THE PRESSURE OF CONCRETE ON VERTICAL FORMWORK IN WIDE SECTIONS

Thesis submitted to the University of London for the degree of Doctor of Philosphy

by

Thomas Alexander Harrison BSc., C.Eng., MICE.

University College, London

December 1979

ABSTRACT

A theory is presented which describes the mechanisms involved in concrete pressures on formwork in wide sections. The main value of the theory is in providing a framework for analysing site data and indicating areas in which potential economies in design might be made.

The horizontal pressure of concrete on formwork comprises two components whose magnitude depends on the proportion of the vertical load taken by the particle structure and the pore water pressure. In normal formwork, the pore water pressure provides the major contribution to the maximum horizontal pressure and therefore any factor which increases the rate of load transfer from the pore water pressure onto the particle structure, will decrease the maximum pressure. For example, porous formwork will give lower horizontal pressures than impermeable formwork and the re-analysis of existing site data supports this prediction.

Normal internal vibration does not have such a significant affect on the maximum horizontal pressure as previously reported, but it can fluidify concrete to the depth of poker immersion.

The elements of the theory are supported by an experimental programme, re-analysis of existing site data and new site measurements. These site measurements have shown that during underwater concreting a rapidly falling tide can cause the horizontal pressure to exceed the vertical pressure.

ACKNOWLEDGEMENTS

I wish to thank Dr G Somerville, my Director of Research, for permitting me to undertake this research. I am also indebted to my Directors of Studies and Supervisor, the late Mr R H Elvery, Professor K O Kemp and Mr W E Murphy for their guidance and constructive comment.

My thanks also go to my colleagues in the Research and Development Division of the Cement and Concrete Association for their help and in particular to Mr M G Habgood for his extensive help with the experimental work, processing data and in the preparation of the Figures and to Mrs P J Ward for typing this thesis.

Thank you all.

CONTENTS

		Page
	TITLE PAGE	1
	ABSTRACT	2
	ACKNOWLEDGEMENTS	3
	CONTENTS	4
	LIST OF FIGURES	7
	LIST OF TABLES	10
	NOMENCLATURE	11
1.0	INTRODUCTION	13
2.0	LITERATURE SURVEY AND ANALYSIS OF EXISTING SITE PRESSURE MEASUREMENTS	16
	Introduction	16
2.1	Mathematical models	16
2.2	Empirical studies and descriptive theories	30
2.2.1	Introduction	30
2.2.2	Rodin	30
2.2.3	ACI Committee 622	34
2.2.4	Ertingshausen	40
2.2.5	Adam, Bennasr and Santos Delgado	44
2.2.6	CERA (CIRIA)	46
2.2.7	Ore and Straughan	49
2.2.8	Ritchie (and McDowall)	51
2.2.9	Murphy	58
2.3	Analysis of existing site pressure measurements	59
2.3.1	Introduction	59
2.3.2	Presentation of the data	59
2.3.3	Discussion of the results	68
2.4	Discussion	70
2.5	Conclusions	74
3.0	EXPERIMENTAL PROGRAMME	76
	Introduction	76
3.1	Objectives of the test programme	78
3.2	Description of apparatus	78
3.3	Method of testing	86
3.3.1	Mould assembly	86
3.3.2	Concrete preparation	87

		Page
3.3.3	Test procedure	87
3.3.4	On completion of the test	88
3.4	Details of the test programme	89
3.5	Results	93
3.6	Discussion of the results	93
3.6.1	Experimental technique	93
3.6.2	Initial tests	104
3.6.3	Tests on the influence of cement chemistry	106
3.6.4	The role of vibration on formwork pressures	110
3.7	Conclusions	113
4.0	A THEORY OF CONCRETE PRESSURE ON FORMWORK	116
4.1	A review of the early hydration of cement	116
4.2	Theory of concrete pressure on vertical formwork in wide sections	123
4.2.1	The dispersal of the hydrodynamic excess	125
4.2.2	The development of suction forces	129
4.2.3	Changes in the head of concrete	131
4.2.4	Vibration	134
4.2.5	Flexible formwork	135
4.3	Mathematical model	136
4.4	Application of the theory	139
4.4.1	Permeability of formwork	139
4.4.2	Rate of placing	143
4.4.3	Mix design	145
4.4.4	The reduction in pressure after the maximum	149
5.0	APPLICATION OF THE THEORY IN INTERPRETING AN UNUSUAL SET OF FIELD DATA	152
	Introduction	152
5.1	Description of the test	152
5.2	Application of the theory to the measurements	154
5.3	Results	156
5.4	Discussion of the results	160
6.0	MAIN CONCLUSIONS AND FURTHER RESEARCH	167
	Main conclusions	167
6.1	Further research	169

		Page
	REFERENCES	171
Appendix A	THE USE OF THE PRESSURE BLEED TEST FOR MEASUREMENTS OF THE FLUID LOSSES IN CONCRETE	178
	Introduction	178
	Description of the equipment and test method	178
	Experimental design	181
	Results	181
	Discussion of the results	183
	Conclusions.	188

LIST OF FIGURES

Figure	Title	Page
2.1	The variation of λ with time.	22
2.2	Setting time against period of working.	25
2.3	Two triaxial test results for values of λ for vibrated freshly mixed concrete at 20°C.	27
2.4	The linear standard viscoelastic solid used as a model for form surfaces.	28
2.5	The effect on pressure distribution of the formwork yielding.	32
2.6	Lateral pressure distribution.	33
2.7	Correction factors for Rodin's basic equations.	35
2.8	The relationship between maximum pressure and the rate of placement at 21°C.	37
2.9	ACI Committee 622's pressure distribution for unlimited rates of pour in columns.	38
2.10	The relationship between formwork pressure and time.	42
2.11	Formwork pressure envelope.	42
2.12	Pressure design envelope.	48
2.13	Stress strain relationship for a 1:3 OPC/gravel concrete.	55
2.14	Effect of workability on lateral pressure in a simulated pressure test equivalent to a rate of placing of 5.4 m/hr.	56
2.15	Site pressure readings on a 450 mm thick wall.	61
2.16	Summary of formwork pressure measurements for low slump concrete.	63
2.17	Summary of formwork pressure measurements for medium slump concrete .	64
2.18	Summary of formwork pressure measurements for high slump concrete.	65
2.19	Comparison of calculated and measured pressures.	67

Figure	Title	Page
3.1	Diagrammatic sketch of the test rig.	79
3.2	Photograph of the test rig.	80
3.3	Cross section of a horizontal pressure gauge.	82
3.4	Tests with plate pressure only (high workability mix).	94
3.5	Test with water pressure only (medium workability mix).	94
3.6	Test with plate and water pressure (high workability mix).	95
3.7	Tests on the influence of cement chemistry (R = 5.3 m/hr.).	96
3.8	Test on the influence of cement chemistry - medium workability concrete (R = 5.3 m/hr.).	97
3.9	Test on the influence of cement chemistry - air entrained concrete (R = 5.3 m/hr.).	97
3.10	Test on the influence of cement chemistry - superplasticized concrete (R = 5.3 m/hr.).	97
3.11	Tests on the influence of cement chemistry (R = 2.6 m/hr.).	98
3.12	Tests on the influence of cement chemistry (R = 1.8 m/hr.).	99
3.13	Test on the susceptibility of the particle structure to vibration (R = 5.3 m/hr.) - high workability concrete.	100
3.14	Scanning electron micrographs of cement paste after 90 minutes of hydration.	108
3.15	The effect of deep re-vibration on three pressure gauges placed 400 mm above the base of a large column.	112
4.1	The components of the vertical and horizontal pressures.	124
4.2	The effect of the consolidation process on pressure.	128
4.3	The development of suction pressures.	130
4.4	Idealised pressure distribution for concrete being placed continuously.	132

Figure	Title	Page
4.5	Idealised pressure distrbution for concrete being placed in lifts.	133
4.6	Reduction in pressure one hour after the maximum.	151
5.1	The trial tremie pour after removal from the river.	153
5.2	The underwater formwork pressure test.	155
5.3	Notation.	156
5.4	Tide levels.	157
5.5	Pressure measurements on an underwater tremie pour.	159
5.6	Graph to obtain coefficient 'a'.	163
5.7	Horizontal pressures adjusted to remove tidal effects.	164
A.1	Pressure bleed test.	179
A.2	Calibration graph.	180
A.3	Pressure bleed test - 35 kN/m^2.	184
A.4	Long duration pressure bleed test - 35 kN/m^2.	184
A.5	Pressure bleed test - 70 kN/m^2.	184
A.6	Pressure bleed test - 85 kN/m^2.	184
A.7	Pressure bleed test - 105 kN/m^2.	185
A.8	Pressure bleed test - 140 kN/m^2.	185
A.9	Pressure bleed test (high workability concrete) - 70 kN/m^2.	185
A.10	Pressure bleed test (high workability concrete) - 140 kN/m^2.	185

LIST OF TABLES

Table	Title	Page
2.1	Comparison of Ertingshausen's site measurements with British formwork design methods.	43
2.2	Summary of the influence of temperature, width of section and slump on the maximum formwork pressure.	45
2.3	Simplified design equations for pure Portland cements.	46
2.4	Comparison of concrete pressures based on the CIRIA work.	50
2.5	Theoretical heights to which various mixes could stand with a vertical face.	53
2.6	Summary of site pressure measurements for concretes containing cements other than OPC.	66
3.1	Mixes used in the experimental programme.	90
3.2	The representative sample of tests reported in this thesis.	92
3.3	The effects of vibration and time on the water movements within a column.	101
4.1	Typical compound proportions of some Portland cements.	117
4.2	The measured horizontal pressure expressed as a percentage of the calculated pressure.	141
4.3	Measured formwork pressures compared with the calculated pressures.	144
5.1	Calculation of the effective formwork pressure and the adjustment to remove tidal effects.	162
A.1	Mix proportions	182
A.2	Fluid loss 6 minutes after the start of the test for the medium workability concrete.	186

NOMENCLATURE

Symbol	Units	Definition
d	mm	Width of section
F	m^2	Horizontal cross sectional area
H	m	Overall depth of section
h	m	Head of concrete above the point being considered
h_1	m	Head of concrete affected by vibration
h_2	m	$(h - h_1)$
h_r	hours	
h_s	m	Head at which the maximum pressure first occurs (often taken as the product of the rate of placing and the setting time*)
k	-	Ratio of pore pressure head to h
k_c	m/hr	Permeability of concrete
m_v	m^2/kN	Coefficient of compressibility
p	kN/m^2	Horizontal pressure
p_{max}	kN/m^2	Maximum horizontal pressure
p_v	kN/m^2	Vertical pressure
R	m/hr	Rate of placing
T	hr	Setting time of the concrete*
t	hr	Time from mixing (it was normally assumed that placing started immediately after mixing and therefore t also represents the time from start of placing)
t_1	hr	Time that the concrete is affected by vibration
t_{max}	hr	Time to reach maximum pressure
U	m	Perimeter of the formwork in plan
u	kN/m^2	Pore water pressure
u_c	kN/m^2	Hydrodynamic excess
u_{max}	kN/m^2	Maximum pore water pressure
u_s	kN/m^2	Potential suction pressure
u_w	kN/m^2	Static water head (γoh)

*The term 'setting time' has been used extensively in the literature without being clearly defined. It is normally meant to represent the time at which the concrete changes from a semi fluid to a solid and at which there will be no further increase in the horizontal pressure. A number of other possible definitions are given in Chapter 2.

Symbol	Units	Definition
γ	kN/m^3	Force or weight density of the concrete
γ_o	kN/m^3	Force or weight density of water
θ	°C	Temperature of the concrete
λ	-	Ratio of horizontal to vertical pressures (see Equation 2.7)
λ_o	-	Initial value of λ
λ_σ	-	Ratio of horizontal to vertical effective pressures (see Section 4.2)
σ	kN/m^2	Effective vertical pressure (i.e. pressure taken by particle structure)
ϕ	°	Angle of internal friction
ϕ'	°	Angle of friction between concrete and formwork.

Chapter 1 INTRODUCTION

Formwork can simply be described as the mould, usually temporary, used to form fresh concrete into the desired shape and size. The distinction between formwork and falsework is not always clear[1,2], but there is agreement that both come under the general heading of 'temporary works'. Perhaps, because they are temporary explains why this is a relatively neglected area of research compared with, say, the design of shell roofs. Comparing the number of shell roof buildings constructed in the United Kingdom with the production and expenditure on formwork (typically one third the cost of a structure[3]), the balance of research effort is not easily explained.

Temporary works range from very simple to highly complex structures, but economy of construction forces factors of safety to be reduced to a minimum. In most cases the design and construction of temporary works have been successful, but the few failures can, and do, cost lives[4,5]. The design of temporary works is similar to the design of the permanent structure in that both the limit states of collapse and deflection are considered, but they differ in the approach to factors of safety. In temporary works, because the loads are of short duration, the permissible stresses in the materials tend to be higher. In addition, the estimated loads are taken as the design loads (i.e. a load factor of 1.0) regardless of whether the loading is due to the self weight of the structure, the construction loads, or the pressure of concrete on the formwork. With such a system it is particularly important that the estimated loads do represent the highest probable loading condition.

In the design of soffit formwork, the design load is the sum of the weights of the formwork, concrete and reinforcement plus the construction load. With normal weight concretes, the density of reinforced concrete (concrete plus reinforcement) is usually taken as 2500 kg/m^3[2]. With lightweight concrete construction, the concrete weight should be calculated using the fresh wet density which is typically 160 kg/m^3 higher than the air dry density[6]. The construction loads consist of the weight of plant and operatives, the impact of the concrete as it is being discharged, any temporary surcharge of concrete and any vibrational loading. The Formwork Report[1] recommends

a range of values between 1.5 to 3.5 kN/ m^2. A CIRIA backed research project[7] measured the construction loads on a number of sites and confirmed that this range was adequate for normal conditions.

In the design of vertical formwork, the horizontal pressure of the fresh concrete has to be assessed. The simple solution of assuming the concrete remains as a fluid is unrepresentative of what happens in most forms and uneconomic, as the costs of initial fabrication are proportional to the pressure[8]. The normal design methods in the United Kingdom[3,9,10] assume that the concrete will reach a maximum pressure which is less than the fluid head of concrete. The pressure envelope follows the fluid pressure to the depth at which this maximum pressure is reached and then remains constant. The maximum design pressure is obtained from design charts[3,9,10] and it depends on the rate of placing, height of lift, width of section, concrete density, temperature and slump. These design charts are limited to pure Portland cement concretes and do not cover cases in which admixtures or cement replacement materials are used. Enquiries continue to come to the Cement and Concrete Association for advice on the maximum pressures in situations not covered by the design charts. Because of the lack of data and the knowledge that a unit load factor was going to be applied, the advice given has tended to be conservative. This project was started with the intention to investigate the maximum formwork pressures for situations not covered by the present design charts. As the literature study progressed and previous site pressure measurements were studied, the complete lack of a sound theoretical basis became apparent. Real progress on the effect of admixtures and cement replacement materials on formwork pressure was unlikely to be made until there was an understanding of the mechanisms by which concrete pressure on formwork was generated. Therefore the emphasis of the research was changed to this more fundamental question.

From the early stages of this project, the indications were that there was a wide range of potential mechanisms to investigate and therefore to make the task more manageable, a start was made with a consideration of un-reinforced concrete being placed in a wide section contained in smooth, rigid, impermeable vertical formwork. Because of this definition, arching of the concrete cannot occur and the factors are reduced to those of the concrete, the rate of placing and vibration.

Whilst concrete pressure on vertical formwork in wide sections is the subject of this thesis, the literature survey includes narrow sections where formwork-concrete interaction is dominant. These are included because the development of the ideas on formwork pressures cannot be sensibly discussed without them, and they help put the research presented in this thesis into an overall context. There is also the intention of continuing with the next stage of the research, the study of formwork-concrete interaction.

The results of the literature survey and a study of existing, though mainly unpublished, site pressure measurements raised many questions. Nevertheless, by deductions based on this information, it was possible to produce a tentative hypothesis suggesting that the maximum formwork pressure was mainly dependent on the dispersal of pore water pressure. An experimental programme which is described in Chapter 3, was devised to test this hypothesis and answer some of the other questions raised by the literature survey. Linking this work in with recent research on the early hydration of cement resulted in the theory presented in Chapter 4. The theory is a descriptive theory and whilst an approach to defining it mathematically is presented, this line of research was not pursued for the reasons given later.

To test quantitatively the theory's predictions, a programme of site pressure measurements was instigated. These were limited to certain areas of specific interest and whilst these measurements are continuing, the results so far obtained are presented in Chapter 5. The degree to which they support the theory's predictions is described.

Chapter 2 LITERATURE SURVEY AND ANALYSIS OF EXISTING SITE PRESSURE MEASUREMENTS

2.0 INTRODUCTION

The literature on vertical formwork pressures is extensive, but the relevance to the modern construction industry of some of the earliest work is doubtful. Rodin in his 1953 paper[11] expressed doubts about both the reliability of some of the early work due to the experimental techniques used, and the relevance of hand spaded and rodded concrete to the 1953 construction industry which was using low to medium workability concretes placed by skip and compacted by internal vibration. Since 1953 the industry has undergone major development with the use of pumped concrete, high rates of placing, finer cements, cement replacement materials and admixtures becoming commonplace. This literature survey reflects these changing conditions by concentrating on the papers that have a relevance to the present day construction industry and those papers that led to the development of ideas about formwork pressures.

The approaches to formwork pressures can be categorised into mathematical theories, descriptive theories and empirical studies. As the descriptive theories were normally contained within an empirical study, the literature survey is considered in just two sections, mathematical theories and empirical studies with their descriptive theories. Comments on the papers are limited at this stage to deductions based on the contents of the paper and on previous work. Comments made on the basis of hindsight are left until the general discussion.

After the literature survey, there is presented a section on the analysis of existing site pressure measurements. Most of this data has not been published and they provide a valuable source of information for checking theory against practice.

These sections are followed by a general discussion on the state of knowledge on formwork pressures. This combines the findings of both the literature survey and the analysis of the site pressure measurements.

2.1 MATHEMATICAL MODELS

In attempts to assess the pressure distribution on vertical

formwork, engineers turned to adapting existing theories in soil mechanics and silo design. The cohesion of concrete was normally, although not always, ignored and concrete was assumed to be a granular material with an angle of internal friction, ϕ . Guerrin[12] categorised concrete into the following groups,

(a) liquid concrete with no internal friction
(b) poured concrete having an angle of internal friction of 20°
(c) stiff concrete, (ϕ = 30°)
(d) concrete after compaction by vibration (ϕ = 50°)
(e) concrete after compaction by rodding (ϕ = 30°)

The angle of friction between the concrete and formwork, ϕ', was given as 23° for timber and 14° for steel. Sections were divided into wide sections and narrow sections. For wide sections, poured concrete was split into a water component and a solids component and the maximum pressure for a concrete of force density 22 kN/m^3 given as,

$$p_{max} = 10\ h_s + 12\ h_s\ c \quad kN/m^2 \qquad (2.1)$$

where h_s = product of the rate of placing and setting time
c = a coefficient given as 0.413 for timber and 0.445 for steel.

Stiff concrete was not assumed to have a water component and the maximum pressure was given as,

$$p_{max} = 0.3\ \gamma\ h_s \quad kN/m^2 \qquad (2.2)$$

With vibrated concrete, the concrete was assumed to act as a fluid to a depth of 0.8m and the maximum pressure given by the equation,

$$p_{max} = 0.8\gamma + 0.13\ \gamma\ (h_s - 0.8) \quad kN/m^2 \qquad (2.3)$$

For narrow sections, Guerrin[12] turned to silo theory. Silo theory takes into account the friction between the material and container and therefore the increase in load or force caused by the increase in head equalled the total load increase less the load taken by the formwork i.e.,

$$d\,p_v F = \gamma F\ dh - p_v U \tan \phi'\ dh \qquad (2.4)$$

This vertical force then has to be modified to give the horizontal force. The two classic solutions to the silo problem are Janssen's method[13] and Reimbert's method[14]. Guerrin used Reimbert's equation to obtain,

$$p = a\gamma \frac{F}{U \tan \phi'} \left[1 - \frac{1}{\left(\frac{h\ U\ b}{F} + 1 \right)^2} \right] \qquad (2.5)$$

where $b = \tan \phi' \tan^2 \left(\frac{\pi}{4} - \frac{\phi}{2} \right)$

a = shape coefficient having values of 1.273 for square sections and 2.546 for walls of infinite length.

With stiff concrete, the lateral pressure was obtained by direct substitution into this equation. Poured concrete was still split into water and solid components and equation 2.5 was substituted for the last term in equation 2.1. Similarly with vibrated concrete, the last term of equation 2.3 was replaced by equation 2.5 giving,

$$p_{max} = 0.8\gamma + \frac{a\ \gamma\ F}{U \tan \phi'} \left[1 - \frac{1}{\left(\frac{(hs - 0.8)\ U\ b}{F} + 1 \right)^2} \right] \qquad (2.6)$$

This equation gave relatively small reductions in pressure when compared with the wide section equation. Guerrin stated that the rate of placing only has a slight effect on pressure with vibrated concrete.

In wide sections where arching was considered to be insignificant, several researchers started their analysis of formwork pressure from the Rankine equation[15] for the ratio of horizontal to vertical pressure, λ, in granular materials,

$$\lambda = \frac{p}{\gamma h} = \tan^2 \left(\frac{\pi}{4} - \frac{\phi}{2} \right) \qquad (2.7)$$

For vertical formwork and a horizontal concrete surface, the Coulomb wedge theory gives the same formulae[16]. The main difference between the papers that have used this approach has been in the variation of λ with time, temperature and concrete mix proportions. In Uspenskij's account of Russian practice[17], in Guerrin's stiff

concrete[12] and Drechsel's wide sections[18] the change in λ with time was ignored and the pressure was taken as

$$p = \gamma h \times \text{constant}$$

where the constant was given numerical values based on their experience.

The maximum pressure was said to be controlled only by the setting time of the cement and would occur when

$$h = h_s = \text{rate of placing} \times \text{setting time}$$

Most of the researchers took λ as a variable with time. At the time of placing, the concrete was normally assumed to act as a fluid in which case the initial value of λ would be 1. At some time later, the concrete would be self supporting and λ must therefore be zero. The researchers differed in both the function used to link these points together and the time taken to reach zero. Böhm[19] took λ as linearly decreasing from 1 to zero at 12 hours for concrete with a temperature of 8 to 10°C. Toussaint[20], whose work was limited to rate of placing of 0.1 to 1.0 m/hr also took a linear reduction in λ from 1 to zero, but this was over an 8 hours period for normal concretes.

The assumption of a linear reduction in λ gives an equation of the form

$$p = \gamma h \left(1 - \frac{h}{h_s} \right) \qquad (2.8)$$

which gives a parabolic pressure distribution in which the maximum pressure,

$$p_{max} = \frac{\gamma h_s}{4} \quad \text{at depth} \quad \frac{h_s}{2} \qquad (2.9)$$

Hoffman[21] attempted to measure the variation of λ with time by measuring the tie bolt loads in a column in which the head of concrete was simulated by superimposed loads. Gaede[22] doubted if such a system would simulate the actual conditions within a column. Hoffman found considerable variations in λ, particularly in the initial stages, but based on his experimental work, he adopted an exponential equation for

the ratio of the conjugate stresses of the form

$$\lambda = \lambda_o \exp \left[- \frac{1}{T} \left(t - \frac{x}{R} \right) \right] \qquad (2.10)$$

where x = height to the level under consideration measured from the base in metres.

The coefficients λ_o and $^1/T$ had to be determined by experiment and Hoffman gave values of λ_o = 0.93 for vibrated concrete and 0.36 for loosely placed concrete. In both cases $^1/T$ was 0.10 hr^{-1}. The Hydro-Electric Power Commission of Ontario[23] evaluated these coefficients for one rate of placing, 0.27m/hr, and when the ACI[24] developed a rate of placing/pressure graph from these results, they finished with a straight line passing through the origin. The ACI suggested that it would be simpler to determine the slope of the line experimentally rather than the constants λ_o and $^1/T$.

Muhs[25] carried out some site measurements on formwork pressures in large concrete sections. The ambient temperatures were low, 0 - 3°C and the placing rate was on average 0.75m/hr. The concrete was compacted by internal vibration. The pressures were found to increase up to a head of 3 to 3.5m, but the numerical measured values of the pressure were less than those predicted by Rodin[11]. Using his results, Muhs suggested that $\lambda = 1$ up to a time t_1 and thereafter decreases hyperbolically until setting occurs.

For t between t_1 and T

$$\lambda = \lambda_o \left(\frac{t}{t_1} \right)^{- \alpha} \qquad (2.11)$$

and the basic pressure equation is,

$$p = \gamma R \lambda_o t_1^{\alpha} t^{(1 - \alpha)} \qquad (2.12)$$

On the basis of his measurements, Muhs recommended for high workability concrete that t_1 = 0.75 hr. and α = 0.6. Muhs appreciated the inaccuracy of his solution and suggested that it only be used to check empirical solutions.

Olsson[26], who derived equations for formwork pressure using silo theory, tried both a linear and expontial decrease in λ with time.

As a representative of this group, Schjødt's papers[27,28,29] are reported in detail as the comments applicable to his work would in principle fit all of these papers. The other reason for choosing Schjødt is that he was the first person to introduce the term pore water pressure into formwork pressure analysis.

Schjødt considered the following variables:

1. Setting time.
2. Workability of the concrete.
3. Weight of the concrete.
4. Pore water pressure.
5. Rate of placing.
6. Depth of vibration.
7. Smoothness of the formwork (for arching).
8. Permeability of the formwork (linked with pore water pressure).
9. Cross section of the formwork.

The concrete model used to develop his formulae was that the concrete acts as a fluid during vibration or working but as soon as the working of the concrete ceases, it acts as a solid porous material with pore water pressure. During the fluid stage the pressure curve follows the hydrostatic pressure.

Concrete as a material exhibits both cohesion and internal friction. Schjødt ignored cohesion in his main calculations, as he showed that it had an insignificant effect on pressure in most circumstances, but for completeness he derived in the Appendix to his paper[28] a formula that included cohesion. This left his model concrete as a granular material with internal friction and pore water pressure. The ratio of the conjugate stresses, λ , was assumed to reduce linearly by the factor

$$\left(1 - \frac{h_2}{h_s}\right) \qquad (2.13)$$

where h_2 = depth of concrete to the point being considered, less the depth of concrete still being worked (Figure 2.1).

Figure 2·1: The variation of λ with time·

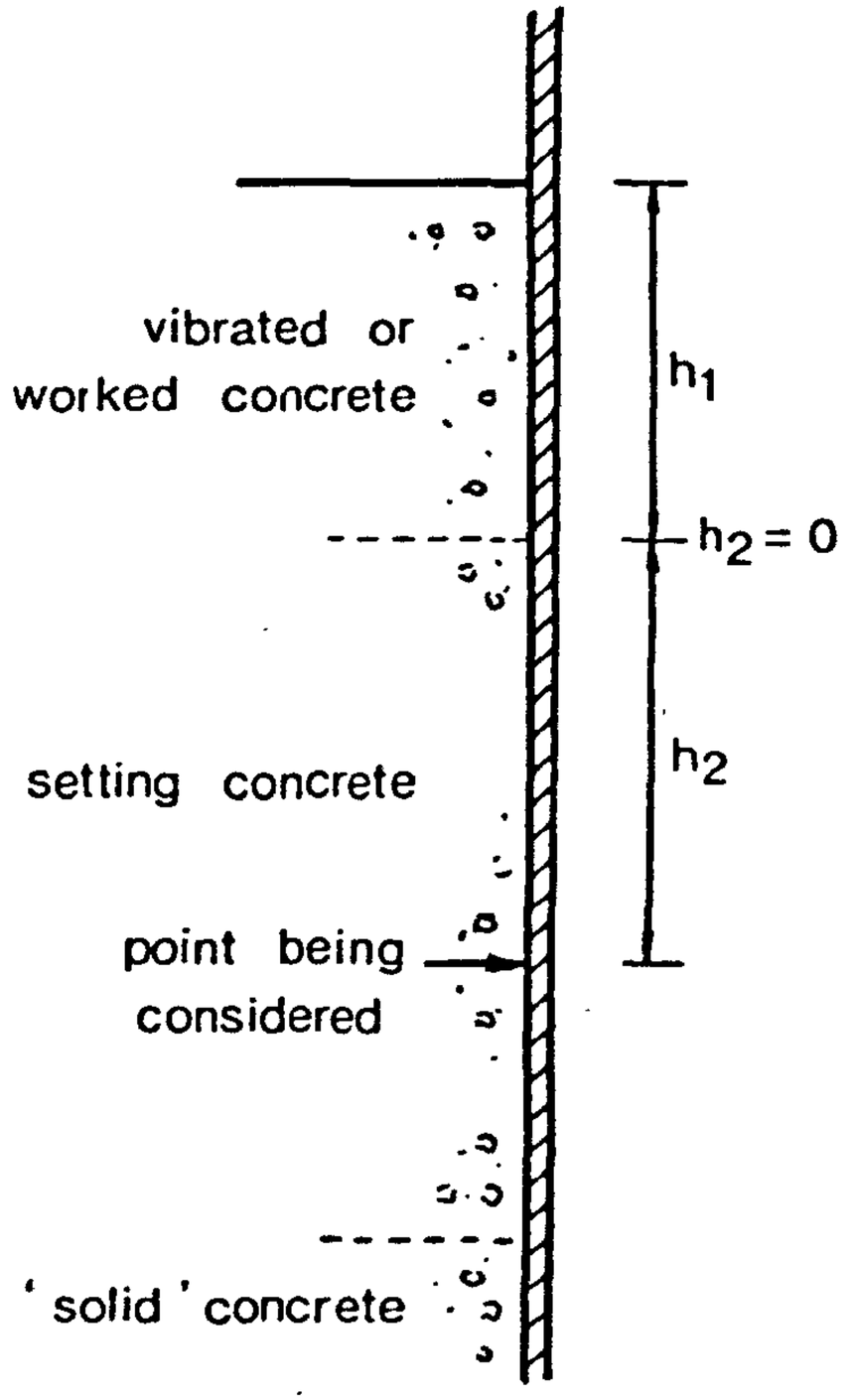

[a]

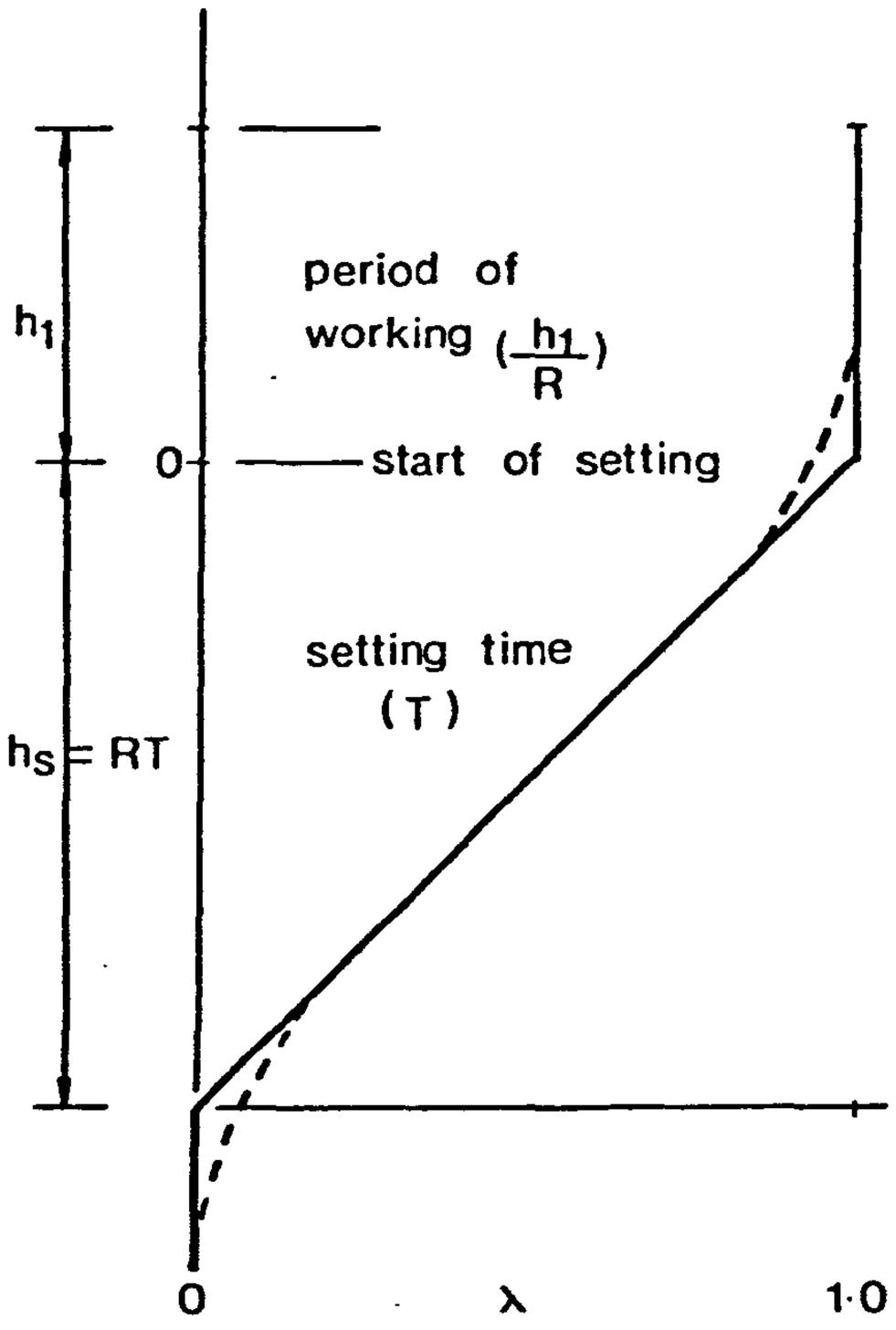

[b]

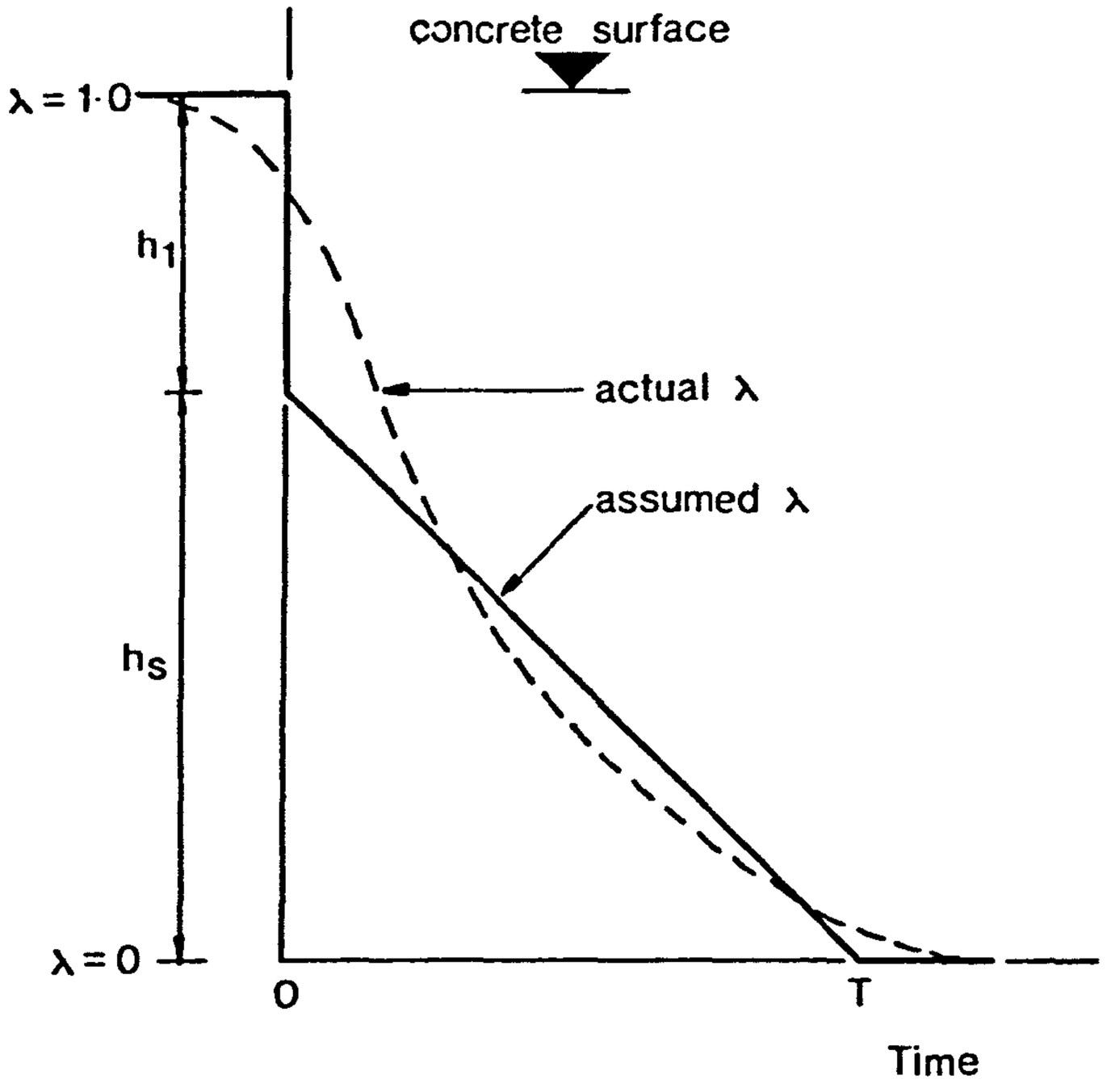

(after Schjødt[28]) - this diagram is not correct as at level $h_2 = 0$ λ should still be equal to 1·0.

[c]

Is DATA FROM SITTING OR PLACING ?

Figure 2.1(a) shows the various zones of concrete described by Schjødt. It should be noted that the setting time, T, does not start until the end of the period of working. Figure 2.1(c) is a reproduction of Schjødt's figure giving the variation of λ with time. The solid line was said to represent the assumed value of λ and the dashed line, the actual value. This figure is confusing and does not appear to be correct for up to time t = 0, λ is still 1. Figure 2.1(b) is my interpretation of Schjødt's definitions.

Schjødt derived equations for formwork pressure without and with friction between the concrete and forms.

Without friction, the maximum lateral pressure was given by,

$$p_{max} = \left[\frac{\gamma\lambda}{2}\left(1 - \frac{h_1}{h_s}\right) + \frac{\gamma_o h}{2}\left(1 - \lambda - \frac{\lambda h_1}{h_s}\right)\right]\left[h_1 + \frac{h_s}{2}\left\{1 - \frac{h_1}{h_s} + \frac{k}{\lambda}\left(\frac{\gamma_o}{\gamma - \gamma_o k}\right)\right\}\right] \quad (2.14)^{*}$$

where k is the ratio of pore water pressure head to height of concrete above the point in question.

In further work[29], Schjødt showed that the depth of vibration was not necessary as it could be covered by modifying λ and k. A simplified equation was proposed where

$$p_{max} = \frac{1}{4}\left[\gamma\lambda + \gamma_o k (1 - \lambda)\right]\left[1 + \frac{1}{\lambda}\,\frac{\gamma_o h}{\gamma - \gamma_o k}\right] RT \quad (2.15)$$

He further simplified this equation for vibrated concrete by assuming that $\lambda = 1$. This implies that the concrete has no internal friction and that it acts as a fluid.

In this case

$$p_{max} = \left(5.97 + \frac{377k}{150 - 63k}\right) RT \quad \frac{kN}{m^2} \quad (2.16)$$

Taking friction between the concrete and form into account, Schjødt derived the following equation for pressure,

$$p = \gamma_1 \lambda \left(Ah_1 - Kh_s\right)\left(1 - \frac{h_2}{h_s}\right) + \gamma_o k (h_1 + h_2) \quad (2.17)$$

---

*Note The term $(\gamma - \gamma_o K)$ was given as $(\gamma + \gamma_o K)$ in the original paper. By re-calculating the equation this was proved to be a printing error. It is also interesting to note how frequently this error has been reproduced in other papers quoting this reference.

where $\gamma_1 = \gamma - \gamma_o\, k$

$$A = \exp\left\{ - a \frac{h_2}{h_s} \left(1 - \frac{h_2}{2h_s} \right) \right\} \quad \text{with } a = \lambda \tan \phi' \frac{h_s}{R}$$

$$\text{and } K = \exp\left\{ \frac{a}{2} \left(1 - \frac{h_2}{h_s} \right)^2 \right\} \sqrt{\frac{2}{a}} \int_{\sqrt{\frac{a}{2}} \left(1 - \frac{h_2}{h_s} \right)}^{\sqrt{\frac{a}{2}}} \exp\left\{ - h_2^2 \right\} dh$$

(Again a printing error in the term K has been corrected).

Because of the complexity of these coefficients graphical aids were given to determine their values.

The main weakness of Schjødt's method is in the selection of the material constants. For example, the pore water pressure constant was taken as 1 for impermeable rigid formwork and zero for porous formwork which gave rapid drainage, but most practical forms fall between these extremes. The guidance given by Schjødt as to the value of k suggests values in the range 0.70 - 0.90, yet in his examples where the calculated pressures fit the experimental results, values of k of 0.2 and 0.53 were used.

There is also considerable difficulty in selecting the depth to which the concrete is affected by vibration. In his second example[28], the experimental results were used to determine that the rodding effect reached down to 1.4 metres. A theory that relies on rodding being ignored in one example and taken as 1.4 metres in the next, suggests that it contains a fundamental weakness.

The setting time, T, was defined as the time after the concrete is left undisturbed for it to achieve its final set and change from a frictional mass to a solid body. Schjødt has assumed that working the concrete neutralizes the setting process and that the setting time can be measured as the period between the end of working and setting. To check the assumption that the setting time is constant when measured by this method, a test was carried out using the Vicat needle test[30] in our laboratory. A standard cement paste[30] was re-worked every few minutes and at various times after batching samples were taken for penetration tests.

Figure 2.2 : Setting time against period of working.

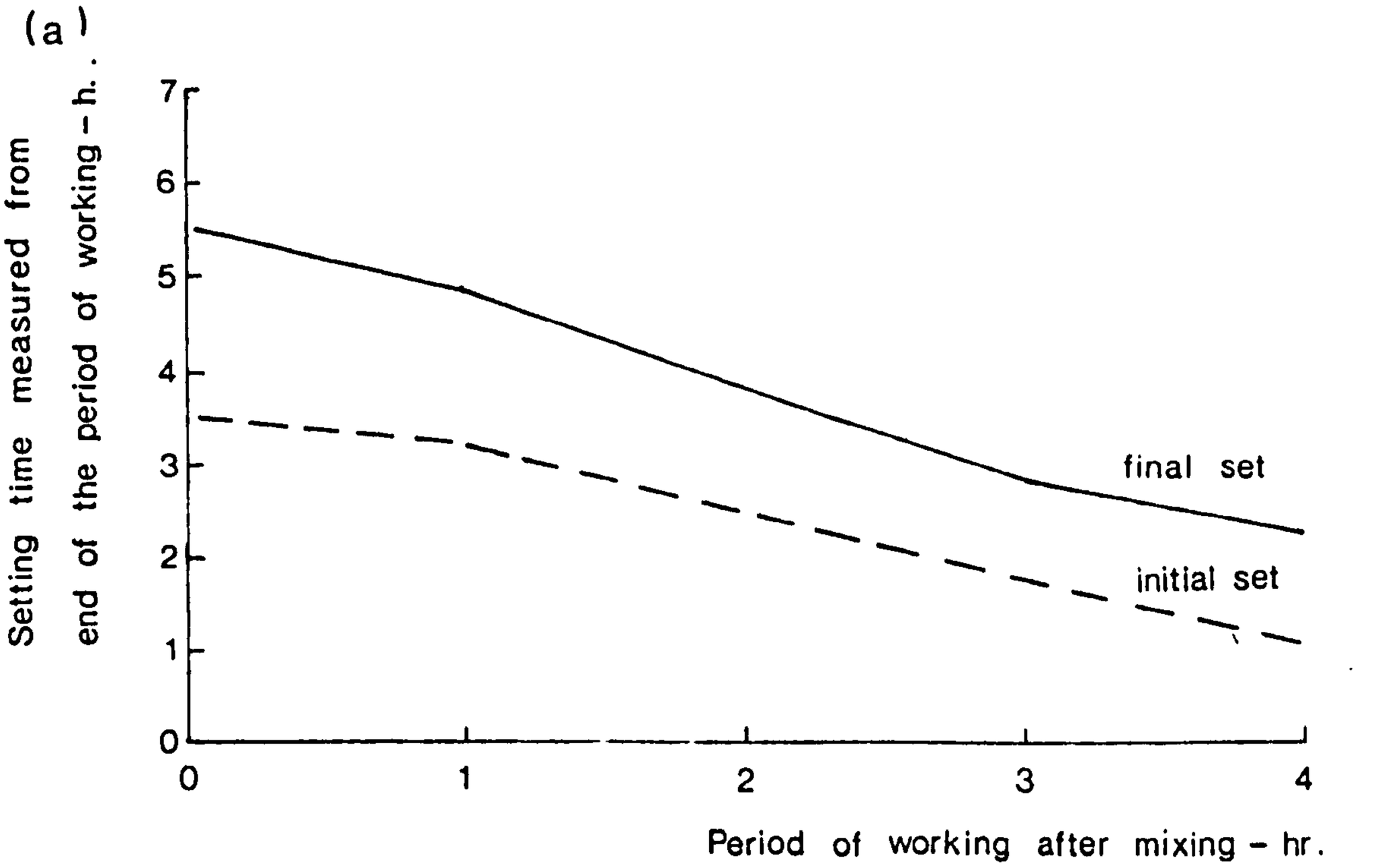

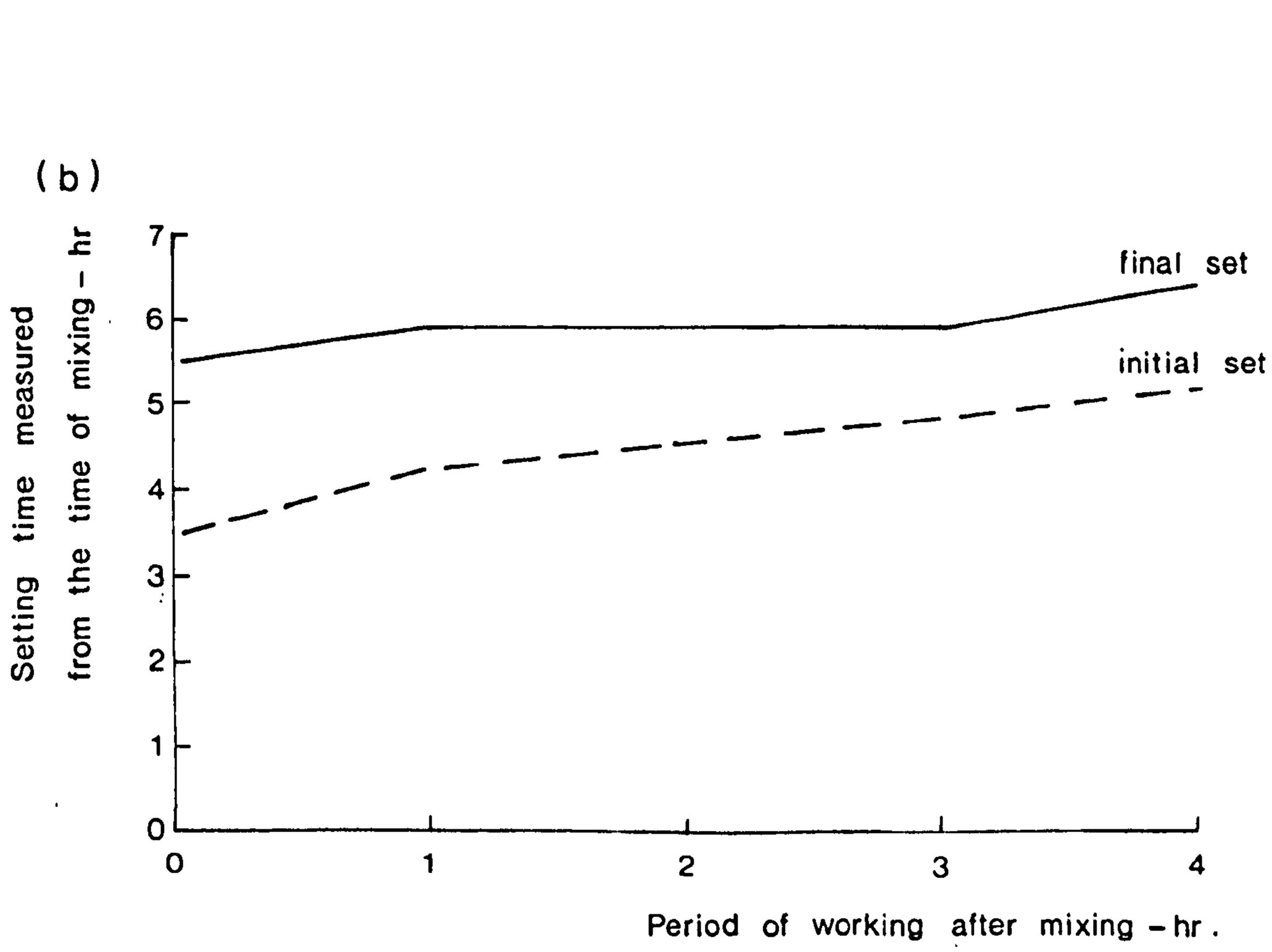

Figure 2.2(a) gives the setting times of these samples measured from the end of the period of working. This figure clearly shows that when the setting time is measured on this basis, it cannot be taken as a constant. On the other hand, Figure 2.2(b) shows that when the setting time is measured from the start of mixing, it is, for practical purposes, a constant. From this one experiment, it was possible to show that Schjødt's assumptions regarding setting times were not correct.

The most useful aspect of Schjødt's papers was the introduction of the term 'pore water pressure' although in the context of his paper the term 'a fraction of the static water head' would have described his approach more accurately. The pore water pressure was treated as a constant proportion, less than or equal to the static water head. Nevertheless, the use of the term was sufficient to start a chain of thought which will be described later in this thesis.

Witte[31] investigated the reduction in the angle of internal friction with time by means of triaxial tests. The samples were compacted by vibration within rubber bags and then at various intervals of time after compaction, tested in the triaxial compression machine. The horizontal pressure was adjusted to prevent the specimen deforming and then the ratio of the conjugate stresses, λ , was obtained directly from the applied stresses. At the time of vibration, λ was taken as 1. Immediately after vibration, the values of λ were lower than expected (Figure 2.3) and this was attributed to frictional losses in the machine.

Witte considered that the reduction of λ with time should follow the exponential form and the experimental results from 2 hours onwards fitted this assumption reasonably well, Figure 2.3. This is not surprising because as λ tends to zero, any of the proposed λ curves could be said to correlate reasonably well with the data. In this paper in particular, one senses an adherence to the mathematical equation regardless of the experimental results.

In all of these methods using soil mechanics or silo theory, the main weakness was the lack of reliable data to feed into the equations; the only cases in which there was any confidence in the

Figure 2.3 : Two triaxial test results for values of λ for vibrated freshly mixed concrete at 20°C.

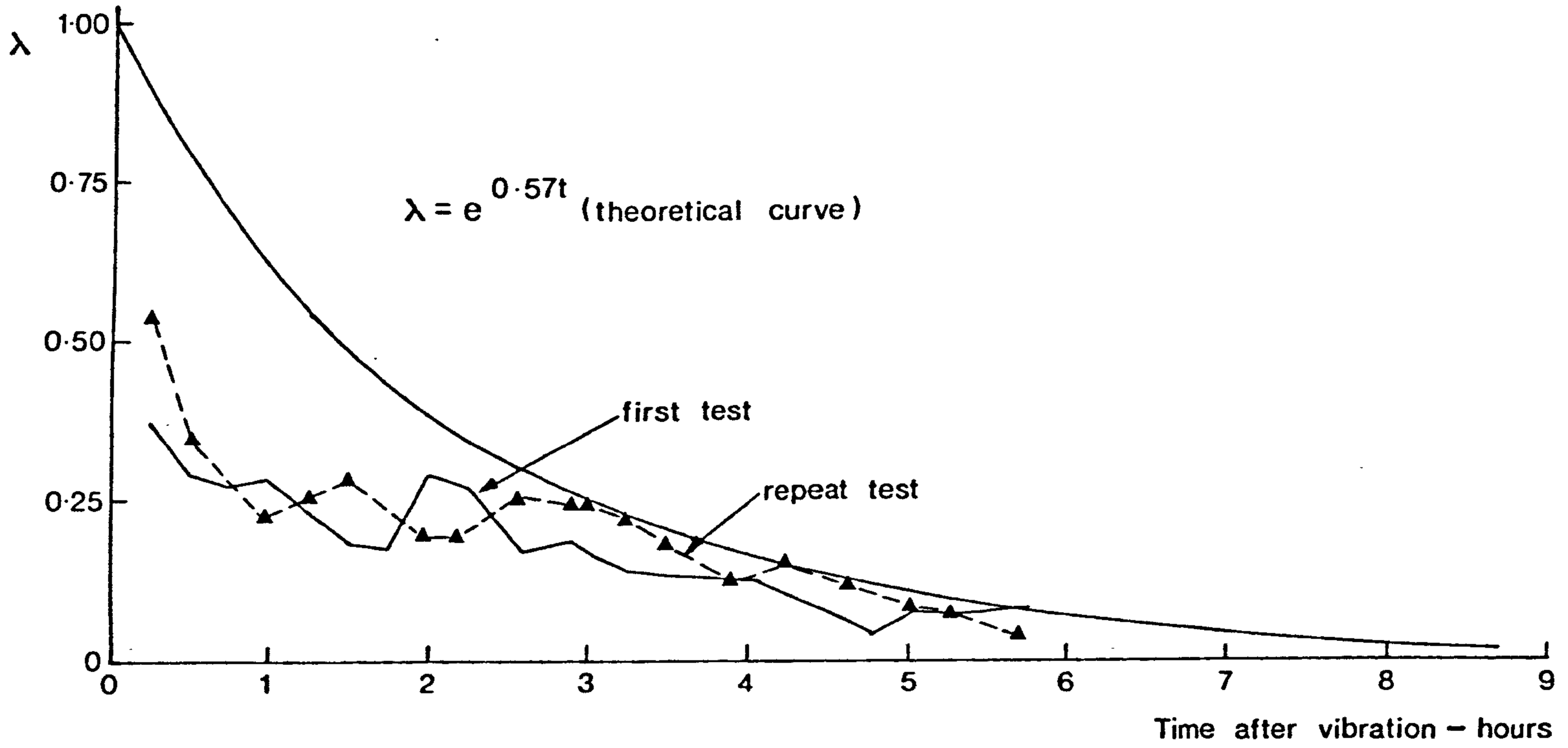

(after Witte[31])

results was when the coefficients had been deduced from the measured formwork pressure and this defeats the point of the exercise.

As well as the failure to produce reliable answers, the modification of soil mechanics theory has theoretical weaknesses. Wedge theory is essentially a failure situation in which the forces necessary to stop a sheared wedge of soil from moving are resolved. With concrete, the settlement of the concrete and the deflection of the forms is unlikely to generate the full potential shear strength of the concrete and the failure situation will not be reached.

In a more recent paper, Levitsky[32] produced an analytical model for form pressure based on an viscoelastic model. In an earlier model[33] he assumed that the shape of the pressure curve to be a result of simultaneous hardening and shrinkage, but this gave neither the correct qualitative nor quantitative results. In the new model the relaxation in the form pressure after the maximum was ascribed to relaxation of the formwork.

For his model he assumed that the concrete mix would firstly act as a fluid and then harden instantaneously into an infinitely rigid material. The formwork is assumed to possess a large initial stiffness that decays to a lesser residual value under the action of the concrete pressure. These characteristics can be described with a standard linear viscoelastic model (Figure 2.4). Shear stresses between the form

---

Figure 2.4 The linear standard viscoelastic solid used as a model for form surfaces

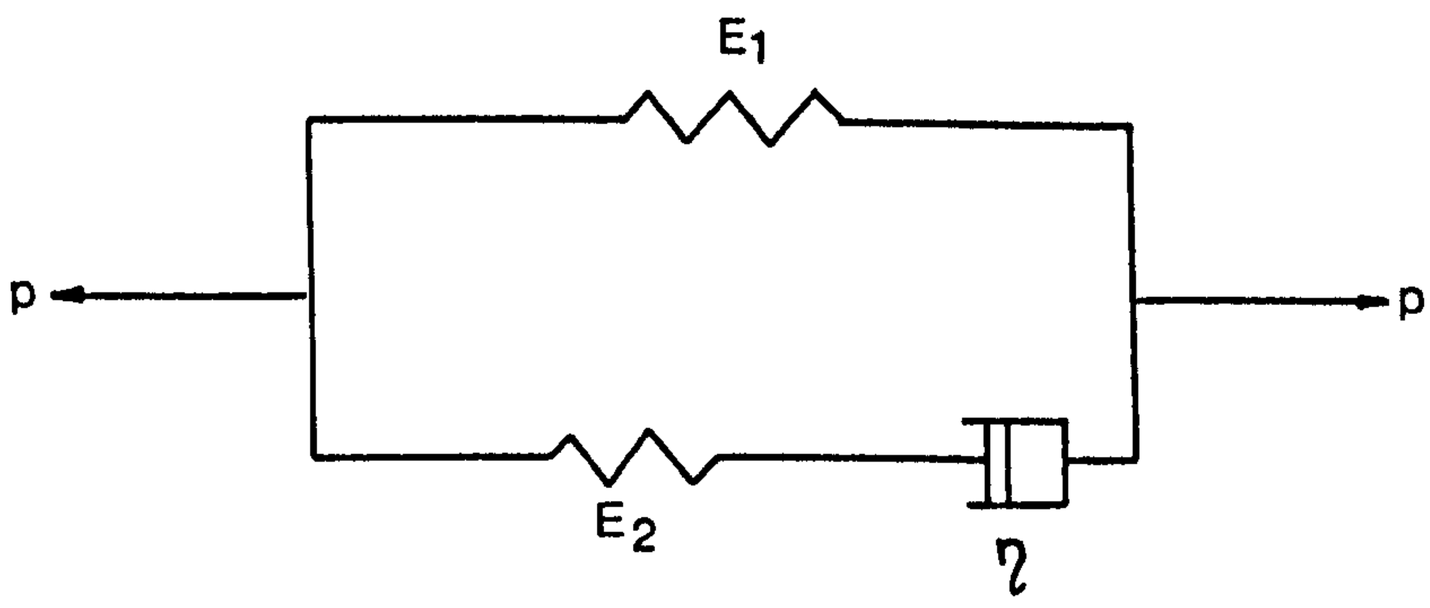

surface and concrete were taken to be negligible and therefore by implication 'arching type' effects are ignored. Levitsky correlated his work to Ritchie's[34,35,36], but Ritchie's work was done on small columns where arching would have been significant.

The model considers two regions. A zone from the pouring surface to the depth at which it instantaneously hardens where the form pressure is hydrostatic and the form is displaced according to the postulated viscoelastic pressure displacement model, and a zone below this where the form displacement is fixed, but the pressure between it and the concrete reduces due to relaxation of the formwork.

In the lower zone, the interface pressure was shown to be:-

$$p = p_{oo} + (p_{max} - p_{oo}) \exp\left(\frac{h_1 - h}{R\, t_r}\right) \qquad (2.18)$$

p_{oo} is the residual form pressure and was calculated from:-

$$p_{oo} = E_1 \; e_{max} = E_1\left(\gamma \frac{RT}{E_1} + \gamma \frac{R t_r E_2}{E_1^2}\left[\exp\left(-\frac{E_1 T}{(E_1+E_2)t_r}\right) - 1\right]\right) \qquad (2.19)$$

where t_r = relaxation time constant of the formwork

E_1 = residual stiffness coefficient of the formwork

E_2 = relaxable form stiffness coefficient.

From existing data, the physical parameters were selected to fit a placing rate of 3m/hr. This gave a setting time of only 0.25h. The pressure distributions were then calculated at other placing rates. The results did not correlate well with the experimental data although the qualitative shape of the pressure distribution was similar.

In an attempt to get better correlation, the setting time was treated as a variable using Rodin's data[11],

$$T = 0.25\left(\frac{3.05}{R}\right)^{\frac{1}{2}} \quad \text{hr.} \qquad (2.20)$$

The correlation between calculated and experimental results was still poor. It was claimed that this poor correlation was due to an anomalous interaction between the pouring rate and the initial setting of the concrete mix. On the basis of his results Levitsky concluded that there was a very rapid initial set a short time after the concrete had been placed and this determined the maximum form

pressure and that the reduction in the form pressure after the maximum was specifically due to relaxation of the formwork.

As neither the very rapid initial set, nor relaxation of the formwork to the degree required are phenomena that have been observed, the assumptions of this theory must be suspect. As the results are not quantitatively reliable, the model has little use as a guide to practical formwork pressures.

2.2 EMPIRICAL STUDIES AND DESCRIPTIVE THEORIES

2.2.1 Introduction

The emphasis in this section is on papers that have either contributed new experimental evidence, or provided a forum for the discussion of descriptive theories. Papers that have just produced design charts based on a survey of existing published data[37,38] are not included. The papers are taken in hisotrical sequence as this helps trace the development of ideas.

2.2.2 Rodin

Rodin[11] carried out an extensive review of the previous work on formwork pressure. However much of this data have little relevance to present day techniques as many of the pressure readings were for hand placed concretes having slumps in excess of 200 mm. Rodin also reviewed the experimental techniques used by the investigators and he argued that some of these techniques cast considerable doubt on the usefulness of the results. The thoroughness of his analysis of the previous data was confirmed by the ACI Committee 622[24] with spot checks.

Before presenting formwork design equations, Rodin described his concept of why formwork pressure was not purely the fluid pressure. When the concrete is placed between forms, the aggregate settles until the grains are in contact and surrounded by a cement mortar matrix. Assuming a particular concrete mix at constant temperature, placed by hand at a constant rate of pour against an infinitely long form of width d, Rodin used Terzaghi's analysis of pressure distributions in granular materials to show the pressure distributions resulting from

a form rotating either about its top, or its base, or moving laterally (Figure 2.5). According to Terzaghi, the change from the fluid pressure distribution is due to an 'arching effect' resulting from a transfer of pressure from a yielding mass into adjoining stationary parts. Arching will also occur if one part of a yielding support moves out more than its adjoining part.

Rodin claims that arching generally occurs and this combined with friction between the concrete and form and chemical stiffening of the mortar, is the prime cause of the lateral pressure distribution. The degree of arching is affected by the yielding and deformation of the formwork and by the ratio d/H. The smaller this becomes, the greater will be the arching effect.

Figure 2.6 shows Rodin's lateral pressure distribution. The reason for the maximum pressure, p_m, was put down to shrinkage strains reducing the total lateral pressure, or to the location of the pressure cells. It was also argued that the distribution of moment to adjacent spans might decrease or increase the pressure cell readings depending on its location in the forms. For simplicity, Rodin recommends that the shape of the pressure distribution be taken as linear between zero and the maximum pressure.

Using his model of formwork pressure, Rodin analysed the experimental results available to him. He fitted empirical curves to the data after making an allowance based on his assessment of the reliability of the data. This gave the following relationship for a 1:2:4 concrete at 70°F, for hand placed concrete.

$$p_{max} = 17\ h_s = 19.16\ (3.28R)^{\frac{1}{3}}\ kN/m^2 \qquad (2.21)$$

and for vibrated concrete,

$$p_{max} = 24\ h_s = 25.9\ (3.28R)^{\frac{1}{3}}\ kN/m^2 \qquad (2.22)$$

This relationship for vibrated concrete was based on very limited data but eleven years later[39], Rodin felt that there was insufficient new published data to warrant any modifications to the relationship.

Figure 2.5 : The effect on pressure distribution of the formwork yielding .

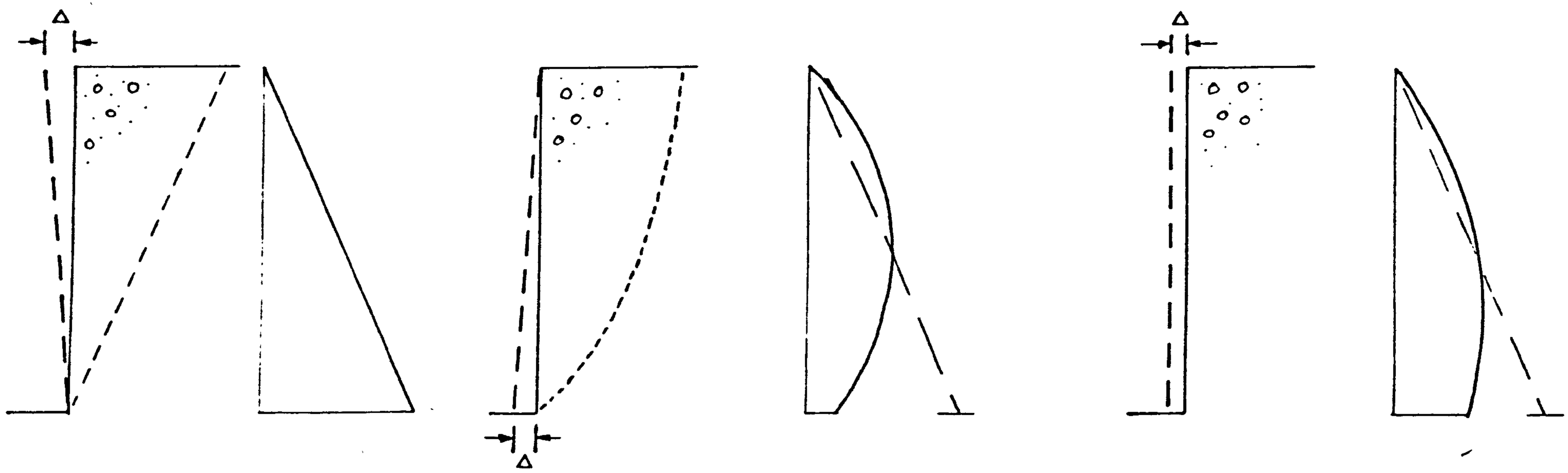

Rotation about the base

Rotation about the top

Lateral displacement

(after Rodin[11])

Figure 2.6 : Lateral pressure distribution .

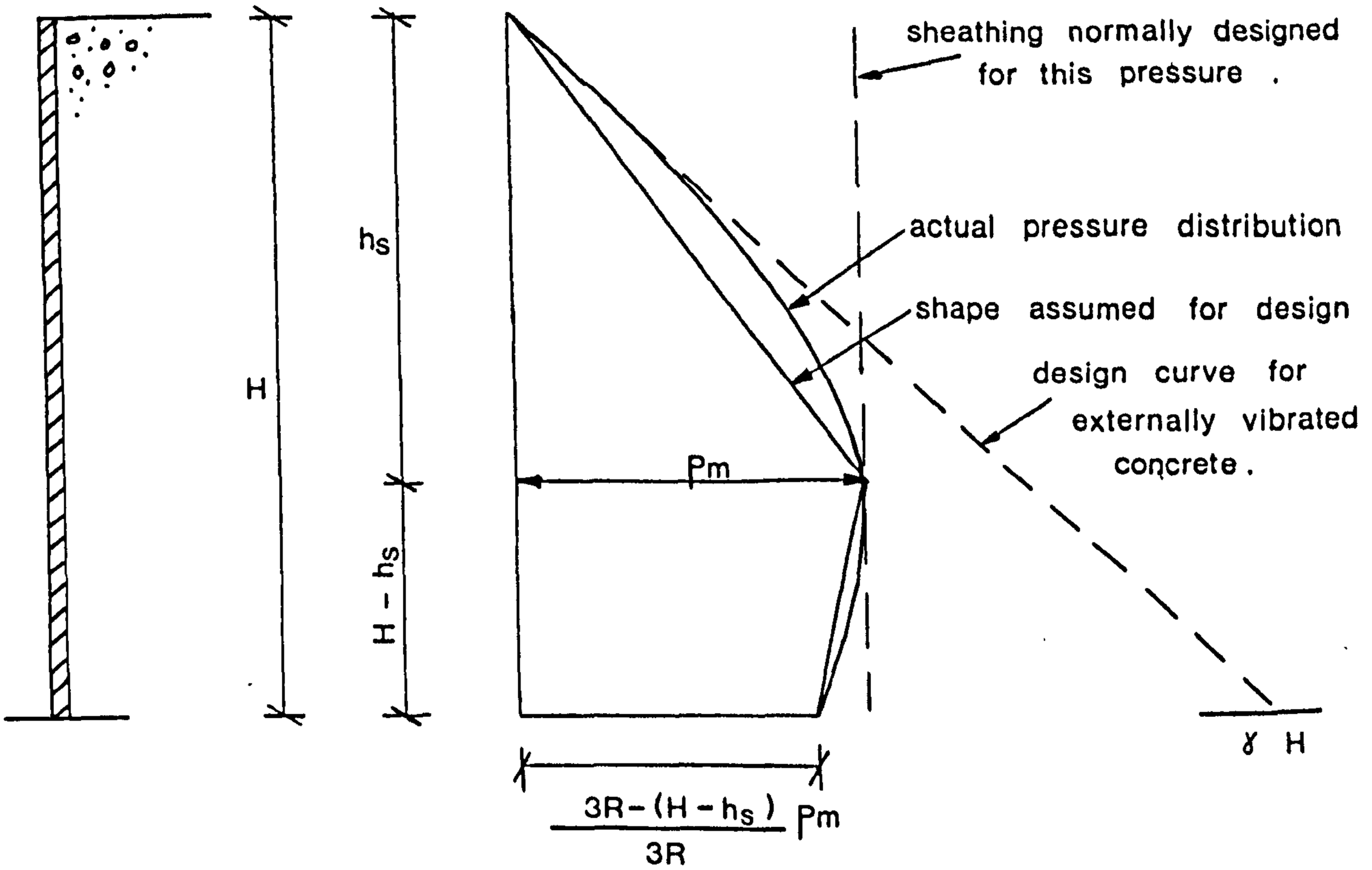

(after Rodin[11])

To allow for different mix proportions, workability and temperature, correction factors were applied. Figure 2.7 gives three factors, but again Rodin had to use his judgement to produce these curves as the data were scant and of variable quality. Due to lack of data, Rodin was unable to establish relationships to take into account setting time and the size and shape of the form. He mentions the importance of these factors and discusses the possible form these relationships would take.

Meyerhof in the correspondence on Rodin's paper suggested that in sections where the ratio d/H was less than one half, silo theory might be applied. Rodin agreed that it might well apply in such cases and referred him to Schjødt's first paper[27].

2.2.3 ACI Committee 622

The ACI Committee 622 review[24] of the work on formwork pressure was published in August 1958. In their study of the data, they utilised Rodin's 1952 survey extensively and also the work of Schjødt, Hoffman and the Ontario Hydro-Electric Power Commission. No new work was instigated but they did make use of unpublished data when determining, for example, the maximum pressure in columns. Their brief was to produce a safe guide to the concrete pressures to use when designing formwork in normal conditions. As such they did not attempt to offer any new theories on formwork pressure, but the papers did provide a focal point for discussing the ideas current at this time.

From the review of the variables affecting concrete pressure, it was concluded that the rate of placement, concrete temperature and the effects of vibration were the most important. These were combined to form a general basic equation,

$$p_{max} = C_1 \left(1 - \frac{C_2 \; R}{\theta}\right) \qquad (2.23)$$

where C_1 is a function of the unit weight of mix

C_2 is a function of the consistency of the concrete.

Assuming Type 1 cement, no admixtures, a weight density of 23.6 kN/m^2 and a slump of 100 mm, the equation becomes

Figure 2.7: Correction factors for Rodin's basic equations.

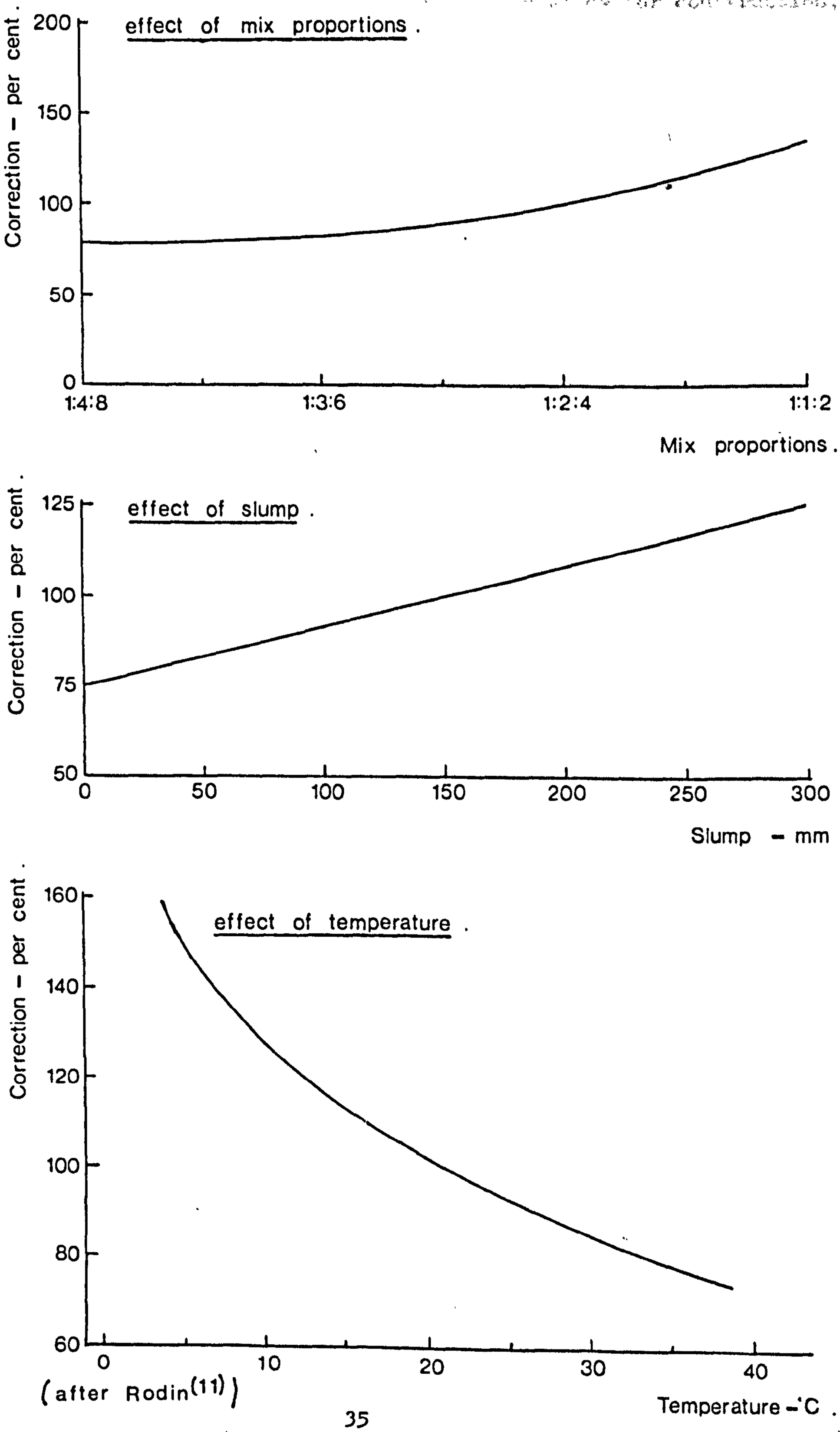

$$p_{max} = 7.2 + \frac{785\ R}{\theta + 17.8} \qquad kN/m^2 \qquad (2.24)$$

The minimum value of 7.2 kN/m^2 was to allow for construction, surcharge and re-vibration loads. Pressures for lightweight and heavyweight concretes were to be obtained pro rata to density.

Figure 2.8, a reproduction of one of the figures in the ACI paper, gives a comparison of this equation with test data. Rodin's pressure equation was also plotted and the Committee felt that it was too conservative at low rates of placing and not conservative enough at high rates of placing. Above rates of placing of 2.1 m/hr for walls, the Committee found equation 2.24 to be conservative. Rodin's curve fitted the experimental results closely in this range, but the ACI choose a simplified empirical straight line following the equation,

$$p_{max} = 35.9 + \frac{244\ R}{\theta + 17.8} \qquad kN/m^2 \qquad (2.25)$$

This was modified in later papers[40,41], without explanation to

$$p_{max} = 7.2 + \frac{1156}{\theta + 17.8} + \frac{244\ R}{\theta + 17.8} \qquad kN/m^2 \qquad (2.26)$$

This modification makes little difference at 21°C but at lower temperatures, it tends to increase the lateral pressure. For example at 5°C, the pressure is increased by 23 kN/m^2.

Equations 2.25 and 2.26 were given a maximum value of 96 kN/m^2 provided the vibration was limited to the top four feet of the lift and only then if the concrete was still plastic.

For columns, equation 2.24 was applied up to a maximum value of 144 kN/m^2. With very high rates of placing, the assumption was made that the whole depth of the column is subjected to vibration and the Committee recommended that the maximum pressure be taken as 144 kN/m^2 at one third the height of the column above the base and varying linearly to zero at the top and the bottom (Figure 2.9).

This recommendation was based on unpublished field tests.

The Committee also recommended that the height of the column should not exceed 5.5m and if it does so, the column should be

Figure 2·8 : The relationship between maximum pressure and the rate of placement at 21°C.

▼ Teller's experimental results.
□ Stanton's experimental results.
△ Blaw-Knox's experimental results.
} all these results are for vibrated concrete.

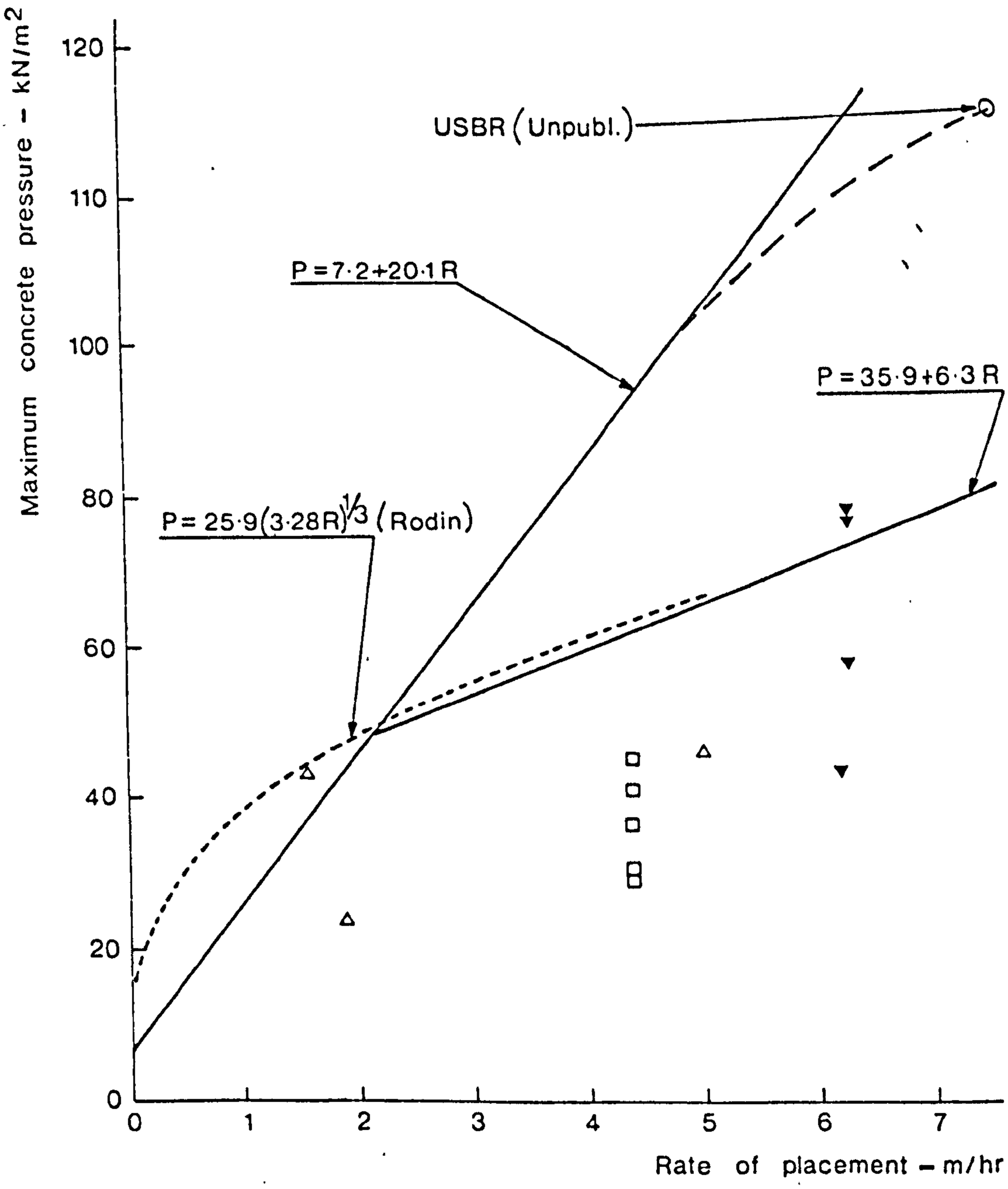

(adapted from the ACI[24])

Figure 2.9 : ACI Committee 622's pressure distribution for unlimited rates of pour in columns .

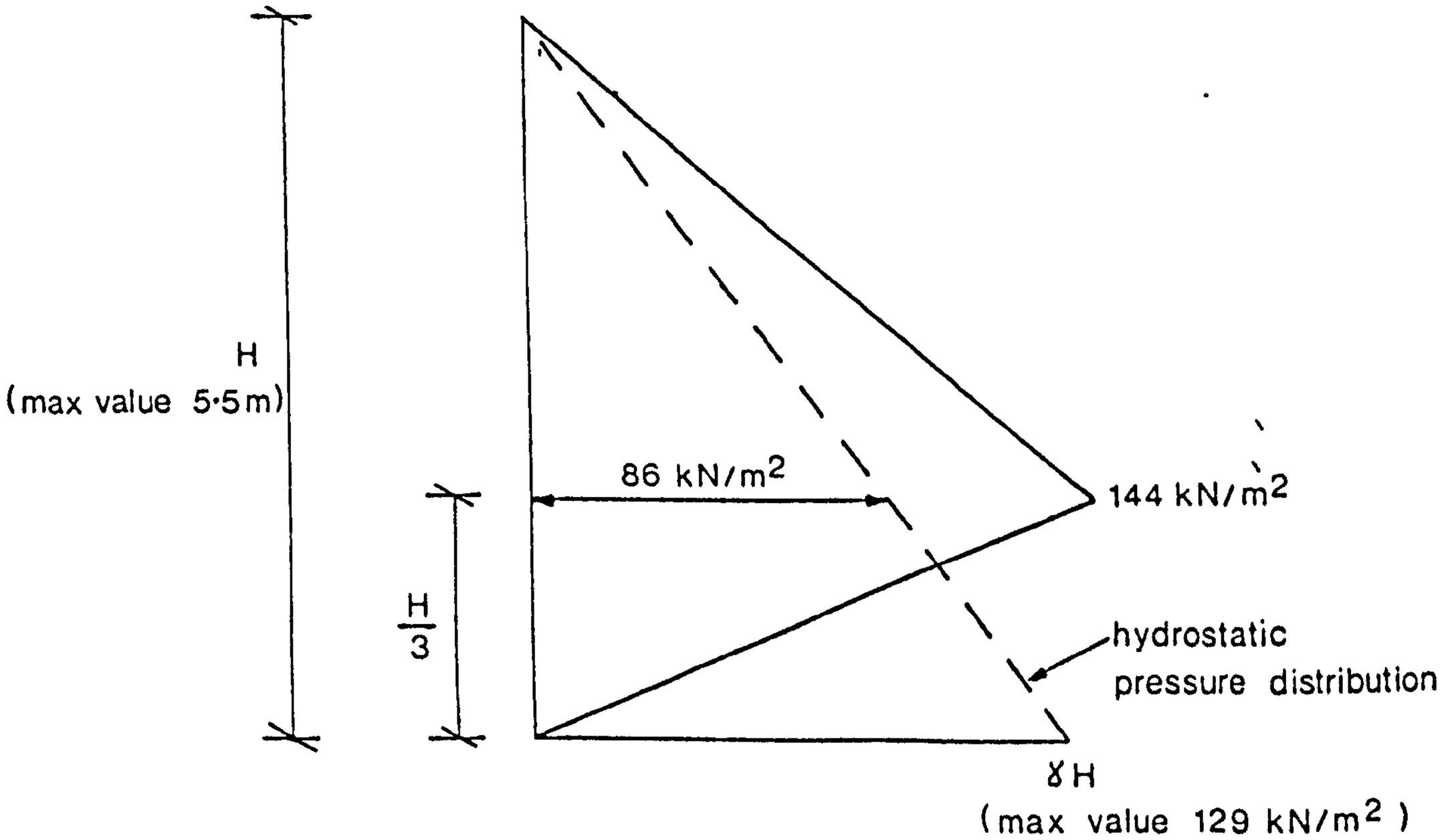

γ has been taken as 23·6 kN/m^3

concreted in 5.5m lengths with periods of at least two hours between concreting successive lengths. This was to permit some chemical stiffening to take place and thereby reduce the lateral pressure.

If these requirements are combined, Figure 2.9, it would appear that the ACI are recommending that columns be designed for pressures that are considerably in excess of the fluid pressure of concrete and that the formwork strength at the base of the column can be less than that at one third the column height. Recommendations for lateral pressure[40] based on this work, have ignored the depth of placement limitations and taken the maximum pressure as equation 2.24, 23.6 H or 144 kN/m^2 whichever is least.

Macklin in the discussion on the Committee's report[29] suggested a hypothesis that concrete pressure is terminated when the particles of aggregate make contact. It was argued that concrete consists of solids suspended in a grout which has liquid characteristics for a variable length of time. The solids having higher densities than the grout, sinks at a uniform rate. Starting from the base, the solids come to rest with a precarious balance, but vibration helps compact these solids into more stable configurations. Water and lighter particles move upwards.

The time taken for the solids to settle is a function of the quality and consistency of the cement paste. Chemical action could affect the settlement and Macklin quotes Teller[42] to show the small effect temperature has on pressure. (It should be noted that Teller used 200 mm square columns and a rate of pour of 6.1 m/hr.) Macklin also quotes Smith[43] to show that an increase in cement caused an increase in pressure whilst an increase in water showed a decrease in pressure.

The Committee did not disagree with Macklin's hypothesis and suggested that the reason why the solids were suspended for so long was the inability of the free water to escape. They also suggested that with time, chemical action would reduce the pore water pressure and thereby create particle contact. The Committee only partially agreed with Macklin's interpretation of Smith's tests and pointed out the differences between the pressure distribution produced by a concrete with particle contact and pore water pressure and that produced by a concrete that had the aggregates suspended in grout.

If chemical action is ignored (i.e. at high rates of placing) Macklin's hypothesis would make the maximum pressure a function of the height above the base. This dependency has not been observed. Furthermore loosely compacted coarse aggregate only occupies about 73 percent of the volume of concrete and therefore particle contact by coarse aggregate alone would result in segregation of the concrete to an extent not observed in practice.

Both Montgomery and Schjødt[29] raised the significance of variables not included in the ACI formulae. Montgomery discussed how form deflection could reduce the pressure and Schjødt updated his work with some simpler equations but no new concepts.

Since its introduction in 1958, the ACI method of calculating formwork pressures has been widely used for formwork design, and the fact that it has been changed so little over the years would indicate that it effectively achieved its objective to be a safe design method.

2.2.4 Ertingshausen

For his thesis[44], Ertingshausen contributed two pieces of work. The first was carried out at the Institute for the Pit and Quarry Industry of the Clausthal Academy of Mining and this showed that heavily vibrated concrete attained its maximum pressure more quickly than lightly vibrated concrete.

The second section of work consisted of monitoring the pressure development in nine structures. The concrete was similar at all of these locations and it consisted of natural gravel and sands with 300 kg/m^3 of OPC cement. The workability was described as being between stiff and plastic and the concrete had flow table spread values of between 328 and 378 mm. The densities ranged between 2380 and 2405 kg/m^3 and compaction was always by internal vibrator. The sheeting material of timber boards or panels was also similar for all the structures.

For the above conditions, Ertingshausen concluded that,

(a) the effect on maximum pressure of the rate of placing was most pronounced for low placing rates and at rates in excess of 4.2 m/hr.

(b) the head to achieve maximum pressure increased rapidly at first with increasing rates of placing.

(c) for placing rates above 1.5 m/hr the effect of temperature is negligible.

(d) setting time does not have the supposed effect of the longer the setting time, the higher the pressure. Ertingshausen's results showed that the maximum pressure was lower, the longer the period to reach maximum pressure (Figure 2.10).

Statistical analysis of the results gave the following equations for maximum pressure:-

For placing rates up to 4 m/hr

$$p_{max} = 30\ (R\ )^{\frac{1}{4}} \qquad (2.27)$$

and for rates of placing between 5 and 6 m/h

$$p_{max} = 36\ (R\ )^{\frac{1}{4}} \qquad (2.28)$$

To aid the calculation of the maximum pressure, Ertingshausen combined these equations in a design chart.

When Ertingshausen compared his results with the formulae proposed by Macklin, Rodin, Guerrin and the ACI, it was Rodin's and Guerrin's proposals for non-vibrated concrete that gave the closest estimates to the measured values. The ACI proposals varied so greatly from the measured values, that their use was not recommended.

It is of interest to compare Ertingshausen's results with the current British formwork design methods which were originally produced in the same period (Table 2.1). At slow rates of placing, they tend to underestimate the maximum pressure and at high rates of placing greatly overestimate the pressure. As British design methods are based on data obtained from site measurements, it appears that some significant variables are not being taken into account.

A discussion on the shape of the pressure envelope highlighted two main factors, shrinkage of the concrete and the flexibility of the

Figure 2.10 : The relationship between formwork pressure and time .

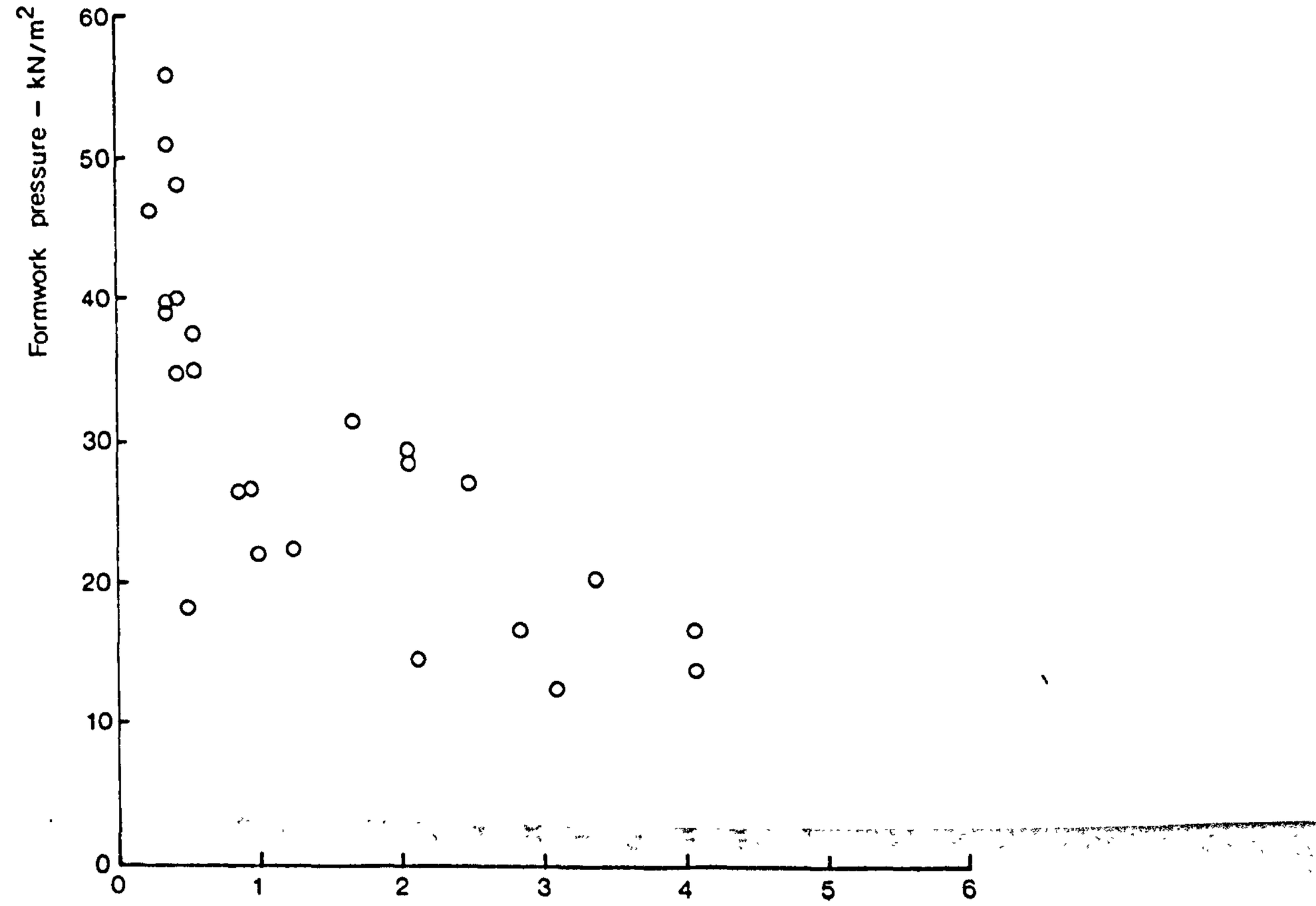

(after Ertingshausen[44])

Figure 2 ·11: Formwork pressure envelope

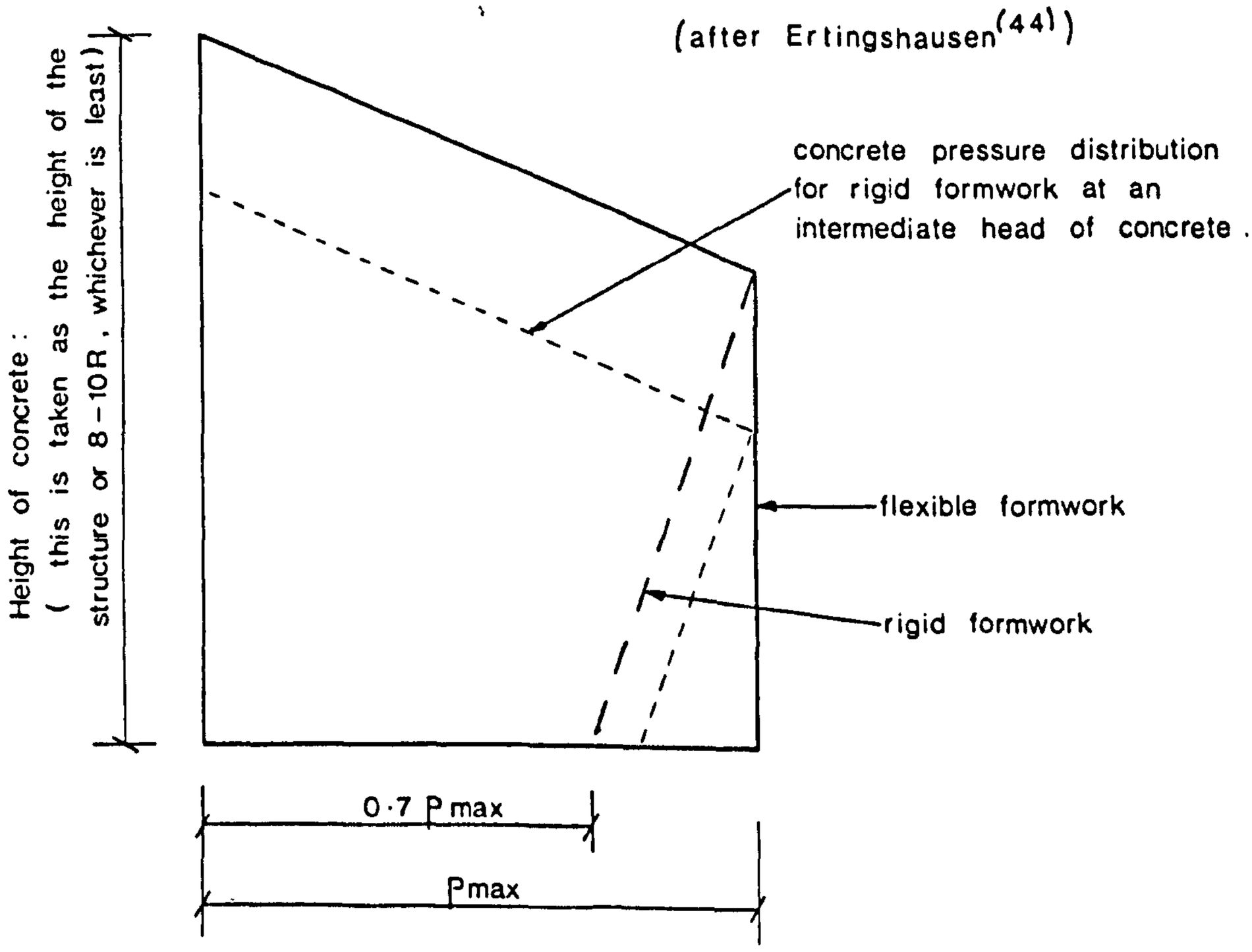

TABLE 2.1 Comparison of Ertingshausen's site measurements with British formwork design methods

Description of unit	Placing rate of time of maximum pressure m/hr	Temperature of concrete °C	Width of section mm	Ertingshausen site measurements kN/m^2	Pressures from the Concrete Society Design Chart[10] kN/m^2	Pressures from the CIRIA metric calculations[9] kN/m^2
Central pier of bridge	2.60	14.0	750	34	54	58
Abutment	0.19	10.8	700	16	9	10
Abutment	0.34	13.8	700	20	13	12
Abutment	0.50	18.0	500	27	13	13
Abutment	1.45	6.5	900	31	53	52
Circular column	5.0	14.9	1250 dia.	50	102	101
Circular column	5.8	15.8	1250 dia.	54	109	112
Wall	9.2	15.2	240	28	70	67
Wall	4.2	13.5	240	39	52	52

formwork. Ertingshausen had deduced that a linear contraction of 0.04 - 0.05 mm/m can occur within half an hour of mixing. With some examples, it was shown that for the same linear contraction of the concrete the reduction in pressure after the maximum would be greater for rigid formwork than for flexible formwork. Using the values for the reduction in pressure given by the site measurements, the pressure envelope given in Figure 2.11 was proposed.

2.2.5 Adam, Bennasr, and Santos Delgado

The authors reported[45] on an experimental programme in which a number of 3m high by 2.3m long walls were cast under controlled conditions. The variables investigated were:

type of cement (French types CPA, CPAC and CPAL*)
gradings of the aggregates
admixtures (retarders, plasticisers and air entraining agents)
width of section (120 to 400 mm)
rate of placing (0.33 to 8 m/hr with a standard rate of 3m/hr in the study of the other variables)
depth of vibration
effects of impact.

The walls were cast outside so there was not control over the ambient temperature, but in the 15 months of testing the temperature ranged from 0 to 25°C.

The conclusions on the influence of temperature, width of section and slump are summarized in Table 2.2. It is interesting to note that at a rate of placing ≤ 1 m/hr, the maximum pressure was independent of these variables and depended solely on the depth of vibration. At rates of placing in excess of 4 m/hr the maximum pressure was independent of the width of section and the slump, but increased as the temperature decreased. With rates of placing between 2 - 3 m/hr all three variables had a significant effect on the maximum pressure.

---

*CPA is a pure Portland cement whilst CPAL and CPAC include about $7\frac{1}{2}\%$ of a secondary active ingredient. With CPAL it is blastfurnace slag and with these particular CPAC's it was coal ash and brown coal ash.

The tests showed that the rate of placing was a significant factor, but not as significant as previous researchers had indicated. Nevertheless it was concluded that the rate of placing and setting time were the most significant factors and that the maximum pressure occurred at a depth equal to the product of the rate of placing and the setting time and that the concrete acted as a fluid up to this depth. From this basis, some simplified relationships for maximum pressure, Table 2.3, were produced. These ignored the affects of width of section and slump. This table has been modified from the original to include the influence of the type of cement. Depending on the type of cement, the basic table was modified by a coefficient, 0.9 for CPA, 1.0 for CPAL and 1.1 for CPAC. The cement types CPAL and CPAC are not normally available in the U.K. so Table 2.3 has included the 0.9 coefficient for pure Portland cements.

TABLE 2.2 Summary of the influence of temperature, width of section and slump on the maximum formwork pressure (after Ref.45)

Rate of placing	For a given concrete, the maximum horizontal pressure is a function of		
	temperature	width of section	slump
> 4 m/hr	As temperature decreases the pressure increases	Independent	Independent
2 to 3 m/hr	As temperature decreases the pressure increases	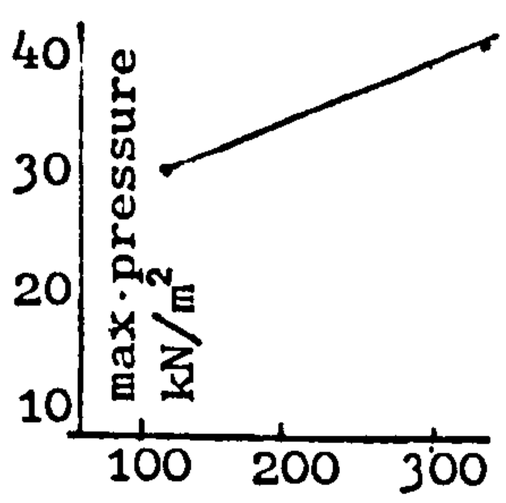	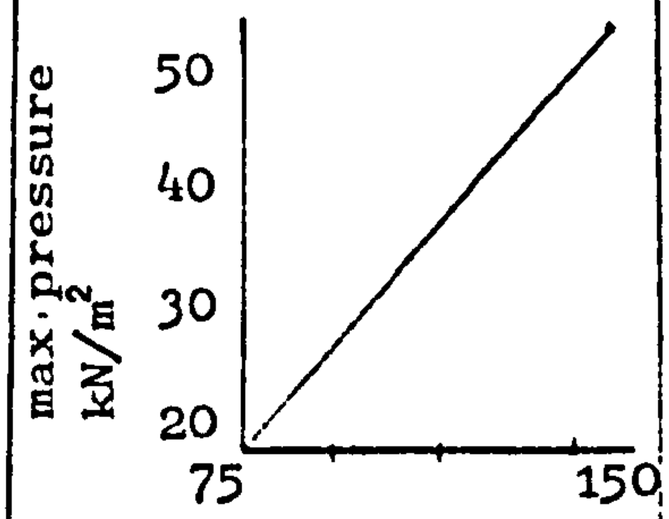
⩽ 1 m/hr	Independent	Independent	Independent

TABLE 2.3 Simplified design equations for pure Portland cement (Based on Ref.45)

Maximum pressure kN/m^2		Rate of placing < 2 m/hr	Rate of placing > 2 m/hr
Temperature	< 5°C	17.7 + 11.1R	36.2 + 1.8R
	15°C	17.7 + 8.8R	31.8 + 1.8R
	⩾ 25°C	17.7 + 7.6R	29.1 + 1.8R

The affects of admixtures were variable. The use of set retarder increased the formwork pressure with one exception; they found that using a plasticiser with a small retardation effect in CPAL cement concretes produced a lower pressure. The effect of air entraining agents was found to be small.

The research showed a clear relationship between the maximum pressure and the grading of the aggregate. Gap graded and crushed rock aggregates gave lower pressures. Some measurements were taken of the pore water pressure. The importance of pore water pressure was mentioned but little detail was given. Re-vibrating and deep vibrating were shown to increase significantly the pressure. At slow rates of placing (< 0.6 m/hr) the affect of impact was to produce a pressure greater than the fluid pressure of the concrete. At higher rates of placing this effect was not observed.

2.2.6 CERA (CIRIA)

A comprehensive study of formwork pressure was carried out by the C and C A for CERA[3]. The approach was based on site measurements using a specially developed pressure balance[46]. Over 200 measurements were taken on site and these were concentrated as far as possible on the extremes of either concrete temperature, rate of placement or section dimension. The heights of lift were not normally less than 3m and in a few cases were over 6m.

No attempt was made to produce a new theory on formwork pressure,

but some observations were made. It was observed that fresh concrete behaves almost as a liquid under the mobilizing influence of vibration. Deviation from the fluid pressure was said to be due to stiffening of the concrete and arching effects.

Stiffening was defined as the progressive increase in resistance to mobilisation and was due to chemical changes in the cement matrix and to physical interlock. As stiffening develops the concrete becomes capable of supporting the additional surcharge without increasing the lateral pressure. Most of the papers on formwork pressure have made similar assertions, yet the accepted physical laws relating stress and strain in solid elastic materials show that an increase in the compressive stress in one direction, increases the tensile strains in the other directions. These strains will produce an increase in loading on the formwork and therefore a head increase on already stiff concrete should still increase the formwork pressure. Small effect only!

The stiffening time was defined as the time at which maximum pressure occurred. For low and medium rates of placing this correlated well with Tuthill and Gordon[47] setting time relationships. These relationships were given as a function of the temperature and workability of the concrete. At high rates of placing the stiffening time relationships did not fit the pressure measurements. This was explained as being due to the insignificant influence of chemical stiffening compared with the time taken to develop physical particle contact. An empirical correcting term of 1.89 (2.44-R) to the basic lateral pressure equation gave improved correlation with the experimental results at high rates of pour. The final empirical equation was of the form

$$p = \frac{\gamma Rt}{1 + C\left(\frac{t}{T}\right)^4} + 1.89\ (2.44 - R) \quad \frac{kN}{m^2} \qquad (2.29)$$

where C = factor depending on the workability of the concrete and the continuity of vibration. Typically it ranges from 0.13 - 0.27 for structural concrete.

When t = T, equation 2.29 reduces to,

$$p_{max} = \frac{\gamma RT}{1 + C} + 1.89\ (2.44 - R) \quad \frac{kN}{m^2} \qquad (2.30)$$

As the section width narrowed, the maximum lateral pressure reduced and this was attributed to 'arching effects'. The arching effect was described as being due to friction between the form faces and the concrete. Insufficient data limited the analysis of the effects of arching to determining upper limits for arching ignoring differences in form smoothness, workability, level of reinforcement and temperature of the concrete. The upper limits were found to be represented by the equation

$$p_{max} = 15 + \frac{d}{10} + 3R \quad \frac{kN}{m^2} \qquad (2.31)$$

This equation held for values of d up to 450 mm but it was not possible to confirm if it held for values greater than 450 mm as in most of the 600 mm sections tested, chemical stiffening controlled the maximum pressure.

A warning is given that the arching limits do not apply to externally vibrated concrete. (In a more recent paper, Palanca[48] claimed that provided resonance is avoided, external vibration would not overload adequately designed formwork, but the definition of 'adequately' appears to be designed to take the full fluid pressure).

Figure 2.12. Pressure design envelope.

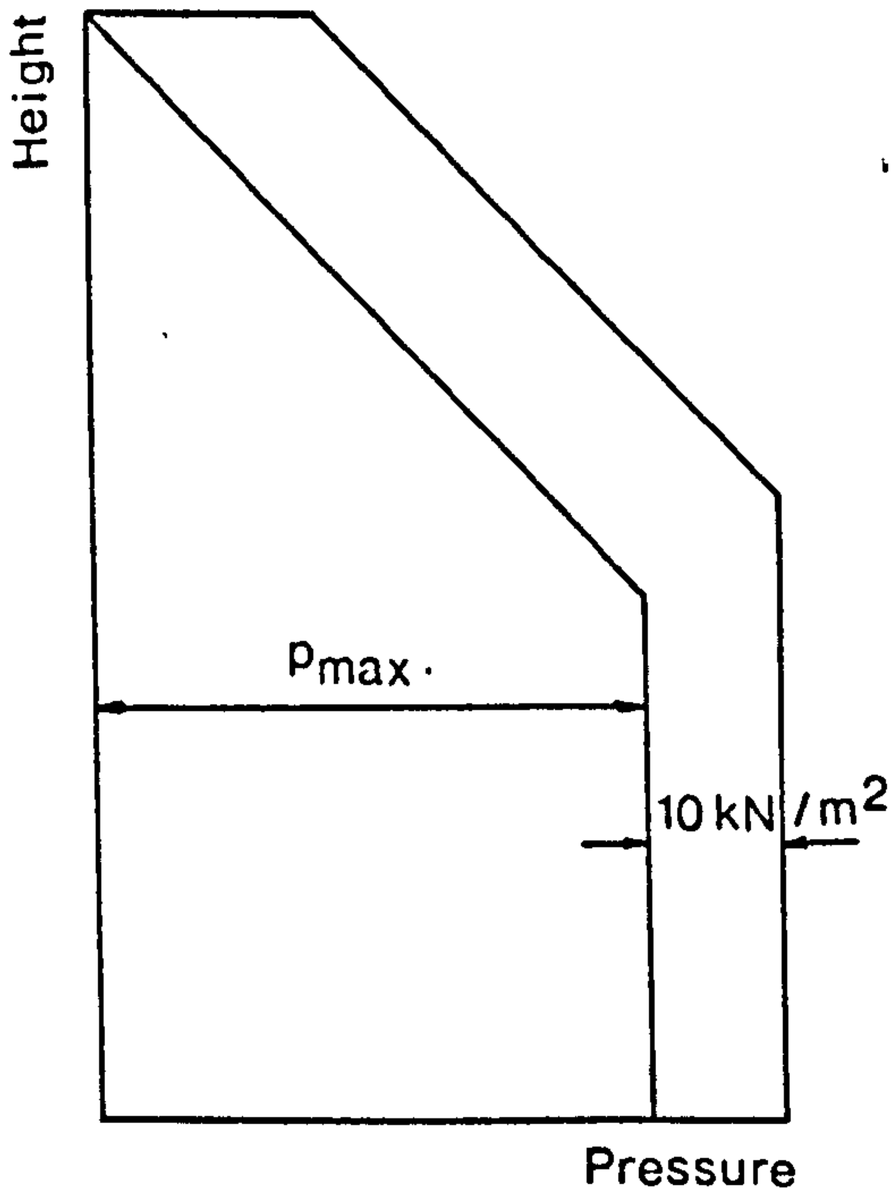

The site measurements gave a good indication of the order of impact loads as the concrete was discharged. Impact loads did not prove to be of critical importance because with shallow lifts they were rarely as great as the maximum lateral pressure produced by the static concrete. Nevertheless it was recommended that an allowance for impact loads of 10 kN/m^2 be applied as shown in Figure 2.12. In the more recent metric design

chart[9] the impact allowance is only applied when there is a free fall of over 2m and in the Concrete Society design chart[10], it is omitted.

As a simpler alternative to the calculation of pressure, various graphical aids[3,49,9,10] have been produced. They have all been based on the same data and should therefore give similar results. Table 2.4 is a check on their consistency. The formwork pressure was calculated from equation 2.30 (column 1), the Imperial design sheet calculations[49] (column 2), the Imperial design conch[49] (column 3), the metric design sheet calculations[9] (column 4), the metric design conch[9] (column 5) and the Concrete Society design graph[10] (column 6).

The calculated pressures are not consistent. Calculations based on equation 2.30 and the Imperial design equations[49] agree closely and these results also agree with the metric equations[9] except for wide sections at high rates of placing. In these cases the metric equations predict higher pressures. What is unusual, is that these design equations are not consistent with the accompanying design chart where stiffening of the concrete controls the maximum pressure. The design charts give pressures approximately 5 kN/m^2 less than the calculations. In some cases a similar inconsistency exists between the Imperial design equations and the Imperial design charts.

The Concrete Society pressure graph[10] agrees well with the metric design equations except at high rates of placing where arching controls. In these cases they predict lower values. In summary, the trend of more recent publications has been to increase the form pressure where stiffening of the concrete controls the maximum pressure and to reduce it with high rates of placing in narrow sections. No evidence is published to back up these changes.

2.2.7 Ore and Straughan

In a series of experiments[50], Ore and Straughan produced some useful information. A series of columns were cast using not only normal concrete, but a water reduced, set retarded concrete and a non-hydrating equivalent to concrete which contained fly ash. The aim of the series was to try and determine if only chemical stiffening controlled the lateral pressure.

TABLE 2.4 : Comparison of concrete pressures based on the CIRIA work

Rate of placing m/hr	Concrete temperature °C	Slump mm	Maximum concrete pressure kN/m²																	
			150 mm section Source of information						450 mm section Source of information						> 500 mm section Source of information					
			1	2	3	4	5	6	1	2	3	4	5	6	1	2	3	4	5	6
1	5	50	32	32	32	33	31	32	48	48	42	51	45	50	48	48	42	51	45	50
		100	32	32	-	33	-	31	60	60	-	63	-	62	67	69	-	71	-	70
	20	50	22	22	20	24	20	24	22	22	20	24	20	24	22	22	20	24	20	24
		100	30	31	-	33	-	32	30	31	-	33	-	32	30	31	-	33	-	32
2	5	50	35	35	35	36	34	32	63	63	63	66	64	64	91	92	80	96	90	95
		100	35	35	-	36	-	31	63	63	-	66	-	62	130	133	-	137	-	136
	20	50	35	35	35	36	34	34	39	39	35	43	39	43	39	39	35	43	39	43
		100	35	35	-	36	-	33	55	57	-	60	-	60	55	57	-	60	-	60
4	5	50	41	41	40	42	42	32	69	69	68	72	71	64	150	150	150	150	150	150
		100	41	41	-	42	-	31	69	69	-	72	-	62	150	150	-	150	-	150
	20	50	41	41	40	42	42	34	69	69	64	72	71	70	74	73	64	82	72	82
		100	41	41	-	42	-	33	69	69	-	72	-	67	105	108	-	115	-	115

Note: This table assumes tall sections (i.e. the maximum pressure is less than γH)

The experiments showed that the physical processes of aggregate interlock and arching were the first factors to limit pressure at the rate of placing of 1.5 m/hr. At this rate of placing hydration played a secondary role. The water reduced and retarded concrete showed a slightly lower maximum pressure than the normal concrete, but it could be re-vibrated for a longer period. The author showed how re-vibration of the plastic concrete could significantly increase the lateral pressure.

2.2.8 Ritchie (and McDowall)

Ritchie's work can be conveniently considered in two parts, the pilot study as progressively reported in 1962[34,35] and 1963[36] and the in depth study researched with McDowall and reported in CIRIA Project Record RP64[51].

Ritchie used a Laboratory experimental approach and in the pilot study supplemented this with a few site readings.

The pilot study looked at the following variables,

1. Mix proportions
2. Workability
3. Method of compaction
4. Rate of pour
5. Formwork size.

Ritchie was unable to treat temperature as a variable in his Laboratory, so he kept the temperature at a constant 20°C.

Pressure readings were taken, with a specially developed gauge, in 152 and 234 mm square columns of rigid, waterproofed timber formwork. The contribution of this pilot study was to show that the concrete pressure in small sections were significantly reduced due to the 'arching effects'. Workability aids and rounded aggregates tended to reduce this arching effect.

Ritchie also showed that the mix proportions also had a significant effect on the concrete pressure. Richer mixes and higher workabilities (in this case simply produced by increasing the water

content) gave substantially higher pressures.

The initial pressure curve was shown to follow the fluid pressure and was stated to be the result of the concrete being affected by vibration. A point not made by Ritchie in this or the later work, was the difference between the depth of vibration (limited to 300 mm) and the depth to which the concrete followed the fluid pressure line. Part of his theory of formwork pressure relies on vibration being transmitted to these relatively deep depths.

In the substantial study with McDowall[51], the meaning of workability was studied. They reasoned that this all embracing term should be split into the characteristics of stability, compactability and mobility. Stability is a measure of the concrete's ability to resist segregation and bleeding whilst compactability is a measure of the ease with which the concrete is compacted. This factor can be easily graded by the compacting factor test. Mobility, the inverse of stiffness, is a measure of the flow characteristics of the concrete and is related to the viscosity, cohesion and most importantly, the angle of internal friction of the concrete. This characteristic according to Ritchie is the one that most affects the concrete pressure.

The stiffness of concrete is formed by both physical and chemical processes, but the initial stiffness is only a function of the physical properties. These are the concentration and angularity of the aggregate, the water/cement ratio and the surface area of the cement. Leaner mixes are initially stiffer than richer mixes, but as chemical stiffening starts to take place (2 - 3 hr at 20°C), a reversal of the relative stiffness takes place.

Having reasoned that mobility (stiffness) was the most important characteristic of workability with regard to formwork pressure, it was studied in detail by means of a vane test. After starting with basic tests, attempts were made to simulate internal vibration, re-vibration and head of concrete (by means of surcharge loads). Shear strengths were found to increase with re-vibration and with increased surcharge loads, but when the numerical values of shear obtained from these tests were substituted in the Rankine-Bell lateral pressure equation (Table 2.5), the free standing height of concrete

TABLE 2.5 Theoretical heights to which various mixes could stand with a vertical face.

Mix	Heights, m, to which fresh, compacted concrete can stand with a vertical face based on calculations from:		
	.Vane test[51] McDowall and Ritchie	Powers[52]	Triaxial test[53] Ritchie
Cement paste	1.05	0.06	-
1:2 mortar	1.25	0.13	-
1:3 concrete (high workability)	0.86	-	2.96
1:3 concrete (medium workability)	1.92	-	3.63
1:3 concrete (low workability)	6.53	-	1.13
1:6 concrete (low workability)	6.37	-	8.54
1:6 concrete (medium workability)	2.62	-	8.54

was found to be far in excess of that obtained in practice.

McDowall and Ritchie suspected that their vane test did not measure basic shear strength and that volumetric dilatant action was occurring. This is where the advancing blades force the aggregate particles into contact thereby greatly increasing the shear strength.

In their initial assessment of properties that affected concrete stiffness, the rate of test was not considered significant. Overriding this initial assessment, some further tests were carried out at low rates of shear (Figure 2.13). These showed that shear strain was time dependent for the first 5 seconds, but not signficantly so thereafter. The anomalous first reading at low rates of shear was explained as being due to the cement paste exhibiting viscous flow until the particles approach each other and increase the shear resistance of the concrete. This was called rheologically dilatant action. Testing at these very low rates of shear was claimed to give better representation of the true stress-strain characteristics of concrete in the initial stages of hydration.

With the background work complete, McDowall and Ritchie turned to the problem of formwork pressure. At first they tried to simulate the head of concrete by using surcharge loads on a short section of column, but when these results were compared with CERA Report No 1[3], their results were up to 60% lower than the site measured values. The differences were explained as being due to no re-vibration and the aggregate particles tending to take more of the superload than the concrete as a whole. In order to overcome this last factor a deeper mould (500 mm approximately) was tried, but still without success. They concluded that formwork pressure could not be simulated by surcharge loads.

This work did produce some useful and unexpected results (Figure 2.14). With rich concretes, the higher the workability, the higher the maximum pressure, but with leaner mixes the reverse was found to apply. No satisfactory explanation was given. In both cases increased workability was obtained by increasing the water content, and if in the case of the leaner mixes this significantly changed the viscosity of thefluid between the particles, a pore water approach might have explained the observed results.

Figure 2.13 : Stress strain relationship for a 1:3 OPC / gravel concrete.

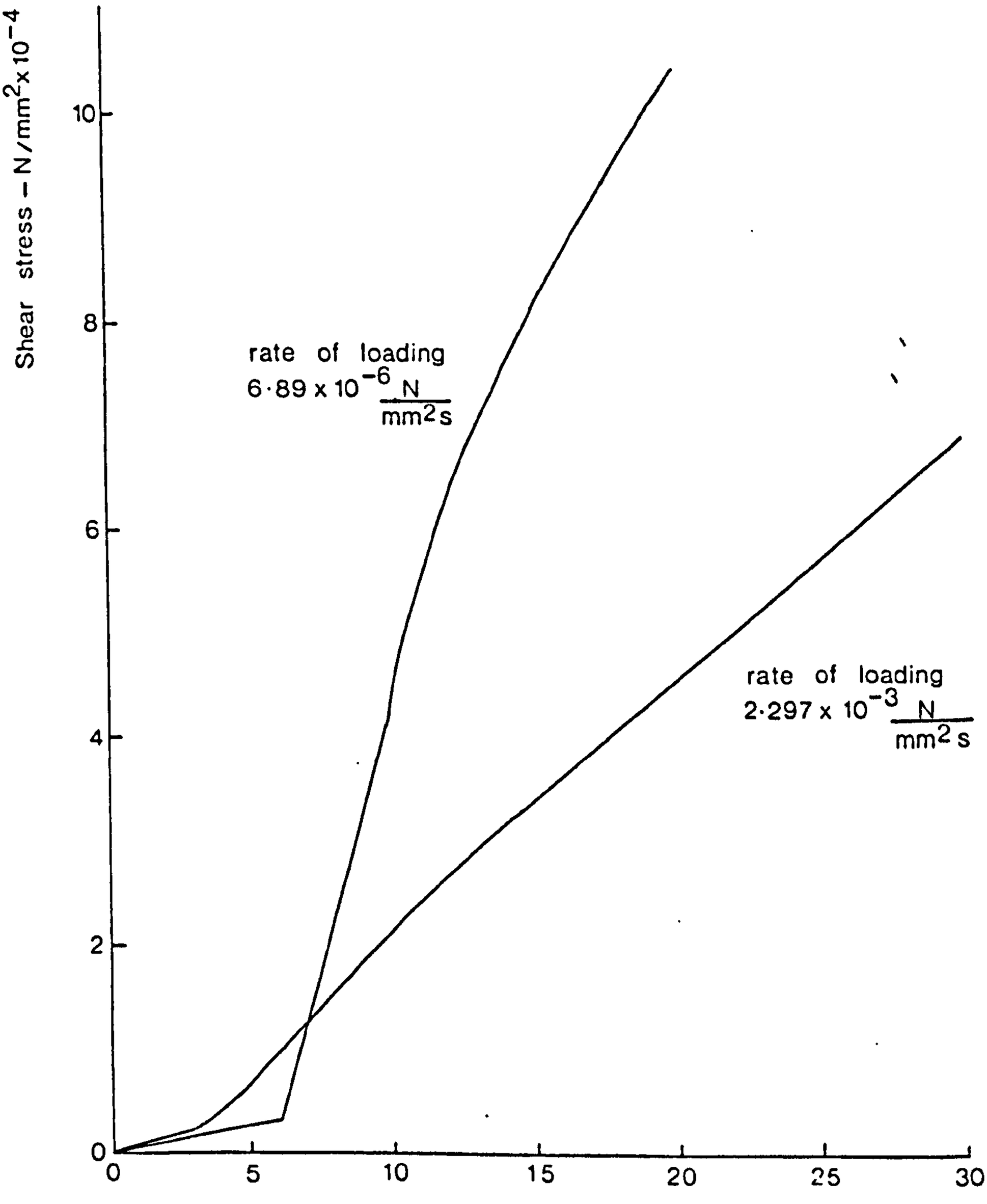

Test started when the concrete had an age of 30 min.

Figure 2.14 : Effect of workability on lateral pressure in a simulated pressure test equivalent to a rate of placing of 5·4 m/hr .

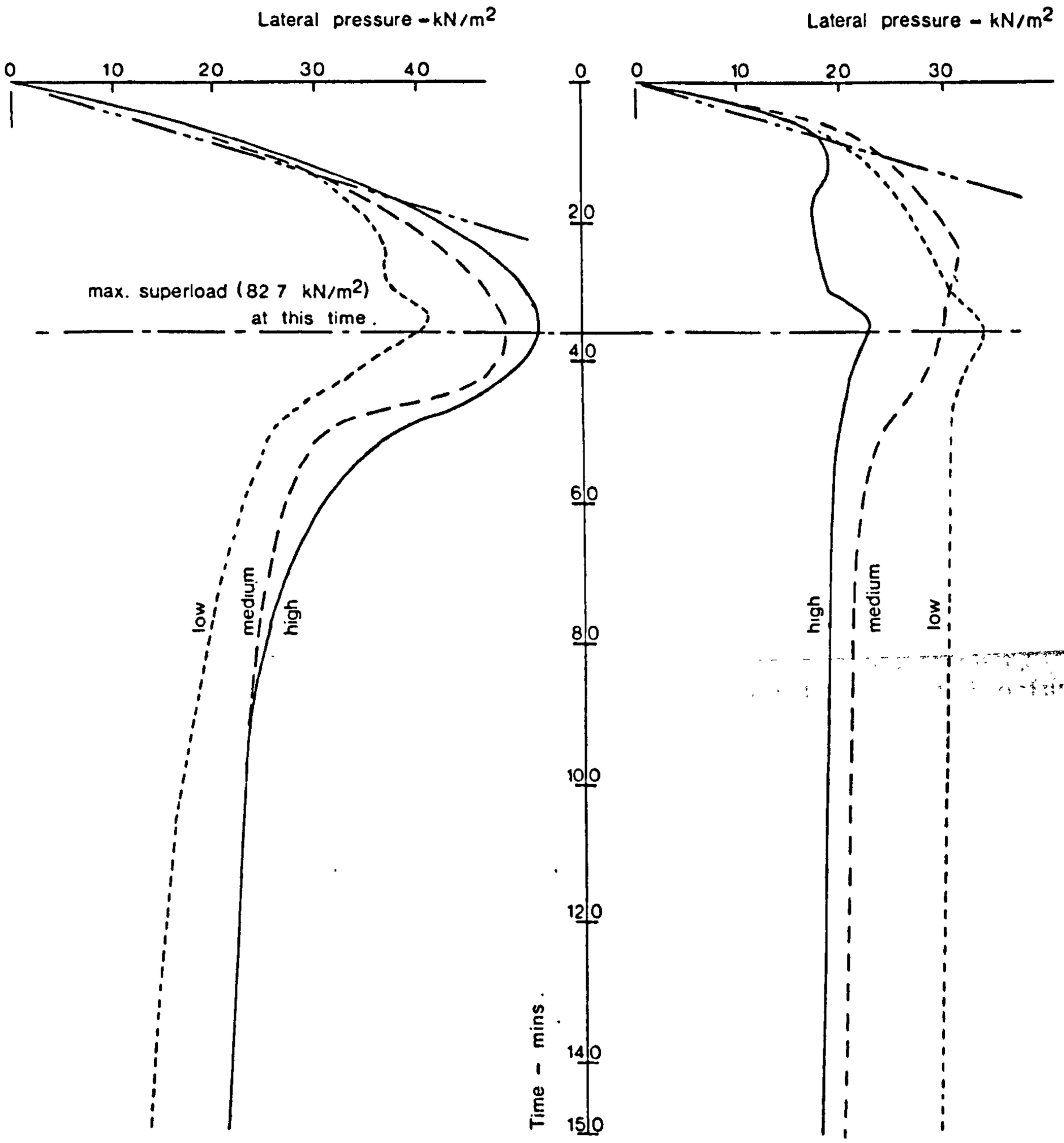

(after McDowell and Ritchie[51])

With the failure of their simulation technique, work was continued using full sized columns. The new conclusions from the main investigation were that,

1. an increase in slump does not necessarily produce an increase in lateral pressure

2. an increase in vibration over 25% of the placing time does not necessarily produce an increase in lateral pressure

3. there were large differences in lateral pressure for concretes of equal slump but different cement-aggregate ratios

4. an increase in angularity at constant w/c ratio reduces the lateral pressure

5. an increase in the surface area of the cement at constant w/c ratio, makes little difference with rich mixes, but increases lateral pressure with lean mixes

6. the correction factor F, in CERA report No 1 was considered to cover too wide a range and predict greater reductions and increases from the standard, than those observed by McDowall and Ritchie.

On the basis of their investigation, the authors gave their concept of formwork pressure. The process was described by considering the changes in a single slug of concrete which has successive slugs of concrete placed above it. When the slug is first placed and vibrated it acts as a fluid of density equal to that of the concrete. When the vibration is withdrawn, the concrete congeals and regains its viscosity. The cohesion of the concrete balances most of the shearing stresses and the aggregate remains suspended in the cement paste matrix.

When a further slug of concrete is placed and vibrated on top of the one under consideration, transmitted vibration and superload will cause the first slug to deform plastically and produce hydrostatic pressure. During this period some particle contact will be established.

Eventually further slugs of concrete and transmitted vibration will cause the formation of a continuous intergranular structure using

all the solid constituents. Lateral pressure may still be induced by pore fluid. As the shearing stresses are transferred to the intergranular structure, a compression of the volume occupied by the particles occurs resulting in the expulsion of interstitial cement paste and water, and transference of vertical pressure to the form walls. (The authors limited the use of the term 'arching' to cases involving non-rigid formwork).

Once maximum density has been attained, further load causes a dilation of the structure and a volume increase. This causes the pore fluid to be drawn back into the interstitial spaces reducing both the lateral and vertical pressures. This concept appears to defy the basic laws of physics, as the mass of concrete has remained the same, yet the external forces have been reduced. The authors might have meant that this difference in load is taken vertically in the forms, but then it becomes necessary to accept that both a volume decrease and increase result in transference of vertical pressure to the form walls. Further lateral pressure reductions are caused by thixotropic regain and the formation of chemical bonds.

The theory, like all the previous theories, has its weaknesses and lacks quantitative data, nevertheless Ritchie and McDowall have made a useful contribution to our knowledge of the factors affecting formwork pressure.

2.2.9 Murphy

Murphy[54] carried out a literature survey on the pressure exerted by lightweight aggregate concrete. There was very little work specifically with lightweight concrete[55] and Murphy found little experimental evidence to support the design equations that included the density as a variable.

Based on theoretical grounds and engineering judgement, Murphy recommended that when using lightweight aggregate concretes, the pressure obtained from the equation for normal density concrete could be reduced proportionally to density.

In the data collected for the CERA work there was one set of results for a Lytag concrete. The maximum pressure was 29 kN/m^2 and the

calculated pressure using this method was 36 kN/m^2 (arching was the controlling factor), so, in this case, the method proved to be satisfactory.

2.3 ANALYSIS OF EXISTING SITE PRESSURE MEASUREMENTS

2.3.1 Introduction

One of the most noticeable features of the literature survey is the lack of published site pressure measurements. Ertingshausen[44] is the only author to give a complete set of results. CERA[3] gives a correlation between the calculated and actual pressures, but the number of points plotted is substantially less than the number of readings taken.

A study of actual pressure measurements would be an extremely valuable way of checking the significance of the postulated variables and it was fortunate that access was available to the data used to compile CERA Report 1[3] as this was by far the largest programme of site measurements. In addition to these data, there were the records from a number of columns cast subsequently at the Cement and Concrete Association using pumped concrete at high rates of placing which have not been previously reported. Combining these results with those of Ertingshausen represents a large proportion of all the relevant formwork pressure measurements that have ever been recorded.

2.3.2 Presentation of the data

Current UK design methods[3,9,10] take the following variables as having a significant affect on the maximum formwork pressure:

rate of placing,
width of section,
slump of the concrete,
concrete temperature,
and, continuity of vibration.

This is assuming that the height of lift is sufficient for the maximum pressure to be reached. As some of the data were used to deduce that these were significant variables and as only the factors that have been recorded can be analysed, these divisions represented a reasonable

starting point.

Taking a typical pressure v time graph for a long wall, Figure 2.15, the effects of placing concrete in layers is demonstrated. Frequently the maximum pressure occurs during the placing of a layer of concrete and if there is a long delay before the next layer is placed, determining the rate of placing is difficult. For example, if the rate of placing up to point A had been continued would the pressure have gone higher ? The relevance of the rate of placing after point B seems doubtful. The concept of an equivalent rate of placing i.e. the uniform rate of placing that gives the same horizontal pressure, is a useful idea but difficult to quantify. It lies between the limits of the rates of placing to points A and B but where it lies in this range cannot be defined. In the summary of data, Figures 2.16, 2.17 and 2.18, when this problem occurs the rate of placing has been indicated as a range between the rates to points A and B. In the calculations used to produce Figure 2.19, the rate to point A is used as this is the assumption that gives the highest calculated pressure.

The reasoning behind the CERA continuity of vibration factor is difficult to accept. The wall in Figure 2.15 would have a low continuity of vibration, but consider the method fo concreting walls. The concrete is vibrated at the point of discharge but both the point of discharge and the vibration move along the wall and back as each layer of concrete is placed. The vibrator is inserted into the previous layer to re-mobilise the concrete and avoid cold joints. The time in which the concrete is subjected to vibration is normally more than sufficient to fully compact the layer of concrete and re-mobilise the top of the previous layer. The time of vibration per unit volume is comparable with small columns being placed at rates in excess of 40 m/h with 100% continuity of vibration, so why should there be a difference due to vibration between the two sections? One can appreciate that there would be a difference between poorly compacted concrete and well compacted concrete, but engineering judgement would suggest that the majority of the concrete monitored by CERA could be classified as being adequately compacted. Because of the doubts about the CERA method of assessing the effects of vibration, continuity of vibration has been omitted from the summary of data, but was retained in the statistical analysis of the data and the calculation of pressure by

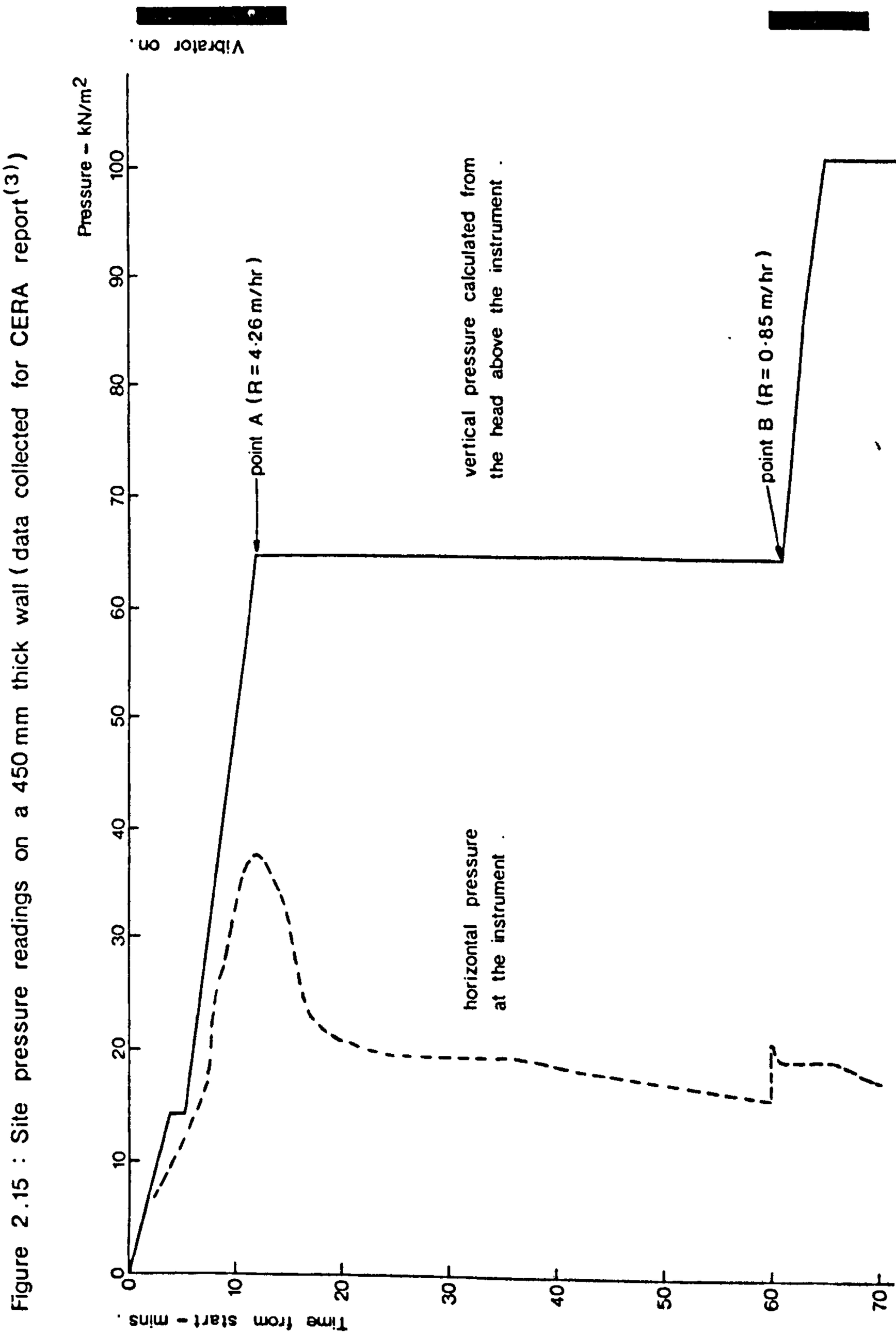

Figure 2.15 : Site pressure readings on a 450 mm thick wall (data collected for CERA report[3]) the concrete was placed at 16 °C with a 25 mm slump.

the CERA method.

The summary of the data is in the form of a series of graphs of maximum pressure on a linear scale against rate of placing on a logarithmic scale. The intersection of these factors has been marked by the temperature of the concrete. The remaining two factors, width of section and slump, have been shown by grouping the results and plotting them on separate graphs. The sections were grouped into widths of $\leqslant$152 mm, 153 - 305 mm, 306 - 457 mm, 458 - 610 mm and $>$610 mm and the slumps were classified as low ($\leqslant$25 mm), medium (26 - 74 mm) and high ($\geqslant$75 mm). There were only four results for walls under 152 mm and these were placed at rates between 0.9 - 2.0 m/hr, were all medium slump, had temperatures of 11°C $\pm$ 1°C and gave maximum pressures of 30, 31, 32 and 39 kN/m^2. The remaining twelve combinations of width and slump were plotted separately in Figures 2.16, 2.17 and 2.18. There were a few results available for cements other than ordinary Portland cements and these have been presented separately in Table 2.6. In Figure 2.19 these results have been indicated by an '*' and in all cases the criterion controlling the design pressure was stiffening.

These data were used in an attempt at curve fitting using a regression analysis. There was no success in producing any statistically significant relationships and from a study of the scatter of results in Figures 2.16 to 2.18, the result is not surprising. What is surprising is the good correlation between the calculated and measured pressures obtained by CERA[3] as CERA used some of these same data. To resolve this question, all these data were analysed by the CERA method and a graph of calculated against measured pressure was produced, Figure 2.19. In the analysis, the actual measured rates of placing, degree of vibration, concrete temperatures and slumps were used, whereas in a normal design situation estimates have to be made for these factors. Assuming that these would normally be conservative estimates, this had the effect of putting an additional factor of safety into the design which is not shown in Figure 2.19. As previously mentioned, the other difference in the method of analysis is the use of the rate of placing up to the maximum pressure rather than an overall rate.

Figure 2 16 · Summary of formwork pressure measurements for low slump concrete.

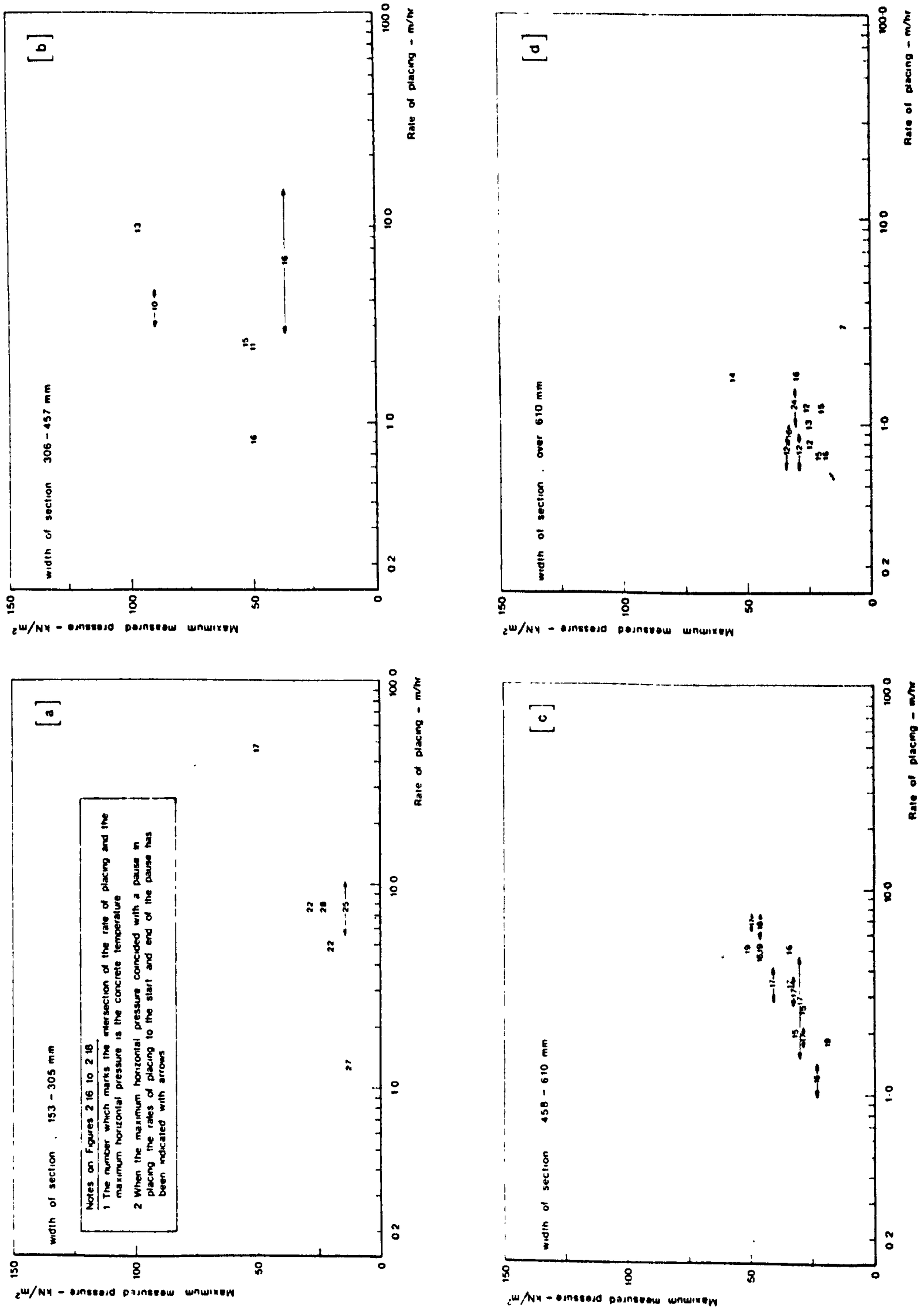

Figure 2.17 : Summary of formwork pressure measurements for medium slump concrete .

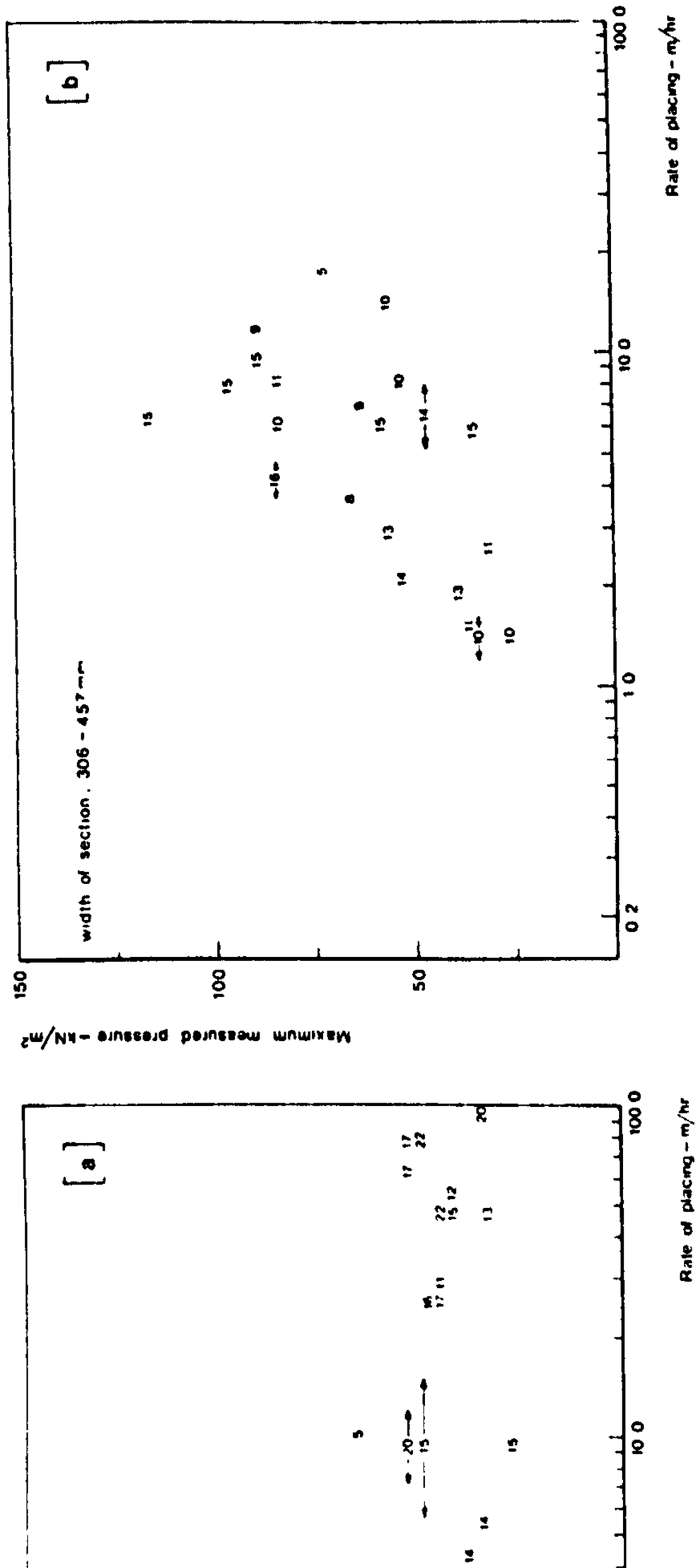

Figure 2.18 : Summary of formwork pressure measurements for high slump concrete .

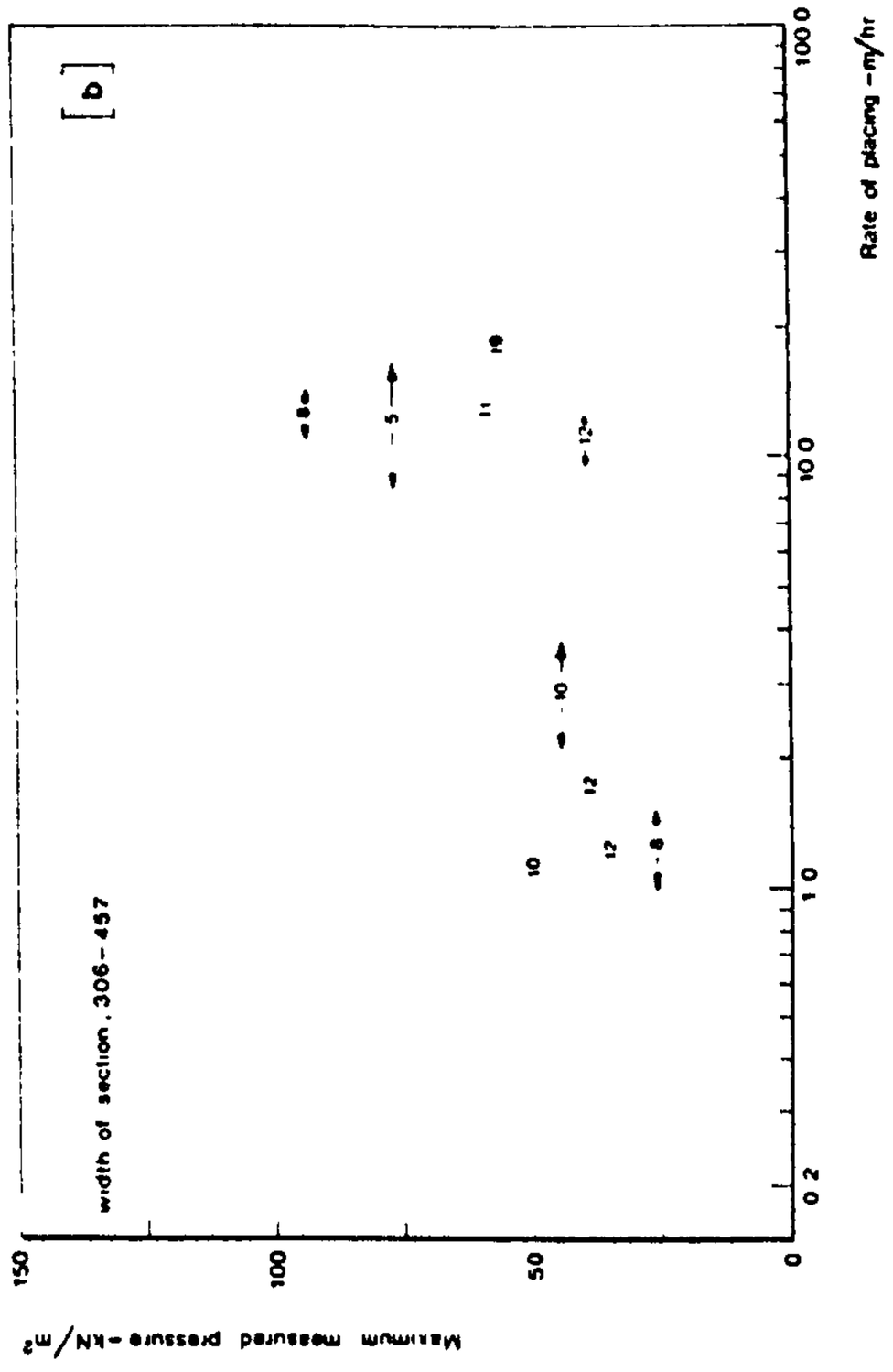

TABLE 2.6 Summary of site pressure measurements for concretes containing cements other than OPC.

Cement	Rate of placing m/hr	Temperature °C	Slump	Maximum pressure kN/m^2
Traβzment	1.4	20	Medium	66
Traβzment	1.4	20	Medium	57
Traβzment	1.6	20	Medium	52
BFPC	0.6	10	Low	31
BFPC	1.0	5	Low	40
BFPC	1.0	10	Low	29
BFPC	1.0 (0.6)	16	Low	37
BFPC	1.2 (1.0)	22	Low	35
BFPC	0.6 (0.5)	5	Low	27
BFPC	0.7	10	Low	55
BFPC	0.8	10	Low	31
BFPC	0.8	20	Low	32
S.R.	1.9 (1.5)	13	Medium	61

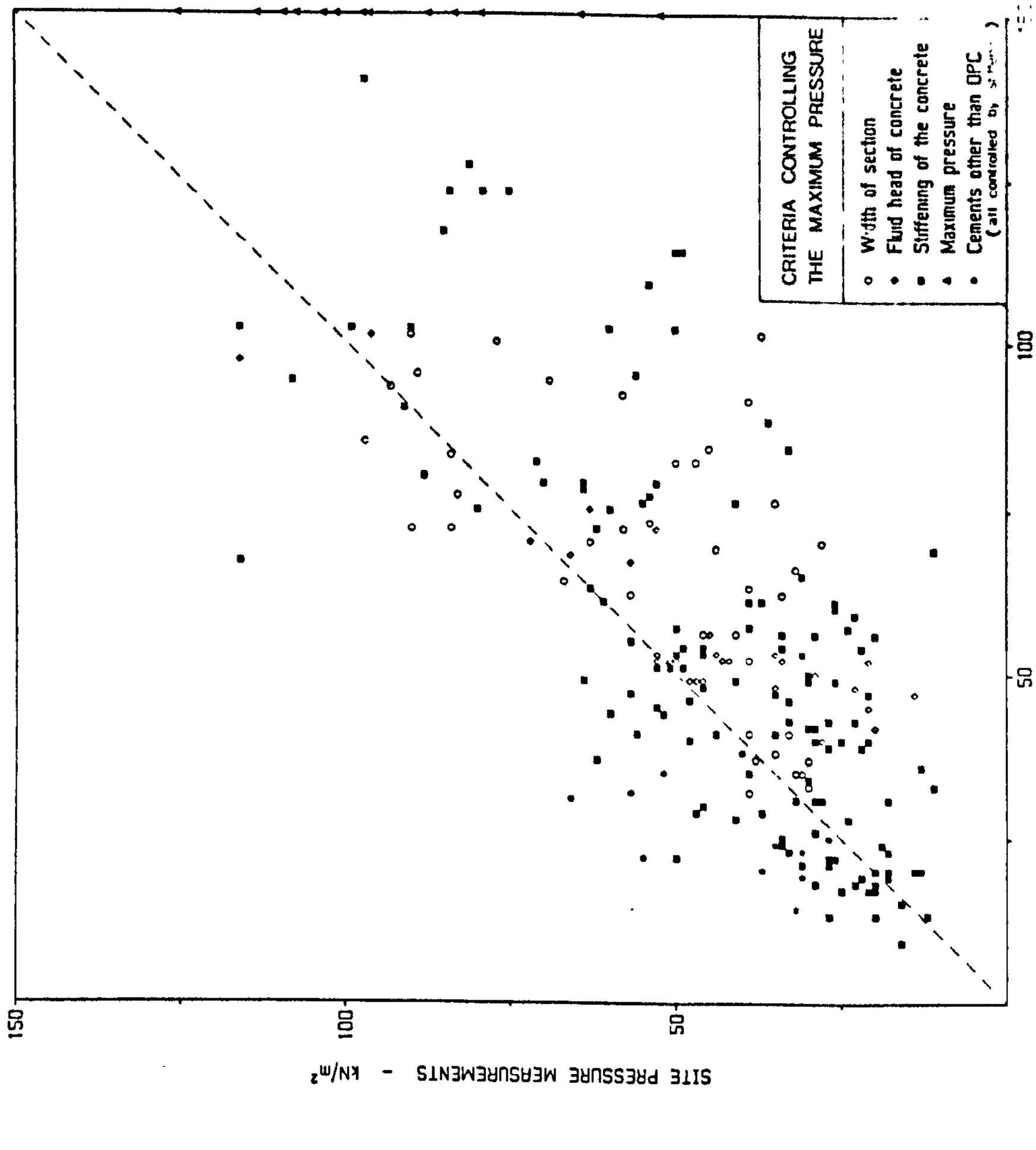

Figure 2.19: Comparison of calculated and measured pressures

2.3.3 Discussion of the results

The most significant observation of these data is the scatter of results and the lack of a clear pattern showing the influence of the normally accepted factors. The scatter of results indicates that some major variables have not been monitored. In the monitoring of the Cement and Concrete Association columns, a number of instruments were used on the same column and even for the same section, the scatter of results was high. For example in one column, the maximum pressure ranged from 75 to 125 kN/m^2, (These figures have ignored the upper level of gauges which effectively followed the fluid head and there were no grounds to doubt the reliability of the gauges). These results indicate that the missing variables are not simply the result of mix design or formwork type and stiffness, but depend on the location of the gauges and/or, localised variations in the concrete mix.

The regression analysis showed that none of the normally accepted variables were statistically significant. A study of Figures 2.16 to 2.18 shows that whilst the overall picture does not show any definite form, within some of the graphs, trends do appear. The low slump concretes tend to create lower maximum pressures than the medium and high slump concretes, but there appears to be little difference between the medium and high slump concretes. There is no evidence of the expected temperature variations in which low temperatures give higher pressures when all other variables are constant. In several of the graphs there appears to be a distinct influence on the maximum pressure by the rate of placing. In Figures 2.17(a) and 2.18(a) a relationship could be masked by the fact that all the results at high rates of placing were for short columns which were effectively giving the fluid pressure of concrete. If these had been taller, a higher pressure might have resulted and a clearer relationship between the rate of placing and maximum pressure displayed. In wide sections with high workability concrete, rates of placing above 1.5 m/hr appear to have no influence on the maximum pressure. The section width appears to have an influence on the maximum pressure up to a width of 305 mm even with an allowance being made for the short column results. There is no conclusive evidence to indicate that width of section influences the pressure for wider sections.

The conclusion from the study of these data is that formwork design charts have been based on what the authors believe from their theoretical models to be the main variables and this has overridden pure statistical analysis of the data. This approach cannot be condemned providing the design method predicts safe upper limits for maximum pressures. To test the reliability of the CERA design method is the objective of Figure 2.19.

If the method of calculation were perfect, all the results should fall on a 45° line and if it is a safe method, all the results should fall on, or below the 45° line. This latter requirement is effectively achieved by the CERA design method except for some of the low calculated pressures where the stiffening criterion controls the maximum pressure or where cements other than OPC have been used. As a proportion of the calculated pressures, the degree of overload can exceed 100%, yet the number of reported failures is small. A check on the results gave no grounds to question the validity of the readings. A possible explanation of these observations lies in the fall off in pressure after the maximum compared with the design assumption of the pressure remaining at the maximum value. Most of the pressure readings were obtained using the C and C A pressure balance and this tends to predict a higher rate of fall off in pressure than other instruments[3]. The reason for this will be described later in this thesis. When the bolt loads were measured as well as the pressure, the unpublished data showed that when the pressure gauges indicated no load, the load in the bolts had only reduced by 13%. Therefore these data cannot be used to assess the reduction in pressure after the maximum.

Figure 2.19 shows that at low rates of placing BFPC and Traβzment* concretes tend to give higher pressures than pure OPC concretes. There were no results available for high rates of placing and the few results that make up this group are given in Table 2.6. It is interesting to note that both of these cements have the same setting time specification as pure OPC.

---

*Traβzment is a Portland cement with some natural pozzolanic material. It is specified in DIN 1164 Blatt 1.

Figure 2.19 also confirms the maximum pressure limit of 150 kN/m^2. In no case did the pressures exceed this value, the maximum recorded being 125 kN/m^2. For walls, ACI have a lower maximum pressure of 100 kN/m^2 [41] which if shown to be a reasonable assumption, could lead to economy of design. Figure 2.19 unfortunately neither verifies nor disproves this assumption. The high pressure results are all for columns although six of the columns would be classified as walls by the ACI system. Three of these columns exceeded the 100 kN/m^2 pressure but by less than 10%. As there were so few examples in which the calculated pressure would have been controlled by a 100 kN/m^2 limit, Figure 2.19 can not be used to prove the ACI assumption.

2.4 DISCUSSION

In drawing together the literature and data survey, the problem is one of finding areas of agreement between authors and between authors and the data. For a subject with such an extensive literature, there are very few proven facts. Even the complete shape of the pressure v time envelope is not known for certain. There is agreement that the horizontal pressure starts by following the pressure of the fluid weight of concrete and, given a sufficient height of lift, it then deviates from this to reach a maximum value. The extent to which the pressure decreases after the maximum is an area where there is not agreement. CERA[3] claim that with rigid formwork the reduction in pressure below the maximum is small, but with flexible formwork there is a redistribution of pressure and it decreases below the maximum. Ertingshausen[44] claims the complete opposite - a reduction in pressure with rigid forms but not with flexible forms. This was reasoned from the effects on pressure of shrinkage of the concrete.

The association between the concrete acting as a fluid only whilst it is being influenced by the internal vibration has general agreement[3,51]. Internal vibrators are either 'parallel' or 'pendulium' action vibrators[56], but in both cases the main compacting effect is radial and there is very little effect beyond the tip of the poker. This would imply that the effective depth of vibration is approximately equal to the depth to which the poker is immersed (assuming it is held vertically), but this is substantially less than the depth to which the concrete continues to give fluid pressure[36].

Either the generally agreed relationship is incorrect or there is some way in which the vibration is transmitted to these lower depths. This latter possibility is unlikely as if for example, the vibration was transmitted into the form which then transmitted it back into the concrete, the effect on the formwork would be obvious and have been reported.

Transmission of vibration via the reinforcement is also unlikely as there would always be a zone in which the vibrating bar is capable of breaking the bond, but not fluidizing the concrete. As the zone progresses up the bar, the result would be unbonded steel. This phenomenon is not normal and it is possible to get this difference between the depth to which the concrete acts as a fluid and the effective depth of vibration in non-reinforced sections[34]. This leaves the most probably explanation as being that this generally assumed relationship is not correct.

Given a sufficiently high lift of concrete, there is substantial evidence to prove that the concrete reaches a maximum value which is less than the fluid weight of concrete. The reasons proposed for this maximum pressure have been,

(i) the concrete is no longer influenced by vibration,

(ii) the concrete sets,

(iii) the concrete develops a sufficiently high shear strength that the loads from further increases in head are taken vertically.

The grounds for questioning the first factor have already been given. After the concrete has reached a peak pressure, it is still possible to increase this pressure by deep re-vibration[50]. This is an abnormal procedure and would not form the basis for a design pressure.

The theory that the maximum pressure is controlled by the concrete setting has a long history in the literature on formwork pressure. The idea is attractive as one can easily picture the hydration products forming bonds between the loose particles and turning the Bingham material[57] into a solid. This change is not instantaneous and there are a number of different ways of defining or determining the setting

time; such as the time at which the cement changes from a Bingham material to a solid, the time to the end of the dormant period (see Chapter 4), the time to make a mark by a standard needle,but not the attachment, on the surface of a cement paste[30], or the time at which there is a sudden change of electrical potential difference[58]. In practise the time differences between these definitions have been ignored and authors have tended to use existing setting time data[47]. The setting time of a cement is controlled by its chemical composition and fineness, temperature and workability and because setting time is considered important these factors are included in the current design charts. If only the setting time controls the time of maximum pressure[12,17,18,11] for the same concrete and temperature, the time at which the maximum pressure occurs would be the same regardless of differences in the rate of placing, width of section, or depth of vibration. The evidence already presented shows that this is not true, for example, a column placed in a few minutes still exhibits a maximum pressure, and in these cases setting time would not control the maximum pressure. The analysis of existing data also showed that cements of different types but with the same setting time specification tended to exhibit different maximum pressures.

Whilst the setting time of cement does not appear to be a key factor controlling the maximum pressure, the early chemistry of cement might well be significant by changing the size of the solid particles. Data on admixtures are scarce. Retarders because they change the setting time of the cement were thought to give substantially increased pressures. Adam's experiment[45] resulted in higher pressures when set retarders were used whilst Ore and Straugham[30] measured slightly lower pressures.

The concept of the maximum pressure being controlled by changes in the shear strength of the concrete allowed the setting time concept to be combined with some physical processes which increase the interlock between particles. This allows for the idea of a particle structure capable of supporting the weight of the concrete and without necessarily the need for the concrete to set. Macklin[29] visualized the solid particles settling in the fluid cement paste to form a particle structure whilst the more recent authors[3,51] have used the concept of vibration preventing the development of shear strength (during the period in which the concrete follows the fluid head) and then a rapid development of

shear strength and the formation of a particle structure. This could be either pure physical interlock or aided by the cement setting.

Most of the mathematical theories also depended on the change in shear strength with time and therefore it is not surprising that various attempts were made at measuring the change in the shear strength of concrete with time either indirectly from form pressure measurements[21] or by triaxial tests[31,53] or vane tests[51]. Figure 2.13 at low rates of shear shows there is initially a rapid increase in strain with little increase in stress. The implication of these experimental results is that before the potential shear strength of the concrete is developed there has to be an appreciable movement. Do movements of this magnitude occur after the concrete has been vibrated ? Furthermore, a fully compacted granular material or a solid material (aggregate bonded together by hydrated cement) are still elastic materials which if loaded vertically would respond with tensile strains in the other principal axes and if these strains are resisted by, say, the presence of formwork, result in a load increase on the formwork. Therefore the loading of a granular material would show an increasing lateral pressure until the placing has been completed and not a distinct maximum pressure.

With narrow sections there is some agreement that the maximum pressures are liable to be lower than with wide sections and this has been attributed to arching effects. The presence of arching has been confirmed by examination of the crack patterns on the cast concrete surfaces[59] but arching is only one of a number of potential mechanisms. As narrow sections are not the subject of this thesis, these mechanisms will not be discussed.

The original intention was to look at the role of admixtures on formwork pressures, but this lack of a sound theoretical basis prevented anything other than a purely empirical approach. The emphasis was therefore changed to the production of a sound theoretical basis for concrete pressures on formwork in wide sections.

During the literature survey some authors[21,28] split the horizontal pressure into two components, one from the solid particles and the other from the static water head or a fraction of the static water head. Taking this idea that the horizontal force is made up from

two components, but then applying the principles of consolidation theory[15,60], it can be quickly deduced that the water pressure will start by being in excess of the static water head due to the partial or complete suspension of solid particles in the water. A piezometer which measures pore water pressure would therefore register a pressure which was the sum of the static water head plus an additional pressure due to the suspended solids called the hydrodynamic excess whilst a horizontal pressure gauge would register the pore water pressure plus the horizontal component of force from the particle structure. The pore water pressure is time dependent and as it disperses, the load is transferred to the interparticle structure where only a component of it will be transferred to the horizontal plane. With a uniform rate of placing, the net result on a horizontal pressure gauge with time would be that it would firstly register the fluid pressure, rise to a maximum and then start to decrease i.e. follow the shape of the characteristic formwork pressure graph.

The direct application of consolidation theory to formwork pressures is not possible as concrete is not an inert material but contains reactive materials which change both the volume of solids and the amount of free water. Also consolidation theory does not allow the water pressure to fall below the static water head, but water does not drain out of concrete as the formwork is removed, so there cannot be an effective static water head remaining. To resolve these questions and the development and testing of the hypothesis that the maximum formwork pressure is dominated by the change in pore water pressure with time, is the main subject of this thesis.

2.5 CONCLUSIONS

1. Most types of concrete pressure gauges give similar readings up to the maximum pressure, but after the maximum has been reached, the type of instrument has a significant effect on the recorded pressure.

2. The concrete pressure on formwork starts by following the fluid pressure of concrete and then deviates to reach a maximum. After attaining this maximum, the pressure may or may not reduce.

3. The assumed association between the depth to which the concrete acts as a fluid and the influence of vibration, does not agree with observations on the compacting ability of internal vibrators.

4. Existing theories for a maximum pressure do not satisfy all the observations.

5. The maximum pressure on formwork might involve both chemical and physical processes.

6. At high rates of placing, the chemical processes are secondary and can be ignored for practical purposes.

7. Provided the concrete has not set, deep re-vibration will increase the horizontal pressure above that normally produced.

8. Within a single section, pressure readings show a wide scatter of results.

9. The data do not confirm the relationships used in design methods.

10. BFPC and TrZ cements tend to give higher pressures than OPC although the setting time requirements are the same.

11. Narrow sections (under 305 mm) have lower maximum pressures than wide sections for all other conditions being equal.

12. Low slump concretes give lower pressures than high or medium slump concretes. The data do not show a clear difference between medium and high slump concrete.

13. The CERA design method generally predicts a safe upper limit for the concrete pressure except at low calculated pressures or where cements other than OPC were used.

14. The ACI maximum pressure limit of 100 kN/m^2 for walls is unproven by these data.

Chapter 3 EXPERIMENTAL PROGRAMME

3.0 INTRODUCTION

The primary aim of the experimental programme was to test the hypothesis that the dispersal of pore water pressure is the dominant factor in determining the maximum horizontal pressure. Three test methods were considered, site pressure measurements, testing full scale sections in the laboratory or experimental simulation by surcharging a small sample of concrete. Site pressure measurement gives the investigator little control over the variables and would therefore not provide the most effective starting point. Once a theory has been established site pressure measurements would provide the most realistic way of checking theory against practice. Testing full scale sections in the laboratory gives the necessary control over the variables but they are expensive in time, labour and materials. In practice this puts severe limitations on the number of sections that can be cast and consequentially, the variables investigated. This leaves experimental simulation.

Experimental simulation of concrete pressure by surcharging a small sample of concrete with static weights has been tried by Hoffmann[21] and by McDowall and Ritchie[51]. The horizontal pressures obtained were lower than those predicted by design charts and McDowall and Ritchie concluded that pressures could not be simulated in this manner. The pore water pressure hypothesis offers an explanation for this; a static weight only reproduces the same total load and not the same pore water pressure gradients (see Chapter 4). With static weights, the hydraulic gradient up the sample of concrete is very much steeper and this causes rapid drainage (Darcy's law) and the rapid formation of a particle structure and consequentially lower horizontal pressures. The implication of the hypothesis is that for the simulation of the conditions in an actual section, both the total load and the pore water pressure distribution have to be reproduced. Achieving this objective is difficult, for the pore water pressure is not simply the static water head (see Chapter 4) and its value is unknown. Nevertheless a test rig in which the static weight of concrete could be simulated by loading a small sample of concrete via a plate and which could simultaneously but independently, apply a water pressure to the concrete, would provide

a valuable tool for studying the mechanisms involved in formwork pressures. Because the applied pore water pressure would not be the same as that in a full sized section, the results of these tests would not be directly applicable to formwork pressure calculations.

A rig of this type was developed and testing started with the application of just one type of loading, either plate pressure (direct loading of the concrete via a porous plate) or water pressure. Next the effects of applying both type of loading simultaneously but at different levels were investigated, followed by studies of the role of cement chemistry and vibration. The dispersal of pore water pressure with time could be a purely physical process or aided by the hydration of the cement. By accelerating the set of cement, retarding it and stopping it altogether, the role of cement chemistry on horizontal pressure could be studied in the test rig.

When the concrete was placed in the test rig, it was compacted with a 25mm diameter internal poker, but during pressure testing the concrete was not normally vibrated. If it is possible to get the horizontal pressure to follow the fluid head without vibration, the concept that the horizontal pressure follows the fluid head because of vibration[3,51] would be disproved. The rig was also used to check the susceptibility of the particle structure to weak vibration.

In a separate series of tests, five 1.2m high columns were cast for direct measurement of the water distribution during the first two hours after vibration. Because of the direct sampling technique used, each column only gave one distribution of water. Nevertheless some interesting conclusions were made on the basis of these tests.

Consolidation theory depends on the principle that as the particles are compacted together, water is expelled. Before detailed test rig design, a pilot series of tests was carried out with a modified Taylor Woodrow pressure bleed test apparatus[61,62]. This series of tests is reported in Appendix A. The tests gave water losses of up to 26% of the total free water and if this had been reflected in consolidation, the settlement of the concrete would have been far in excess of that normally observed. The main conclusion from these tests is that the large potential settlement of concrete is never

fully achieved in real sections.

3.1 OBJECTIVES OF THE TEST PROGRAMME

The objectives of the test programme are summarized as:

1. To understand the relative roles of the two components of the horizontal force i.e. that contributed by the solid particles and that by the pore water pressure.

2. To understand the influence of the rate of loading on the horizontal pressure.

3. To understand the role of the chemistry of cement on the horizontal pressure.

4. To understand the role of vibration on the horizontal pressure.

3.2 DESCRIPTION OF APPARATUS

The test rig (Figures 3.1 and 3.2) consists of a rigid, smooth, steel mould which can contain a 294 mm diameter by 402 mm long cylinder of fresh concrete. The size was a compromise between being too large to handle and being so small that arching might be significant. The mould can be split vertically in half to aid the removal of the concrete after the test. At mid-height there are three horizontal pressure gauges and two piezometers. On top of the concrete rests a fabric filter and a porous loading plate. The cover carries three deflection gauges to monitor the movement of the porous plate and a hydraulic piston to apply a central load via a ball joint to the porous plate. The space between the cover and porous plate is filled with water. The applied water pressure is obtained by pressurizing this water with air.

In principle, the test rig was simple, but the actual achievement of a water and air tight rig took a long time to develop. Once achieved, constant maintenance was necessary as the constant stripping and re-assembly gave a relatively short life to the rubber seals.

The basic instrumentation was not novel. The settlement of

Figure 3·1 Diagrammatic sketch of the test rig·

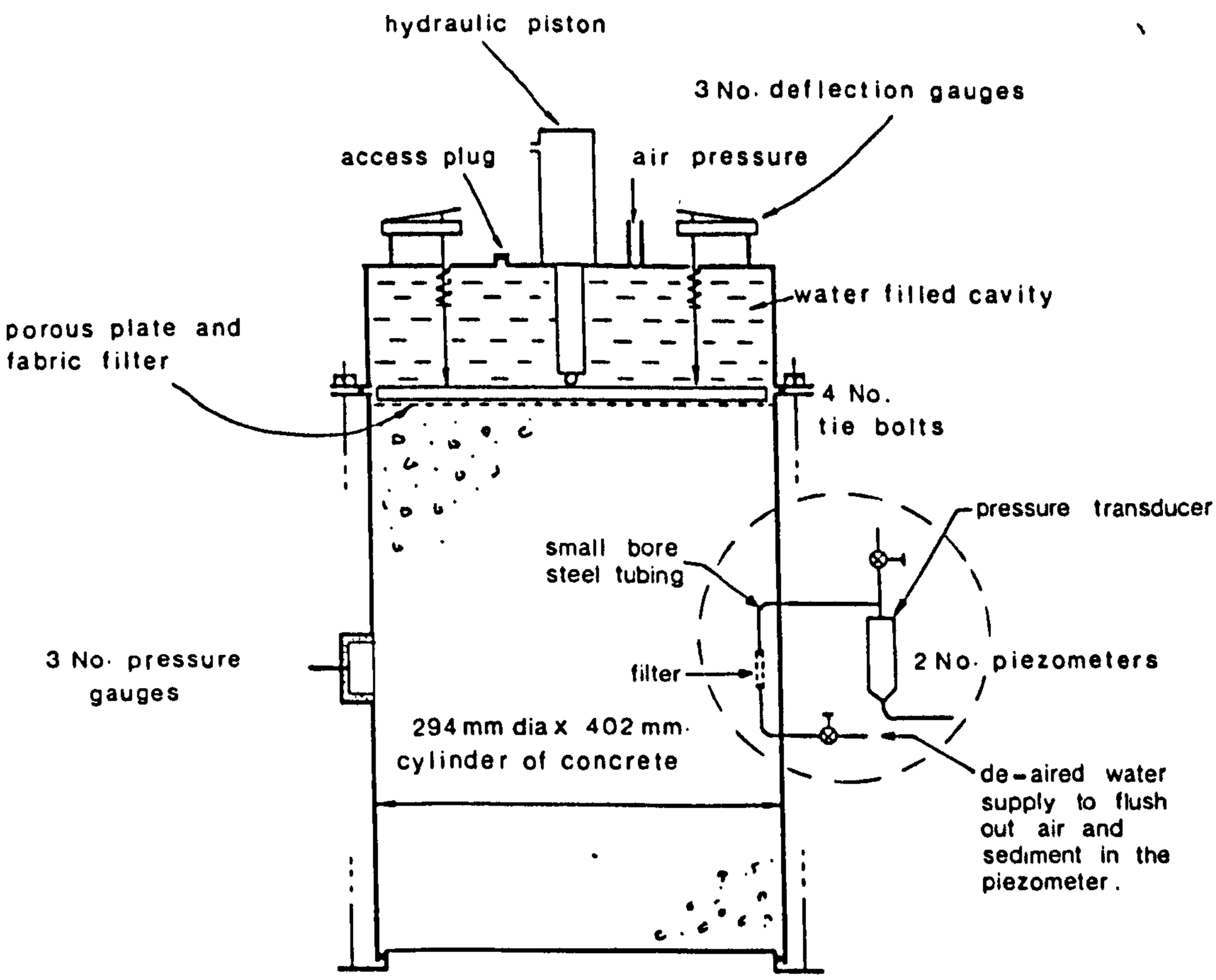

Figure 3·2 : Photograph of the test rig·

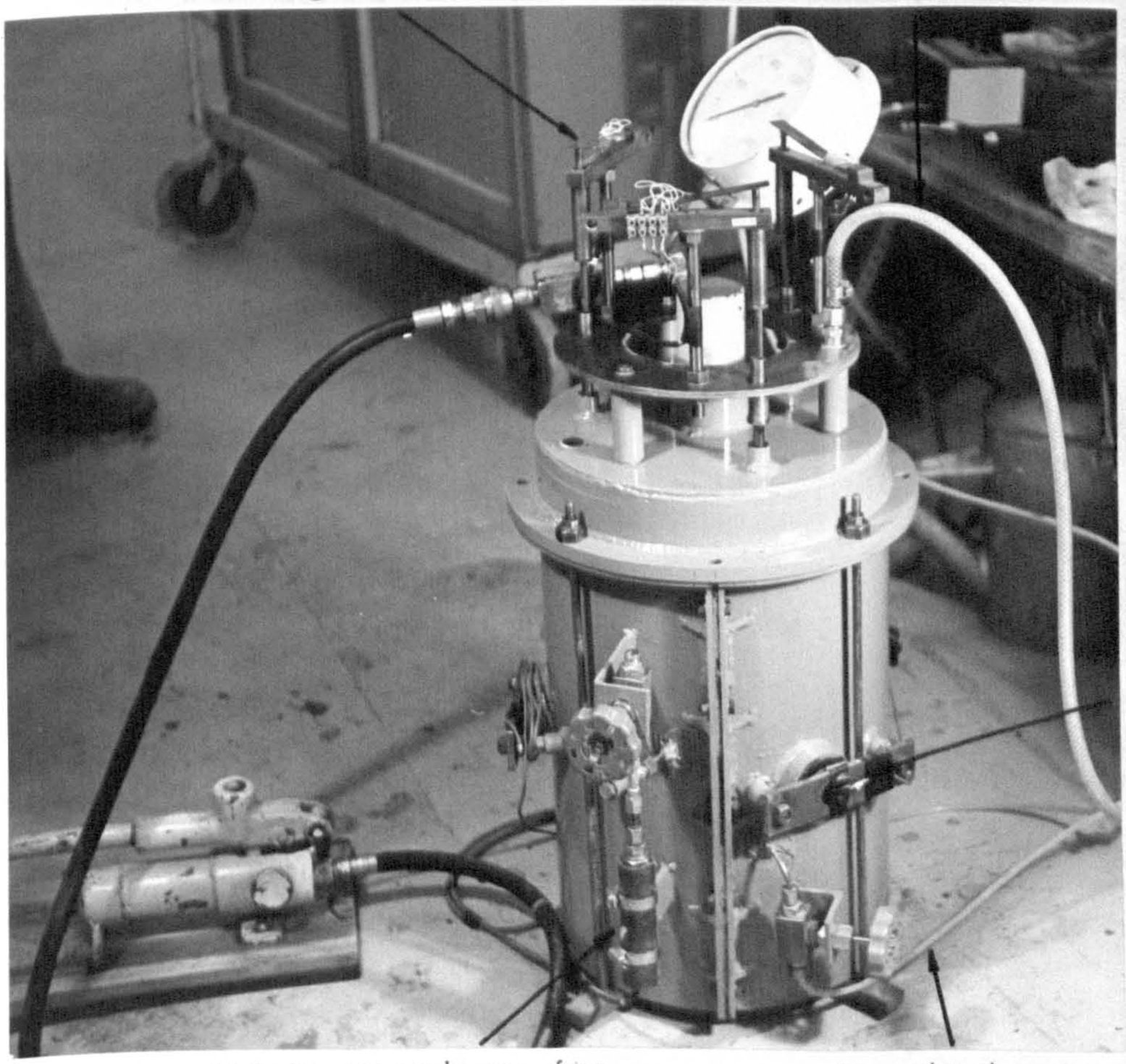

the porous plate was measured with three cantilevered half bridge deflection gauges[63]. These gauges were of proven reliability and were calibrated regularly against a micrometer scale. During the development of the rig, additional deflection gauges were used to check that the cover was not lifting away from the base of the mould.

Concrete is not a homogeneous material on the microscopic scale and to get a representative pressure reading it is normal to maximise the ratio of the gauge diameter to maximum aggregate size. With the cylindrical mould it was not possible to fit large diameter horizontal gauges and therefore only 50 mm O.D. gauges were used. These had a diaphragm of 32 mm diameter which gives a gauge to aggregate ratio of only 1.6:1. This is smaller than that normally used, but the consistency between the three horizontal gauges was a check on whether these small gauges yielded reliable results.

The horizontal pressure gauges worked on the principle of measuring the strains in a thin diaphragm with clamped edges. Figure 3.3 shows the details of the pressure gauge and housing. The diaphragm was a nominal 0.86 mm thick and was gauged with a full strain gauge bridge of 20 mm diameter and a nominal resistance of 240 Ω. Using a full strain gauge bridge had two main advantages[64]; firstly this arrangement is temperature compensating and secondly the strain gauge bridge was so arranged that one pair of opposite arms of the bridge was in the compression zone on the diaphragm and the other pair in the tension zone. This gives a magnification of sensitivity, depending on the relative values of the compressive and tensile strains, up to a maximum of 4 times that of a bridge with only one arm strained[64].

The pressure gauges were fitted with a balancing circuit so that prior to each test, the gauges were adjusted to give approximately zero voltage in the voltmeter at no load. This refinement helped to minimise the errors due to large out of balance currents heating the voltmeter.

The method of fixing the gauges into the moulds was novel. The gauges were sealed into position using a cold mixed and cured urethane, Flexane 60. In addition, a thin non-bonded film of Flexane

Figure 3·3 : Cross section of a horizontal pressure gauge

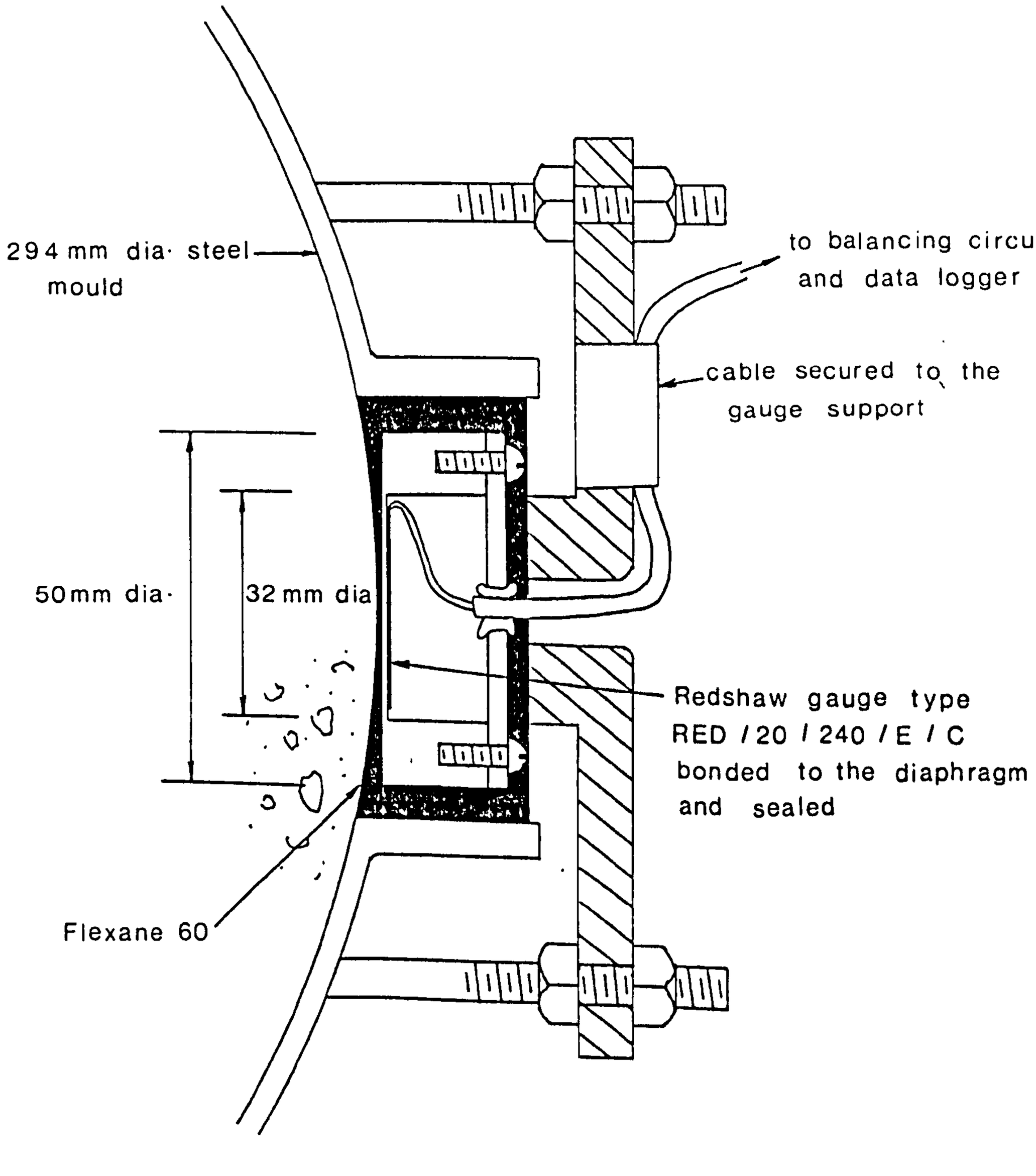

was placed over the face of the gauge to give a flush surface on the cylindrical mould and to afford some measure of protection from handling and vibration damage. This resulted in a loss of sensitivity but direct calibration of the gauges in position against a water pressure gave adequate resolution. This varied from 0.54 to 0.65 kN/m^2 per mV.

The procedure for fixing the gauges was as follows:

1. Stick, with a contact adhesive, a temporary card former over the inside of the gauge position. The Flexane is cast against this former to maintain the cylindrical profile of the mould.

2. Clamp the mould with the gauge position horizontal.

3. Clean and prime the inside of the housing.

4. Paint release agent (supplied by the manufacturer of Flexane) over the card face to prevent it bonding to the Flexane.

5. Mix 10 ml of Flexane 60 according to the manufacturer's instructions and pour into the gauge position. This is to form the protective cover and give a flat surface onto which the gauge is mounted.

6. Paint release agent over the face of the pressure gauge but not the sides.

7. When the Flexane has just solidified (3 - 4 hr at normal room temperature) place the gauge face down centrally in the gauge position.

8. Mix 10 ml of Flexane and pour around the sides of the gauge and over the back of the gauge until the screw heads are just covered.

9. Leave to cure.

10. Remove the card former and clean the mould.

11. Place and clamp the solid support behind the gauge. Secure the cable to prevent accidental damage.

12. Test and calibrate the gauge.

This system of fixing the gauges was excellent provided the gauges did not need replacing. Once opened, Flexane 60 only has a shelf life of 2 months and it had to be re-ordered each time a gauge was changed. With curing times and re-calibration, the replacement of a pressure gauge took a week.

The piezometer consisted of a low displacement pressure transducer which was connected to the concrete via a filter. Changes in the pore pressure of the concrete were transmitted through the filter and were registered on the pressure transducer. The literature[65,66] indicated that a filter of 1 μm fineness would be suitable for cement paste, but a filter tube of this fineness was not found. Tests with a coarser porous plastic tube provided a fair filter although a small quantity of fines did penetrate it. The programme went ahead using this filter. During the tests, the piezometers were frequently flushed with de-aired water to remove the sediment and air which had entered from the concrete. The coarseness of the filter created problems for despite frequent flushing out of the fine steel tubes connecting the filter and pressure transducer, there was a build up of solids which blocked the tubes and necessitated their replacement.

The plate loading system was calibrated directly. Firstly, the gauge on the hydraulic piston was calibrated against a loading rig. Then the force in the springs holding the extension of the deflection gauges against the porous plate were measured and the porous plate weighed. When plotting the results, the pressures were resolved to equivalent pressures at the centre line of the horizontal pressure gauges. The plate pressure was therefore the sum of the force from the piston, the spring forces, the weight of the porous plate divided by the area of the porous plate, plus the weight of the concrete above the centre line of the horizontal pressure gauges and the weight of the additional water in the cover space divided by the cross sectional area of the concrete.

One of the assumptions about the rig was that it was rigid. To verify this assumption a test was carried out. Two resistance strain gauges were bonded to the mould at the level of the horizontal gauges

and positioned in the direction of maximum hoop strain. These were linked to a pair of dummy gauges and then into the data logger. At mid height on the vertical joints between the sections of mould, pairs of cantilevered deflection gauges were placed to monitor any joint movement. The cylinder was pressurised in increments up to 83 kN/m^2 (leaks prevented it being taken any higher). At each pressure increment, the strains in the cylinder wall and joint movements were recorded.

These measured movements were then extrapolated assuming a continued linear relationship to give the following movement for a pressure of 150 kN/m^2 ; an increase in diameter of 0.005 mm due to the hoop strain in the steel and joint movements of 0.013 and 0.123 mm. No rig will be absolutely rigid and as the measured movements are under 1/16 of typical formwork deflections (1/300 of 450 mm), the assumption that the rig is relatively rigid is valid.

The possibility of developing shear forces between the walls of the container and the concrete was considered at the design stage. If shear forces were to develop in the test rig, the magnitude of the vertical load on the concrete at the level of the horizontal pressure gauges would not be known.

The following measures were taken to reduce any shear effects:

1. A large diameter in relation to the maximum aggregate size (over 14 X).

2. A small height to diameter ratio.

3. Rigid wall construction.

4. Walls of turned steel to minimise friction between the wall and concrete.

5. The use of an oil based release agent on the mould.

These features were considered to be sufficient to reduce any shear effects to an insignificant level, but no attempt was made to measure shear forces. The experiments which followed the development of this rig showed that about 80 percent of the maximum horizontal pressure came from the pore water pressure and this would not develop shear forces. Any

small shear effect influencing the remaining 20 percent would not invalidate any of the conclusions drawn from the experimental programme.

3.3 METHOD OF TESTING

The procedure for the tests was standardized into the following routines:

3.3.1 Mould assembly

1. Apply a thin layer of contact adhesive to the outside 5 mm of the steel tube on either side of the filter location. Make sure that the adhesive does not block the tube (Figure 3.1).

2. Slide the filter tube onto the lower half of the pipework. There are two of these filters to be fitted and they are both on the same section of the mould.

3. Locate this section of the mould onto the base including its two tie rods.

4. Manoeuvre the other section of mould into position and push the two filter tubes onto the upper section of pipework.

5. Bolt the sections together and locate the remaining two tie rods.

6. Fix the pressure transducer to the piezometer tubing.

7. Close all valves (two on each piezometer).

8. Connect the supply of de-aired water to the piezometer.

9. Connect the cables from the pressure gauges and deflection gauges to the data logger.

10. On the cover, check that the piston is fully retracted and that the deflection gauges are central on their extensions through the cover plate.

3.3.2 Concrete preparation

1. Batch the aggregates and sand from single sized materials in the air dry condition into a 0.04 m^3 pan mixer.

2. Add the mixing water less one litre and mix for 30 seconds.

3. Leave for $4\frac{1}{2}$ minutes.

4. Add the cement and cover with aggregate.

5. Start mixing and add the remaining litre of water into which the admixture has been diluted. In the case of the superplasticized concrete only the water was added as the Melment was not added until after the slump test.

6. Mix for two minutes.

7. Make three control cubes.

8. 20 minutes after the start of mixing the concrete, carry out a slump test.

9. In the case of the superplasticized concrete, mix for one minute whilst adding the admixture.

10. Transport to the test rig in the laboratory.

3.3.3 Test procedure

1. Switch on the data logger.

2. Prepare the concrete as given in section 3.3.2.

3. Fill the piezometers with de-aired water and then close the valves to hold this water in the piezometers.

4. Remove from the mould any water that had leaked from the piezometers.

5. Take a set of zero readings for the pressure gauges and piezometers. Note the time.

6. Fill the mould with concrete, then vibrate with a 25 mm diameter internal vibrator for 60 seconds whilst topping up with concrete so that the finished level is 5 mm below the rim.

7. Lightly trowel the surface.

8. Place the fabric filter, porous plate and ball bearing.

9. Clean the rim and fit the cover.

10. Connect the hydraulic pump and the air pressure line from the manometer (Figure 3.2).

11. Fill the top of the mould with water through the plug hole.

12. Take a set of readings on all the gauges. Note the time. This is the second set of readings for the pressure gauges and piezometers but the first set of readings for the deflection gauges connected to the porous plate. The porous plate is assumed to have no settlement at this time.

13. Apply an increment of pressure to the concrete with either or both the pump and manometer. Take a set of readings and note the time.

14. Continue to apply pressure in increments and take readings as required for the particular test. Bleed the piezometers occasionally.

3.3.4 On completion of the test

1. Disconnect the hydraulic pump, the manometer, all cables and the hosing to the piezometers.

2. Remove the plug and drain off the water in the top of the mould.

3. Remove the cover, ball bearing, porous plate and fabric filter. Rinse out the fabric filter.

4. Dig out the concrete carefully to just below the gauges.

5. Cut through the piezometer filters and split the mould to ease the removal of the remaining concrete and to reduce the risk of damage to the gauges.

6. Remove the piezometer pressure transducers and flush out their diaphragms. If necessary clean with dilute acid.

7. Clean the mould including flushing out the piezometer tubes working from the valve side (to wash the debris away from the valve).

8. Apply release agent to the mould surfaces.

9. Push back the piston in the cover to the fully retracted position.

10. Re-assemble.

3.4 DETAILS OF THE TEST PROGRAMME

The test programme can be conveniently split into three groups, the initial tests, tests on the influence of cement chemistry and tests on the influence of vibration. The initial tests started with the application of just one form of loading, either the plate or water pressure and then progressed to the application of both types of loading simultaneously but at different pressures. The objectives of these tests were to develop an experimental method, prove that tests were reproducible and understand how the pattern of loading influences the horizontal and pore water pressures. Only two concrete mixes were used in this group of tests, the medium and high workability OPC concretes (Table 3.1).

The initial tests showed that the most useful method of testing was to apply an increment of load and then hold this load for a period of time whilst changes in horizontal pressure, pore water pressure and plate settlement were recorded. This technique was adopted as standard for the remaining tests.

Also adopted as standard was a ratio of plate pressure to water pressure of 2.32:1.0. The plate pressure would therefore represent the full weight of concrete and the water pressure represents the static water head. This ratio of loading resulted in sufficient difference between the applied pressures to enable the influence of each type of loading to the analysed. The increments of loading were therefore standardized at 10 kN/m^2 of plate pressure and 4.31 kN/m^2 of water pressure applied in increments at either 5,10 or 15 minute intervals.

TABLE 3.1 Mixes used in the experimental programme

Mix title		Medium workability	High workability	Retarded	Sugared	Accelerated	Air-entrained	Superplasticized
Mean 28 d strength N/mm^2		47	45	47	None	50	39	49
Target slump, mm		50 mm	100 mm	100 mm	100 mm	100 mm	100 mm	75 mm before adding Melment
OPC kg/m^3		320	350	325	350	325	350	350
Water, l/m^3		184	196	185	170	185	185	190
Admixture, $/m^3$		None	None	Conplast R 1.3 l	Sugar 3.5 kg	Cormix P8 6.5 l	Conplast AEA 150 ml	Melment 7 kg
Single sized Thames Valley aggregates, kg/m^3	20 - 10	805	760	760	760	760	760	760
	10 - 5	410	380	380	380	380	380	380
	5 - 2.5	60	61	67	61	67	58	61
	2.5 - 1.25	60	61	67	61	67	58	61
	1.25- 600	120	122	133	122	133	116	122
	600 - 300	225	229	251	229	251	217	229
	300 - 150	120	122	133	122	133	116	122
	pass 150	15	15	16	15	16	15	15

As the plate pressure represents the weight of concrete, these rates of loading can be converted into the equivalent rates of placing of 5.3 $\left(\frac{120\ kN/m^2}{2.320 \times 9.81}\right)$ hr) 2.6 and 1.8 m/hr.

To study the influence of cement chemistry on the horizontal and pore water pressures, admixtures were used. By accelerating, retarding and stopping the set completely (with sugar at 1% by weight of cement), the influence of cement setting on the horizontal pressure could be investigated. Included in the group were a few tests with air-entraining agents as they reduce bleeding[67] and superplasticising agents as there is little known about their effects on formwork pressure[68].

In general, the concrete mixes were designed using the basic mix method[69] and philosophy to give a mean 28 day strength of 45 N/mm^2 and a slump of 100 mm. Air dried, single sized Thames valley aggregate and sands (blended to give a zone 3 sand) with ordinary Portland cement were used throughout the experimental programme. Table 3.1 gives the mix proportions used in the experimental programme.

The work of Raffle[70] showed that the particle structure in a cement paste was very susceptible to weak vibration. Tests were programmed to show if concrete was also susceptible to weak vibration.

In addition to the main experimental programme, five 1.2 m columns were cast and directly sampled to measure the water movements. As the main conclusions from these tests concern the zone of influence of vibration, they have been included with the other work on vibration.

The main experimental programme included over 35 tests of which only a representative sample are reported in this thesis. Some of the tests not reported were situations in which a complete set of results was not obtained due to one of the gauges being defective. Nevertheless these tests were useful in that they helped confirm that the results were reproducible. The other tests which are not presented are simply repeat or similar tests.

The tests reported in this thesis are summarized in Table 3.2.

TABLE 3.2 The representative sample of tests reported in this thesis

Initial tests

Title of test	Concrete mix	Figure
Plate pressure only	High workability	3.4 (a)
	High workability	3.4 (b)
Water pressure only	Medium workability	3.5
Plate and water pressure	High workability	3.6

Tests on the influence of cement chemistry

Concrete mix	Rate of placing - m/hr.		
	5.3	2.6	1.8
Accelerated set	Fig. 3.7 (a)	Fig. 3.11 (a)	
High workability	3.7 (b)	3.11 (b)	Fig. 3.12 (b)
Retarded set	3.7 (c)	3.11 (c)	3.12 (c)
Sugared	3.7 (d)	3.11 (d)	3.12 (d)
Medium workability	3.8		3.12 (a)
Air entrained	3.9		
Super plasticized	3.10		

Tests on the influence of vibration

Title of test	Concrete mix	Figure
Vibration	High workability	3.13
Column tests	Medium workability	Table 3.3

3.5 RESULTS

The main experimental results have been presented as a series of graphs of pressure against time, Figures 3.4 to 3.13. The graphs show the average value of the three horizontal pressure gauges and the average value of the two piezometers. The consistency between the gauges was good, and therefore averaging the results does not lead to invalid conclusions. The exception to this general rule was the super plasticized concrete; with these mixes there were large differences between the horizontal gauges and therefore in these graphs the range of scatter is indicated.

In Figures 3.4 to 3.13 a standard notation has been used; the solid line represents the plate pressure and the dashed line represents the water pressure. Both pressures are resolved into the equivalent pressures at the centre line of the horizontal pressure gauges. The average of the three horizontal pressure gauges has be symbol O and the average of the two piezometers the symbol Δ . The average plate settlement is indicated by the symbol $\blacktriangledown$.

The results of the tests on the direct measurement of water movements are given in Table 3.3.

3.6 DISCUSSION OF THE RESULTS

3.6.1 Experimental technique

The experimental rig worked as well as could be expected for such a complex experimental method. After the development stages, there were still occasional problems with blockages in the piezometer tubing, damage to the wires connecting the gauges to the logger, and a variety of internal problems with an elderly data logger. In such cases the tests were repeated and the reliable information from the incomplete tests was used to help assess how reproducible the tests were.

The ability to repeat a test and get similar results is important. If the results are not consistent, a detailed study is necessary to determine if this is due to the experimental technique or the material under test. The initial group of tests of which only a small sample are reported, showed that the rig gave a consistent pattern

Figure 3 4 . Tests with plate pressure only (high workability mix)

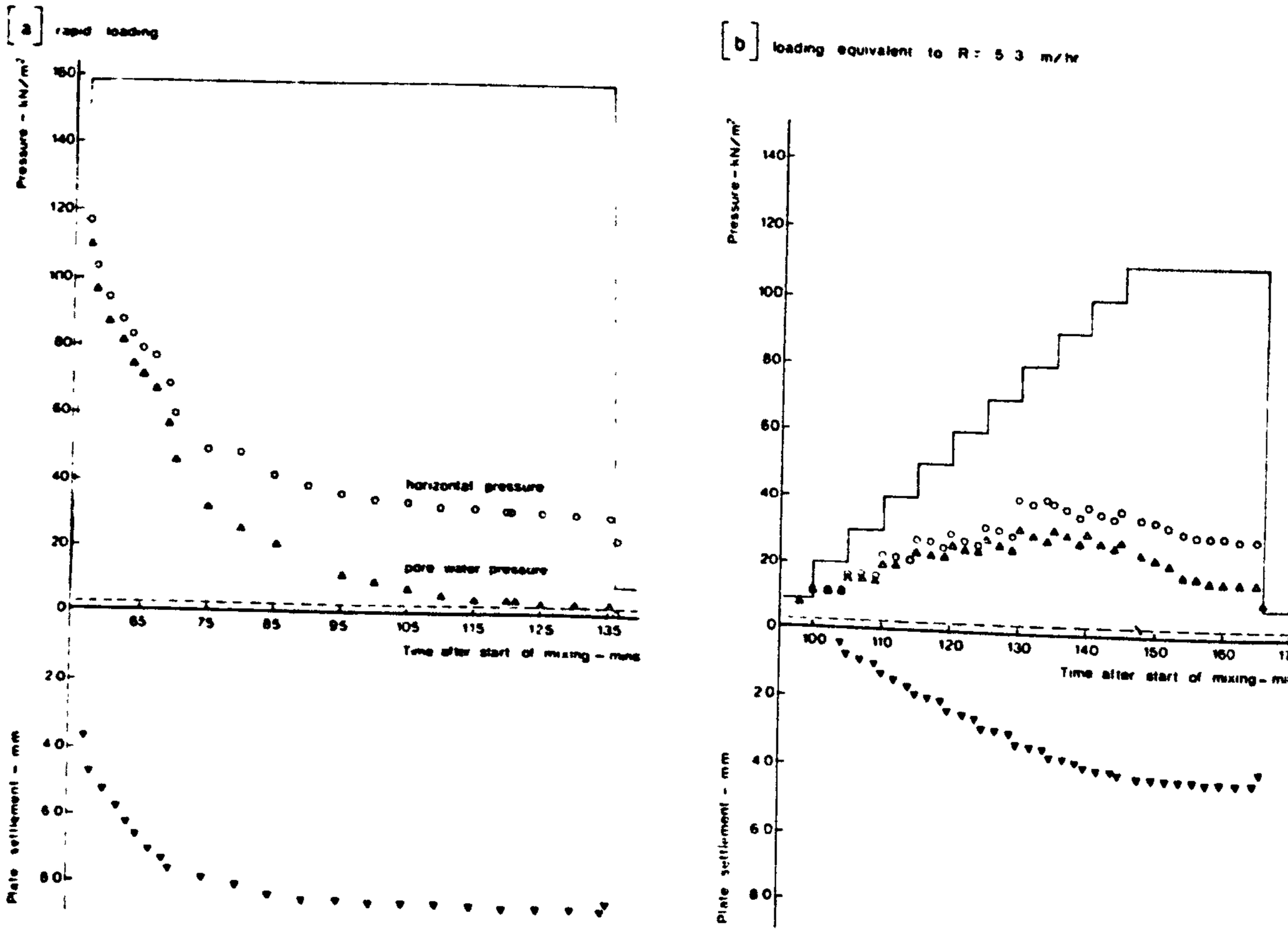

Figure 3 5 . Test with water pressure only (medium workability mix)

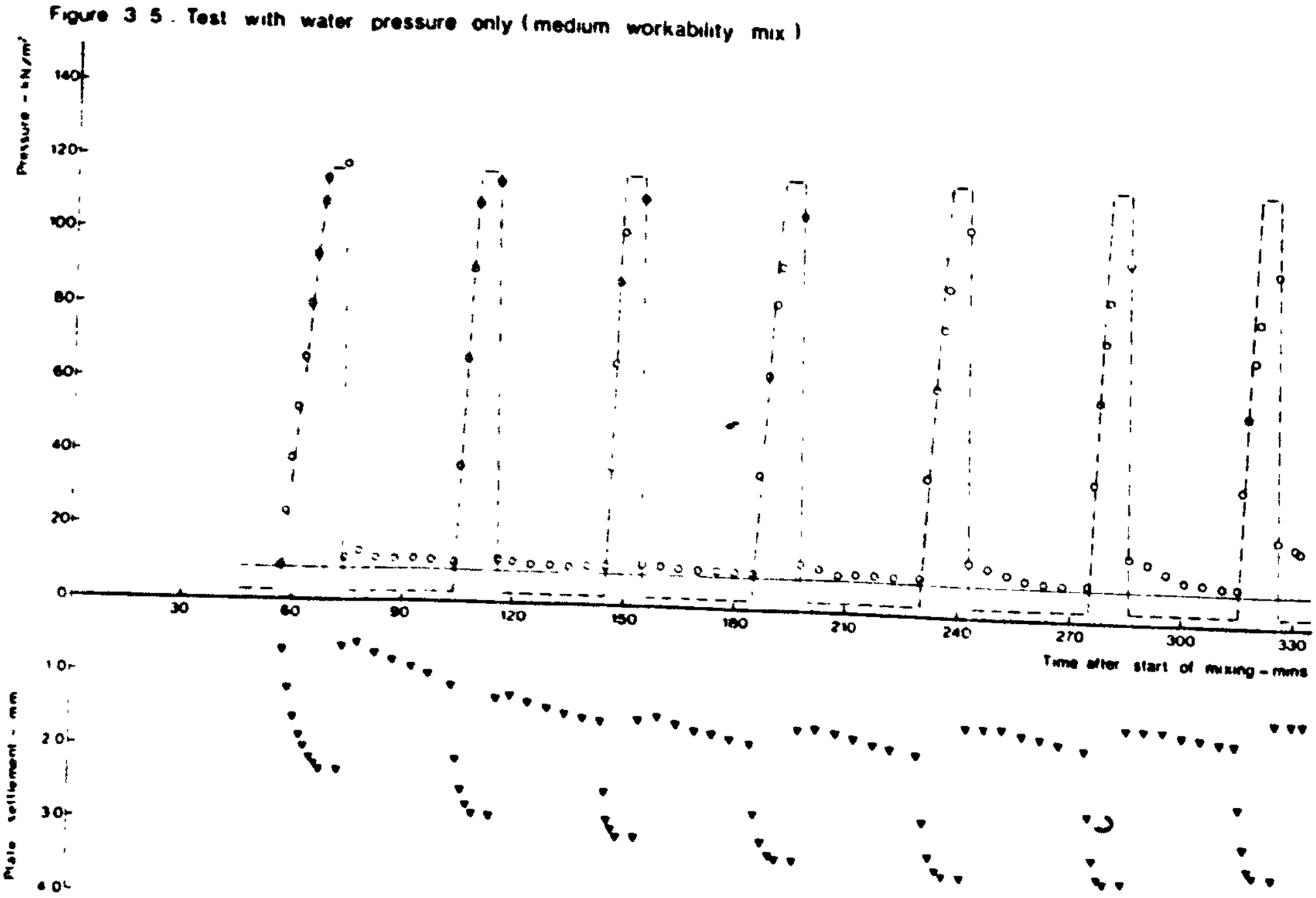

Figure 3.6 : Test with plate and water pressure (high workability mix).

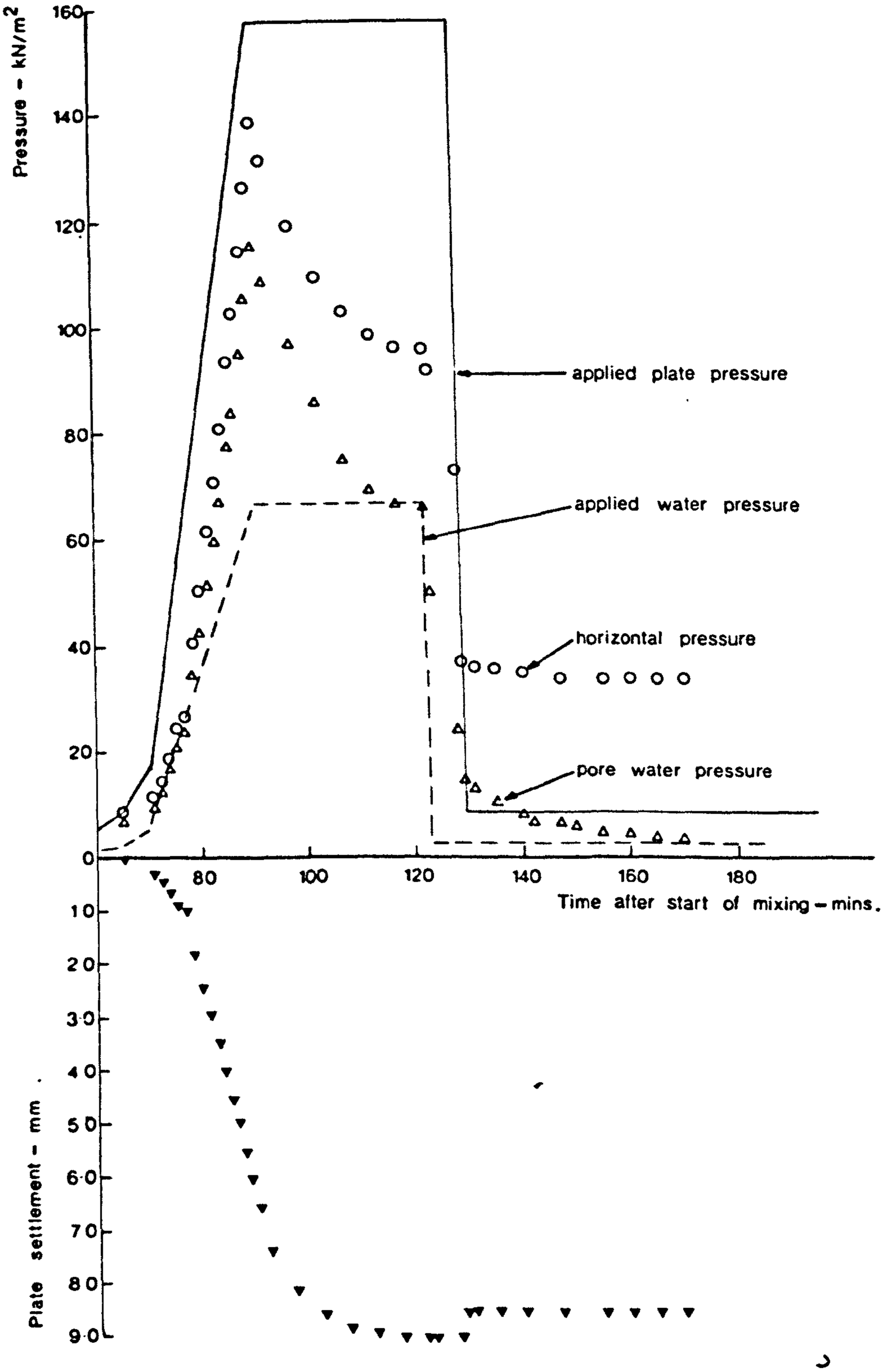

Figure 3 7 Tests on the influence of cement chemistry (R = 5 3m/hr)

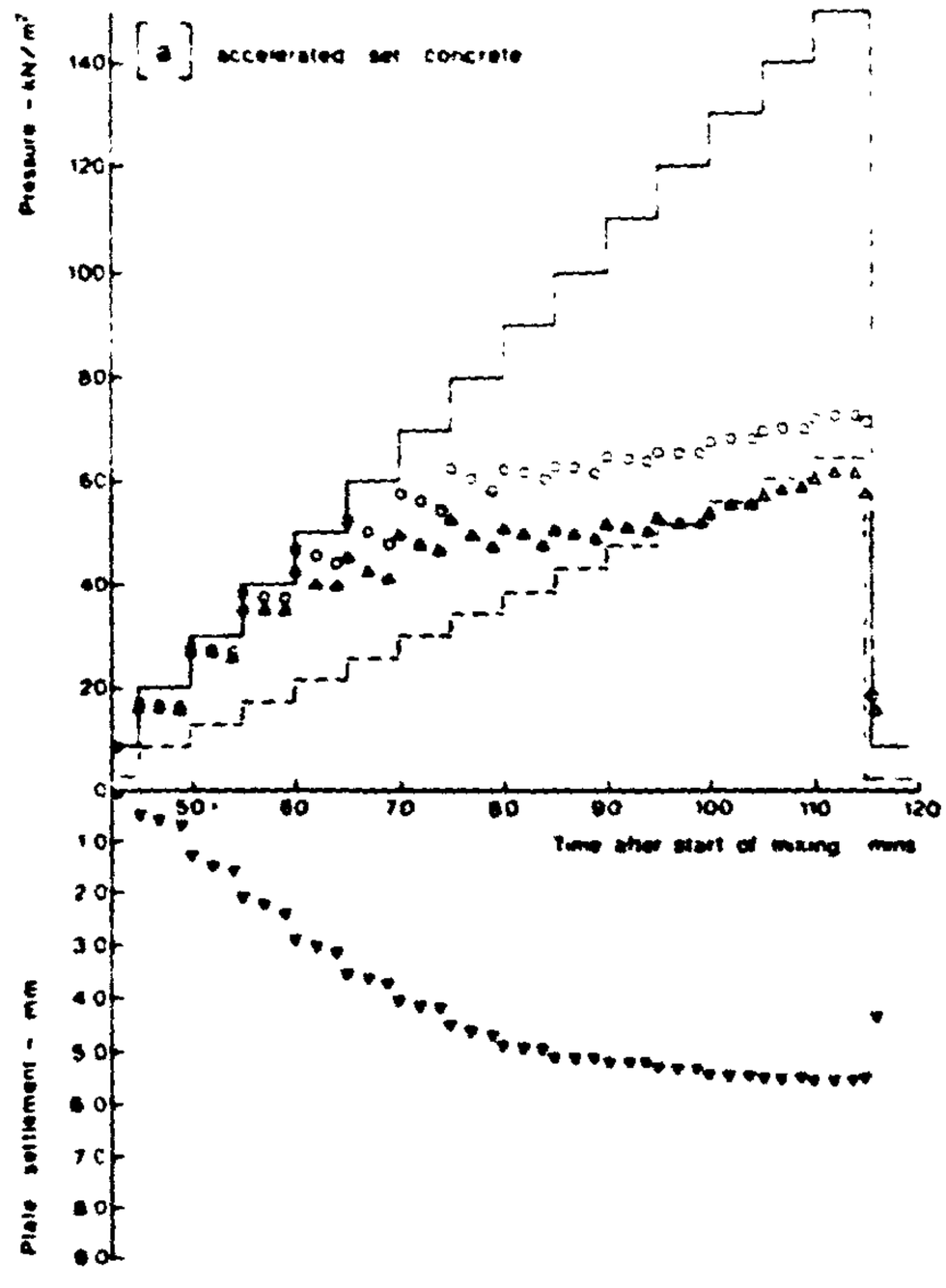

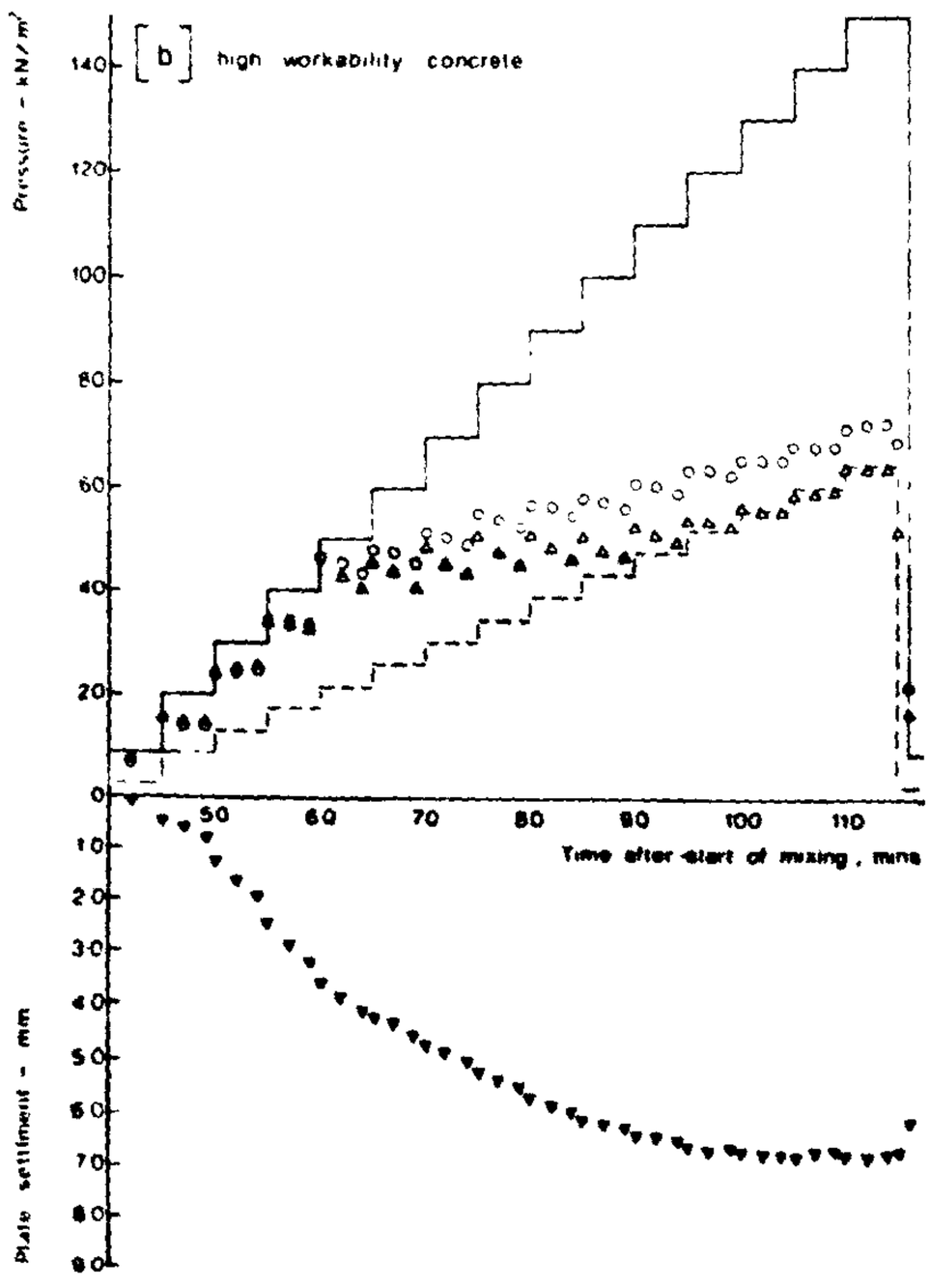

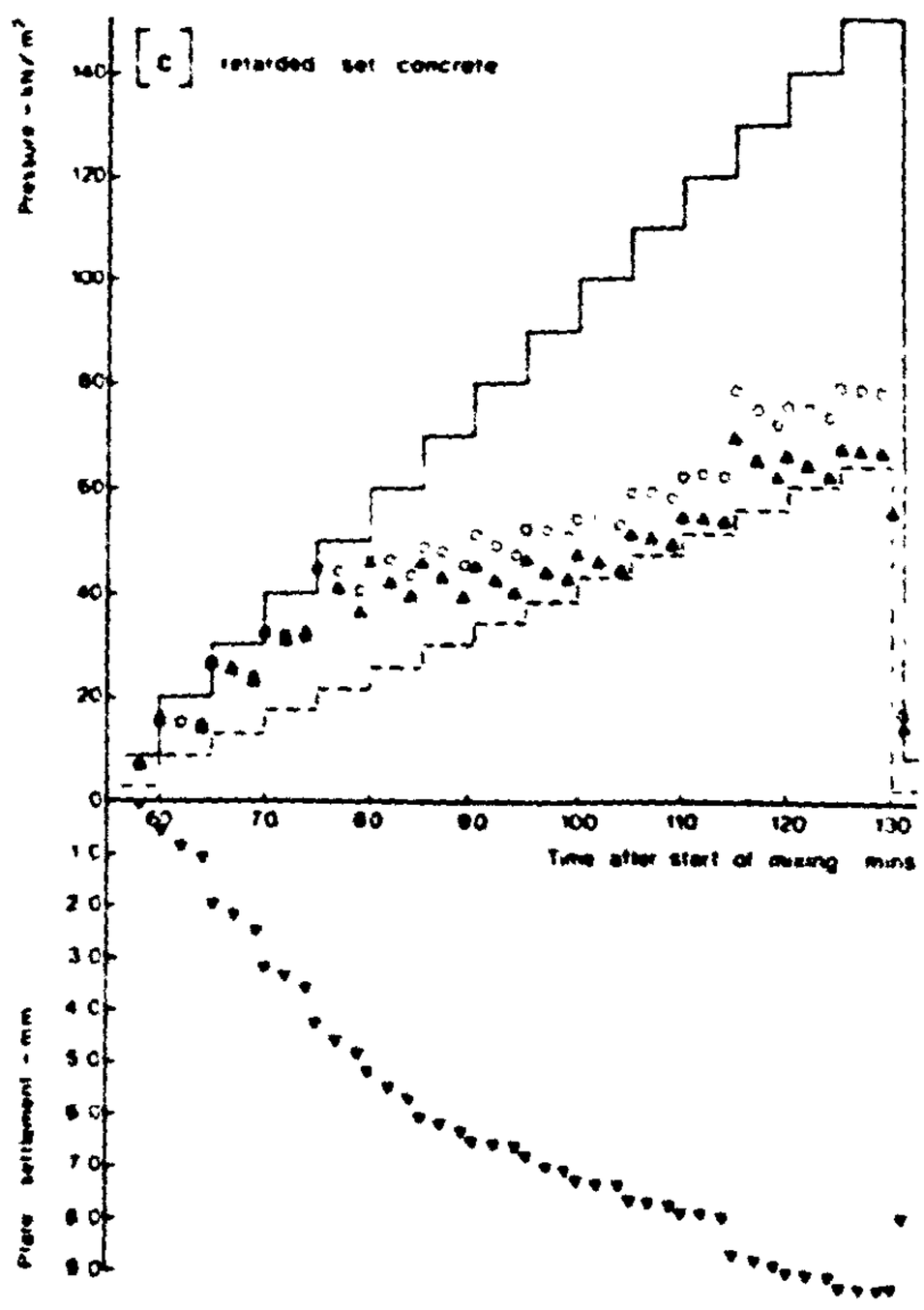

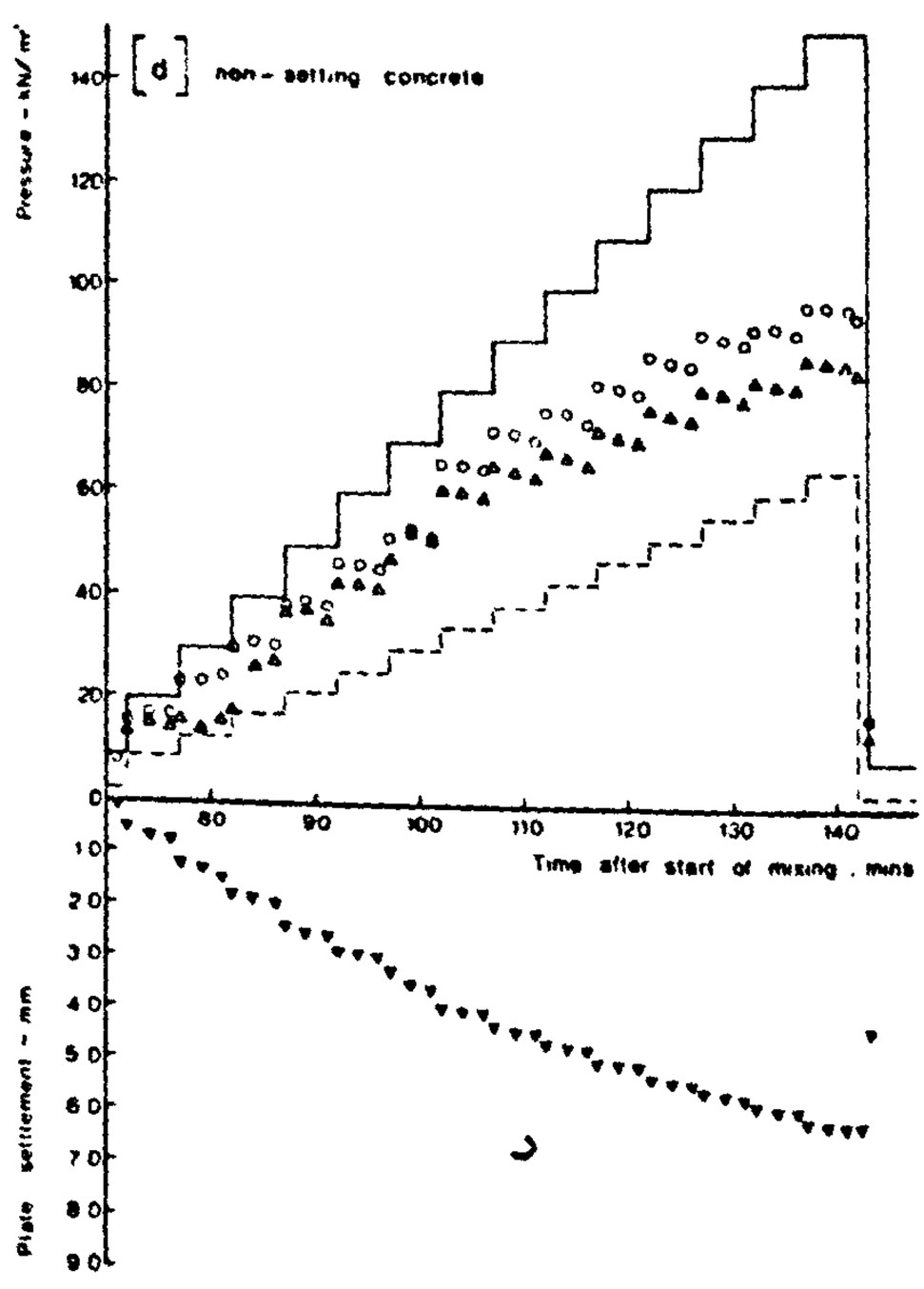

Figure 3 8 Test on the influence of cement chemistry - medium workability concrete (R = 5 3 m/hr)

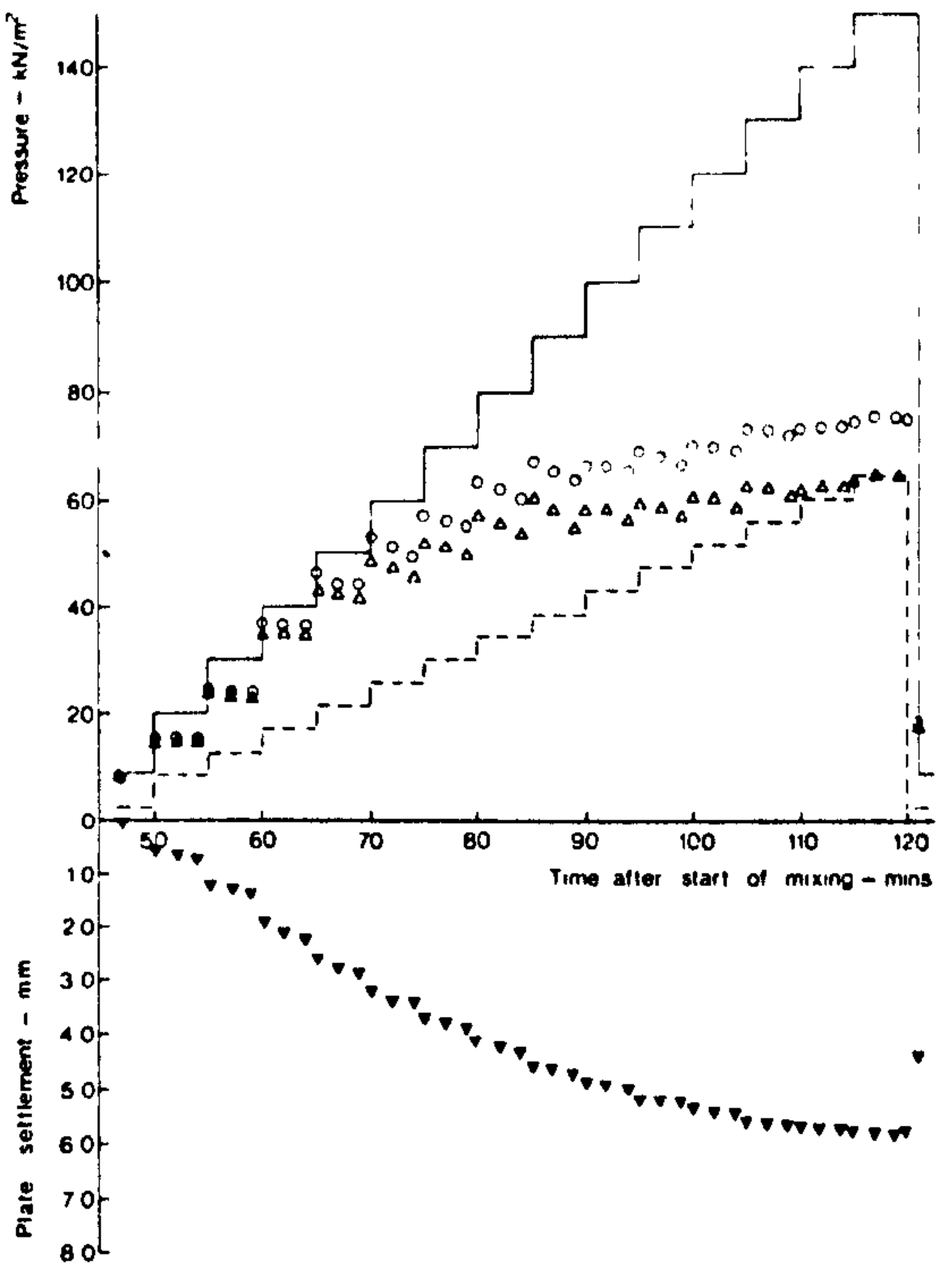

Figure 3 9 Test on the influence of cement chemistry - air entrained concrete (R = 5 3 m/hr)

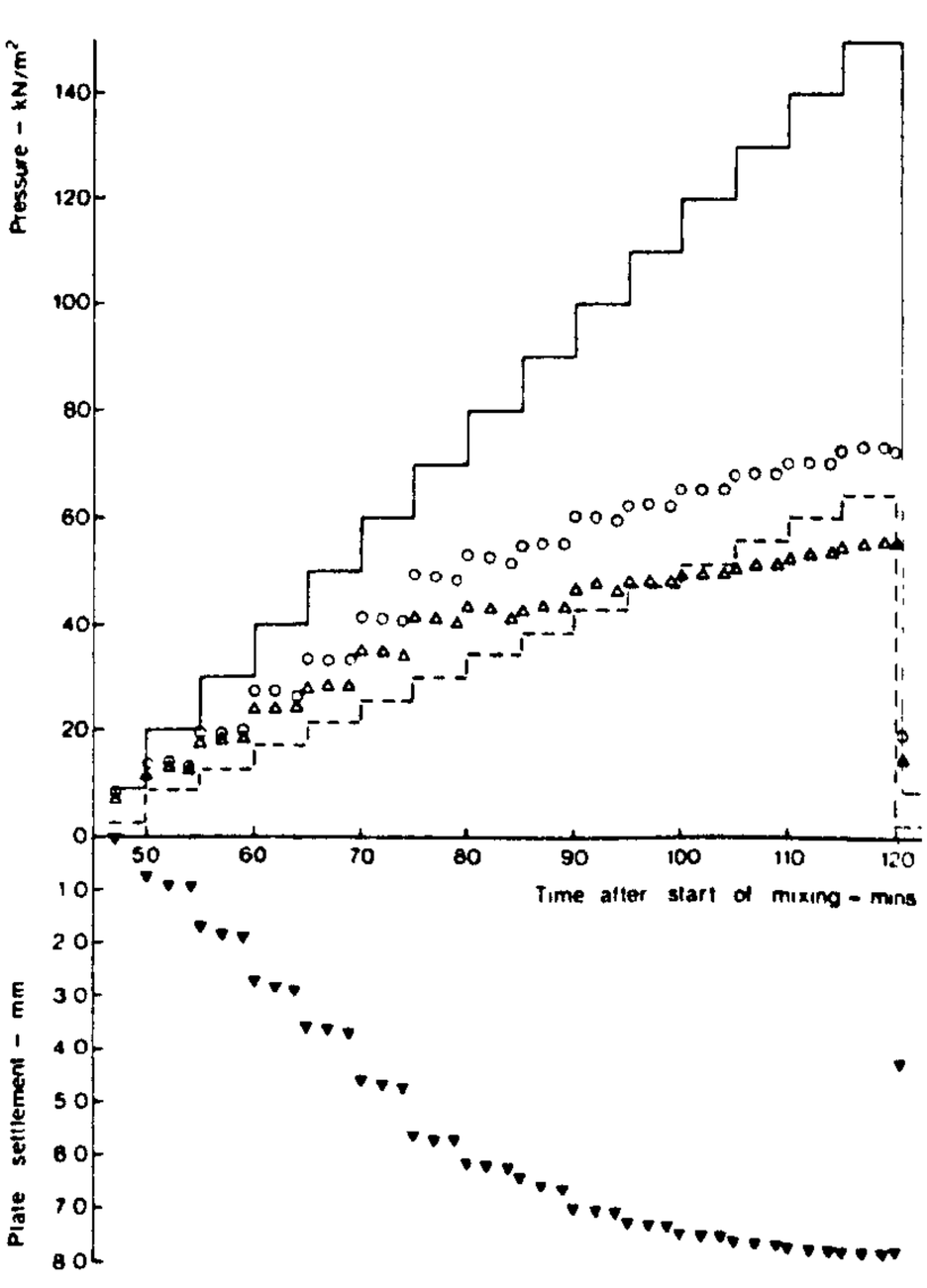

Figure 3 10 Test on the influence of cement chemistry - superplasticized concrete (R = 5·3 m/hr)

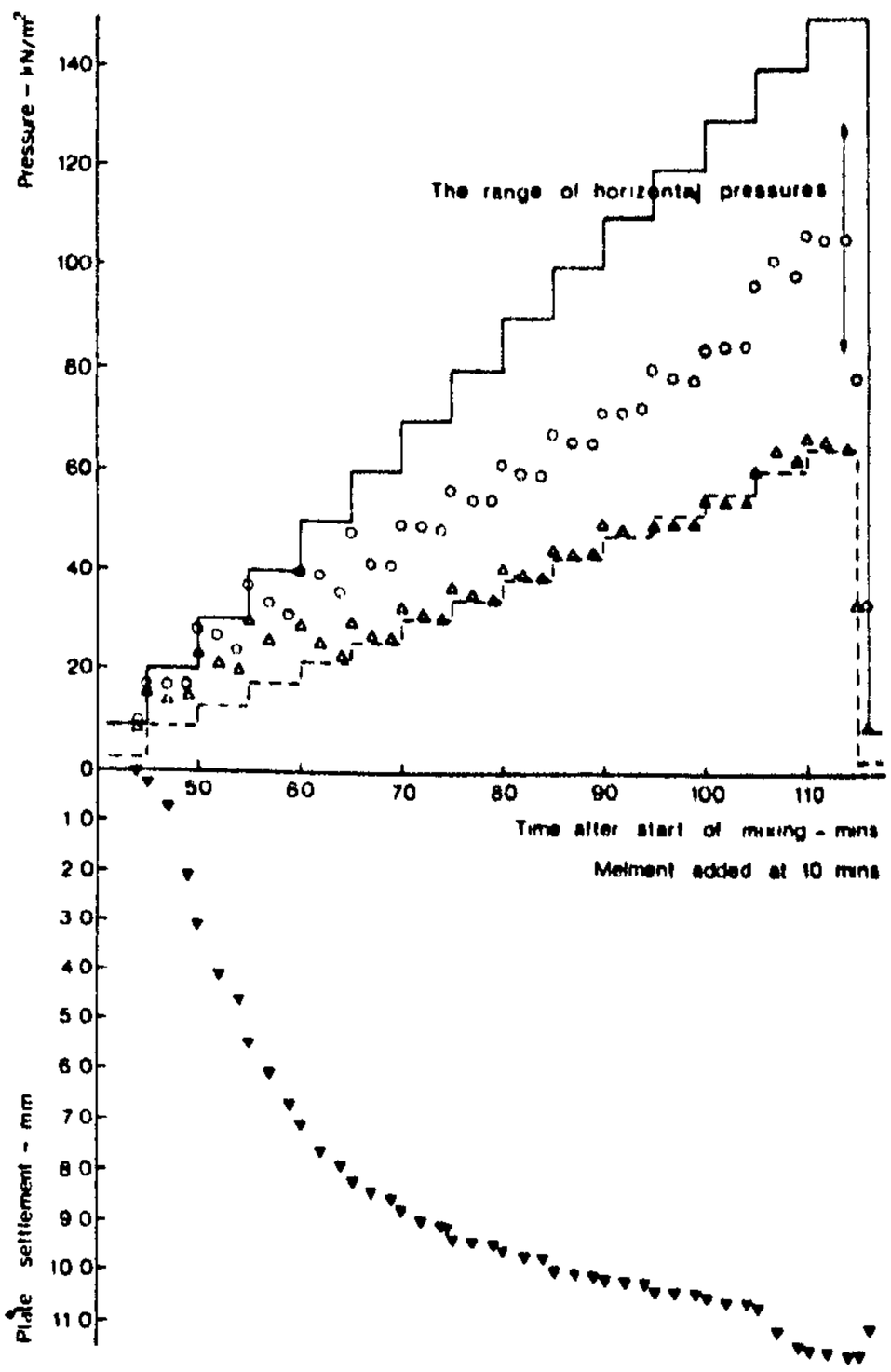

Figure 3 11 Tests on the influence of cement chemistry (R = 2 6 m/hr)

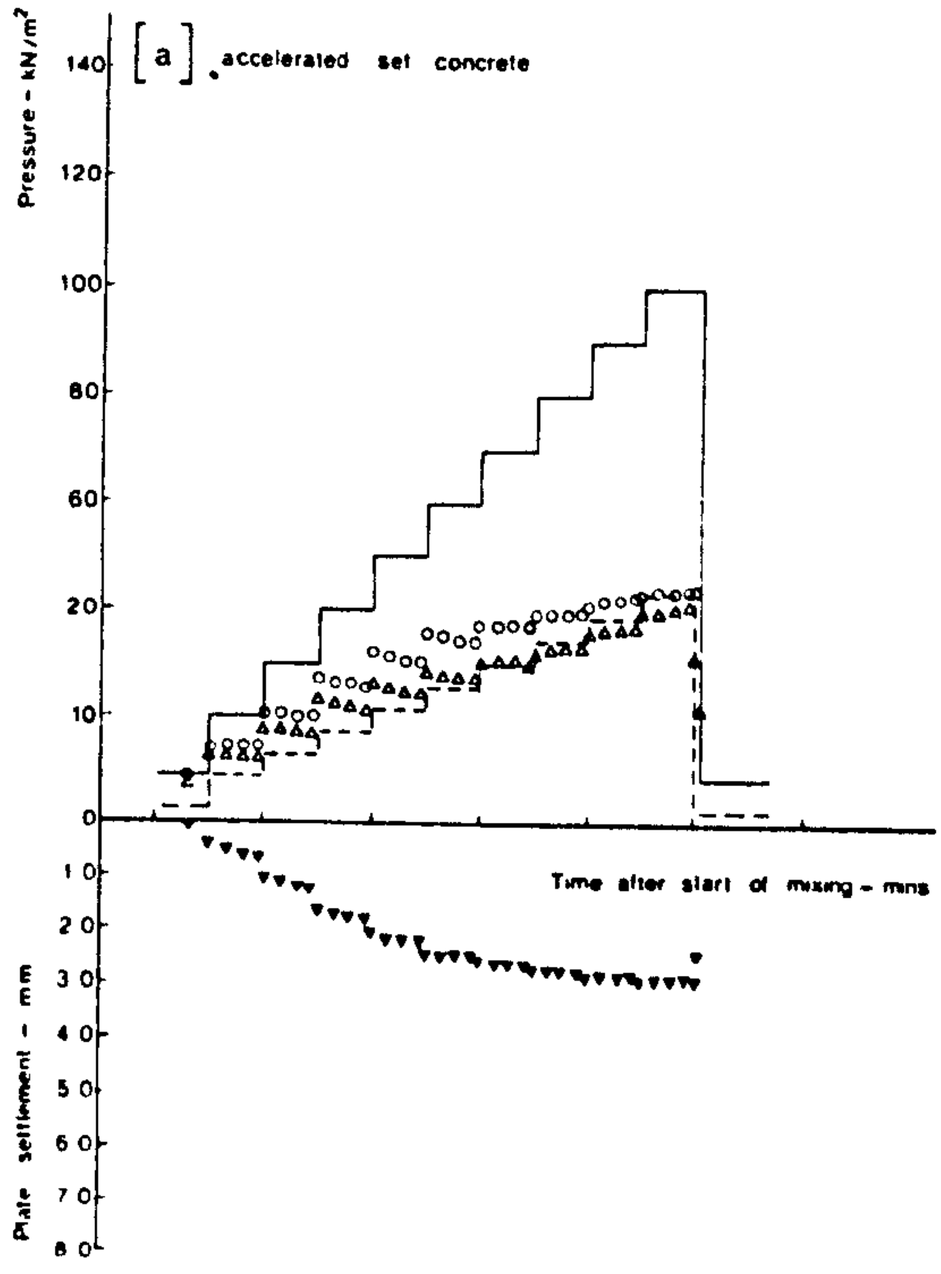

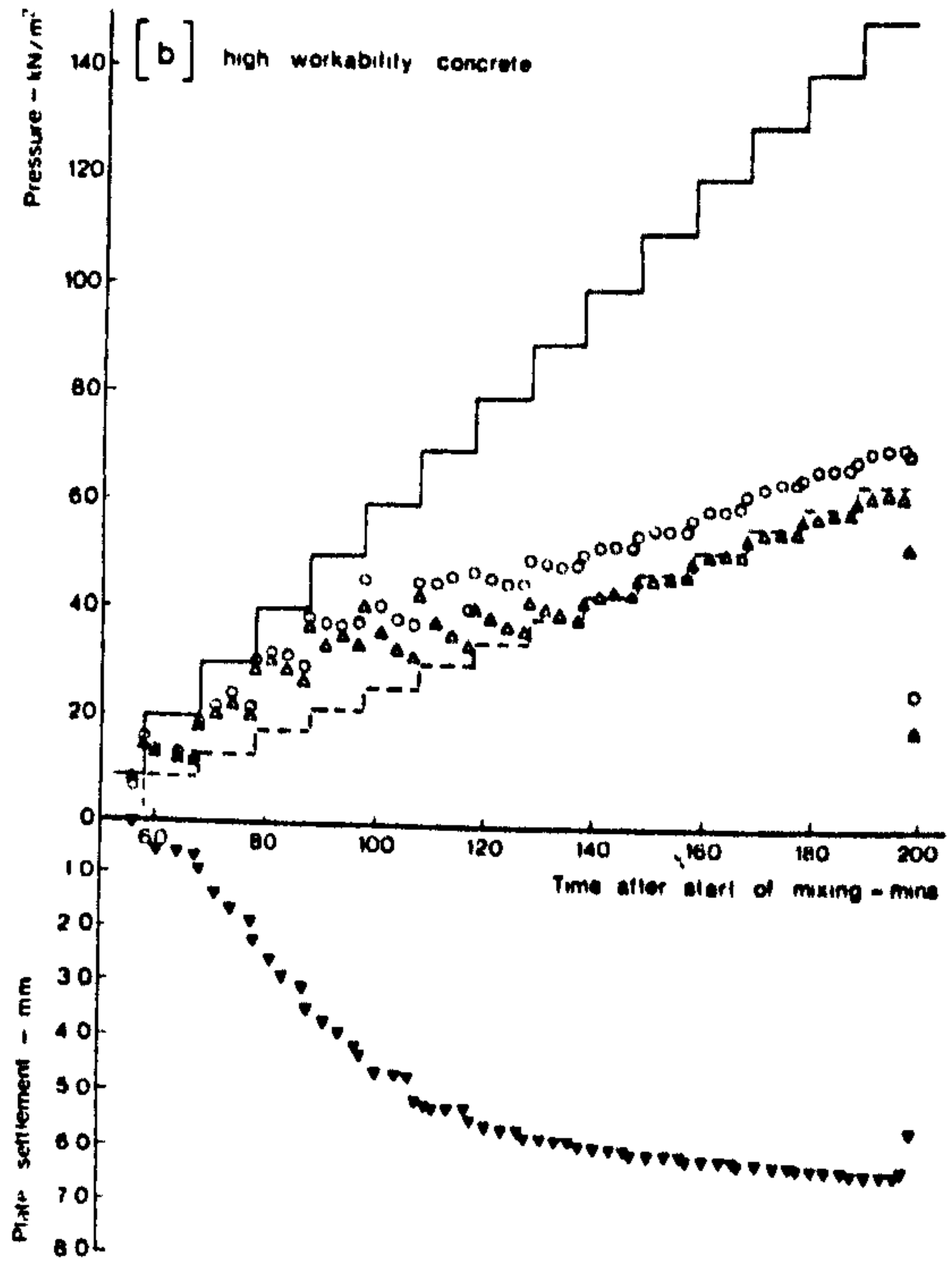

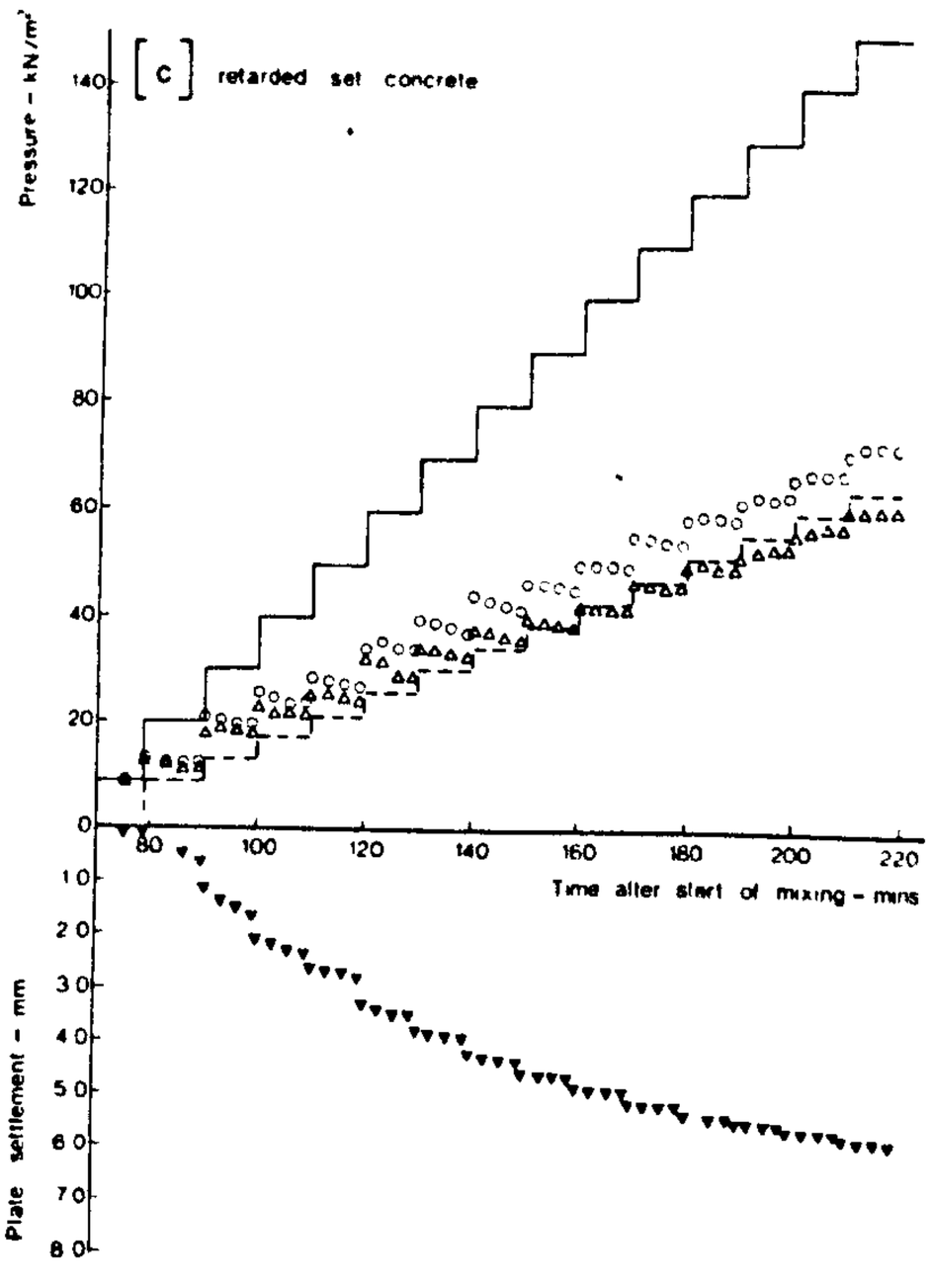

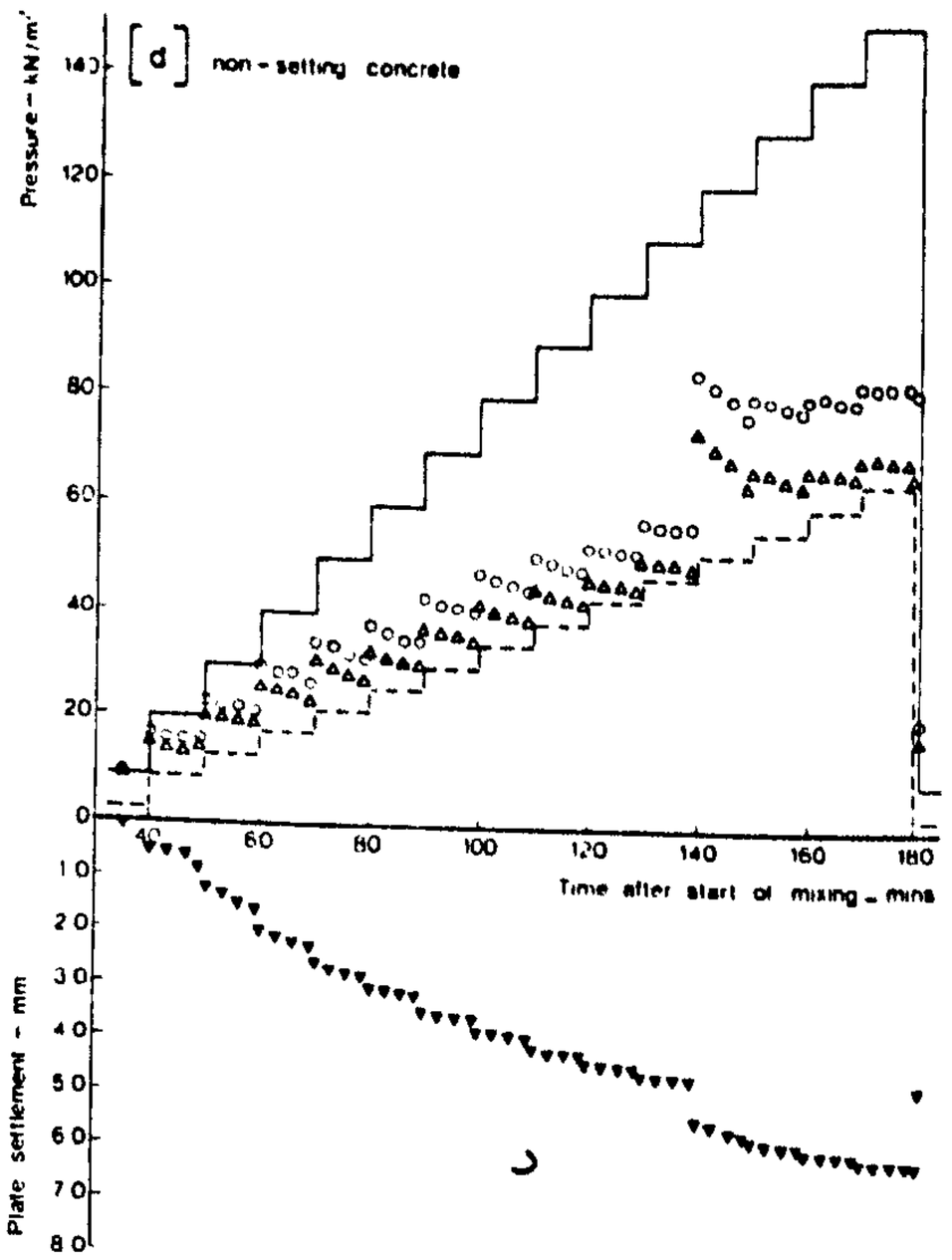

Figure 3 12 Tests on the influence of cement chemistry ' R = 1 8 m/hr '

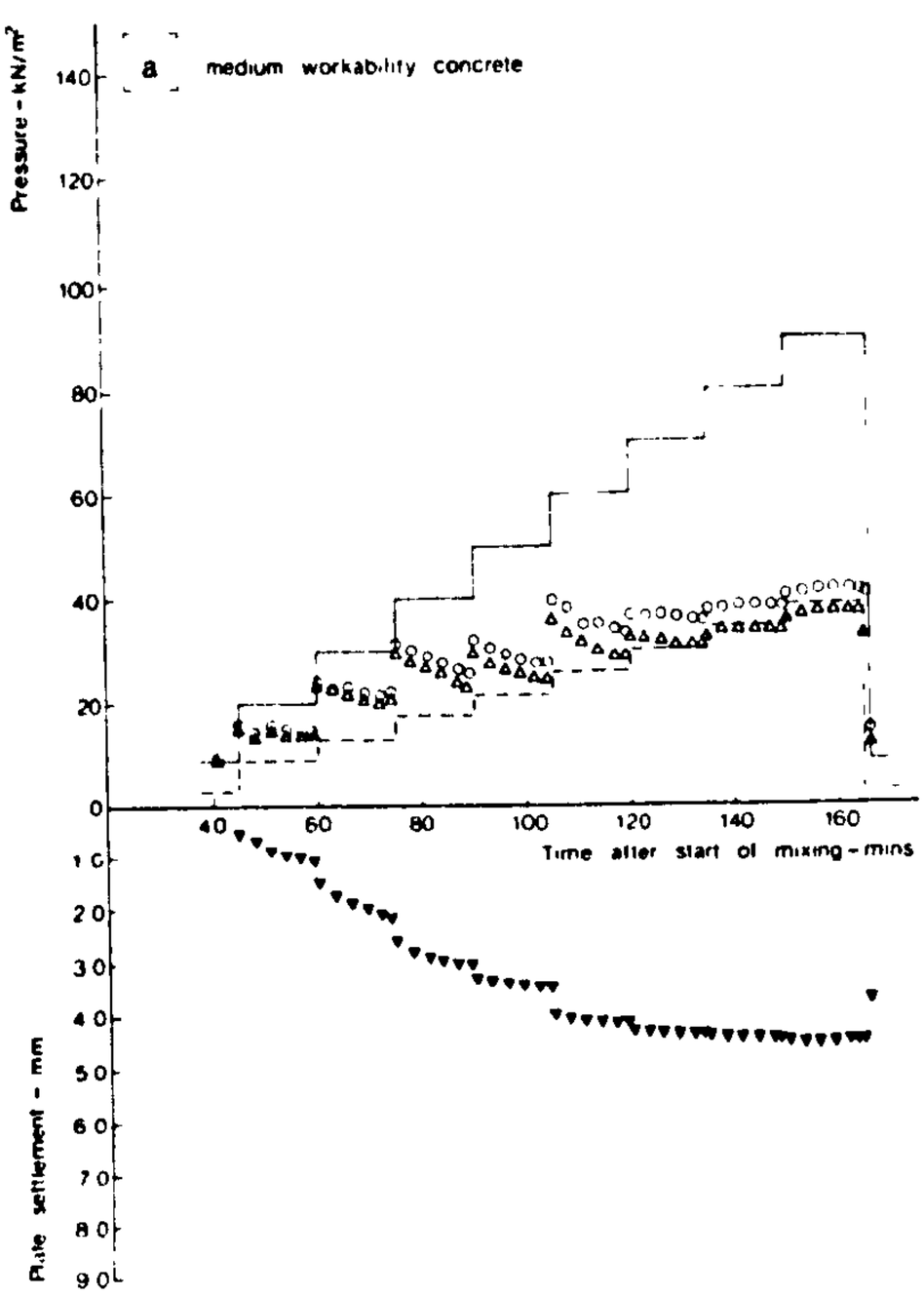

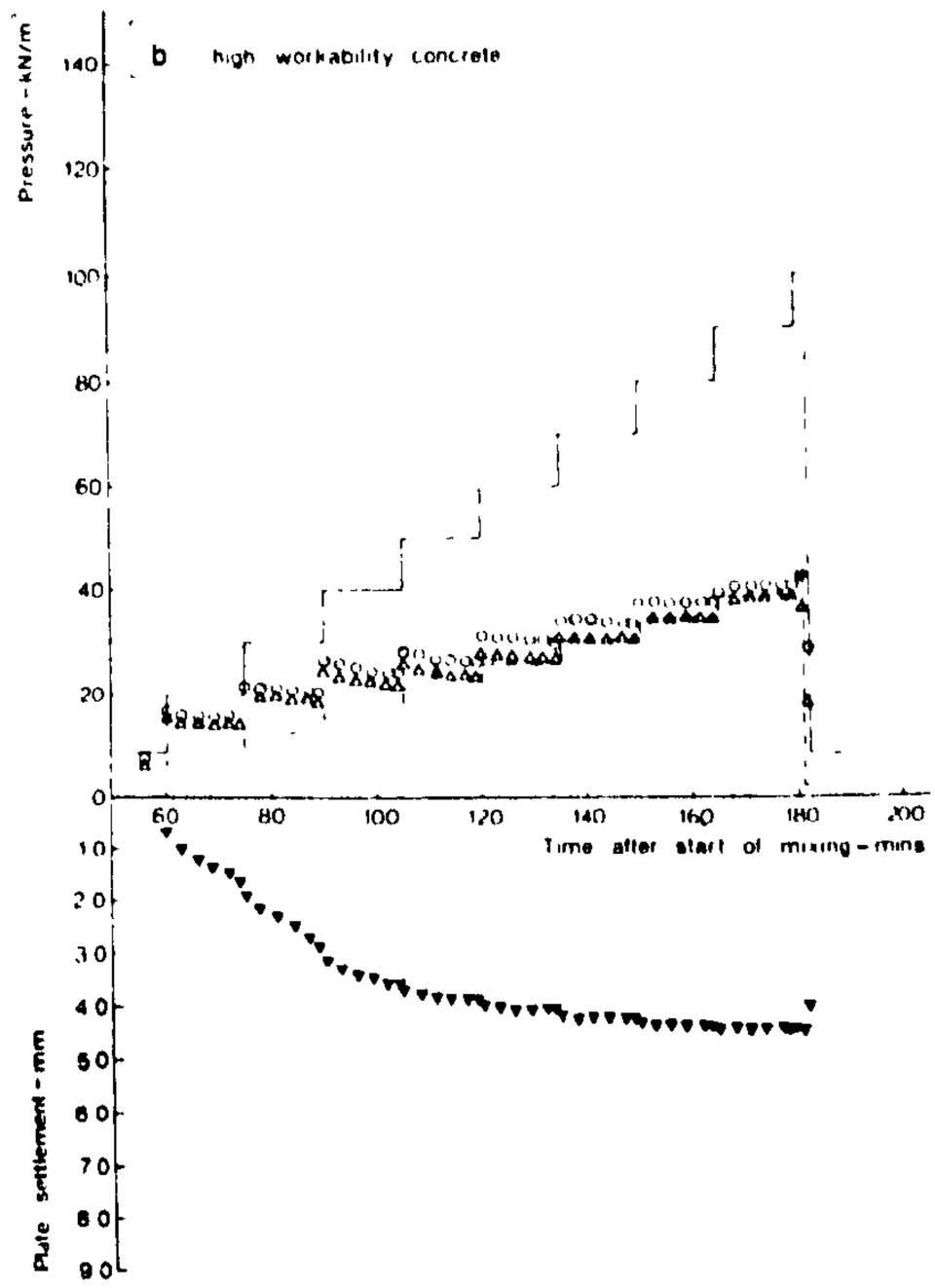

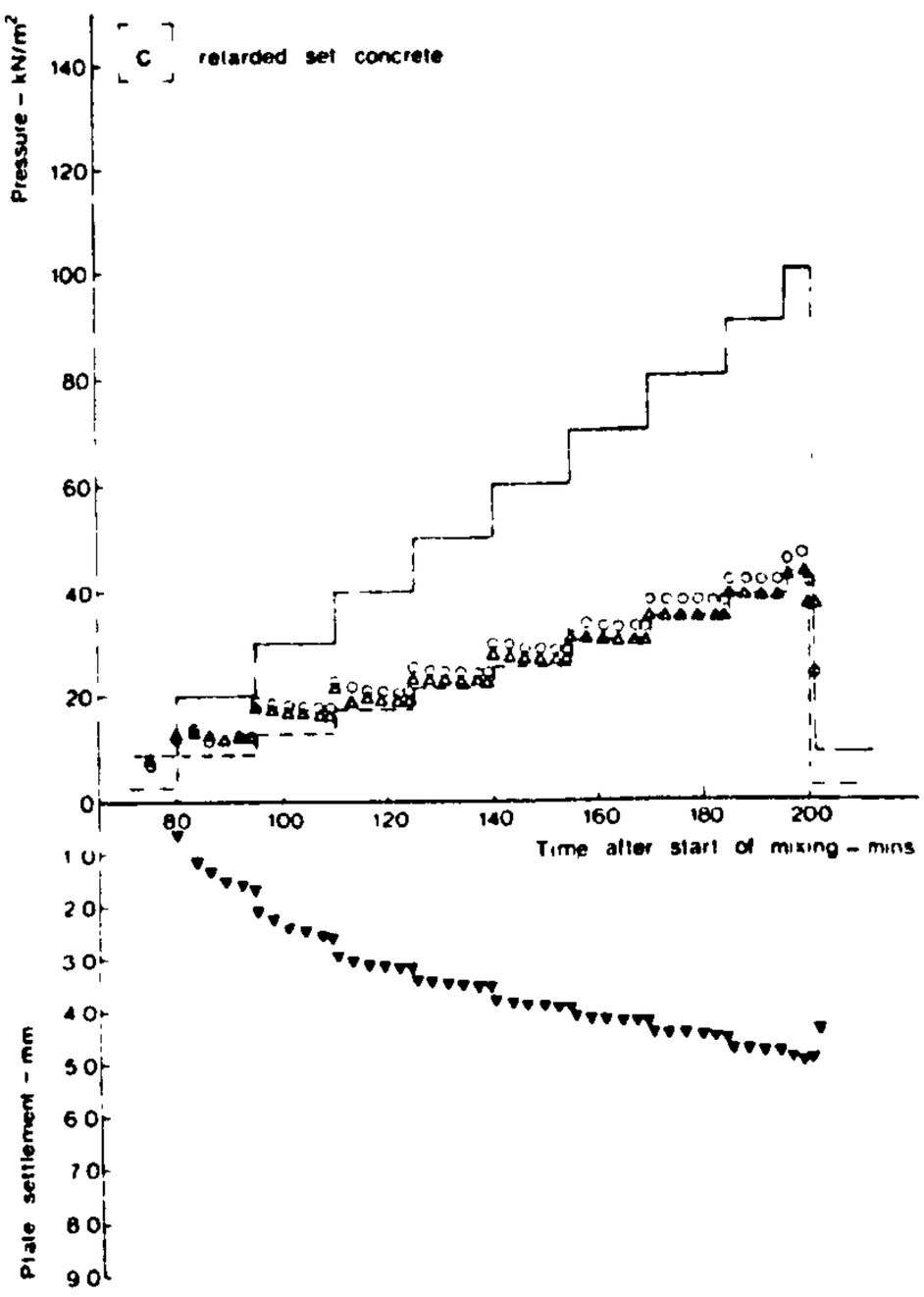

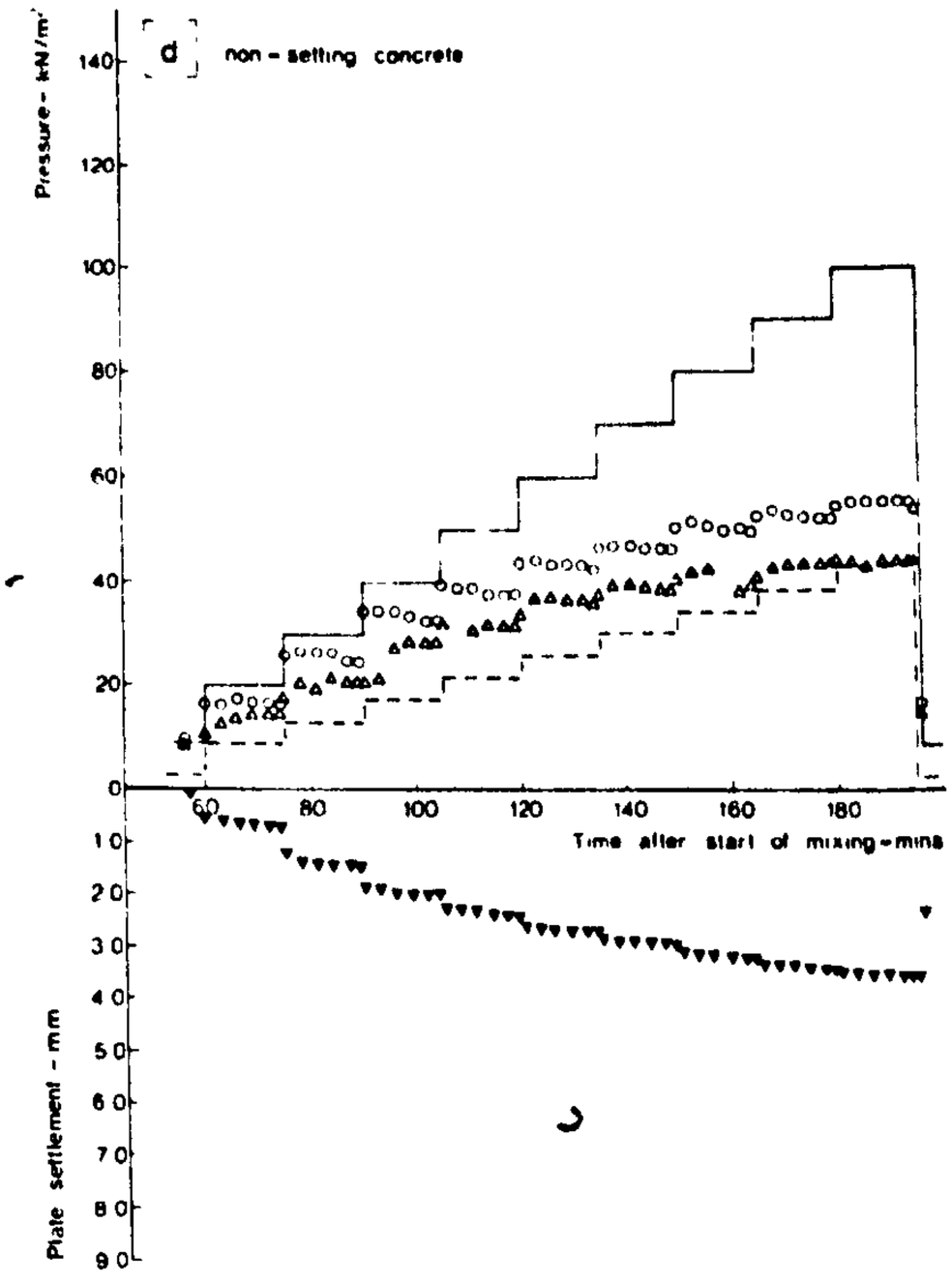

Figure 3.13 : Test on the susceptibility of the particle structure to vibration (R = 5·3 m/hr) – high workability concrete .

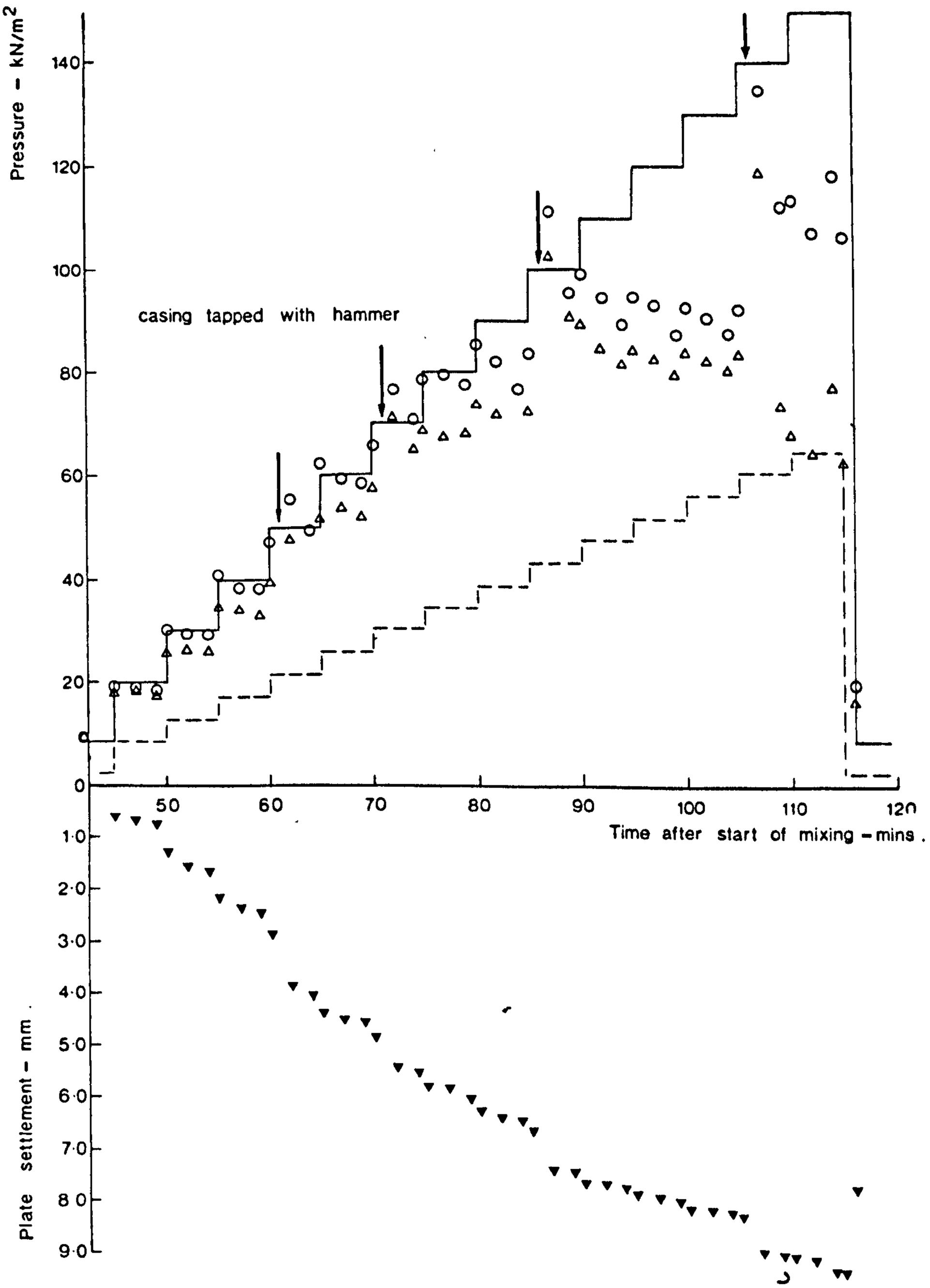

TABLE 3.3 The effects of vibration and time on the water movements within a column

Cube strength, N/mm^2	47.1	48.2	47.6	45.6	46.3
Slump of the concrete, mm	30	25	30	25	20
Diameter of the internal poker, mm	50	25	25	25	25
Time of vibration, minutes	4	4	4	5	6
Rate of placing, m/hr	14.4	14.4	14.4	12	12
Period between completion of placing and sampling from the column	5 min.	5 min.	35 min	1 hr 5 min	2 hr 5 min

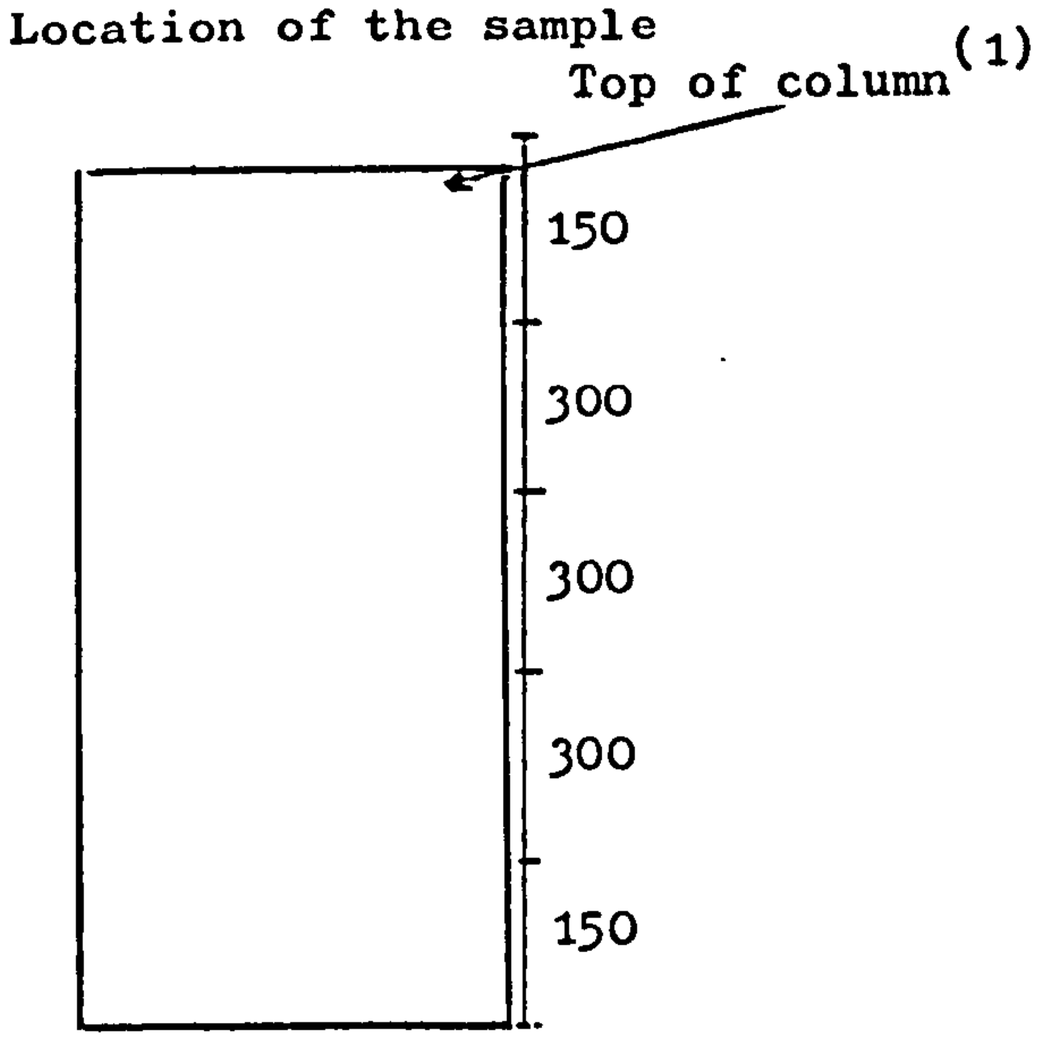

Notes

1. The free standing water and laitence were removed prior to sampling.

2. Water was lost through the joint between the column and base.

of results and in most respects consistent numerical values. Frequent calibrations of the instruments showed that the applied loading and recording systems were reliable and therefore there are no general grounds for doubting the numerical values obtained from the tests. Faults in the instruments gave such gross errors they could be spotted very quickly. During the tests, the piezometers were bled to remove any air or sediment that had collected in the system and sometimes after bleeding there was a sudden drop in pressure for one or two readings. This was normally obvious when the pattern of results was studied and these anomalous results have been omitted from the graphs.

The response of the horizontal pressure gauges and piezometers to the loading of the concrete was consistent in pattern and, in general, consistent in magnitude. The initial tests where just a water pressure was applied (8 tests) or where both a plate and water pressures were applied (3 tests) gave very consistent results due to the dominant role of the pore water pressure. A test in which plate pressure only is rapidly applied, Figure 3.4(a), is the situation in which a wide scatter of results should be expected as the resultant pressures are changing very rapidly during the first few minutes of test and they are only being intermittently recorded. With this type of test, two similar experiments gave maximum horizontal pressures of 117 and 103 kN/m^2.

The plate settlement results are not so consistent. The pattern of results gives the typical consolidation curve[15] but the magnitudes of the settlements are not consistent (compare the magnitudes of settlement in Figures 3.7, 3.11 and 3.12). This inconsistency in the magnitude of settlement is believed to be partially due to the experimental technique, but mainly due to the nature of concrete. After the concrete had been placed and the rig fully assembled, a set of readings was taken. These readings were called zero settlment, but already the weight of the porous plate would have caused some settlment. Differences in the time taken to assemble the rig and in the bedding conditions of the plate would affect the 'zero settlement' point, but these effects would be confined to the first segment of the settlment curve. The main cause of these differences in the magnitude of settlment is believed to be due to the nature of the particle structure being formed. The consolidation obtained with the pressure bleed test.

(Appendix A) proved that the concrete in the test rig was not fully consolidated and therefore the particle structure must be in some intermediate stage of consolidation. The settlement required to form this metastable particle structure would not be the same even for two identical mixes. If two particles touched at a certain location in one mix, the chances of the two identical particles touching in the second mix would be slight. As a consequence of the random nature in which the particle structure is built, some variation in settlement should be expected.

As described in more detail later, the plate settlement readings provided a valuable link between the changes in the particle structure and the sudden jumps in the horizontal pressure which were observed in a number of tests.

Prior to building the rig, it was realised that the pore water pressure gradients obtained in full sized sections could not be reproduced in the test rig, but the rig also failed to reproduce the conditions within a full sized section in another important respect, the development of suction forces. King and Raffle[71] showed that from the time of mixing, cement pastes had the potential to develop suction forces. This important concept is described in detail in Chapter 4, but briefly these suction forces will change the role of water in concrete from a fluid with suspended solids to discrete pockets of fluid within a solid. These suction forces do not manifest themselves until a particle structure is developed, but then they can develop into powerful forces[71]. In the test rig, there was a reservoir of water above the porous plate, so as soon as these suction forces started to develop, water was drawn into the capillary spaces and the suction forçes were relieved.

The rate at which these suction forces are relieved depends on the permeability of the concrete, the path length, the rate of increase in applied water pressure and the potential rate of development of these suction forces. But in general terms, the reservoir of water will prevent the development of substantial suction forces in the test rig and consequentially the horizontal pressure does not fall substantially below the applied water pressure. As the applied water pressure was being increased continuously in the majority of the tests, the effect was to

produce a progressively increasing horizontal pressure and not the clear peak observed with site pressure measurements (see Chapter 2).

3.6.2 Initial tests

The experimental programme started by applying either a plate pressure, Figure 3.4, or a water pressure, Figure 3.5. Even when the plate pressure was applied very rapidly, Figure 3.4(a), the maximum horizontal pressure was less than the applied pressure. After the maximum, both the horizontal and pore water pressures decay rapidly. This is consistent with the theory given in section 4.2 which argues that the higher the hydraulic gradient (i.e. the change in pore pressure up the section), the quicker particle contact will be established. As there is no applied water pressure in Figure 3.4(a) the hydraulic gradient will be at a maximum and the hydrodynamic excess will disperse very rapidly. As the horizontal and pore water pressures fall, the pressure lines diverge and when the pressure in the hydraulic piston is removed, the horizontal pressure gauges register a pressure that is higher than the residual applied pressure. This can be explained by considering the movement of the diaphragm of the pressure gauge. As the pressure increases, the diaphragm deflects and water and solids move into the deflected shape, but when the pressure starts to decrease, the solid particles hinder the return of the diaphragm to the unstrained position and therefore the gauge continues to register a pressure. Whilst to every action there is an equal and opposite reaction, it is useful to consider that at this stage in the test, the gauge is causing a pressure on the concrete and not the concrete on the gauge. If the gauge and concrete were parted at this stage of the test, the gauge would return to its unstrained position, but the concrete would retain its deflected shape as the elastic strain recovery of the concrete would be minute. In Chapter 4, the application of this argument to formwork deflections and residual loads on formwork will be developed.

The application of plate pressure at low rates of loading produces a low maximum pressure, Figure 3.4(b). Again this is consistent with the theory given in section 4.2, as the rapid drainage plus time prevents the build up of a large hydrodynamic excess and therefore large horizontal pressures.

Figure 3.5 is the most interesting example from a series of tests with only an applied water pressure. Tests had shown that the water within the concrete and the reservoir of water above the plate were interconnected and that any change in the applied pressure was immediately reflected by an equal increase in the horizontal pressure.

The test shown in Figure 3.5 was to check if this relationship was time dependent. Water pressure was applied in increments up to a maximum of 116 kN/m^2. At each increment the horizontal pressure and plate settlement were measured (at this stage of the project the piezometers had not been installed). The pressure was held at 116 kN/m^2 for five minutes and then released. After 30 minutes without an applied pressure, the cycle was repeated. In Figure 3.5 and in all the other Figures, before a surcharge load is applied, the horizontal gauges register the fluid head of concrete. As the concrete had been recently internally vibrated, this was to be expected. In the test shown in Figure 3.5, the horizontal gauges started by responding immediately to changes in the applied water pressure, but as time progressed there was a delayed response. Towards the end of the test, the horizontal gauges did not reach the same pressure as the applied loading due to the short period in which the applied pressure was maintained. With a longer period of loading, the gauges would have reached the applied pressure. Examination of the concrete not used in the test rig showed that before the test was ended, the concrete was no longer workable. The interesting point to note from this test is that the concrete shows a progressive reducation in permeability and does not remain unchanged for a period of time (the dormant period) and then show a sudden change in characteristics at, say, the point at which the main reaction starts. After the first two cycles, there is little change in plate settlement and therefore the changes in permeability cannot be related to better compaction of the solids and must therefore be related to progressive changes in the hydration products.

When both a plate and water pressure are applied, Figure 3.6, the rate of decay in the horizontal pressure after the maximum is reduced to 27 kN/m^2 in 10 minutes compared with the 40 kN/m^2 in 10 minutes of Figure 3.4(a). By applying a water pressure simultaneously with a plate pressure, the hydraulic gradient up the section is reduced by an amount

equal to the manometer pressure and this will reduce the rate at which the hydrodynamic excess disperses and consequently the rate of reduction in the horizontal pressure.

Figures 3.4(a) and 3.6 show the pore water pressure provides the dominant contribution to the horizontal pressure. In Figure 3.4(a) pore water pressure accounts for 94% of the maximum horizontal pressure and in Figure 3.6, 83%. Even with the low maximum pressure in Figure 3.4(b), pore water pressure provides 78% of the maximum horizontal pressure.

3.6.3 Tests on the influence of cement chemistry

The series of tests given in Figures 3.7 to 3.10 are the most useful for studying the role of cement chemistry on formwork pressures. All these graphs are for an equivalent rate of placing of 5.3 m/hr. At lower rates of placing, Figures 3.11 and 3.12, the applied water pressure has dominated the results and therefore these figures provide less understanding of the processes involved.

The most noticeable feature of Figures 3.7 to 3.10 is their similarity despite the wide range of setting times. All of these graphs are similar with the exceptions of the non-setting concrete and the superplasticized concrete. A typical graph, say Figure 3.7(b), starts with the horizontal and pore water pressures following the applied plate pressure and then they fall away until the pore water pressure is equal to the applied water pressure and the horizontal pressure curve is parallel to, but slightly above, the applied water pressure curve. The existence of a pore water pressure in excess of the applied water pressure is proof of the existence of a hydrodynamic excess. The short drainage path and large hydraulic gradient (the difference between the pore water pressure and applied water pressure) causes this hydrodynamic excess to disperse rapidly. After this stage, further increases in plate pressure are taken by the particle structure and therefore only a small proportion of the load increment will be transferred into the horizontal direction (see Section 4.2). As discussed in Section 3.6.1, the reservoir of water above the porous plate hinders the development of suction forces, nevertheless in some of the figures, for example Figure 3.9, the rate of development of suction forces is greater than

the rate of increase in applied water pressure and consequently the pore water pressure falls below the applied water pressure. From Figures 3.7(a) to (c) cement setting appears to have little influence on the maximum formwork pressure, but because there is a difference between these figures and the non-setting concrete, Figure 3.7(d), it was deduced that cement chemistry was having some influence on the maximum formwork pressure. The early hydration of cement is reviewed in the next chapter and it is not an area that is particularly well understood at the present time. A current concept of the early hydration of cement is that in the first few minutes of reaction, the cement particles are coated with a dense layer of ettringite and then according to some authors[72,73] this layer of ettringite is recrystallised during the dormant period into long crystals that bridge the spaces between particles. The structure formed would be weak and liable to damage. At the end of the dormant period the main reactions start and the weak structure is quickly strengthened by long fibre calcium silicate hydrate (C-S-H). This strengthened structure is unlikely to be damaged by small disturbances. From Figures 3.7, 3.8 and 3.9 it is postulated that chloride based accelerators, hydroxycarboxylic acid based retarders and neutralised vinsol resin based air entraining agents do not significantly affect the re-crystallisation of ettringite during the dormant period. In the case of retarders, there is other circumstancial evidence that supports this hypothesis. When a concrete is retarded, it still has a loss of slump of a similar order to plain concrete[74,75]; the re-crystallisation of ettringite is a reasonable explanation of this phenomenon. In an attempt to prove that the structure of plain and retarded concrete were similar during the dormant period, some scanning electron micrographs of a cement paste with and without a retarder after 90 minutes of hydration were commissioned. The method of sample preparation was the same as reference (72). The interpretation of scanning electron micrographs is always difficult, but the two samples looked as if they would have similar mechanical properties. There was no clear evidence showing the re-crystallisation of ettringite, but the use of the dry test method could have destroyed this evidence. Imperial College are developing a wet test method of taking scanning electron micrographs, but for this the samples have to be very dilute. The progress of their work is awaited with interest.

Figure 3·14: Scanning electron micrographs of cement paste after 90 minutes of hydration.

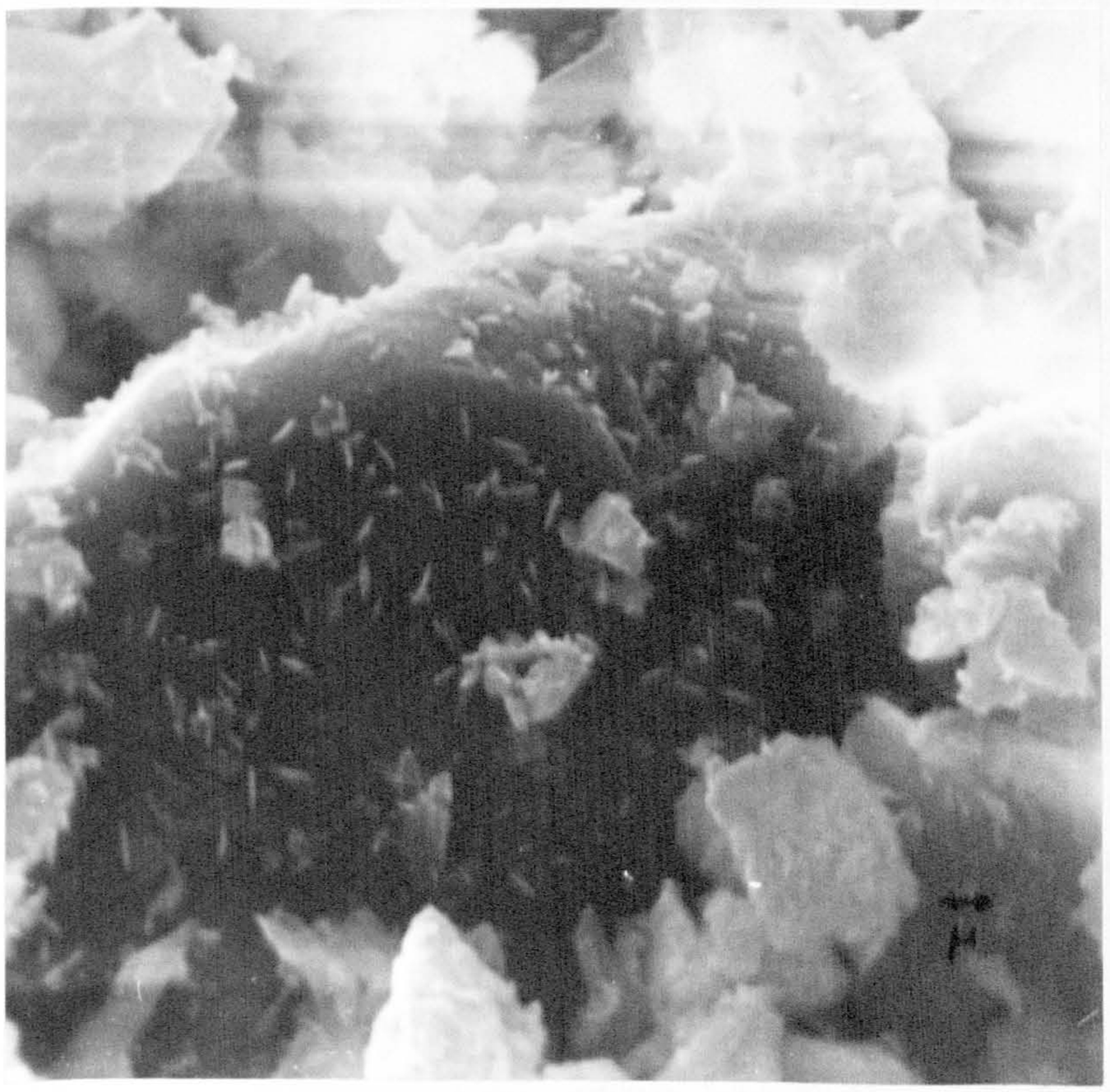

X 4800

plain OPC
(W/C = 0·55)

X 5000

same OPC with
Conplast R at
0·72 ml/l
(W/C = 0·55)

Apart from the non-setting concrete, the only tests which did not fit the general pattern of results were those with Melment. Three tests were completed, one being shown in Figure 3.10. Melment deflocculates the cement grains[68] and therefore the solid particles should pack together more closely and give larger than normal plate settlements. This deduction was confirmed by the experiments.

Only two of the horizontal gauges were working during the tests with Melment and in all cases there was a wide discrepancy between the two gauges. In Figure 3.10, this range of pressure readings is indicated. In the tests with Melment, the contribution to the horizontal pressure from the solid particles is higher than normal and the contribution from the hydrodynamic excess was very small. These results show that Melment produces high permeability in the concrete and rapid drainage and that it reduces the cohesion of the concrete. The concrete appears to act as a saturated granular material during the period in which the Melment is effective. The horizontal pressure comes from the pore water pressure plus a component from the particle structure. The thrust from the particle structure is not uniform and it will have peaks and troughs depending on the particular particle arrangement, but whilst its contribution to the horizontal pressure is small, the variation between pressure gauges at the same level will be small. With Melment concretes, the particle structure provided a substantially higher proportion of the horizontal force and consequently a higher scatter of pressure readings.

When the period between pressure increments was increased, Figures 3.11 and 3.12, the hydrodynamic excess had time to disperse and the horizontal pressure was controlled by the applied water pressure. Figures 3.11 and 3.12 demonstrate that as the applied pressure is maintained, both the pore water pressure and horizontal pressures fall. This provides an important confirmation of the pore water theory for formwork pressures; as the hydrodynamic excess disperses, the load is transferred onto the particle structure and as the particle structure only transmits a proportion of its load in the horizontal direction (pore water pressures are equal in all directions), the horizontal pressure falls.

3.6.4 The role of vibration on formwork pressures

The literature survey was inconclusive on the role of vibration in formwork pressures. Ritchie[51] and others[3] stated that the initial period in which the horizontal pressure followed the fluid head was due to vibration, but this statement is not consistent with the effective zone of vibration. As this association between vibration and the horizontal pressure following the fluid head of concrete is one of the major facets of the previous theories on formwork pressures and as the author had argued in Chapter 2 that this relationship is invalid, experimental proof of this claim was necessary. This proof came from two sources.

Apart from the initial compaction, the concrete was not vibrated during the tests that have just been reported. During rapid loading, Figures 3.4(a) and 3.6, the horizontal pressure before it reached its maximum, was of the same order as the fluid head of concrete. This showed that it is possible to produce the fluid head without vibration.

The next piece of evidence comes from the tests on water movements in five 1.2 m columns, Table 3.3. Five 1.2 m columns were cast in the laboratory to check the effects of vibration and time on the water movements within a column. The columns were cast by the same two experienced technicians and then at the previously decided time after placing, the columns were turned on their side and directly sampled. The mass of the samples was of the order of 3 kg and they were dried to constant weight at 105°C. From the original free water content of the concrete, the percentage water gain or loss was calculated. The weights were recorded to the nearest gram and this gave an accuracy of $\pm$ 0.33 percent. From the results taken immediately after vibration, columns 1 and 2, the water movements do not show an overall water movement up the column, but tend to form layers. If internal pokers have a large effective zone, localised irregularities in vibration would be small and there would be an overall water movement up the column. These two columns confirmed the localised nature of vibration and showed that the more powerful 50 mm diameter poker caused greater water loss than the less powerful 25 mm diameter poker.

Columns 3 to 5 were all compacted with the 25 mm diameter poker and then left for various periods before sampling. The clear lack of an overall pattern in the results shows the difficulty in reproducing identical starting conditions and the inability of water flow due to the hydrodynamic excess to remove the irregularities in the water content. This last observation may be due to the columns only being 1.2 m high, but it would be reasonable to assume that even in tall sections, these initial differences in water content would not be removed completely. Because of the localised nature of these water movements, it would be impossible to predict the water content at a particular location in a section and the water content affects the time taken to develop a particle structure. These variations in water content could be one of the reasons for the variation in the maximum horizontal pressure within a single section (see Chapter 2).

In a number of graphs, for example Figures 3.7(c) and 3.11(d), there were sudden jumps in the horizontal pressure which were coincident with jumps in the pore water pressure and plate settlment. These are exactly the results that would be obtained from a sudden collapse of the particle structure; some of the vertical load would be transferred onto the pore water and this gives an immediate rise in the horizontal pressures. The sudden jumps in pressure appears to be random within the test period, but they are more prevalent in the retarded and non-setting concretes. There were no sudden pressure jumps in the later stages of the experiments with accelerated set concretes. At this stage of the test, this concrete was not workable and it had 'set'[30,58]. The results indicate that pressure jumps are limited to the period before setting.

There was a reasonable amount of evidence indicating that the particle structure within the concrete was weak (see Chapter 4) and therefore a simple increase in head could be sufficient to cause the particle structure to collapse. Collapse could also be induced with weak vibration, Figure 3.13, or by deep re-vibration, Figure 3.15. The characteristic sharp peak in the horizontal pressure indicates that the particle structure quickly re-establishes itself.

The length of time in which an area of formwork is susceptible

Figure 3·15 The effect of deep re-vibration on three pressure gauges placed 400 mm above the base of a large column.

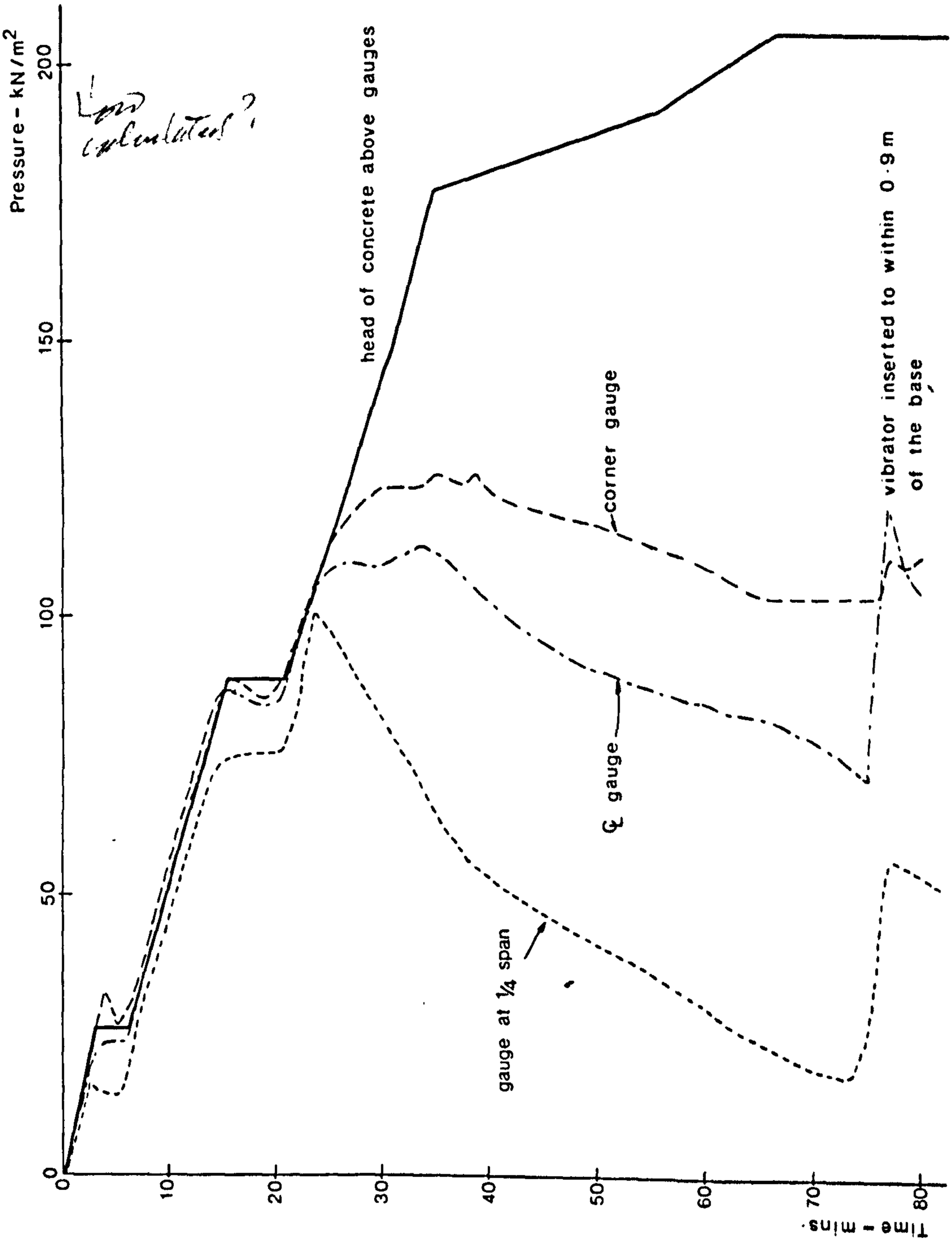

to sudden pressure increases appears to depend on the setting time of the concrete. Even after the main reactions have strengthened the weak particle structure, it would be susceptible to some level of loading, but the probability of achieving this loading would be small. The time between forming a weak particle structure and setting can be considerable. The pressure on the formwork could therefore range between that produced at the moment of forming the first weak particle structure to that obtained by assuming sufficient disturbances to produce the fluid head right up to the time of setting. Neither of these two extremes would form a practical basis for design, one being an unsafe assumption and the other being too conservative. Because the development and stability of a particle structure is such a haphazard event, site pressure measurements will produce a wide scatter of results. This could explain some of the scatter of results in Figure 2.19. Even within the same section the pressures will not be uniform. For example, if a strip of concrete were discharged at one point, this could cause a localised collapse of the particle structure and a localised increase in the horizontal pressure. As the structure rapidly reforms after a collapse, by the time the next strip is discharged the pressure at the first location is receding. Pressure gauges at the two locations would have given different results. For the economic design of formwork, a balance between the theoretical possibility of a pressure increase and the probability of it occurring, needs to be made. Site pressure measurements are the only reliable way of achieving this assessment of risk.

3.7 CONCLUSIONS

1. The experimental technique developed gave reproducible horizontal and pore water pressure distributions. Plate settlments were similar in shape, but variable in magnitude; this was mainly due to the nature of concrete and not the experimental technique.

2. The tests did not reproduce the conditions within a large section.

3. With the concrete loaded with just plate pressure, the horizontal pressures were less than the applied pressure even at high rates of loading. With slow rates of loading, the horizontal pressure

was very low.

4. When the concrete was loaded with just water pressure, the horizontal and pore water pressures followed the applied pressure. At first the response was immediate but at later ages, with a delayed response.

5. The permeability of concrete changes gradually throughout the dormant period.

6. When concrete was loaded with both plate and water pressure, the rate of fall in horizontal and pore water pressure was a function of the hydraulic gradient. The higher the hydraulic gradient, the more rapidly the pressure will reduce.

7. The horizontal pressure consists of a component of the vertical load taken by the particle structure and the pore water pressure.

8. The pore water pressure provides the dominant contribution to the maximum horizontal pressure. For the tests with plain concrete, 78 to 94% of the maximum horizontal pressure came from the pore water pressure.

9. The chemistry of cement contributes to the development of horizontal pressure in at least two ways; firstly by producing progressive changes in structure during the dormant period and secondly by controlling the time at which the initial structure is reinforced with C-S-H.

10. In these tests, accelerators, retarders and air entraining agents had little effect on the formation of the initial particle structure, but they did influence the period in which this structure was susceptible to disturbance.

11. Melment concretes developed only a small hydrodynamic excess and the particle structure gave a significantly higher than normal contribution to the horizontal pressure. The horizontal pressures were higher than in similar tests with plain concrete.

12. There is no relationship between the depth to which the horizontal pressure follows the fluid head and the effective depth of

vibration.

13. Internal vibration causes localised variations in water content and not an overall water movement up the section.

14. The initial particle structure is weak and it can be broken by head increases or weak vibration. This causes a sudden jump in the horizontal and pore water pressures. After disturbance the particle structure quickly re-establishes itself.

15. The horizontal pressure in a section could vary from that given at the time of creating the initial particle structure to the fluid head just prior to setting. Even at one level, the pressure could be variable depending on whether the particle structure was stable or had just collapsed.

16. Site pressure measurements are the most reliable way of assessing the probability of disrupting the particle structure and the level of the consequential jump in horizontal pressure.

Chapter 4. A THEORY OF CONCRETE PRESSURE ON FORMWORK

4.1 REVIEW OF THE EARLY HYDRATION OF CEMENT

Portland cements consist of four main compounds, tricalcium aluminate (C_3A), tetracalcium aluminoferrite (C_4AF), tricalcium silicate (C_3S) which is also known as alite, and dicalcium silicate (C_2S) which is also known as belite. Small amounts of gypsum, free lime, moisture, magnesia and other minor compounds complete the composition. The 'minor' in minor compounds refers to the proportion of these compounds and not to their significance in the hydration process. Some of these minor compounds have a major influence on hydration.

The proportions of these compounds vary, depending not only on the type of cement but also on the source of raw materials (Table 4.1). British Standards do not define the proportions of the main compounds directly except in a few specific cases. For example, the hydrated tricalcium aluminate is the compound susceptible to attack by sulphates and therefore in sulphate resisting Portland cements it is limited to a maximum of 3.5 percent[76]. Some indirect control of the proportions of the compounds is obtained from the lime saturation factor[76,77]. This effectively puts limits on the ratio of tricalcium to dicalcium silicates. The proportions of the minor compounds are fixed in the British Standards, except for the moisture content. Some control on this is given by the loss on ignition test.

Frequently the main compounds are not 100% pure. Molecules of alumina can be replaced by molecules of silica and some investigations[78,79] have shown a tricalcium aluminate with 20% of aluminate replaced by silica. Strictly speaking this compound should be classed as a aluminosilicate.

The ground particles of cement clinker contain all the main compounds of the cement but not the gypsum. This is an interground material added in carefully controlled proportions to regulate the rate of setting.

When water is added to anhydrous cement, a complex series of reactions is started which continue for many years. The principal

TABLE 4.1 Typical compound proportions of some Portland cements

Compound	Compound abbreviation	Portland cement type					
		Ordinary			Sulphate resisting	Low heat	White
		A	B	C			
Tricalcium silicate (Alite) $3CaO \cdot SiO_2$	C_3S	35	40	57	43	30	51
Dicalcium silicate (Belite) $2CaO \cdot SiO_2$	C_2S	34	29	16	28	41	26
Tricalcium aluminate $3CaO \cdot Al_2O_3$	C_3A	8.5	14	9	2.5	2	11
Tetracalcium aluminoferrite $4CaO \cdot Al_2O_3 \cdot Fe_2O_3$	C_4AF	10.5	8	7	19	19	1

The remaining material is made up of gypsum, free lime, magnesia, moisture and other compounds.

stable hydrates are given by the generalised form of Brandberger's formula[80]

$$c\ Ca(OH)_2 \cdot s\ SiO_2 \cdot a\ Al(OH)_3 \cdot f\ Fe(OH)_3 \cdot n\ H_2O$$

where c, s, a, f and n are in general whole numbers.

The hydroxyl groups, OH, are no longer those of water and are generally not evaporable at 100°C even at low vapour pressures. The H_2O molecules whilst slightly distorted are still those of water and can be removed or replaced relatively easily.

The aluminates are the most soluble of the cement compounds[81] and these react with the sulphate to form ettringite ($3CaO\ Al_2O_3\ 3CaSO_4\ 31H_2O$). The aluminates influence the initial stages of hydration whilst the silicates are responsible for the strength development. Most of the early strength of cement comes from the hydration of the alite and Joisel[81] managed to show the similarity between the rate of water penetration into alite and the early gain of strength of the cement paste. Belite liberates less lime and hydrates in a similar manner to alite, but slower. Therefore its main contribution to the hydration process is in the long term strength gain of cements. As only the first few hours of hydration are relevant to the subject of this thesis, the rest of this section will concentrate on the hydration processes during this period.

The early hydration of cement is not fully understood and a number of theories exist which explain the mechanisms involved. There is agreement that the early hydration starts with a short burst of reaction between the water and cement in which a small quantity of ettringite and calcium hydroxide are formed. A 'dormant' period follows in which the concrete becomes stiffer and this in turn is followed by the start of the main reactions and the concrete rapidly gaining strength. The dormant period is of particular interest as this is the normal period for placing concrete in formwork.

A number of theories explain why there is a dormant period in the hydration process, what occurs during this period and the mechanism (s) that terminate it. Portland cements contain gypsum as an interground addition to control the setting process and one theory[81] describing the dormant period is based on the effects that gypsum

($CaSO_4 : 2H_2O$) has on the solubility of clinker in water. In water, calcium sulphate ionises into a calcium cation and a sulphuric anion and the solution effectively becomes a weak acid which promotes the dissolving of lime from the silicates and consequently accelerates the hydration of the calcium silicates. On the other hand, the sulphuric anion slows down the dissolving of the alumina and ferric oxides in the C_3A and C_4AF (see Table 4.1 for the standard compound abbreviations) and it therefore acts as a retarder with respect to these compounds. As the C_3A and, in low C_3A cements, C_4AF control the setting process in Portland cement, the net effect of gypsum according to Joisel[81] is that of a set retarder. The sulphate in the pore water retards the dissolving of the C_3A and reacts with it to form ettringite (trisulphoaluminate). Once all the sulphate has been consumed, the C_3A continues its hydration unhindered and this point would be described as the end of the dormant period. Joisel[81] emphasizes that the main mechanism controlling the dormant period is the gypsum acting as a solubility reducer, but acknowledges that the process can be aided by a secondary mechanism in which the reaction products of the C_3A and gypsum form a relatively thick gel over the cement grains and impede the migration of ions from the clinker.

Joisel's theory depends on there being a progressive reduction of the sulphate in the pore water to zero at the end of the dormant period. More recent research[72,73] has shown that this is not the case; the sulphate content of the pore water was found to reach a maximum value within the first few minutes of mixing and then remain at this value for about 6 hours after which it decreased rapidly. These same researchers showed that although the initial paste was much stiffer, ground clinker without added gypsum still exhibted a dormant period. The dormant period of C_3A was practically unchanged by the addition of gypsum to the clinker, but the addition of gypsum reduced the dormant period of calcium silicates. This last observation is in agreement with Joisel[81] who claimed that gypsum acts as an accelerator on silicates. Locher, Richartz and Sprung[72] concluded that the dormant period in the hydration process could not be attributed to gypsum.

Skalny[82] suggests that the dormant period in silicates is due to a diffusion process within the original boundaries of the cement

grains. When water and calcium silicates first come into contact there is a rapid loss of calcium ions from the surface layer of the grains resulting in a silicate rich layer between the unaffected core of calcium silicates and the calcium rich pore water. This layer slows down the rate of migration of the calcium ions into solution. Because of the lack of nuclei or supersaturation, hydration products are not formed until the critical levels are reached. When these are reached, the reaction proceeds at an accelerated rate thus ending the dormant period. Again it is the work of Locher et al[72] that puts doubt on this theory. They showed that after the initial reaction, the calcium content of the pore water does not change in the first few hours; Skalny's theory depends on there being a gradual increase in the calcium content of the pore water. They also showed experimentally that the retarded formation of nuclei for the crystallization of the hydration products could not be the cause of the dormant period.

Locher et al[72] proposed a theory for the early hydration processes based on the temporary obstruction of the surface of the cement grains. In the first few minutes of hydration a small quantity of calcium hydroxide and ettringite are formed. The ettringite forms a thin dense layer over the cement grains preventing further immediate reaction (in clinker without added gypsum, some of the calcium aluminate hydrate does not coat the cement grains but forms an open structure that bridges the pore spaces and rapidly stiffens the concrete). The thin layer of ettringite over the cement grains leaves them free to move in relation to each other. No new hydration products are formed during the dormant period, but the ettringite formed in the first few minutes of reaction, re-crystallises into long crystals that bridge the spaces between the solid particles causing a progressive stiffening of the cement paste. As the ettringite is re-crystallised, the obstruction to the surface of the cement grains is removed and the hydration reactions start for all the clinker compounds.

One check on the validity of a theory is to see if it presents a reasonable explanation of other observed phenomena. In this case Locher et al's[72] theory does offer a reasonable explanation of the slump loss in concrete. Slump loss[74,83,84] is the normal loss of workability during the dormant period; the process of re-crystallization of ettringite would produce a progressively stiffer concrete and

consequently a reduction in slump with time. Concretes with retarders also have slump losses[83,84] which suggests that the re-crystallization of the ettringite is not affected significantly by the retarder, but that the retarder is still capable of delaying the start of the main reactions, perhaps, by forming a slightly thicker layer of primary hydrate.

An attempt to photograph the re-crystallization of ettringite, Figure 3.14, failed, but as already stated in Chapter 3, this could have been due to the dry testing technique. As previously mentioned, this is an area of active research and any suggestions regarding the behaviour of retarders should be regarded as tentative until there is more direct experimental evidence.

The surface layer theory for the dormant period has other variations. Double and Hellawell[86,87] have micrographs of the gelatinous layer over the cement grains and they argue that where the cement grains touch, this gelatinous layer weakly bonds the cement grains together and this is the process known as setting. After 3 - 5 hours, osmotic pressure behind the gelatinous layer causes it to burst. As the aqueous silicate solution comes into contact with the calcium rich fluid surrounding the cement grains it instantaneously precipitates into calcium silicate hydrate gel forming a tube structure radiating from the cement grains. Each cement grain has a large number of these fibrils radiating from it and they interlock with the fibrils from adjacent grains reinforcing the initial weak bonds and rapidly increasing the strength of the matrix.

The micrographs given in Figure 3.14 would support this model of behaviour. The bonding of the cement grains together via the gelatinous layer is not described in any detail, but it is implied that it is a progressive phenomenon. In Chapter 3 some evidence was presented to show that the permeability of concrete changed during the dormant period, and as no new hydration products are formed during the dormant period[72], it is difficult to imagine how an increase in bond at the points of contact could change the permeability of the concrete. When the Double and Hellawell theory is used to try and explain slump loss it runs into problems; during the preparation of the slump core, the bonds between the grains would be broken and in the short period of time between filling

the core and testing, the bonds would have to be re-established. The problem lies in that the longer the period of time between mixing and testing, the more the bonds have to re-establish themselves in the same short time period. With the re-crystallization of ettringite theory, the broken crystals of ettringite would still stiffen the concrete and this theory offers a more reasonable explanation of slump loss.

Both the Locher et al[72] and Double and Hellawell[87] theories of hydration have an initial reaction which would occur in the mixer or during transportation to the formwork location, followed by a dormant period in which the solid particles are held together by weak bonds. The dormant period finishes when the main reactions start and the weak structure is rapidly strengthened with C-S-H.

Another aspect of the early hydration of cement that is of relevance to formwork pressure is chemical shrinkage. Ertingshausen[44] reasoned that the reduction in pressure after the maximum was due to chemical shrinkage. Locher et al[72] showed that dilute Portland cement pastes underwent some rapid shrinkage immediately after mixing and then the rate of shrinkage slowed down to give a very small but steady increase up to 4 - 6 hours after mixing. After this period, there was a rapid increase in shrinkage. The increase in surface of the re-crystallised ettringite could account for the small increase in shrinkage during the dormant period. Drying shrinkage, because of its time scale, is irrelevant to the formwork pressure problem, but one paper by Wittmann[88] on drying shrinkage is interesting as it describes how the role of water changes from that of a fluid with suspended particles to discrete zones of capillary water within a solid skeleton.

Horizontal pressure reductions have been recorded[3] of the order of 45 kN/m^2 in 20 minutes. This order of pressure reduction is not easily explained by shrinkage. In Chapter 3, it was shown that the majority of the maximum horizontal pressure came from the pore water, so rather than thinking in terms of shrinkage to explain the pressure reduction after the maximum, an alternative approach based on the reduction in the pore water pressure is given in the next section. This involves two mechanisms, the reduction in the hydrodynamic excess due to water movements and the development of suction forces. This

last mechanism is simply the effects of the forces which cause shrinkage on the pore water. Raffle and King[71,89] have shown with cement suspensions that from the time of mixing there is the potential to develop suction forces, but these suction forces do not manifest themselves until a particle structure is created. These suction forces can be very powerful and are easily capable of changing the role of water to that of discrete pockets of capillary water within a solid framework. The work of Raffle and King[71,89] was all on cement suspensions and the assumption in the next section is that the same principles apply to concrete. This is not a major assumption for water does not drain out of concrete as the formwork is removed and therefore it must be held within the concrete by some force. Previous work[90] has how release agents are sucked into the surface of concrete and the existence of suction forces can be easily demonstrated by splashing with water the surface of a sealed cured concrete specimen.

4.2 THEORY OF CONCRETE PRESSURE ON VERTICAL FORMWORK IN WIDE SECTIONS

The theory proposed assumes that the concrete is unreinforced and that the formwork is smooth and rigid and consequentially there is no arching to cause load transfer to the form or reinforcement. As arching reduces the horizontal pressure on formwork, the assumption of no arching gives a conservative analysis.

At a depth h below the concrete surface, Figure 4.1, the vertical pressure is γh (as there is no load transfer to the forms) and this pressure is taken partially by the particle structure, σ, and partially by the pore water, u, so that

$$p_v = \gamma h = \sigma + u \qquad (4.1)$$

The pore water pressure being a fluid pressure, is equal in all directions but the effective pressure comes from the particle structure and only a proportion of it is transmitted in the horizontal direction.

Therefore the horizontal pressure, (4.2)

$$p = \lambda_\sigma \sigma + u$$

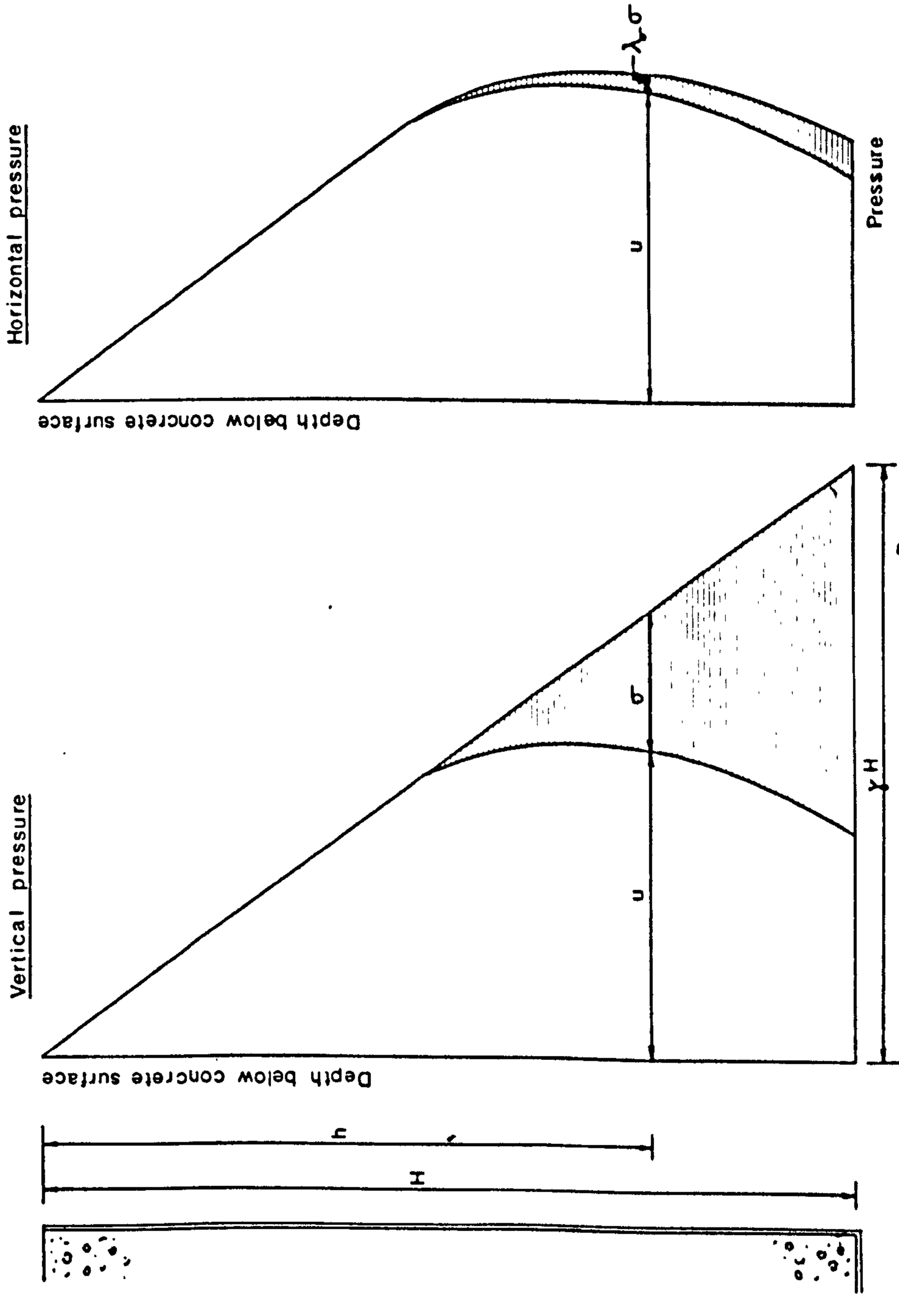

Figure 4·1: The components of the vertical and horizontal pressures·

The numerical values of the terms of this equation vary with time depending on,

1. the dispersal of the hydrodynamic excess,
2. the development of suction forces,
3. the changes in the concrete head,

and 4. vibration.

All these processes are superimposed, but for ease of understanding, they are described separately.

4.2.1 The dispersal of the hydrodynamic excess

The pore water pressure, u, can be split into two components, the static water head, $u_w = \gamma_o h$, and a term called the hydrodynamic excess, $u_c = u - \gamma_c h$. As the name implies, this is a transitory pressure and is a measure of the proportion of the solids supended in the water. If all the solids are suspended in the water,

horizontal pressure, $p = p_v = u = u_c + u_w$

To form a particle structure from the suspended state, the particles must settle and/or hydration products must bridge the gaps between the particles. Whilst appreciating that both of these mechanisms are in operation, the approach used in this theory is to treat the establishment of particle contact as a physical process and then incorporate the affects of continued hydration by establishing which of the coefficients in the physical model are dependent on cement chemistry and adjusting their values accordingly. When the volume concentration of solids exceeds 40 percent, particles do not settle individually according to their size and Stoke's law, but settle in the hindered settlement mode[91]. Concretes have free water contents of about 180 l/m^3 and therefore have volume concentrations of solids in the order of 80 percent. With such high concentrations of solids, it is debatable whether the process of settlement is hindered settlment or consolidation of a very open particle structure. In practice this is not of great importance as in both mechanisms the flow of water out of a layer is controlled by Darcy's Law[15,91]. With a hindered settlement model of particle contact, it is necessary to decide when the hindered settlement ceases and consolidation starts, but this problem is avoided with the

consolidation model as particle contact is assumed to exist from the time of placing. The initial load taken by this particle structure will vary depending on the mix type. With stiff, low workability mixes, the particle structure immediately takes a substantial proportion of the total load, but with medium and high workability mixes, the most reasonable assumption is to assume that the particle structure exists but it carries no initial load. The no initial load case is developed in this section, but the principles described, if not the starting conditions apply to stiff mixes.

Consolidation theory[15] equates the loss of water to the consolidation of the layer, The water loss is obtained using Darcy's Law and is equal to the change in the hydraulic gradient over the layer δh, multiplied by the permeability of the concrete,

$$\text{Water loss in layer } \delta h = \frac{k_c}{\gamma_o} \frac{\partial^2 u_c}{\partial h^2} \cdot \delta h \qquad (4.3)$$

By way of example, assume that the concrete is being placed continuously at R m/hr. In time increment Δt, the head has increased by $R\,\Delta t$, the vertical pressure by $\gamma R\,\Delta t$ and the static water head by $\gamma_o R \Delta t$. During the same time increment, the hydrodynamic excess will have changed by $\frac{\partial u_c}{\partial t} \cdot \Delta t$.

Then the mean effective pressure in time increment Δt is the average $(p_v - u)$

$$= \gamma h + \frac{1}{2} \gamma R \Delta t - \left(u_c + \frac{1}{2} \frac{\partial u_c}{\partial t} \Delta t \right) - \left(\gamma_o h + \frac{1}{2} \gamma_o R \Delta t \right) \qquad (4.4)$$

and the rate of increase in effective pressure

$$= \gamma R - \frac{\partial u_c}{\partial t} - \gamma_o R = (\gamma - \gamma_o) R - \frac{\partial u_c}{\partial t} \qquad (4.5)$$

This effective pressure gives a rate of change of volume in the layer δh of,

$$- m_v \left((\gamma - \gamma_o) R - \frac{\partial u_c}{\partial t} \right) \delta h \qquad (4.6)$$

(The negative sign indicates a decrease in volume).

Equating the loss of water (Equation 4.3) to the change of volume in the layer (Equation 4.6) gives

$$\frac{k_c}{m_v \gamma^o} \frac{\partial^2 u_c}{\partial h^2} - \frac{\partial u_c}{\partial t} + (\gamma - \gamma o) R = 0 \qquad (4.7)$$

This part of a mathematical solution to concrete pressures on formwork is complicated by the continuing hydration of the cement, This changes the mechanical properties of the concrete and in particular two key properties, the coefficient of compressibility, m_v, and the permeability of the concrete, k_c. So as well as being functions of the degree of compaction of the particle structure[15], they are functions of the cement, time and temperature. This mathematical approach will be developed further in section 4.3.

An understanding of the consolidation process can be obtained from Figure 4.2. Initially all the vertical load is taken on the pore water. A relatively large initial value of the coefficient of compressibility gives a slow development of the effective pressure and therefore the horizontal pressure starts by being approximately equal to the fluid pressure. As the particle structure develops it takes an increasing proportion of the load increase until a point is reached at which further increases in head are proportioned between the particle structure and the static water head in the ratio $(\gamma - \gamma^o) : \gamma^o$. (This idealized model assumes a smooth progressive consolidation of the particle structure and does not provide for the sudden collapse of the particle structure as observed in the experimental programme and on site (Chapter 5). The consolidation process for rigid, impermeable formwork will not give a maximum pressure because any increase in concrete head produces an increase in the static water head and therefore consolidation does not provide the complete explanation of concrete pressures on formwork. Experience has shown that concrete does not contain a static water head and this is due to the development of suction forces.

Before discussing the developing of suction forces, it is interesting to consider the effect of permeable formwork. At any free surface the pore water pressure must be zero and the formwork will act

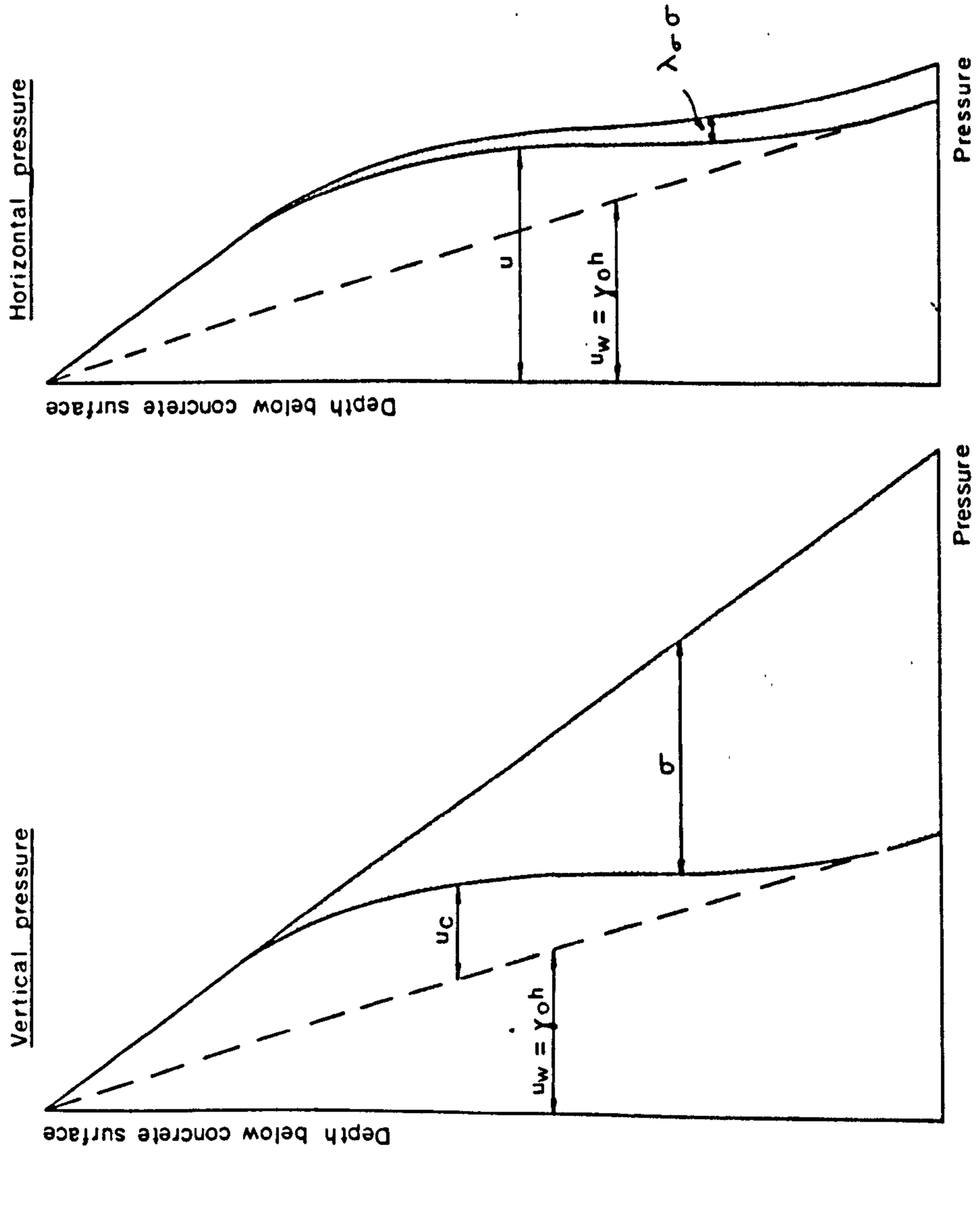

Figure 4·2: The effect of the consolidation process on pressure.

as a filter with a hydraulic pressure gradient across it. The size of the pressure drop across the formwork will depend on the permeability and thickness of the formwork and it can be as low as zero with steel mesh as fabric formwork. With impermeable formwork, the force causing water flow is the hydrodynamic excess, but with permeable formwork the whole of the pore water pressure is causing water flow because there can be no static water head in permeable formwork. This gives a very high hydraulic gradient across the section, rapid particle contact and low horizontal pressures. Section 4.4 on the application of the theory uses site data to quantify the reduction of horizontal pressure due to form permeability.

4.2.2 The development of suction forces

In the previous section it was shown how particle contact is developed by consolidation and how this particle contact is aided by hydration. Cement hydration effects the coefficient of compressibility and permeability of the concrete and therefore the consolidation process, but this is not the complete role of hydration.

During the dormant period, ettringite is re-crystallized into long, thin crystals that bridge the gaps between the particles. During the re-crystallization, water is adsorbed on the surface of crystals giving a small but steady decrease in the free water[72]. Before a particle structure is formed, this demand for water is satisfied without creating stresses by producing a small reduction in the total volume of concrete. Once a particle structure is formed, this demand for water creates suction forces which hold the water within the concrete. A very simple way of picturing this process is to imagine the water is being hung onto the particle structure increasing the effective pressure and reducing the pore water pressure by equal amounts. At first these suction forces will reduce the hydrodynamic excess until it reaches zero and then start to reduce the static water head until that reaches zero. At this stage, all the water is either chemically combined, held water or trapped within the capillary spaces.

Figure 4.3 gives the development of suction forces with time for a concrete without consolidation. The numerical values of the curve would depend on the properties of the cement and admixtures, the mix proportions and the time and temperature from mixing (this is not

Figure 4·3: The development of suction pressures.

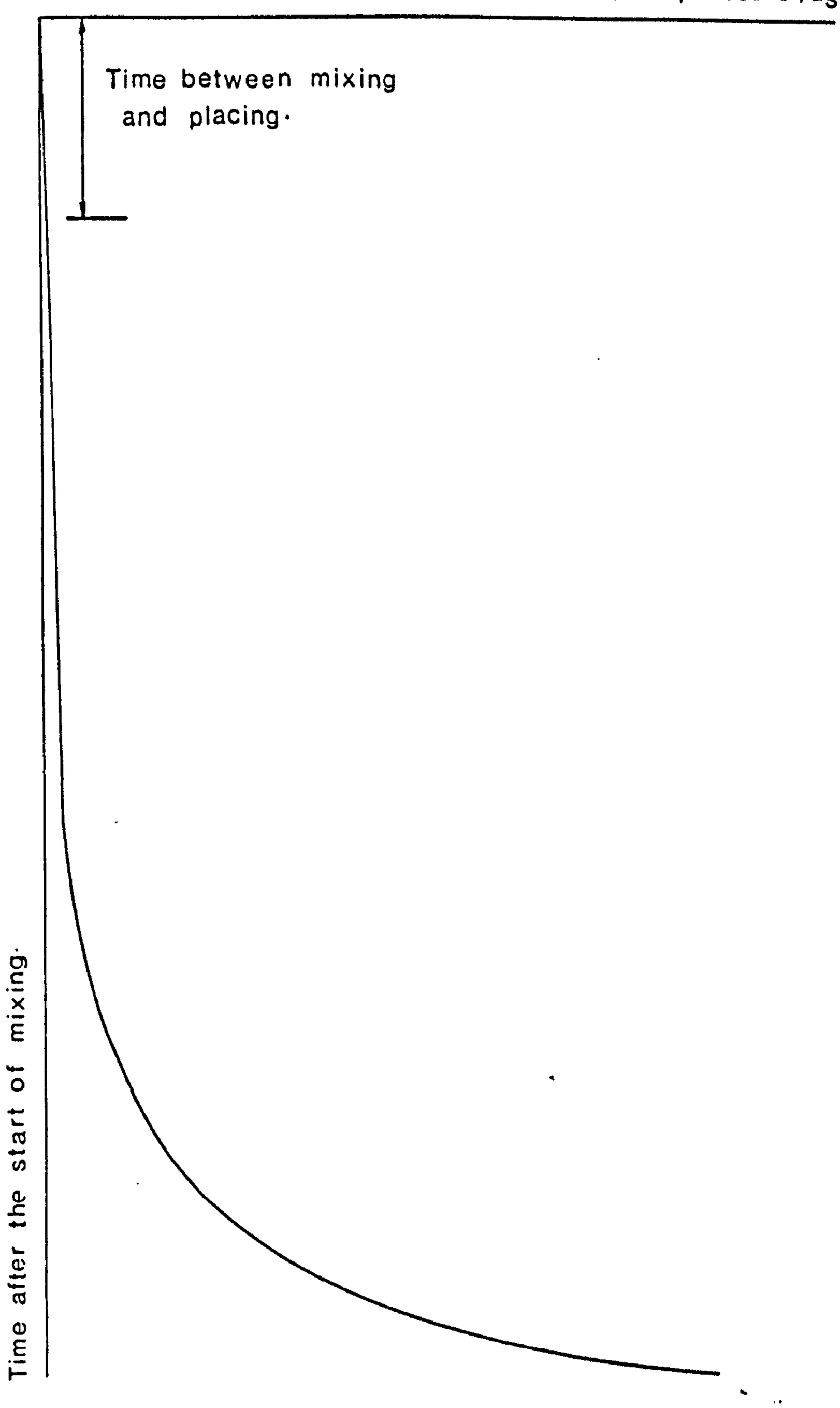

necessarily the same as the time from the start of placing). For formwork pressures, the important aspect of the suction force is its effect on the pore water pressure and the combination of this with the consolidation process. The imposition of Figure 4.3 on Figure 4.2 is done by removing from Figure 4.3 the section of the graph between the times of mixing and the start of placing and then converting the time axis to concrete head using $h = Rt$. The graphs can then be combined to give Figure 4.4. The shaded areas represent the pressures from the particle structure and the clear areas, the pore water pressure. The analysis gives a horizontal pressure distribution that is typical of those measured in CERA Report No 1[3].

When the pore water pressure has fallen to zero, there will be a residual loading on the formwork of

$$p = \lambda_\sigma \sigma = \lambda_\sigma \gamma h \qquad (\text{as } u = 0)$$

Therefore after the cycle shown in Figure 4.4, the horizontal pressure will continue to increase if the concrete head increases. In the practical situation, this is of little importance.

4.2.3 Changes in the head of concrete

In the previous sections, a constant rate of placing was assumed for the analysis. An alternative to this approach is to assume that the concrete is placed in equal lifts. During the first lifts the particle structure will take such a small proportion of the load, the horizontal pressure will effectively equal the vertical pressure. As the particle structure develops, the horizontal and pore water pressures will fall between lifts, but each new lift will cause the particle structure to collapse and the horizontal pressure to return to the fluid head. As the particle structure develops further, the pressure from each new lift is immediately split between the particle structure and the pore water. Eventually, each new lift is taken completely on the particle structure. Figure 4.5 shows this process diagrammatically with a graph of concrete pressure against time.

Included in Figure 4.5 is an example of the sudden collapse of the particle structure, a phenomenon observed in the experiments reported in Chapter 3 and on site (Chapter 5). The weight of a lift of concrete,

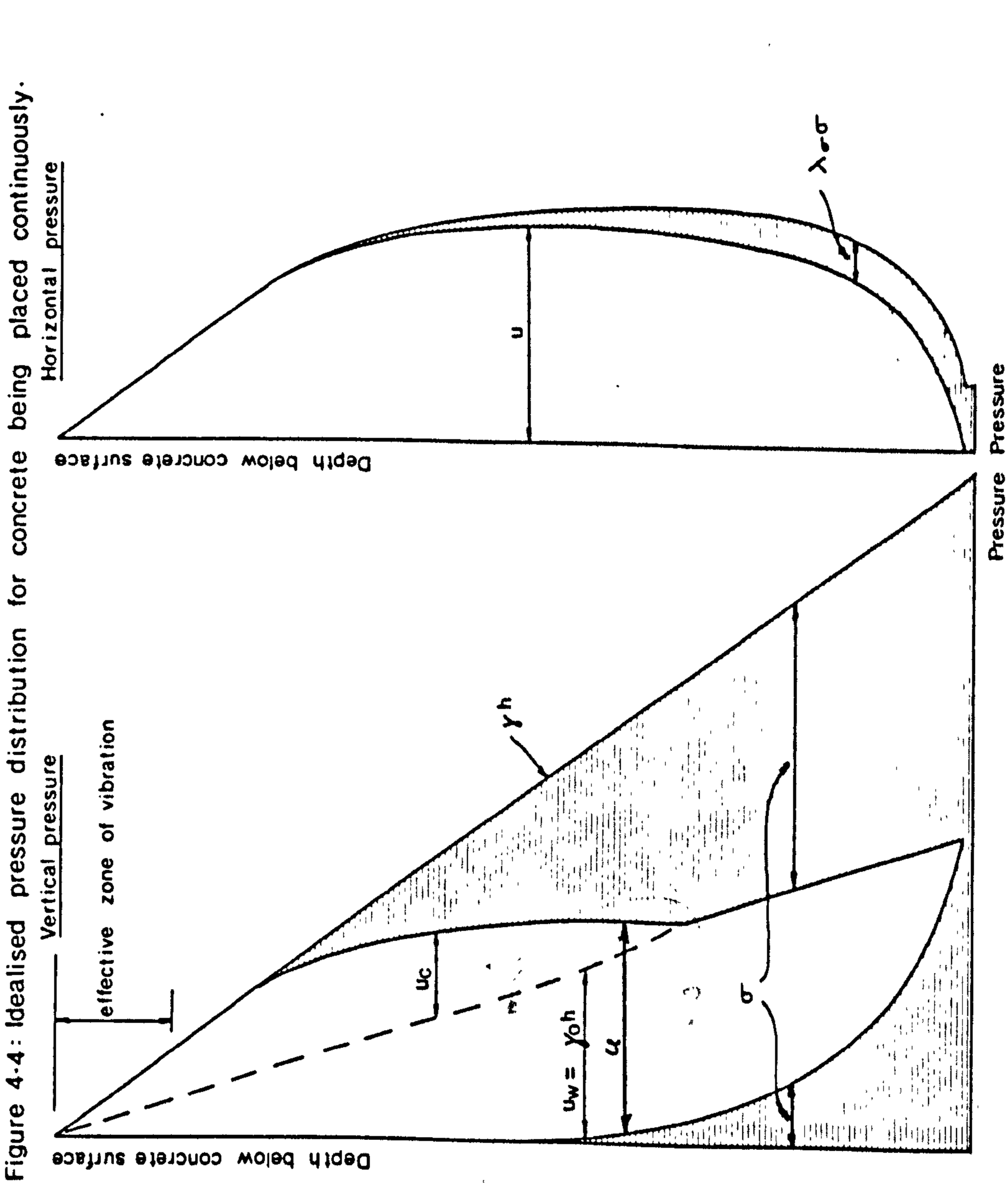

Figure 4-4: Idealised pressure distribution for concrete being placed continuously.

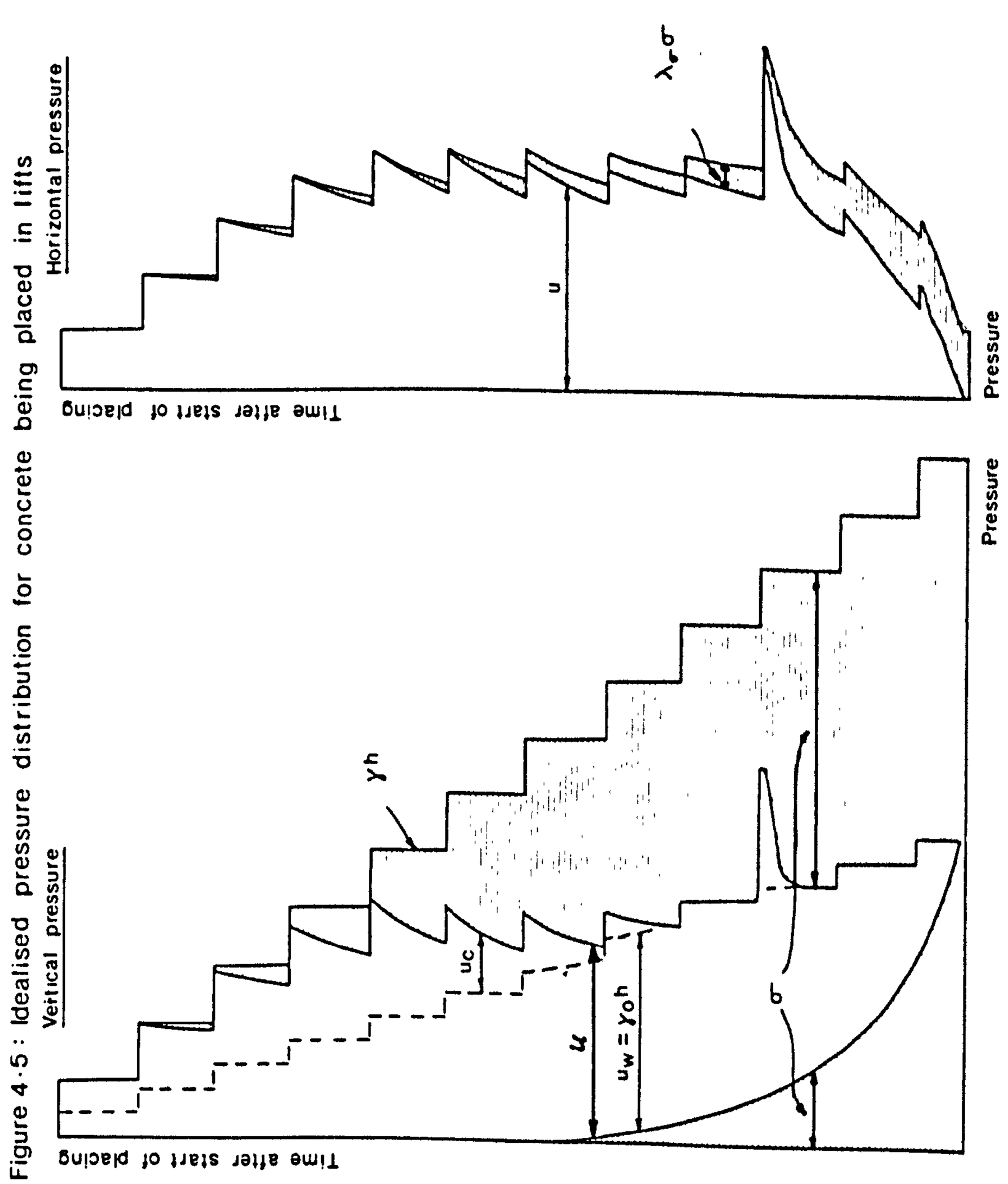

Figure 4·5 : Idealised pressure distribution for concrete being placed in lifts

or the impact as the lift is discharged causes the particle structure to collapse, transferring pressure to the pore water. This has the immediate effect of increasing the horizontal pressure (Equation 4.2). After the collapse, the particle structure is rapidly re-established and the horizontal pressure falls, giving the characteristic pressure peak associated with this phenomenon.

4.2.4 Vibration

In Chapter 3, it was shown that internal vibration does not fluidify the concrete to considerable depths below the depth of poker immersion. Yet in the vicinity of the poker, partially stiffened concrete can be reworked sufficiently for it to exert fluid pressure. Assuming normal vibration and that the poker is placed vertically in the concrete, the concrete will be fluidified at least to a depth that is equal to the depth of immersion, but there are no data on the normal depths of poker immersion. An estimate based on previous site experience is 0.6 to 1.0 m for large sections. A minimum design pressure which is equivalent to the fluid pressure at normal depths of vibration would be a prudent inclusion in all design methods. In wide sections, this minimum value would be 25 kN/m^2. The theory has shown how the concrete can exert a horizontal pressure approximately equal to the fluid head for depths greater than the effective depth of vibration during the period between the end of effective vibration and the particle structure taking a significant proportion of the load.

Deep re-vibration is not a technique that is recommended[3] unless the formwork has been designed to take the full fluid head. Subsequent evidence, for example Figure 3.15, has shown that this is a prudent design recommendation.

Vibration causes water movements, but the experiments presented in Chapter 3 have shown there are localised water losses and gains rather than an overall movement. The water content affects the spacing between the particles and therefore the time taken to form a particle structure will vary. As formwork pressure calculations are concerned with the total load on the formwork, this effect could be ignored and the assumption made that the water content has remained unchanged during placing.

4.2.5 Flexible formwork

In the previous sections, the theory was developed from the assumption that the formwork was rigid and there was no interaction between the concrete and formwork. Movements of the formwork are important as they have been shown to significantly reduce the horizontal pressure[92]. The theory supports this observation as a yielding of the formwork would tend to reduce the mean vertical spacing between the particles, improve the particle contact and therefore reduce pore water pressure. In zones where the movement is not a result of the adjacent concrete pressure but due to loading on another part of the form, the 'void' produced by the movement will provide a drainage area for pore water and this will reduce the pressure even further. Rigid formwork is not common and with flexible formwork the response of the formwork to changes in the pore water pressure is of major importance when assessing the total load on a form. Four factors relating to the formwork need to be considered,

(a) the flexibility of the formwork,
(b) the design of the formwork,
(c) the creep under load,
and (d) swelling effects due to water absorption.

Flexible formwork deflects under load and this deflection often controls the design of sheeting materials[93]. As the formwork deflects between two rigid supports, the deflected space is filled with water and solid particles. When the pore water pressure starts to fall, the formwork tries to respond, but is prevented from returning to its unstressed shape by the solid particles (the unstressed shape is not necessarily its original shape due to irreversible creep). A 'passive pressure' situation exists and because the formwork remains deflected, the tie bolts will remain under stress. A reduction in pressure after the maximum will occur due to the deflected shape being partially filled with water, but deflection measurements on three $1.2m^2$ chipboard walls has shown that the reduction in deflection is small. Walls which were being cast for another programme[94] were monitored for movement after the maximum pressure. The average reduction in deflection one hour after the maximum (100%) was 2.4 percent for a high workability concrete (2 walls) and 2.7 percent for a low workability concrete (1 wall).

The formwork design will influence the reduction in pressure after the maximum. It has just been shown that formwork designed to span between supports gives no significant reduction in pressure, but this is not necessarily the case with single sided cantilevered wall formwork. Successive lifts of concrete will cause the form to progressively deflect, moving the form away from the previous lifts. Initially the concrete will follow these movements because it remains fluid but as the particle structure starts to develop, the movements of the formwork will accelerate the transfer of load onto the particle structure and consequentially accelerate the fall in horizontal pressure. In Section 4.4, this theory is used to re-analyse site data to assess the rate of fall in pressure for rigid and cantilevered wall formwork.

Creep of the formwork does not significantly affect the pressure envelope for the time in which the concrete is capable of responding to formwork movements is short. This is confirmed by the formwork in the wall tests not showing any tendency to increase in deflection with time. There are creep effects in which the formwork sheeting takes on a permanent set[94], but this is outside the scope of this thesis.

When concrete is first placed in unsealed plywood formwork there is a rapid absorption of water. The swelling associated with this water absorption does not cause stresses in the tie bolts because the concrete is still a fluid. The theory has shown that once a particle structure is formed, suction forces start to develop and these would try and suck into the concrete, the water within the formwork. Whether this is successful or not, there will be no increase in the water content of the formwork and therefore no increase in swelling. The net result is that formwork swelling is unlikely to have any significant effect on formwork loading.

4.3 MATHEMATICAL MODEL

A mathematical solution to determine the maximum formwork pressure needs to combine the consolidation process with the development of suction forces. For a uniform rate of placing, the consolidation process has already been described with Equation 4.6 and therefore the next stage of a solution is to develop a mathematical expression for the suction forces.

Inspection of Figure 4.3 shows that the development of suction forces has the form of part of a e^t curve and could be expressed by the equation,

$$u_s = ae^{(bt-c)} - ae^{-c} = ae^{-c}(e^{bt} - 1) \qquad (4.8)$$

where a, b and c are coefficients obtained by curve fitting to experimental data; the data are not available at the present time. The appropriate choice of coefficients can also take into account the time difference between the start of mixing and the start of placing and therefore put the consolidation and suction force processes on the same time basis.

From Equation 4.8, the rate of development of suction forces with time is,

$$\frac{\partial u_s}{\partial t} = a\,b\,e^{(bt-c)} \qquad (4.9)$$

As explained in Section 4.2, these suction forces will reduce the pore water pressure and therefore the pore water pressure will be the sum of the hydrodynamic excess and the static water head less the suction pressure. Therefore the rate of change of pore water pressure is,

$$\frac{\partial u}{\partial t} = \frac{\partial u_c}{\partial t} + \gamma_o R - \frac{\partial u_s}{\partial t} \qquad (4.10)$$

Before Equation 4.7 can be substituted into Equation 4.10 the rate of change of the hydraulic gradient needs to be modified. As explained in Section 4.2, the suction pressure starts by reducing the hydrodynamic excess and therefore the pore water pressure causing water flow is the total pore water pressure less the static water head, less the suction pressure, or,

$$(u - \gamma_o Rt - ae^{(bt-c)} + ae^{-c}) \qquad (4.11)$$

This modifies Equation 4.7 to

$$\frac{\partial u_c}{\partial t} = (\gamma - \gamma_o) R + \frac{k_c}{m_v \gamma_o} \frac{\partial^2 (u - \gamma_o Rt - ae^{(bt-c)} + ae^{-c})}{\partial h^2}$$

Then substituting in Equation 4.10 for $\frac{\partial u_c}{\partial t}$ and $\frac{\partial u_s}{\partial t}$ with Equations 4.12 and

4.9 gives

$$\frac{\partial u}{\partial t} = \gamma R + \frac{k_c}{m_v \gamma_o} \cdot \frac{\partial^2 (u - \gamma_c R t - a e^{(bt-c)} + a e^{-c})}{\partial h^2} - a b e^{(bt-c)} \quad (4.13)$$

Equation 4.13 defines the rate of change of pore water pressure with time for a constant rate of placing. When $\frac{\partial u}{\partial t} = 0$, the pore water pressure will be a maximum and the horizontal pressure will be a maximum. Therefore the numerical values of u and t at $\frac{\partial u}{\partial t} = 0$ will be the maximum values to be substituted in Equation 4.2 to give

$$p_{max} = \lambda_\sigma (\gamma R t_{max} - u_{max}) + u_{max} \quad (4.14)$$

Before attempting a solution to Equation 4.13, it is pertinent to consider the problems in determining the numerical values of the coefficients and the probability of determining them to an accuracy that will give an economic solution of the concrete pressure on formwork. The factors which influence the values of the permeability, k_c, the coefficient of compressibility, m_v, and the ratio of horizontal to vertical effective stress, λ_σ, are the cement, its type, source and fineness, admixtures, time, temperature, mix proportions, aggregate shape and grading, and the degree of consolidation. The coefficients a, b and c are simpler as they are only dependent on the hydration process and therefore on just the quantity of cement, its type, source and fineness, admixtures and the concrete temperature. The complexity of the factors controlling the coefficients makes it very doubtful if a mathematical solution would ever give an economic design. The doubts are reinforced when the conservative assumption of rigid formwork is considered. Also the experimental work has shown that the compression of the particle structure is not uniform, but is subjected to sudden jumps and would be dependent on the site placing techniques.

The theoretical solution to concrete pressure on formwork is considered to be less likely to produce economic design values than the alternative of using the theory to interpret existing and new site data and therefore this avenue of investigation was not pursued any further.

4.4 APPLICATION OF THE THEORY

The main value of the theory lies in its ability to provide a logical framework in which site data can be analysed. The crux of the theory is the more rapidly pore water pressure is dispersed, the lower the maximum horizontal pressure. Therefore any factor that increases the rate of pore water pressure dispersal or particle contact would also reduce the maximum horizontal pressure. The permeability of formwork provides an excellent example of one of the factors.

4.4.1 Permeability of formwork

At any free surface, the pore water pressure is zero and the outer surface of permeable formwork will provide a free surface. The shorter drainage path results in a higher hydraulic gradient, faster water movements and rapid dispersal of pore water pressure. In extremely permeable formwork, for example fabrics and steel mesh, the horizontal pressure will only be due to the effective pressure component, $\lambda_\sigma \sigma$. For all other conditions being equal, the more permeable the formwork, the lower the maximum horizontal pressure i.e.

highest horizontal pressure

↓

lowest horizontal pressure
($p = \lambda_\sigma \sigma$)

impermeable formwork
(steel, GRC, plastic faced plys)

↓

sealed plywoods

↓

unsealed plywoods

timber boards

↓

fabric formwork and steel mesh

This analysis is developed from purely theoretical grounds and to numerate this analysis, the data for wide sections (Chapter 2) was re-examined.

The data gave only one example of similar materials and placing conditions, but different formwork facings. This is the two columns cast at the Cement and Concrete Association in 1968 (upublished data); the formwork for one column was steel and the other, Rapid ply panels.

The concrete and the placing temperature were similar and both columns were placed rapidly by pumping (at 32 m/hr in the steel formwork and 22 m/hr in the Rapid ply formwork). For similar gauge locations, the maximum pressures were,

Depth below final concrete surface	Steel formwork	Rapid ply formwork
9.05 m	103 kN/m^2	78 kN/m^2
6.4 m	91 kN/m^2	50 kN/m^2

The more permeable Rapid ply formwork gave the lower pressures which were 76 and 55 percent of the steel formwork pressures. Rapid ply is a sealed plywood and since 1968 the source of sealed plywood for these panels has changed several times. Therefore these results cannot be shown to be typical for sealed plywoods. As the techniques and coatings for sealing plywood are being continually improved, the trend is towards making these boards effectively impermeable.

Apart from this one example, there were no other sets of data in which the only variable was the formwork facing material. This is not surprising as normally one set of formwork is used for a number of pours and if there are more than one set of forms, the construction materials are normally the same. Therefore some other way of analysing the data was necessary. The CIRIA formwork pressure design method does not include formwork permeability as a variable and being an empirical method, it should predict a safe design value for all conditions. As an upper bound solution, this, according to the theory, should be coincidental with impermeable formwork; the measured pressures in permeable formwork should be less than the calculated value. The wide section data used to obtain Figure 2.19 was grouped by formwork facing material and the measured and calculated pressures were compared. The calculated pressures were obtained using the new CIRIA design chart[95]. This chart is partially based upon the data analysis given in Chapter 2 and it attempts to correct for the underestimation of pressure at low calculated values. The analysis, Table 4.2, expresses the measured pressure as a percentage of the calculated pressure. The obvious weakness of this approach is that it assumes the design chart gives an accurate portrayal of the other factors and this has not been shown to be the case (Chapter 2). Nevertheless, with the exception of timber

TABLE 4.2 The measured horizontal pressure expressed as a percentage of the calculated pressure.

Formwork facing material				
Steel	Sealed plywood	Unknown type of plywood	Unsealed plywood	Timber
54)	88	64)	39	48
67)	53	81)	41	50
53)	83	68)	43	59
70)	71	64) 1 col.	41	60
60)	74	61)	24	173)
93)	Mean 74	89)	49	73) See text
30)		82)	40	69)
47)		72)	47	115)
57)		114	45	Mean 81
45) steel formwork, but instrument placed in plywood stopend		41	98	
51)		Mean 74	Mean 47	
55)				
49)				
53)				
87)				
73)				
73)				
59)				
96				
59				
61				
107				
100				
95				
124				
103				
42				
60				
48				
Mean 68				
Mean of results not in the plywood stopend, 81.				

board formwork, the general pattern in Table 4.2 shows lower pressures with the more permeable formwork facing materials.

A group of four measurements taken in timber board formwork do not fit into the pattern of results. These results are from four columns all cast using the same tall, elliptical column form made with 75 mm timber board. The workmanship was excellent and there was very little fluid loss from the joints between the boards; therefore the form was probably less permeable than normal timber board forms. In addition, measured pressures of 173 and 115 percent of the design value suggest that the design charts are suspect for the actual placing conditions.

The remaining four measurements with timber board formwork are all from Ertingshausen's data (Table 2.1) and these give lower than calculated pressures. This data is insufficient to quantify the possible reduction in calculated horizontal pressure when timber boards are used.

Numerical data on extremely permeable formwork is scarce, but observations of practice support the contention that the horizontal pressure is low. The fabrics in the formwork illustrated[96,97] would have burst if the pressures had been in the same order as normal formwork. With steel mesh stopends[98] the recommended framing is very light when compared with normal formwork.

From these results, the following tentative modification to the CIRIA stiffening limit is proposed; calculate the stiffening limit in the normal manner and then multiply it by the following reduction factors depending on the formwork facing:

Formwork facing	Reduction factor
Impermeable formwork (steel, GRC, plastic faced ply)	1.0
Sealed plywoods	0.8 to 1.0
Unsealed plywoods with normal release agents	0.5 to 0.6
Steel mesh or fabric	(0.25)

Timber board formwork has been omitted from this table until

more data is available. The 0.25 given for steel mesh and fabric is only an estimated figure based on the experimental work and it is not supported, as yet, with site data.

To demonstrate the benefits obtained from these reduction factors, the plywood data given in Table 4.2 is represented in Table 4.3. This table compares the measured pressure with the calculated pressures obtained with and without the reduction factors. The table shows that the reduction factors substantially improve the correlation between the calculated and measured pressures. These data indicates that further site measurements to confirm or otherwise these tentative reduction factors could lead to significant economies in design.

4.4.2 Rate of placing

The rate of placing is the increase in head with time and for a better understanding of the fundamentals, the influence of time and head are considered separately. Whatever the rate of placing, there will be an effective zone of vibration in which the energy imparted into the concrete is sufficient to fluidify the concrete and destroy any particle structure. With very low rates of placing, this effective zone of vibration will control the maximum formwork pressure. With normal rates of placing, the maximum pressure is controlled by the consolidation process and the development of suction forces both of which are time dependent. The longer the period of time between the start of placing and the maximum pressure, the lower the numerical value of the maximum pressure.

The role of the head of concrete is more complex. A head increase will increase either or both the effective and pore water pressures depending on the state of development of the particle structure, but the theory has shown that the rate of consolidation depends on the hydraulic gradient and not the numerical value of the pore water or effective pressures. Also, the development of suction forces is only a function of the cement chemistry, time and temperature and it is therefore independent of head.

In impermeable formwork, a head increase will increase the length of the drainage path as water can only drain upwards. Therefore the head increase is unlikely to alter the hydraulic gradient

TABLE 4.3 Measured formwork pressures compared with the calculated pressures (all units in kN/m^2 rounded to nearest 5 kN/m^2)

Sealed plywood			Unsealed plywood		
Measured pressure	CIRIA calculated[94] pressure	Calculated pressure with red. factor at 0.8	Measured pressure	CIRIA calculated[94] pressure	Calculated pressure with red. factor at 0.5
90	100	80	25	60	30
30	35	30	20	50	25
25	35	30	25	60	30
25	35	30	20	55	30
			10	45	25
			25	50	25
			20	45	25
			20	40	20
			20	45	25
			40	40	20

significantly. With the hydraulic gradient being independent of head, the logic of the argument leads to the conclusion that in rigid, impermeable formwork where the maximum pressure is not controlled by vibration, the time to achieve the maximum pressure will be a constant.

In permeable formwork, the length of the drainage path between the formwork and concrete remains the same and therefore as the head increases so does the hydraulic gradient between the formwork and concrete. Therefore in rigid, permeable formwork the maximum formwork pressure is dependent on both time and head.

The majority of formwork is not rigid, but flexible and as the head increases it progressively deflects. This small increase in the contained volume can have significant effects on the formwork pressure. It will reduce the mean vertical spacing between the particles and improve the particle structure aiding the rapid transfer of pore water pressure to effective pressure. In flexible formwork, the maximum formwork pressure is therefore dependent on both the head of concrete and time.

4.4.3 Mix design

The development and maintenance of a particle structure depends not only on the rate of dispersal of pore water pressure, but on the initial particle spacing and therefore on such factors as the shape of the aggregate, mix proportions, cement type and admixtures. The problem in attempting to analyse the influence of mix design on formwork pressure is that there are always a number of corresponding[99] mixes. Corresponding mixes have equal gradeand workability as assessed by one of the standard workability tests. Where the influence of mix design has been studied[45,51], the method of comparison was rarely directly applicable to normal mix design. For example, McDowall and Ritchie[51] simply increased the water content to get higher slumps and thereby reduced the 28 day characteristic strength of the mix. In normal mix design[69] higher workabilities are achieved by increasing both the water and cement contents, so that strength is maintained. The following is an attempt using the theory, to describe the influence of mix design on formwork pressures.

The shape of the aggregate will influence its loose bulk density. Assuming equal specific gravities and gradings, the more rounded the aggregate, the higher the loose bulk density[100]. In a discussion on particle contact it is more convenient to use the volume occupied by a fixed weight of aggregate rather than the bulk density. The larger the volume occupied by a fixed weight of aggregate, the quicker the establishment of particle contact when this aggregate is used in concrete.

The loose bulk densities of three coarse aggregates used frequently at the Cement and Concrete Association were measured and after adjustment for their differing specific gravities, gave the following volumes for 1000 kg of loosely placed coarse aggregate of equal specific gravity:-

Shape	
Rounded to irregular	705 litres
Irregular	736 litres
Angular	792 litres

These figures show that in concretes which are identical except for the shape of the aggregate, the more angular aggregates have to move less to establish particle contact. The same argument applies to the shape of the sand and cement, but it does not apply to materials that are elongated or flaky because internal vibration tends to orientate these materials so that the long axis is horizontal. The analysis, so far, agrees with McDowall and Ritchie[51] who showed that for a fixed water cement ratio, the more angular aggregates gave lower horizontal pressures.

However in normal mix design[69], concretes with angular aggregates have lower weights of aggregate per cubic metre and this will tend to offset the advantage of being more angular. Using the same three aggregates with equalised specific gravities and the typical mix proportions for a 20 mm aggregate concrete with zone 2 sand[69], the loosely placed volumes per cubic metre of concrete of the combined

10 and 20 mm agregates were calculated as:-

Shape	Low workability	Medium workability	High workability
Rounded to irregular	888 l	816 l	764 l
Irregular	898 l	821 l	765 l
Angular	899 l	808 l	737 l

This demonstrates that the advantage of angularity is offset by the reduction in the volume of the coarse aggregate.

The particle structure is formed from all the solid materials, the coarse aggregate, sand, cement and hydration products. The strength of the particle chain depends on the stability of the contact points and therefore a harsh mix (one with a high proportion of coarse aggregate) will give a more rapid and stable particle structure and consequently lower horizontal pressures. From the figures given above, the coarse aggregate in the low workability concrete is capable of occupying nearly 90 percent of the concrete volume. As such the sand and cement need only provide a relatively small proportion of the particle structure. The result is a rapid formation of a relatively stable particle structure and low horizontal pressures. As the workability increases, the sand and cement are required to form a larger part of the particle structure and the resultant structure will be less stable and the horizontal pressures higher.

As the water content of a concrete mix is increased, the average spacing between the particles will be increased, but the permeability of the concrete is also increased. So, although the particles have to move on average further to establish contact, the dispersal of the hydrodynamic excess is quicker due to the higher permeability. McDowall and Ritchie[51] found that when they increased the water content of their concretes, the increased slump did not necessarily increase the horizontal pressure. With normal mix design, strength is maintained in high workability mixes by compensating for the higher water content with more cement. This is in effect putting more finer particles into the concrete and keeping the water cement ratio constant[69]. As the cement particles and the water cement ratio control the permeability of the concrete, changes in workability coupled with maintaining the 28 day strength will have little effect on the permeability.

Therefore the role of mix proportions in determining the maximum horizontal pressure is mainly in the fixing of the mean particle spacing and in the relative stability of the particle structures. Considering, for example, the range and gradings of coarse aggregates and sands and that the specific surface of ordinary Portland cements varies between 272 to 401 m^2/kg[101], it is not surprising that the data given in Chapter 2 did not show a clear correlation between horizontal pressure and workability.

The data given in Chapter 2 showed that BFPC or Traβzement concretes tended to give higher formwork pressures. This can be simply the result of the type of cement affecting the development of suction forces, but often the mix proportions are different from the corresponding OPC mix. For example, a PFA consists of fine spherical particles which increase the workability of a mix and therefore to obtain a corrèsponding mix, the water content is reduced. So, on the one hand, formwork pressures will be increased due to the fine spherical particles, and on the other hand, decreased due to the lower water content. The balance between these competing factors is not known.

The two main groups of admixtures that might increase the formwork pressures above the normal design values are retarders and plasticizers especially superplasticizers. These admixtures normally require modifications to the mix proportions as most retarders act as water reducers and superplasticized concretes have to be designed against segregation.

The consolidation process is a physical process and will not be significantly affected by the addition of a retarder (there might be some small changes in the numerical value of k_c and m_v). Also the experiments in Chapter 3 showed that the re-crystallisation of ettringite appears to be unaffected by the addition of a hydroxycarboxylic acid based retarder in which case the initial part of the suction force curve will be similar. The suctionforce curves will differ significantly in the time at which the suction forces start to increase rapidly[89]. The theory indicates that the initial formation of a particle structure is similar in retarded and plain concretes, but that the particle structure in the retarded concrete is not reinforced with the hydration products

of the main reactions until a significantly later time. Therefore the particle structure in the retarded concrete will be susceptible to disturbance for a longer period than plain concrete and as a consequence of this could give higher formwork pressures.

Superplasticizers deflocculate the cement grains[68] and as the cement forms part of the particle structure, dispersing them will result in the particle structure taking longer to form. This effect is offset to some extent by an increase in the permeability of the cement paste which will give a more rapid dispersal of the hydrodynamic excess. The horizontal pressure in superplasticized concretes will be influenced by the consolidation process and the development of suction forces and therefore the pressure envelope will be similar in shape to that of normal concrete.

4.4.4 The reduction in pressure after the maximum

The theory has explained why the pressure on the formwork will reduce after the maximum in rigid and cantilevered formwork and this section attempts to quantify that reduction in pressure by reference to site data. A number of instruments have been used to measure the formwork pressure on site and they all give similar results up to the maximum pressure[31]. After the maximum, the readings diverge with the pressure balance giving the highest rate of fall in pressure. The pressure balance works by adjusting the pressure behind a piston to maintain it within the same very small fixed range of movement. This gauge does not have the progressive deflection of the diaphragm gauges and therefore it is not so susceptible to having its return movement hindered by solid particles (see Section 3.6.2). Therefore the pressure balance gives a most accurate representation of the fall in pressure in rigid formwork. With cantilevered formwork, the form is progressively moving away from the concrete and as explained in Section 4.2.5, movements of the form away from the concrete tends to reduce the horizontal pressure on the form. Therefore the pressure balance results for normal wall forms will tend to register a conservative reduction in pressure compared with the obtained in cantilevered formwork. The assumption made in the remainder of this section is that the pressure balance readings are a reasonable

representation of the actual fall in pressure in rigid and cantilevered formwork.

Using the CERA data for wide sections with OPC concretes where placing had continued for at least one hour after the maximum pressure, Figure 4.6 gives the measured reductions in pressure one hour after the maximum. These data give a skew distribution of results and indicate that some reduction in pressure after the maximum could be included in the formwork pressure calculations.

This potential saving in the design pressure is not as significant as it may at first appear. Most cantilevered formwork is 2 m or less in height. Using the new CIRIA design chart[95] and assuming R = 1.0 m/hr, slump = 50 mm and a concrete temperature of 10°C, the maximum pressure is 40 kN/m^2 at 40/25 = 1.6 m below the top of the form. Assuming a reduction in pressure of 30% per hour with a 2 m height of pour, the reduction in pressure is

$$(2.0 - 1.6)\ m \times \frac{hr}{1m} \times \frac{30}{100} \times 40\ \frac{kN}{m^2} = 5\ kN/m^2$$

Therefore the pressure at the base of the pour will only have reduced to 35 kN/m^2. Considering the accuracy of the other parameters, the reduction in pressure after the maximum is not of any practical significance in most cantilevered formwork. In cases of rigid formwork and cantilevered formwork with lift heights in excess of 2 m, applying a reduction in pressure after the maximum could provide some economy in design.

Figure 4·6: Reduction in pressure 1 hour after the maximum.

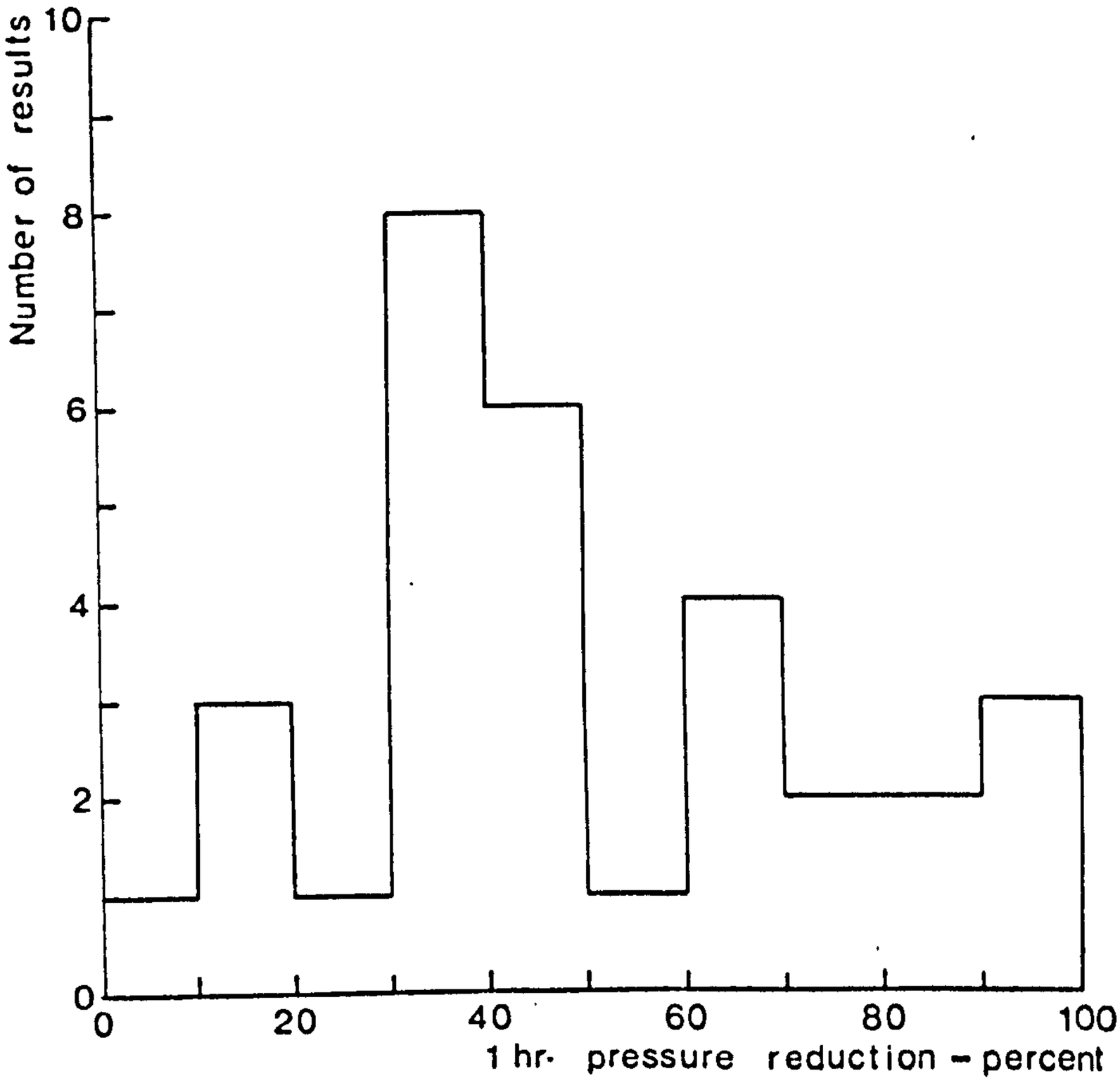

Chapter 5 APPLICATION OF THE THEORY IN INTERPRETING AN UNUSUAL SET OF FIELD DATA

INTRODUCTION

The practical application of the theory is demonstrated with this example of site pressure measurements on an underwater tremied concrete pour at the Thames Barrier. The Thames Barrier consists of a series of insitu concrete piers spanned with precast concrete sills. These sills are located onto the piers with an insitu key of structural grade tremie concrete. As this concreting operation was so critical and as the contractor was concerned that the formwork holding down bolts which had been previously cast into the piers and sills, may not have been strong enough to take the formwork pressures, a full sized trial pour was instigated. The trial consisted of casting a 1 m x 1 m x 6 m high castellated section, Figure 5.1, in a sealed plywood formwork mould under the River Thames. The section was unreinforced except for one lifting bar which was used to raise the whole section out of the river for inspection.

5.1 DESCRIPTION OF THE TEST

The formwork consisted of 19 mm Wisaform plywood on RMD soldiers. This gave an effectively impermeable form. In the centre of one form face, pressure gauges were installed at 0.3, 0.8, 1.8, 2.8 and 3.8 m above the base. The gauges were of the same basic type as used in the test rig described in Chapter 3, but each was sealed in a steel housing with Flexane to make the complete gauge waterproof. The gauges were calibrated prior to water proofing. After water proofing, they were put into a water pressure vessel and checked for malfunction or any change in the calibration factor.

After installation in the form, the cables from the gauges were bunched and wrapped with a double layer of strong adhesive tape. This was to try and protect the cables in the 11 km/hr currents. The cables were also secured to the form to prevent any stress in the connections between the cables and gauges. The gauges were connected into a multi-channel selector and Wheatstone bridge. Before the first lift of concrete was placed, all the gauges were balanced to give zero voltage and the tide

Figure 5.1: The trial tremie pour after removal from the river.

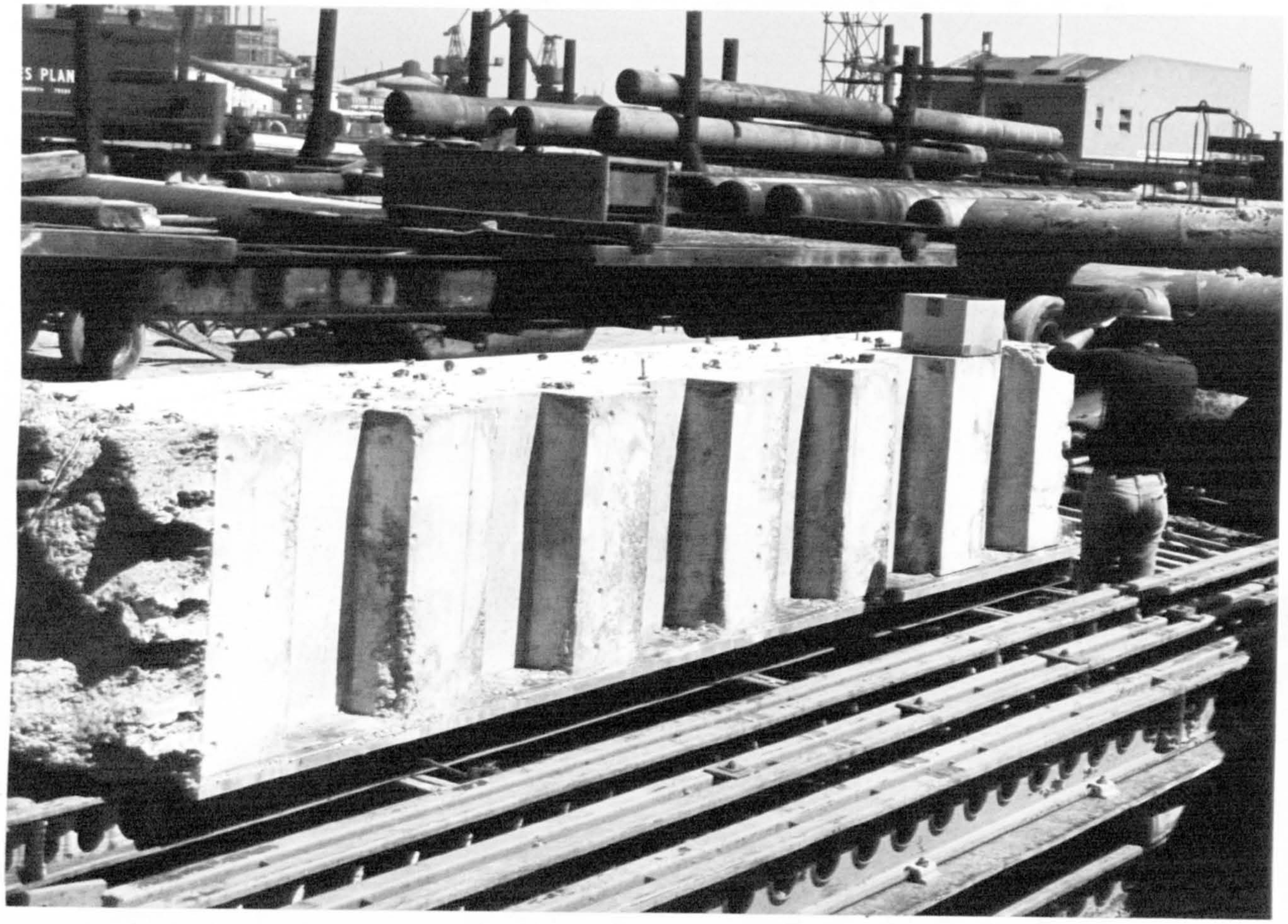

level was recorded.

The Grade 40 concrete contained a retarding water reducer, Cormix P2. The dry batch mix proportions were:

sulphate resisting cement	500 kg
sand	693 kg
10 mm aggregate (gravel)	169 kg
20 mm aggregate (gravel)	828 kg

The mix also contained 210 l/m^3 of water and 1.4 l/m^3 of Cormix P2. This concrete was of exceptional strength for tremied concrete and one function of the trial pour was to prove that it could be placed by the tremie method. The concrete was site batched and delivered to the location of the test in 0.6 m^3 batches. Each batch was tested for slump, samples for control cubes were taken and then it was discharged into a skip which in turn was discharged into the tremie tube, Figure 5.2. A vermiculite plug was used to separate the river water and the first batch of concrete.

Pressure readings were taken just prior and immediately after placing each lift of concrete. A number of intermediate readings were also recorded. Tide levels were noted frequently as there was a large tide fall during the test. The insitu concrete temperature was recorded with a thermocouple and Comark electric thermometer.

5.2 APPLICATION OF THE THEORY TO THE MEASUREMENTS

Consider the vertical pressure at a gauge level AA. Vertical

$$\text{pressure} = \sigma' + u_c + u_w + \gamma_o x = \sigma' + u_c + \gamma_o (h + x) \qquad (5.1)$$

The horizontal pressure on AA above atmospheric, (Figure 5.3),

$$= \lambda_\sigma \sigma' + u_c + \gamma_o (h + x) \qquad (5.2)$$

All this pressure is not transferred to the formwork ties as part of it is balanced by the static water head on the outside of the form. The effective formwork pressure is that given in Equation 5.2 less the static water head, i.e.

$$\text{Effective formwork pressure} = \lambda_\sigma \sigma' + u_c \qquad (5.3)$$

Figure 5·2: The underwater formwork pressure test·

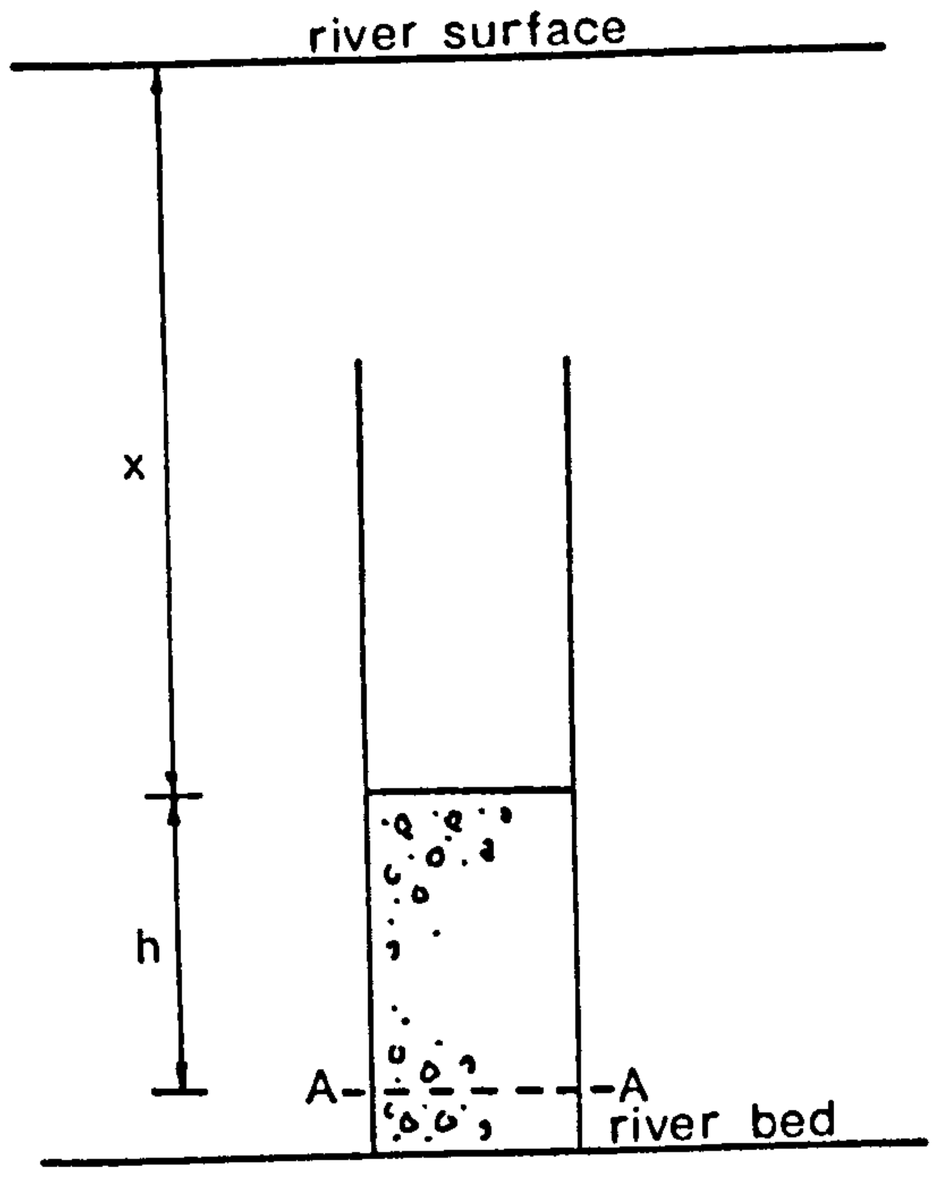

Figure 5·3· Notation.

At an initial head of water, x_o, above AA (h = o), the gauges were set to read zero, but the actual pressure above atmospheric at level AA was $\gamma_o x_o$. As the diaphragm of the gauges deflected against a sealed air void, the measured pressure changes are above atmospheric and not above external water pressure. Therefore at any time, the horizontal pressure above atmospheric is

$\gamma_o x_o$ + calibration factor x bridge reading (5.4)

Equations 5.2 and 5.4 are equal, giving

$\lambda_\sigma \sigma + u_c + \gamma_o (h + x) = \gamma_o x_o$ + calibration factor x bridge reading

Re-arranging

$\lambda_\sigma \sigma + u_c = \gamma_o (x_o - h - x)$ + cal. factor x bridge reading = effective formwork pressure

$\therefore$ Effective formwork pressure = γ_o x tide fall + cal. factor x bridge reading (5.5)

Before concrete covers the gauge, the reduction in pressure due to the tide fall will be balanced by the change in the bridge reading times the calibration factor and the effective formwork pressure will remain at zero.

5.3 RESULTS

Because of the wave action, tide boards cannot be read precisely and therefore the spot tide levels were plotted, Figure 5.4, and the best fit curve drawn. Tide changes for insertion into Equation 5.5 were obtained by interpolation from the best fit curve.

Figure 5·4 : Tide levels.

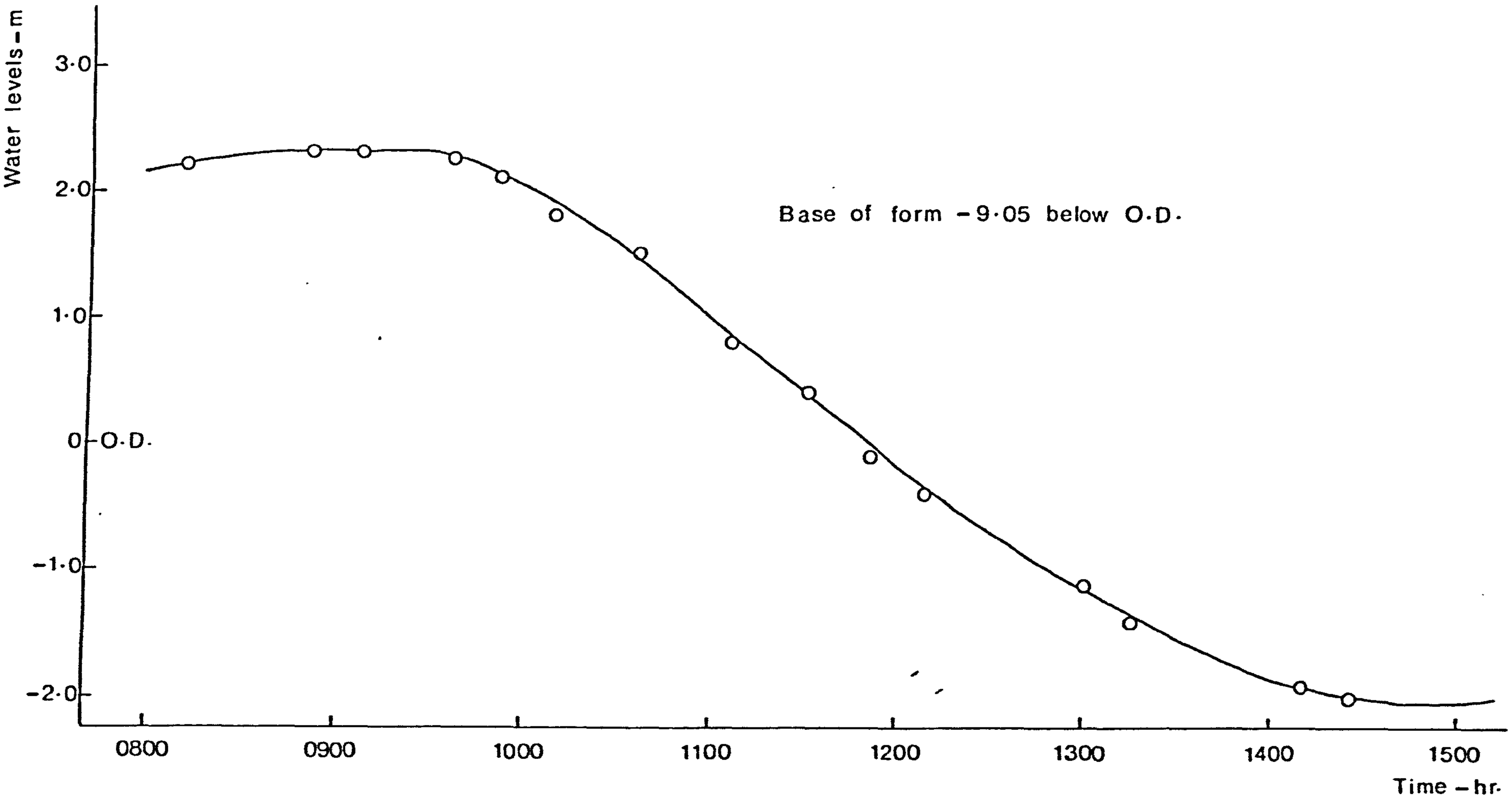

The gauge calibration factors were obtained by direct calibration of the gauges against a known pressure. The gauges were calibration before waterproofing and the waterproofing operation did not affect the face of the gauge. When the calibration factors were checked by inserting the whole gauge in a water pressure vessel, two of the gauges registered different calibration factors. In the time available before the test, there was no way of proving which, if either, of the two calibration factors was correct. Therefore the three most reliable gauges were placed in the lower positions in the form and the two suspect gauges at 2.8 and 3.8 m above the base. It was intended to recover the gauges and check them after the site test, but there was a delay of several weeks before the formwork with the gauges was removed from the river Thames. During this period and the subsequent transportation around the site, the gauges were damaged so that re-calibration was not possible.

During the site test, one of these suspect gauges proved to be defective as it gave random bridge readings during recorded tide changes. The results from this gauge which was 3.8 m above the base, have not been plotted in Figure 5.5. Figure 5.5 gives the effective formwork pressure, calculated from the gauge readings using Equation 5.5, against time for the four remaining gauges. In Figure 5.5(d) the effective formwork pressure has been calculated and plotted using both of the calibration factors.

Comparing the effective formwork pressure with the pressure from the submerged weight of concrete, $(\gamma - \gamma_o)\, h$, is not straightforward with underwater tremied concrete pours. Firstly, is the concrete head measured inside or outside the tremie tube ? The concrete heads will not be the same. Whichever it is, trying to measure it accurately in an opaque, fast flowing river is difficult. A simpler and probably as accurate method of assessing the vertical pressure from the concrete is to assume the batch quantities are correct (with the very strict quality control during this test, this assumption is reasonable) and then calculate the pressure. The pressure from the submerged weight of concrete, calculated by this method, has been plotted in Figure 5.5 to give a comparison between the vertical and horizontal stresses. Figure 5.5 shows that in some areas the horizontal stress substantially exceeds the

Figure 5 5 · Pressure measurements on an underwater tremie pour ·

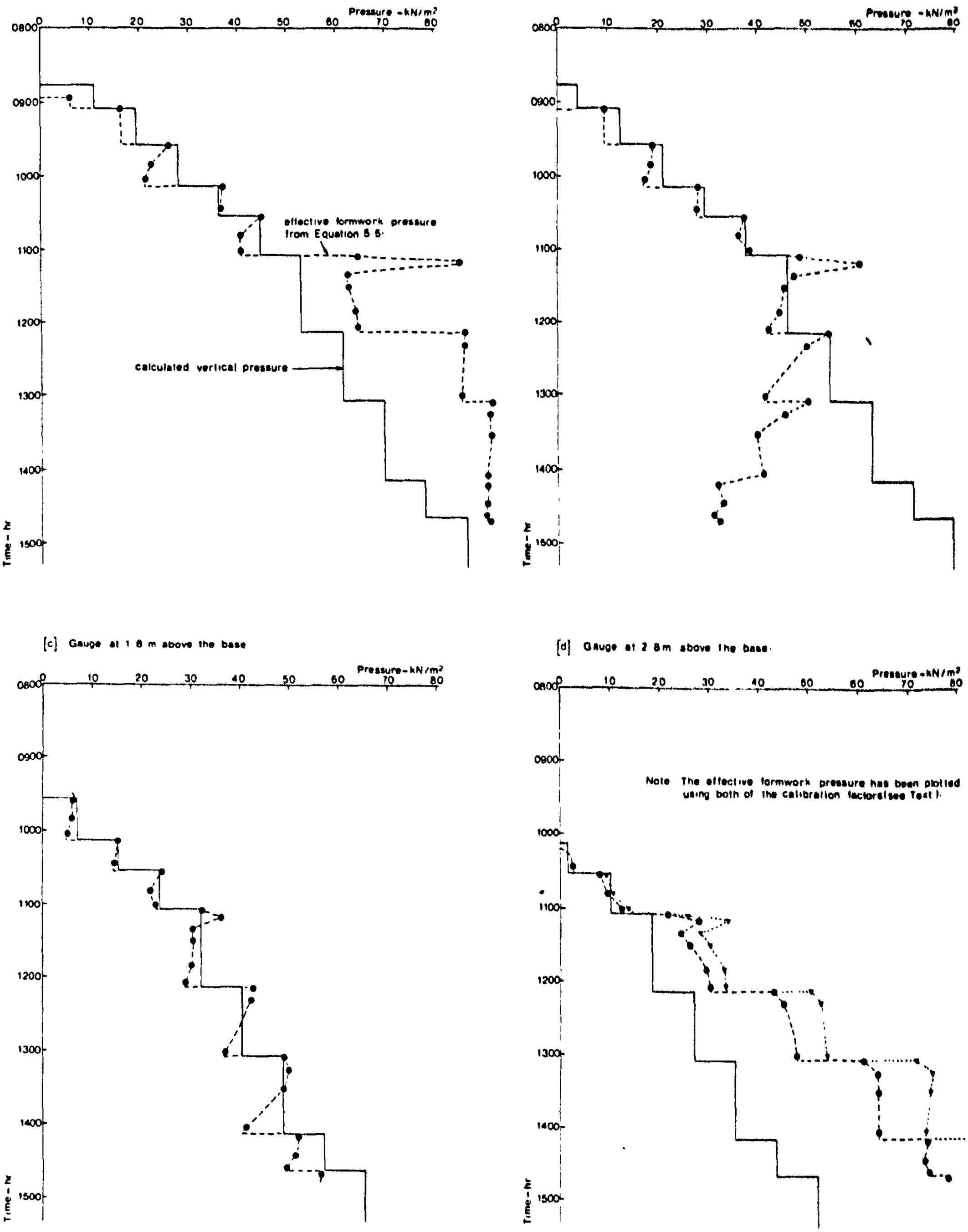

vertical stress.

5.4 DISCUSSION OF THE RESULTS

One of the traditional ways of checking formwork pressure measurements is to compare the horizontal pressure with the fluid pressure of the concrete; if the horizontal pressure exceeds the fluid pressure other than during impact, the results are rejected as an impossible condition. On this basis, half of the results presented in Figure 5.5 should be rejected, but the new theory presented in Chapter 4 offers a logical explanation of these results.

The horizontal pressure is made up from two elements, a component of the effective pressure and the pore water pressure (Equation 4.2). The rate of transfer of load from the pore water onto the particle structure depends on the hydraulic gradient through the section and the development of suction forces. A change in tide level will change the hydraulic gradient. If the drainage path length is short and the concrete is fresh, a change in tide level is rapdily followed by an equal change in pore water pressure. This is demonstrated in Figure 3.5. As the drainage path length increases and time passes, a change in tide level takes an increasing period of time to be reflected by an equal change in pore water pressure at the gauge location. Although there is this delayed response in the concrete to the tide changes, the support to the formwork from the external water is instantaneously affected. With an ebbing (falling) tide, the reduction in support to the formwork without an equal reduction in the pore water pressure produces an increased load on the formwork. In zones of rapid tide fall, this can result in the situation given in Figure 5.5. With a flooding tide, the effective formwork pressure which is the concrete pressure on the formwork less the support to the formwork from the water, is reduced. The understanding of this phenomenon and the acceptance of the site measurements are a direct result of the theory given in Chapter 4.

The contractor wanted to know what would have been the effective formwork pressure if there had been no tide change. The intention was to design the ties to the no tide change situation and then only concrete on a flooding tide. The benefits from the rising tide

were going to be used as an additional factor of safety. In order to estimate the formwork pressure if there had been no tidal effects, Figure 3.5 was re-studied as this gave the response of a short length of concrete (approximately 200 mm) to changes in applied water pressure. This figure showed how changes in the applied water pressure produced instantaneous changes in the gauge pressure at first, but delayed changes at latter ages. In the site test, the temperature of the concrete was lower, but the length of the drainage path larger and increasing with each lift. The effective pressure consolidating the particle structure would also have been larger than in the laboratory test. The data only justified a simple adjustment to the measured pressure to exclude the effects of tide change. Therefore it was assumed that the tide changes had produced an instantaneous and equal change in the pore water pressure at the instrument for the first half hour after covering it with concrete and that 4 hr after covering the instrument, the permeability of the concrete and length of drainage path were such that a change in tide level produced no affect on the pore water pressure at the gauge level. Between these two extremes of instantaneous response and no response in the pore water pressure at the gauge location, linear change was assumed. In effect, these assumptions make no change in the effective formwork pressure given by Equation 5.5 for the first $\frac{1}{2}$ hr. after placing. After $\frac{1}{2}$ hr., the effective formwork pressure obtained from Equation 5.5 needed to be reduced by the amount of the tide fall not matched by a change in pore water pressure at the gauge location. An estimate of this is obtained from:

$$\text{Pressure on formwork due to tide fall} = \gamma_o \sum_{t=\frac{1}{2}hr}^{t=t} a \, \Delta (h + x)$$

where a is a coefficient obtained from Figure 5.6 and

$\Delta (h + x)$ is the incremental tide change.

An example of the calculation of the effective formwork pressure and the adjustment to remove tidal effects is given in Table 5.1

TABLE 5.1 Calculation of the effective formwork pressure and the adjustment to remove tidal effects

Time	Col. factor x bridge reading kN/m²	Tide level m	Incremental change in tide level m	Coefficient 'a' from Figure 5.6 -	$\gamma_o \Delta(h \cdot x)$ kN/m²	$\gamma_o \sum \Delta(h \cdot x)$ kN/m²	$\gamma_o \sum a\Delta(h \cdot x)$ kN/m²	Effective formwork pressure Col.2-Col.7 kN/m²	Adjusted pressure Col.9-Col.8 kN/m²
0850	0	$2.3+x_o$	0	0	0	0	0	0	0
0856	6.1	2.3	0	0	0	0	0	6.1	6.1
0906	16.2	2.3	0.05	0	0	0	0	16.2	16.2
0935	25.5	2.25	0.15	0.1	0.15	0.5	0	26.0	26.0
0950	20.6	2.1	0.1	0.17	0.17	2.0	0.15	22.6	22.4
1002	18.4	2.0	0.15	0.21	0.32	3.0	0.32	21.4	21.1
1008	32.5	1.85	0.25	0.27	0.68	4.5	0.64	37.0	36.4
1026	29.8	1.6	0.15	0.33	0.49	7.0	1.32	36.8	35.5
1033	36.4	1.45	0.25	0.38	0.95	8.5	1.81	44.9	43.1
1048	29.8	1.2	0.25	0.45	1.13	11.0	2.76	40.8	38.0
1100	27.2	0.95	0.10	0.49	0.49	13.5	3.89	40.7	36.8
1105	50.1	0.85	0.10	0.51	0.51	14.5	4.38	64.6	60.2
1110	69.3	0.75	0.20	0.55	1.10	15.5	4.89	84.8	79.9
1120	45.2	0.55	0.15	0.60	0.90	17.5	5.99	62.7	56.7
1130	43.9	0.4	0.45	0.67	3.01	19.0	6.89	62.9	56.0
1150	40.8	-0.05	0.25	0.75	1.88	23.5	9.9	64.3	54.4
1204	38.6	-0.3	0.05	0.79	0.39	26.0	11.78	64.6	52.8
1208	59.7	-0.35	0.15	0.82	1.23	26.5	12.17	86.2	74.0
1218	58.4	-0.5	0.65	0.95	6.17	28.0	13.4	86.4	73.0
1300	51.4	-1.15	0.05	1.0	0.5	34.5	19.57	85.9	66.3
1304	57.1	-1.2	0.15	1.0	1.5	35.0	20.07	92.1	72.0
1315	54.9	-1.35	0.20	1.0	2.0	36.5	21.57	91.4	69.8
1330	53.5	-1.55	0.30	1.0	3.0	38.5	23.57	92.0	68.4
1402	49.6	-1.85	0.05	1.0	0.5	41.5	26.57	91.1	64.5
1410	49.2	-1.9	0.1	1.0	1.0	42.0	27.07	91.2	64.1
1425	47.8	-2.0	0	1.0	0	43.0	28.07	90.8	62.7
1435	47.8	-2.0	0.05	1.0	0.5	43.0	28.07	90.8	62.7
1440	47.8	-2.05				43.5	28.57	91.3	62.7

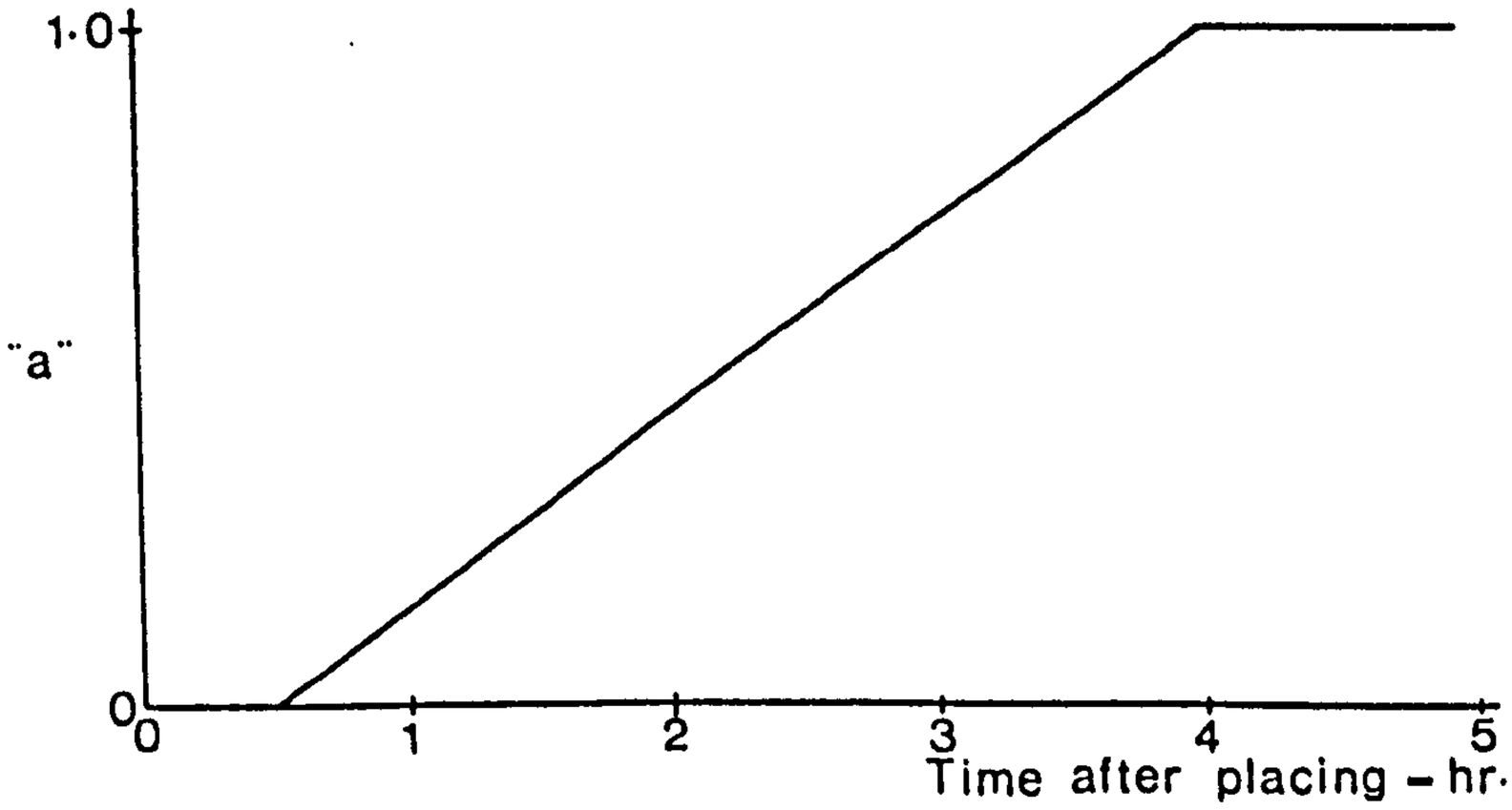

Figure 5·6 Graph to obtain coefficient "a"

The results of this adjustment are given in Figure 5.7. The results from the three lower gauges show the horizontal pressure following the predictions of the theory (Figure 4.5). These site measurements demonstrate the horizontal pressure returning to the fluid pressure (without vibration) as a fresh lift is placed and the pressure falling during the interval between lifts. At 1110 there is a clear example of the collapse of the particle structure. At 1104, a lift of concrete had been placed and then the operatives started to raise the tremie tube ready for the next lift. It was during this raising of the tremie tube, that this collapse of the particle structure took place. All the gauges that were covered with concrete recorded this phenomenon. The next lift of concrete at 1208 also caused a particularly large jump in the horizontal pressure, but not all the gauges showed it decaying as rapidly as the previous collapse. This may be due to the repeated impact as the lifts are discharged causing particles to be wedged against the diaphragm preventing its free return. With this retarded concrete, the particle structure was susceptible to the impact on discharge for 5 hours after placing. The suspect gauge, Figure 5.7(d), is plotted with the calibration factor that was similar to the three lower gauges. Even after adjustment, this gauge still gave a horizontal pressure that consistently exceeded the vertical pressure. Several possible explanations exist; the calibration factor is incorrect; the change in pore water pressure at the gauges due to

Figure 5 7 Horizontal pressures adjusted to remove tidal effects.

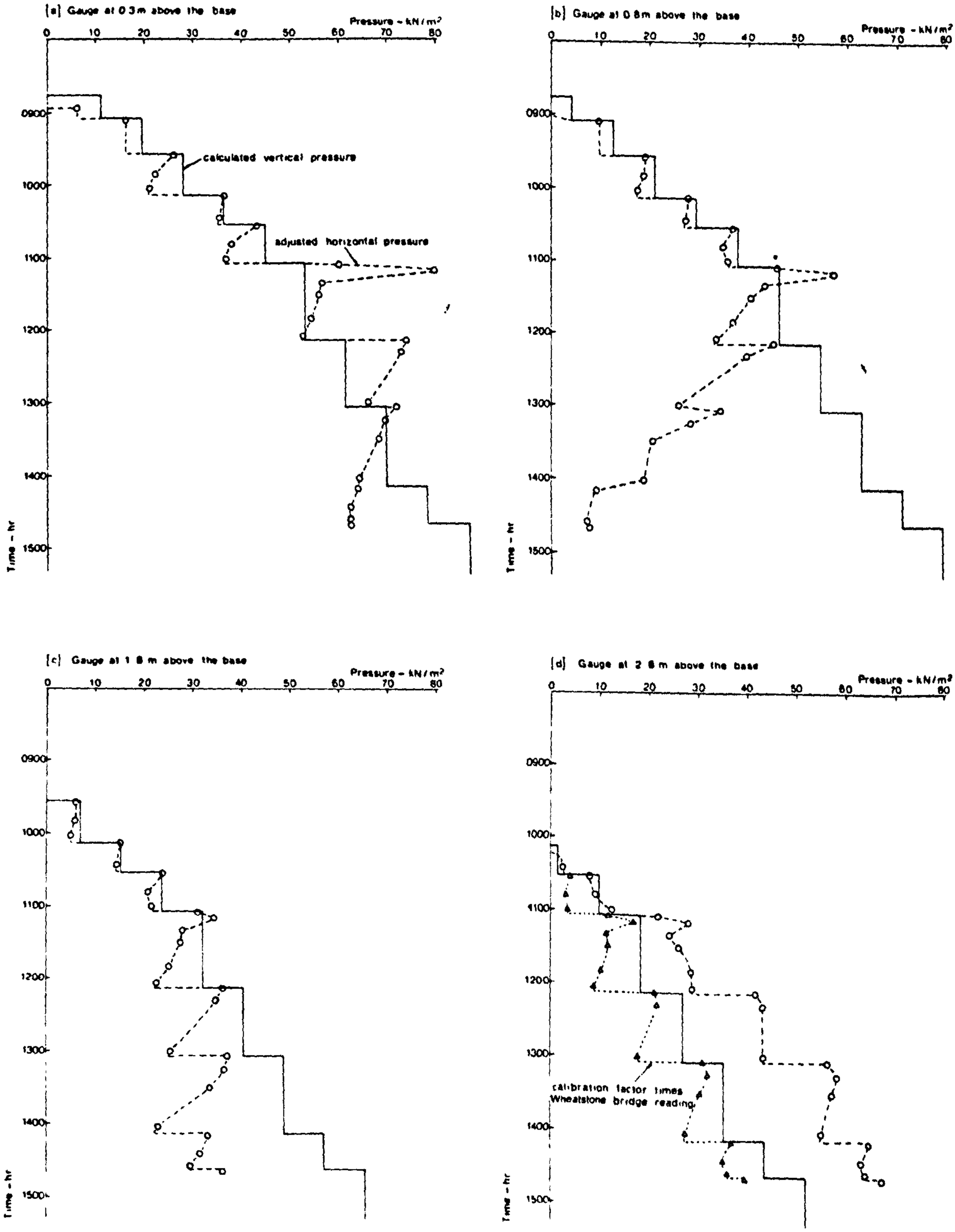

tidal effects is slower than estimated; the head of concrete is not as estimated or the results are due to impact loading and wedging of the diaphragm.

The gauge did not appear to exhibit any gross defect and a small error in the calibration factor would not make a major difference to the results. The rising horizontal pressure between 1030 to 1100 and 1120 to 1204 without an increase in the head of concrete suggests that the adjustment for tidal effects was not adequate. When the previous gauges were covered with concrete, the rate of tide change was slow, but this gauge was covered in concrete during a period of rapid tide change. Plotting the calibration factor times the Wheatstone bridge reading component of Equation 5.5 onto Figure 5.7(d), shows that on its own, it is almost equal to the vertical pressure. This could imply that the pore water pressure at the gauge is insensitive to tide changes once the head of concrete exceeds one full 0.6 m lift. This cannot be reconciled with the theory and applying this implication to the gauges at 0.8 and 1.8 m results in them producing negative formwork pressures. Nevertheless some overestimation of the rate at which the pore water pressure at a gauge responds to tide changes at early ages may be a contributing factor to the results obtained in Figure 5.7(d).

As already described the vertical pressure and head of concrete above a gauge was calculated. On site when the originally calculated volume of concrete had been placed, a diver showed that the concrete was about 200 mm below the top of the form. There had been some loss of concrete from the first lift and consequentially the vertical pressure had been calculated on the basis of a 0.5 m first lift as opposed to the normal 0.6 m lifts. The error from the remaining 0.1 m of concrete is negligible.

The most probable explanation of the results for the gauge at 2.8 m is impact loading and the wedging of the diaphragm. The three lifts at 1104, 1208 and 1304 all resulted in jumps in horizontal pressure that were significantly greater than the increase in static vertical pressure. These large jumps in pressure were recorded on the other gauges, but they in general showed a reduction in pressure after the peak. With the 2.8 m gauge there was little tendency for the

pressure to reduce which could be the result of the gauge being wedged with solid particles.

This site test has produced evidence in support of the concepts of the theory, and has also proved the value of the theory in interpreting unusual site data.

Chapter 6 MAIN CONCLUSIONS AND FURTHER RESEARCH

6.0 MAIN CONCLUSIONS

The literature survey and analysis of existing site data showed:-

1. The horizontal pressure on formwork starts by following the fluid pressure of concrete and then deviates to reach a maximum value. There was not agreement as to whether or not the pressure reduced after the maximum.

2. The assumed association between the depth to which the concrete acts as a fluid and the influence of vibration did not agree with observations on the compacting ability of internal vibrators.

3. Theories for a maximum horizontal pressure did not satisfy all the observations.

4. The maximum pressure on formwork might involve both chemical and physical processes.

5. The role of pore water pressure in the development of the maximum horizontal pressure had not been examined thoroughly and warranted further research.

6. For OPC concretes, CIRIA design method generally predicts a safe upper limit for the concrete pressure except at low calculated pressures.

A laboratory experimental programme proved:-

1. Concrete can be consolidated by static loading.

2. The permeability of concrete changes gradually throughout the dormant period.

3. The horizontal pressure can equal the vertical pressure without vibration.

4. There is no relationship between the depth to which the horizontal pressure follows the fluid head and the effective depth of

vibration.

5. The horizontal pressure consists of two components, a component from the particle structure and the pore water pressure.

6. The pore water pressure provides the dominant contribution to the maximum horizontal pressure in normal formwork.

7. The chemistry of cement contributes to the development of horizontal pressure by producing progressive changes in the structure during the dormant period and by controlling the time at which the initial structure is reinforced with C-S-H.

8. The initial particle structure is weak and is susceptible to dislocation. Dislocation of the particle structure results in the load being transferred onto the pore water pressure and a sudden increase in the horizontal pressure. After disturbance the particle structure quickly re-establishes itself.

From the experimental work, a theory for concrete pressures on formwork in wide sections was formulated which has as its main elements:-

1. The horizontal pressure consists of a component of the effective pressure and the pore water pressure.

2. The pore water pressure provides the main contribution to the maximum horizontal pressure in normal formwork.

3. The transfer of stress from the pore water onto the particle structure depending on consolidation, the development of the hydration products and the development of suction forces.

4. The slower the dispersal of pore water pressure, the higher the horizontal pressure.

5. Any factor which increases the rate of dispersal of pore water pressure, reduces the maximum horizontal pressure.

6. The reduction in pressure after the maximum is small with flexible formwork due to the inability of the form to return to the

undeflected shape.

7. The minimum depth of concrete fluidity is equal to the depth of poker immersion.

It was also concluded that the data needed to evalue the coefficients in a mathematical model would not be known to a precision that would give an economic design of form. The theory provides a logical framework for analysing site data and indicates areas in which potential economies in design might be made.

Site pressure measurements on an underwater tremied concrete pour confirmed many of the elements of the theory and showed its value in interpreting unusual site data. These measurements also showed that during a rapidly falling tide, the horizontal pressure can exceed the vertical pressure.

6.1 FURTHER RESEARCH

There is an urgent need for more site data in a number of specific areas. A programme of measurements has been instigated to obtain these data. The areas specified for further measurements in this programme are:-

1. Concretes with admixtures especially retarders and super-plasticizers.

2. Concretes with replacement materials.

3. Wall forms designed to formwork pressures exceeding 100 kN/m^2 (This is to check if the ACI limit of 100 kN/m^2 for walls[41] is valid for modern construction).

In addition to these, there are two further areas of interest which are a direct result of the work presented in this thesis, namely,

4. Unsealed plywood formwork.

5. Porous formwork such as steel mesh or fabrics.

This programme of measurements will require at least 50

separate site measurements and because of the problems of finding suitable sites will probably take 2 to 3 years to complete.

The fundamental investigation into formwork pressures needs to be continued with the consideration of narrow sections. Arching (the transfer of vertical load to the formwork or reinforcement) does not appear to be the complete explanation to the lower pressures obtained. There are strong indications that formwork movements will be of major importance in narrow sections and this warrants further research. Formwork permeability is also likely to be a major factor.

REFERENCES

1. THE CONCRETE SOCIETY. Formwork - report of the joint Committee. London, Concrete Society Technical Report No. 13, March 1977.

2. THE CONCRETE SOCIETY. Falsework - report of the joint Committee. London, Concrete Society Technical Report No.4, July 1971.

3. KINNEAR et al. The pressure of concrete on formwork. London, Civil Engineering Research Association Report No.1, April 1965.

4. FERGUSON, H. Collapses. New Civil Engineer, 11th March 1976. pp 26, 27 and 29.

5. FELD, J. Formwork failures - failure lessons in concrete construction. A collection of articles from Concrete Construction Magazine. June 1974, pp 6 - 10.

6. NESBIT, J.K. Structural lightweight - aggregate concrete. Concrete Publications Ltd. 1966, pg 77.

7. BIRCH, N., LEE, C.T. and WALKER, M.B.A. The distribution of loading on props to soffit formwork. London, Construction Industry Research and Information Association. March 1977.

8. GATES, M. and SCARPA, A. Concreting and formwork logistics and optimization. Journal of the Construction Division. Proc. of the ASCE, Vol. 104, No. CO2, June 1978, pp 219 - 240.

9. CONSTRUCTION INDUSTRY RESEARCH AND INFORMATION ASSOCIATION. Formwork Loading Design Sheet (Metric). London, Construction Industry Research and Information Association, 1969.

10. THE CONCRETE SOCIETY. Concrete pressure graphs for formwork design. London, July 1972. ISCS4. (52.023).

11. RODIN, S. Pressures of concrete on formwork. Proceedings of the ICE, Vol. 1, Nov. 1952, pp 709 - 746. Correspondence Part 1, Vol. 2, 1953, pp 460 - 462.

12. GUERRIN, A. La poussée exercée par le béton frais sur les coffrages. Technique des Travaux 26 JHG 1950, pp 309 - 320.

13. JANSSEN, H.A. Versuche Über Getreidedruck in Silozellen. UDI Zeitschrift (Düsseldorf) 39, 31st Aug. 1895, pp 1045 - 1049.

14. REIMBERT, M. and REIMBERT, A. Silos - Traité Théoretique et Pratique. Editions Eyrolles, Paris 1961.

15. CAPPER, P.L. and CASSIE, W.F. The mechanics of engineering soils. Span's Civil Engineering Series 1966.

16. SCOTT, C.R. Soil mechanics and foundations. Applied Science Publishers Ltd. pp 213 - 215.

17. USPENSKIJ, V.P. Über den Schalungsdruck von Frischbeton in Trudy Leningrad. Politechn. Inst. No. 208, 1960, pp 321 - 327.

18. DRECHSEL. Die Gleitschalung. Berlin 1950.

19. BOHM, F. Über den Seitendruck des frisch eingebrachten Betons. Beton und Eisen, Vol. 28, Part 18, 1929, pp 329 - 335.

20. TOUSSAINT, F. Schalungsdruck bei grossen Betonkorpern. Österreichiesche Bauzeitschrift, 5. H.1. 1950, pp 11 - 13.

21. HOFFMANN, R. Der Schalungsdruck von frischem Beton. Beton und Stahlbeton 42. H. 17/18, 1943, pp 130 - 134.

22. GAEDE, K. Zuschrift zu Hoffmann : Der Schalungsdruck von frischem Beton. Beton und Stahlbetonbau 43 H.15/16 1944, pp 95-96

23. HYDRO-ELECTRIC POWER COMMISSION OF ONTARIO. Summary of Laboratory Investigations of Concrete Form Pressure. Unpublished, Feb. 1957.

24. ACI COMMITTEE 622. Pressures on formwork. Journal of the ACI, Title No. 55-10, Vol.30, No.2, Aug. 1958.

25. MUHS, H. Zum Schalungsdruck des Betons. Beton und Stahlbeton 50 H.6. 1955, pp 158 - 163.

26. OLSSON, G. Betongs sidetrykk. Teknisk Ukeblad 19 Feb. 1953, pp 140 - 148.

27. SCHJØDT, R. Betons sidetrykk mot forskalling. Teknisk Ukeblad 30 Aug. 1951, pp 611 - 614.

28. SCHJØDT, R. Calculation of pressure of concrete on forms. Proc. of the ASCE, Vol.81, Paper 680, May 1955, pp 1 - 16.

29. ACI COMMITTEE 622. Discussion on Ref. 24. Journal of the ACI, June 1959, pp 1335 - 1348.

30. BRITISH STANDARDS INSTITUTION. Methods of testing cement. BS 4550 : Part 3 : 1978.

31. WITTE, A.M. Les facteurs qui influent sur la poussée laterale exercée par le béton fais sur les parois du coffrage. Béton arme 5 JHG 1961, No. 32, pp 24 - 30 and No. 33 pp 23 -37.

32. LEVITSKY, M. Form pressure and relaxation in formwork. Journal of the Engineering Mechanics Division, Proc. of ASCE, Vol. 101, No. EM3, June 1975, pp 267 - 277.

33. LEVITSKY, M. Analytical determination of pressure on formwork. Journal of the Engineering Mechanics Division, Proc. of ASCE, Vol. 100, No. EM3, June 1973, pp 551 - 564.

34. RITCHIE, A.G.B. Pressure developed by concrete on formwork, Part I. Civil Engineering and Public Works Review, Vol. 57, No. 672, July 1962, pp 885 - 888.

35. RITCHIE, A.G.B. Pressure developed by concrete on formwork, Part II. Civil Engineering and Public Works Review, Vol. 57, No. 673, Aug. 1962. pp 1027 - 1030.

36. RITCHIE, A.G.B. Research on pressures developed by concrete on formwork. Structural Concrete, Vol. 1, No. 10, July-Aug. 1963, pp 454 - 463.

37. ADAM, M. Emploi des pannaux de fibres de bois comme coffrage. Annales de l'Institute Technique du Bâtiment et des Travaux Publics, No. 161, Mai 1961.

38. ROHLING, S. Pressure by fresh concrete on vertical formwork. Translation from " Bauplanung - Bautechnik, Vol. 28, No. 12, Dec. 74, pp 580 - 582 ". C and C A Translation Number 0741.

39. RODIN, S. Pressure of concrete on formwork. Structural Concrete, Vol. 1, No. 10, July - Aug. 1963, pp 445 - 453.

40. ACI COMMITTEE 622. Proposed recommended practice for concrete formwork. Title 59 - 37. Proc. of the ACI, Vol. 59, Aug. 1962, p 999.

41. ACI COMMITTEE 347. Recommended practice for concrete formwork. Title 74 - 38, ACI Journal, Sept. 1977, p 403.

42. TELLER, L.W. The effect of vibration on the pressure of concrete against formwork. Public Roads, Vol. 12, No. 1, March 1931, pp 11 - 15.

43. SMITH, E.B. Concrete pressure against forms. Public Roads, Vol. 2, No. 23, March 1920, pp 15 - 20.

44. ERTINGSHAUSEN, H. Uber den Schalungsdruck von Frischbeton Ph.D Thesis. Faculty of Building of the Technological University of Hanover, 1965, pp 97. (Translation into English of text held at C and C A Library, Wexham Springs, England, No. 69.057, pp 1 - 186).

45. ADAM, M., BENNASR, M. and SANTOS DELGARDO, H. Poussée du Béton frais sur les coffrages. Annales de l'Institut Technique du Bâtiment et des Travaux Publics, No. 207 - 208, Mars-Avril, 1965. pp 402-425.

46. KINNEAR R.G. The formwork pressure balance. London, Cement and Concrete Association Technical Report, 42.373, August 1963.

47. TUTHILL, L.H. and GORDON, W.A. Properties and uses of initially retarded concrete. Journal of ACI, Vol. 27, No. 3, Nov. 1955

48. PALANCA, J.M. La vibracion de encofrados. Madrid, Instituto Eduardo Torroja de La Construccion y del Cemento. Monografias n. 347, diciembre, 1977.

49. CONSTRUCTION INDUSTRY RESEARCH AND INFORMATION ASSOCIATION. Formwork Loading Design Sheet (Imperial) London, Construction Industry Research and Information Association, Undated.

50. ORE, E.L. and STRAUGHAN, J.J. Effect of cement hydration on concrete form pressure. Journal of ACI, Title No. 65 - 9, Feb. 1968, pp 111 - 120.

51. McDOWALL, D.C. and RITCHIE, A G.B. The effect of mix characteristics on the early stiffening process of concrete allied to the pressure of concrete on formwork. London, Construction Industry Research and Information Assoc. Project Record RP64, Nov. 1969. In three volumes.

52. POWERS, T.C. The properties of fresh concrete. John Wiley and Sons Inc., 1968.

53. RITCHIE, A.G.B. The triaxial testing of fresh concrete. Magazine of Concrete Research, Vol. 14, No. 40, March 1962, pp 37 - 42.

54. MURPHY, W.E. The pressure exerted on formwork by lightweight aggregate concrete. Slough, Cement and Concrete Association, Internal Note, June 1973, pp 4.

55. KONDO, M and YAMANE, S. Lateral pressure of concrete. Part 1 Experiments relating to lateral pressures in pumpcreting. Part 2. Reinforcement ratio and rate of placement affecting lateral pressure. Takenaka Technical Research Laboratory, Sept. 1970.

56. TAYLOR, R.W. The compaction of concrete by internal vibrators - an investigation of the effects of frequency and amplitude. Slough, Cement and Concrete Association Technical Report 42.511, March 1976.

57. TATTERSALL, G.H. The principles of measurement of the workability of fresh concrete and a proposed simple two - point test. Dept. of Building Science, University of Sheffield pp 32.

58. ASCHAN, N. Determining the setting time of cement paste, mortar and concrete with a copper - lead electrode. Magazine of Concrete Research, Vol. 18, No. 56, Sept. 1966, pp 153 - 160.

59. MURPHY, W.E. The influence of concrete mix proportions and type of form face on the appearance of concrete. London, Cement and Concrete Association Technical Report 384, May 1967.

60. TERZAGHI, K. Theoretical soil mechanics. J. Wiley, 1943, pp 265 - 296.

61. BROWNE, R.D. and BDAMFORTH, P.B. Tests to establish concrete pumpability. ACI Journal, May 1977, pp 193 - 203.

62. TAYLOR WOODROW RESEARCH LABORATORIES. The Taylor Woodrow Construction pressure bleed test. Pamphlet MD 75/005, p 4.

63. MAYNARD, D.F. and MACLEOD, G. Factors influencing the deflection of plywood sheeting in formwork. London, Construction Industry Research and Information Association, Report 37, Oct. 1971.

64. PERRY, C.C. and LISSNER, H.R. The strain gage primer. 2nd Edition 1962, McGraw-Hill Book Company, pp 332.

65. VAUGHAN, P.R. The measurement of pore pressures with piezometers. Proc. Symposium Field Instrumentation in Geotechnical Engineering, Butterworths, London 1973, pp 411 - 422.

66. BISHOP, A.W., VAUGHAN, P.R. and GREEN, G.E. Pore pressure measurements in the field and in the laboratory. Proc. 7th Int. Conf. Soil Mech. and Foundation Engineering, 1969, pp 427 - 444.

67. BRUERE, G.M. Actions of admixtures in plastic concrete and cement - admixture interactions. Workshop on the use of chemical admixtures in concrete. The University of New South Wales, Dec. 1975, pp 29 - 41.

68. CEMENT AND CONCRETE ASSOCIATION. Superplasticizing admixtures in concrete. Slough, Cement and Concrete Association, January 1976. Report 45. 030.

69. OWENS, P.L. Basic mix method. Slough, Cement and Concrete Association, 1973. Publication 11.005.

70. RAFFLE, J.F. The formation of structure in cement slurries. First International conference on the hydraulic transport of solids in pipes. Sept. 1970, Paper D2, pp 33 - 40.

71. KING, A. and RAFFLE, J.F. Studies on the settlment of hydrating cement suspensions. J. Phys. D : Appl. Phys., Vol. 9, 1976.

72. LOCHER, F.W., RICHARTZ, W. and SPRUNG, S. Setting of cement - Part 1. Reaction and development. Zement - Kalk - Gips, Heft 10, Oct. 1976, pp 435 - 442. (English translation of text, No. 12/ 1976, pp 257 - 261).

73. LOCHER, F.W., RICHARTZ, W. and SPRUNG, S. Studies on the behaviour of C_3A in the early stages of cement hydration. Summaries of contributions to a seminar at the University of Technology, Eindhoven, The Netherlands, April 13- 14 1977, p 5.

74. PREVITE, R.W. Concrete slump loss. ACI Journal, Aug. 1977, Title No. 74 - 35, pp 361 - 367.

75. McCARTHY, M. and HODGKINGSON, L. Admixtures for concrete in hot climates. Publication by Cormix Division of Joseph Crosfield and Sons Ltd (Ref. M 667) Feb. 1978, p 10.

76. BRITISH STANDARDS INSTITUTION. Sulphate-resisting Portland cement. B.S. 4027 : Part 2 : 1972.

77. BRITISH STANDARDS INSTITUTION. Ordinary and rapid-hardening Portland cements. B.S. 12 : 1978.

78. TERRIER, P. and HORNAIN, H. Sur la composition de l'aluminate tricalcique. Revue des Materiaux (France) mar 1971.

79. HORNAIN, H. Sur la répartition des éléments de transition et leur influence sur quelques propriétés du clinker et du ciment. Revue des Materiaux (France) Aug. 1971.

80. BRANDENBERGER, E. Kristallstructur und Zementchemie; Grundlagen einer Stereochemie der Kristallverbindungen in den Portland zementen. Compte rendu n° 114 du Laboratoire Fédéral d'Essai des Materiaux (Suisse) 1938.

81. JOISEL, A. Admixtures for cement, physico-chemistry of concrete and its reinforcement. Published by the author, 1973 pp 253.

82. SKALNY, J. The preacceleration stages of hydration - new data. Cembureau. Summaries of contributions to a seminar in Koge, Denmark, May 1975, pp 3.

83. TUTHILL, L.H. Slump loss·Concrete International, Jan. 1979, pp 30 - 35.

84. MEYER, L.M. and PERENCHIO, W.F. Theory of concrete slump loss as related to the use of chemical admixtures. Concrete International, Jan. 1979, pp 36 - 43.

85. RIXOM, M.R. et al. Concrete admixtures : Use and applications The Construction Press, 1977.

86. DOUBLE, D.D. and HELLAWELL, A. The hydration of Portland cement. Nature, Vol. 261, June 10, 1976, pp 486 - 489.

87. DOUBLE, D. D. and HELLAWELL, A. The solidication of cement. Scientific American. Vol.237, 1977, pp 82 - 90.

88. WITTMANN, F.H. On the action of capillary pressure in fresh concrete. Cement and Concrete Research, Vol. 6, 1976, pp 49 - 56.

89. RAFFLE, J.F. and KING, A. The effect of cellulose ethers and lignosulphonates on the settling and flow properties of cement suspensions. J. Phys. D : Appl. Phys., Vol. 10, 1977.

90. HARRISON, T.A. Mechanical damage to concrete by early removal of formwork. Slough, Cement and Concrete Association, Technical Report 42.505, Feb. 1975, pp 28.

91. RAFFLE, J.F. Pressure variations within concentrated settling suspensions. J. Phys. D : Appl. Phys., Vol. 19, 1976.

92. GARDNER, N.J. and HO, P.T.J. Lateral pressure of fresh concrete. ACI draft manuscript in the review process. Rev. 12/76.

93. COFI. Design of plywood formwork with COFI exterior Douglas fir plywood. Trade literature COFI. Undated.

94. LANE, F.E. The use of chipboard as a formwork sheeting material. Slough, Cement and Concrete Association Test Memorandum. Also TDH 3642, April 1978, pp 19.

95. CIRIA. Concrete pressure on formwork. London, CIRIA 1SBN : 086017 1043, Undated but first published in 1978, pp 2.

96. INTRUSION PREPAKT. Fabriform. Trade literature. Intrusion Prepakt (UK) Ltd. 1978, pp 6.

97. CANNON, E.W. Grouting using fabric shuttering. Intrusion Prepakt (UK) Ltd. Jan. 1978, pp 4.

98. EXPAMET. Expamet Hy-rib in concrete construction work. Trade literature leaflet No. BP 15, Sept. 1978.

99. ANGLES, J.G. Why use admixtures in concrete. FEB (Great Britain) Ltd. Undated, pp 12.

100. GRAY, W.A. The packing of solid particles. Chapman and Hall Ltd. 1968.

101. OWENS, P.L. Private communication. May 1978.

Appendix A THE USE OF THE PRESSURE BLEED TEST FOR MEASUREMENTS OF THE FLUID LOSSES IN CONCRETE

INTRODUCTION

The Taylor Woodrow pressure bleed test[61,62] is used to simulate the dewatering of concrete in pumping pipelines. The pressure applied to the concrete is high, 3500 kN/m^2, and this produces a very rapid dewatering of the concrete. In an attempt to assess the volume of fluid lost by consolidation at pressures equivalent to the static weight of concrete, the bleed test equipment was borrowed for examination and trial tests.

DESCRIPTION OF THE EQUIPMENT AND TEST METHOD

The equipment consists of a mould made from a section of 125 mm diameter cylinder and a base plate, Figure A.1. Above the base plate is a filter of 50 mesh gauge and a retaining plate. Fluid lost through this filter drains via a bleed tap into a measuring cylinder. The sample of concrete in the mould is compressed by a piston operated by a double acting hydraulic cylinder. The applied pressure is calculated from the reading on a pressure gauge located in the hydraulic oil pipeline.

For these tests, the equipment was only required to work up to an applied pressure of 150 kN/m^2 and therefore the normal pressure gauge was replaced with one of a lower range and greater sensitivity. To calibrate this gauge, the bleed tap was temporarily removed and replaced with a second pressure gauge. With the mould filled with water, the gauge measuring oil pressure was calibrated in terms of applied concrete pressure, Figure A.2. It was immediately apparent that the force required to overcome the system friction was significant and that gauge pressures under 1200 kN/m^2 did not give a reliable indication of the applied pressure.

The normal procedure for the pressure bleed test was unsuitable for the purposes of these trials, so after a few trials, the following test method was evolved.

Figure A·1: Pressure bleed test·

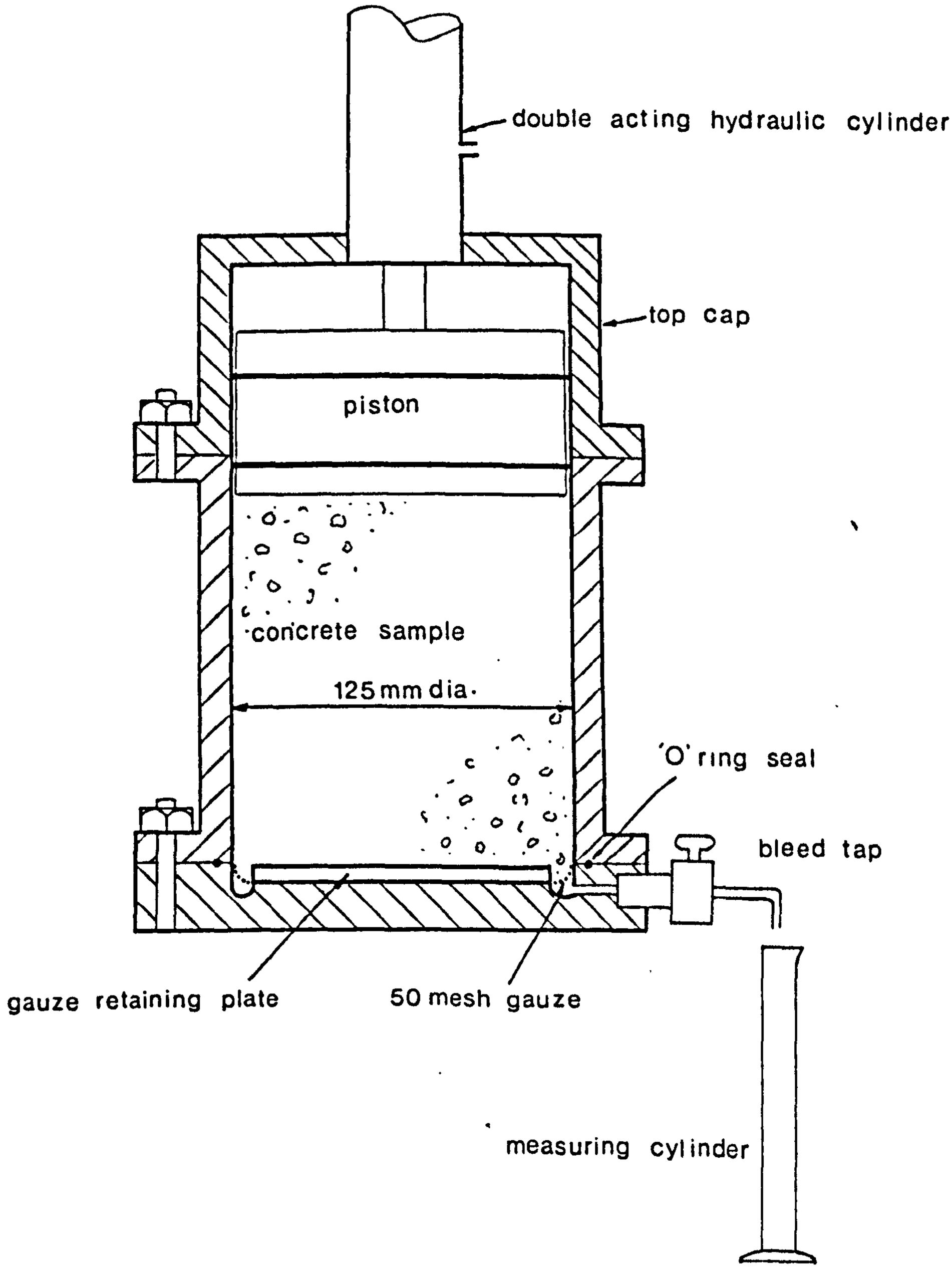

Figure A·2 : Calibration graph·

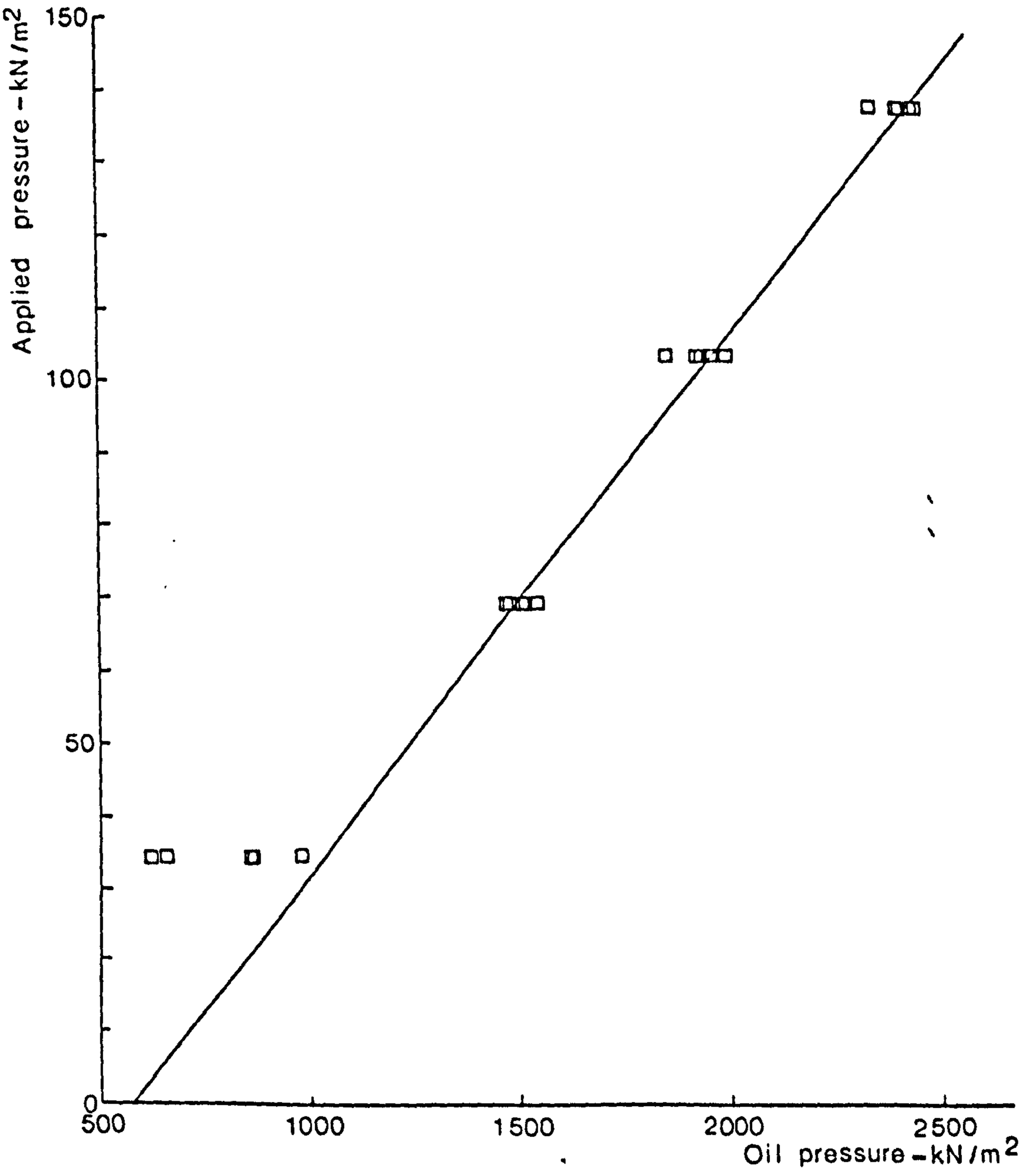

Sufficient concrete for three tests was batched using ordinary Portland cement and singled sized air dry aggregate and sand and then hand mixed to a given workability. The clean mould with the bleed tap closed was placed on a vibrating table and filled with concrete, vibrating continuously, until the concrete was 25 mm from the top of the mould. With the tap cap bolted to the mould, the bleed tap was opened. The piston was rapidly jacked against the concrete until the required gauge pressure was reached and this pressure was maintained for the remainder of the test.

The fluid loss (water plus any solids that had bled from the concrete) was measured against time. At the completion of the test, the fluid that had bled from the concrete was allowed to settle and the volume of solids was recorded. This was to check if the loss of solids was proportional to the fluid loss.

EXPERIMENTAL DESIGN

The first objective of the test programme was to establish whether the experimental technique was reliable and repeatable and the second objective was to assess the fluid loss caused by consolidation.

For the main series of tests, one medium workability, OPC concrete was used. The mix proportions are given in Table A.1. At applied concrete pressures of 35, 70, 85, 105 and 140 kN/m^2, three fluid loss tests were carried out from each of two batches of concrete. This gave six individual results for each pressure level. Normally the three tests from a batch of concrete took under one hour to complete. For one of the tests at 35 kN/m^2 applied pressure, the fluid loss was measured for a period of one hour.

Two batches of high workability, OPC concrete (Table A.1) were tested at applied pressures of 70 and 140 kN/m^2 to check if the fluid losses were significantly different from the medium workability concrete.

RESULTS

The results of the tests have been plotted in Figures A.3 to

TABLE A.1

Mix proportions

Mix materials		Mix proportions /m³	
		Slump 50 mm	Slump 100 mm
Free water(1), Litres		175	190
Ordinary Portland cement, kg		310	340
Coarse aggregate, kg	20 - 10mm	745	705
	10 - 5mm	413	378
Fine aggregate, kg (zone 3 sand)	5 -2.5mm	69	70
	2.5 -1.2mm	69	70
	1.2 - 600	137	139
	600 - 300	258	264
	300 - 150	137	139
	pass 150	17	17

Note

(1) Extra water is required for aggregate absorption

A.10. Where two batches of concrete have been tested at the same pressure, the tests from the first batch have been plotted with a solid line and those from the second batch with a dashed line. The symbols ▲ , ■ and ● represent the first, second and third tests respectively from each batch. The figures in brackets at the end of each plot is the volume of settled solids that were washed out with the water. Table A.2 compares the fluid losses after 6 minutes of applied pressure for all the medium workable batches of concrete.

The fluid losses in the 1580 ml samples of concrete ranged up to 72 ml; after correcting for the volume of solids, this corresponds to losses of up to 26% of the total free water.

DISCUSSION OF THE RESULTS

The calibration curve, Figure A.2, indicates that below a gauge pressure of 1200 kN/m^2 the equipment did not give consistent applied pressures. This high system friction is not significant at the equipments normal applied pressure, 3500 kN/m^2, but as these tests only had an operational range of up to 140 kN/m^2, the system friction was too high for good experimental design. The tests at applied pressures of 70 to 140 kN/m^2 inclusive were on the linear part of the calibration curve. Formwork design pressures are frequently in the range of 35 to 50 kN/m^2 and therefore a set of readings at 35 kN/m^2 was desirable, but this applied pressure was below the consistent and linear section of the calibration curve. The decision was made to make a linear extrapolation of the straight line portion of the calibration curve and take the gauge reading of 1040 kN/m^2 to represent 35 kN/m^2.

On many of the plots, a sudden random increase in the slope occurs. This was coincident with a sudden outrush of solids and water followed by a number of air bubbles. A possible explanation of this phenomenon is when the piston is lowered onto the concrete it traps and compresses a volume of air. This compressed air exploits the weakest path through the concrete causing these blow outs as it finally breaks through. These blow outs would not occur in normal concrete sections and therefore the fluid loss figures obtained from these experiments may be an overestimation.

Figure A 3 Pressure bleed test - 35 kN / m²

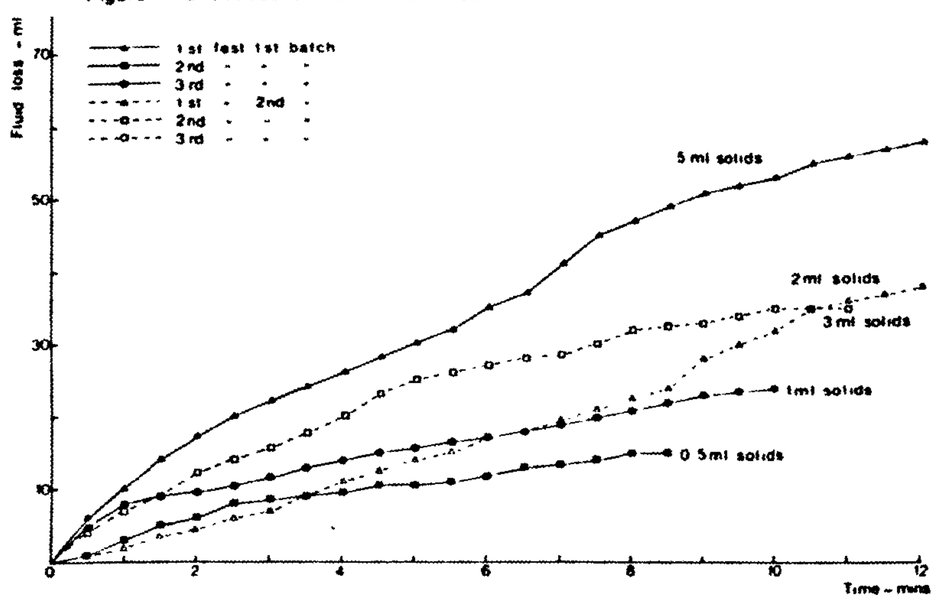

Figure A 4 Long duration pressure bleed test - 35 kN / m²

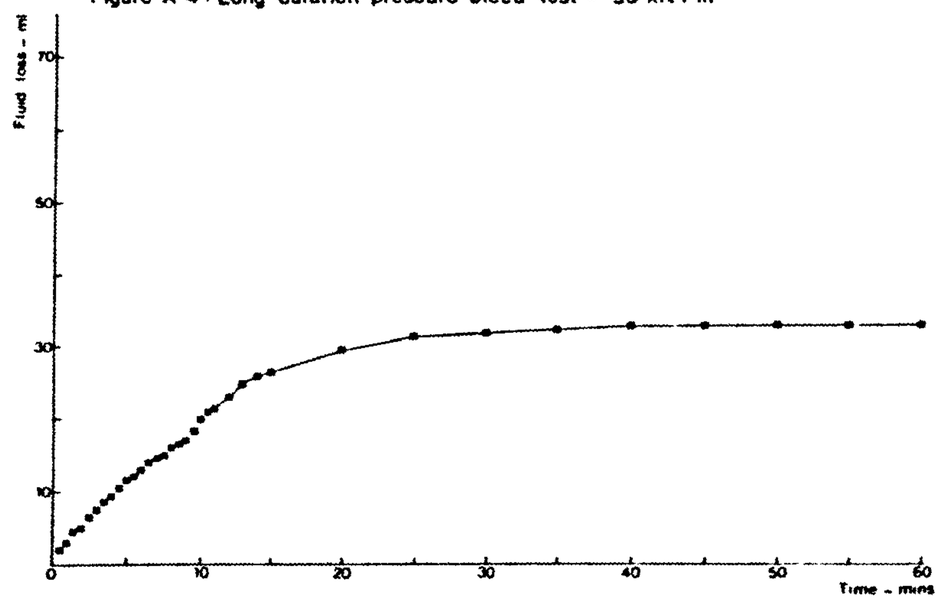

Figure A 5 Pressure bleed test - 70 kN / m²

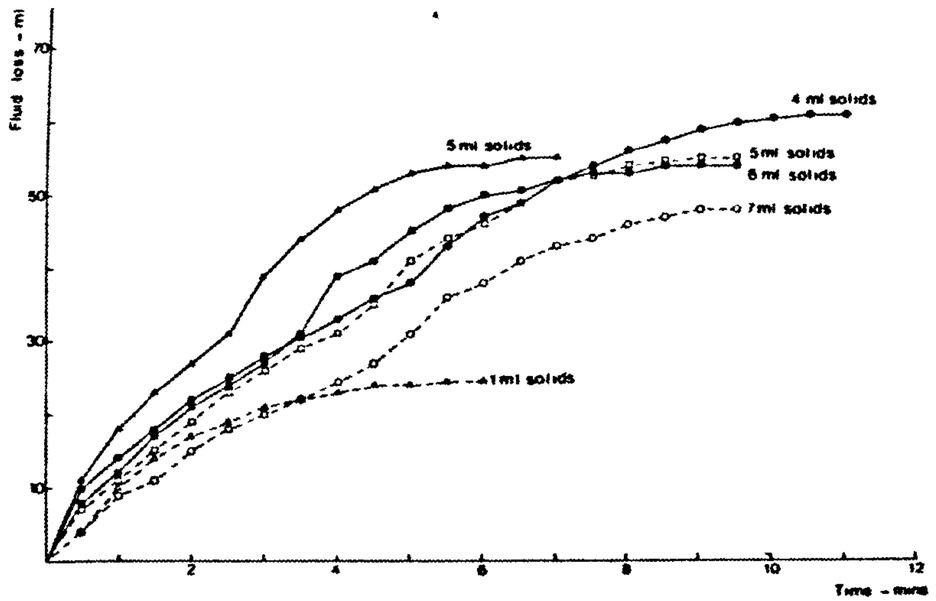

Figure A 6 Pressure bleed test - 85 kN / m²

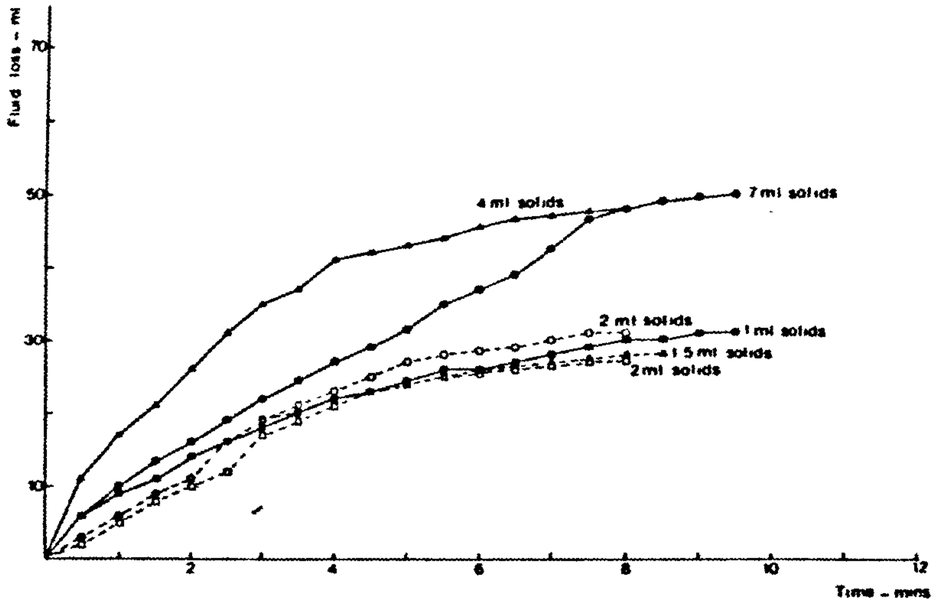

Figure A 7 Pressure bleed test - 105 kN / m²

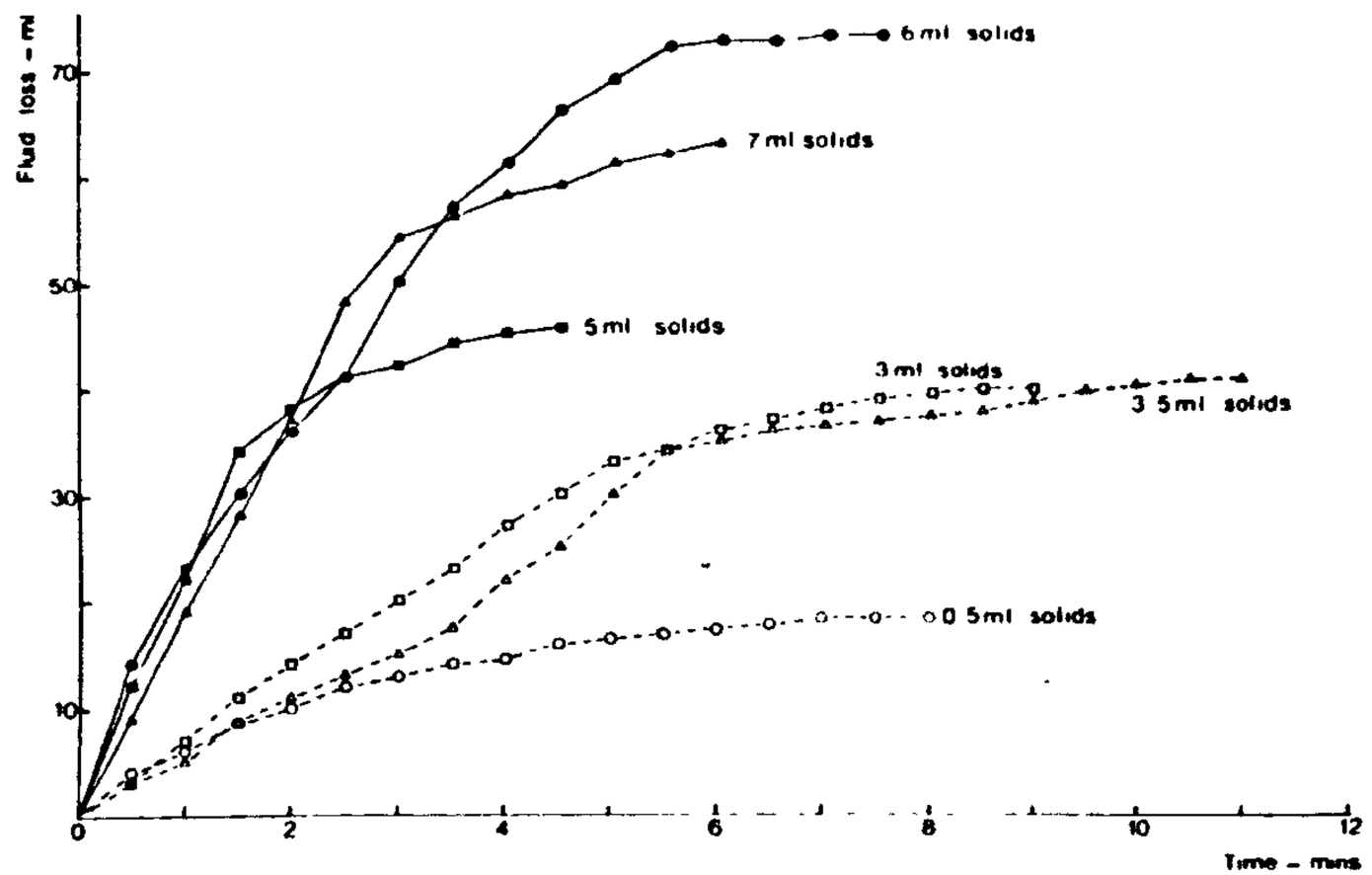

Figure A 8 Pressure bleed test - 140 kN / m²

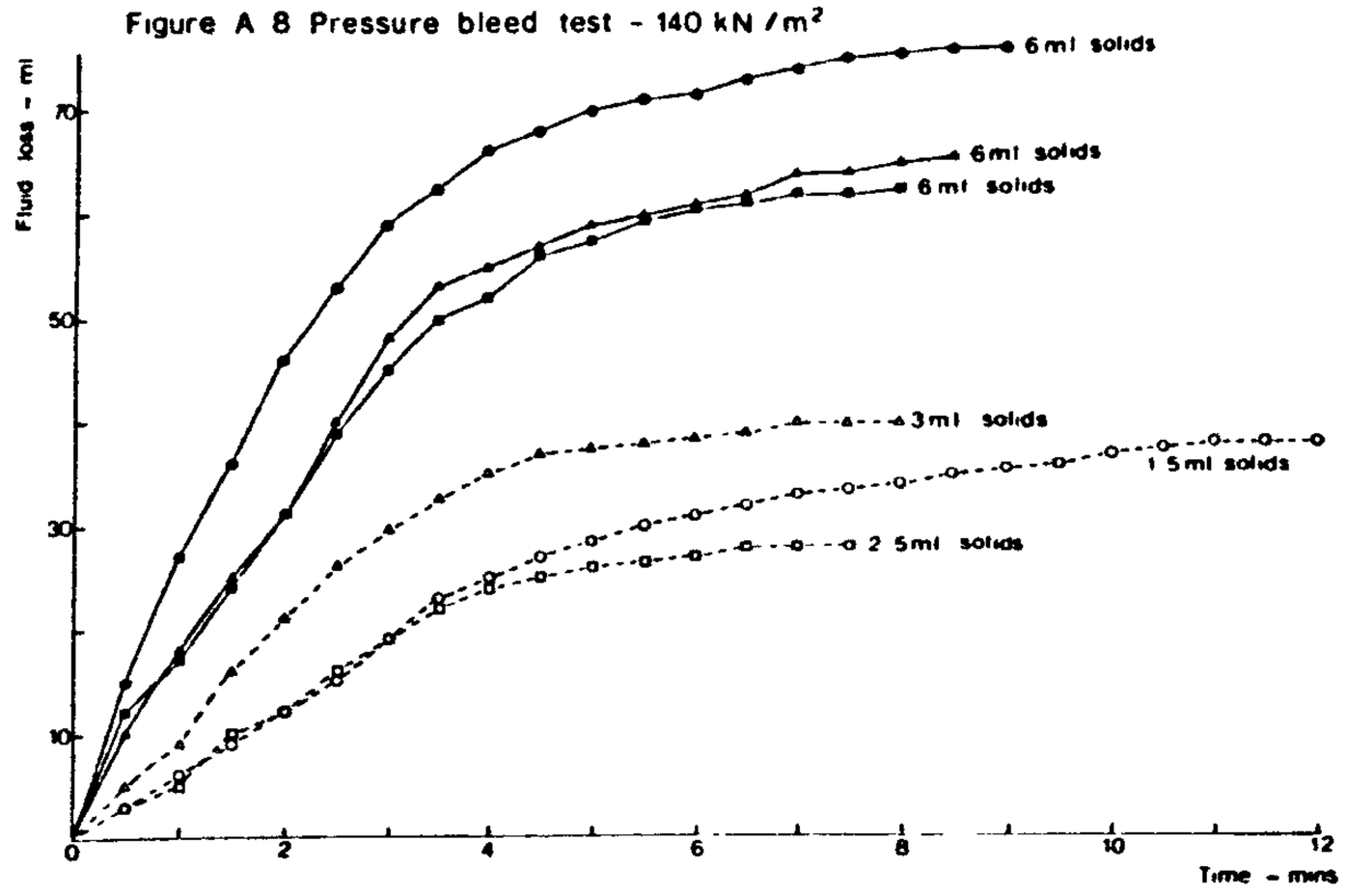

Figure A 9 Pressure bleed test (high workability concrete) - 70 kN / m².

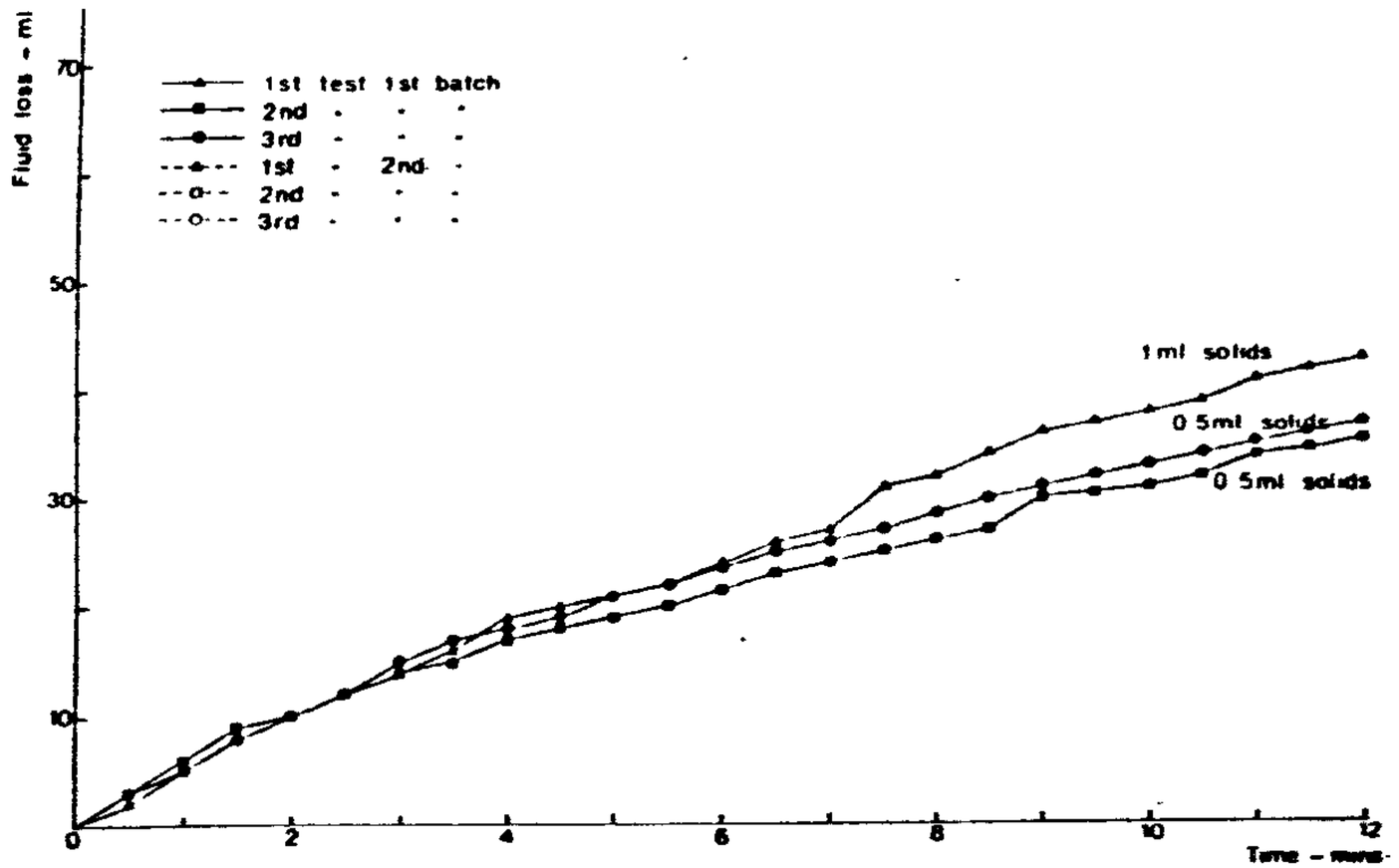

Figure A 10 Pressure bleed test (high workability concrete) - 140 kN / m².

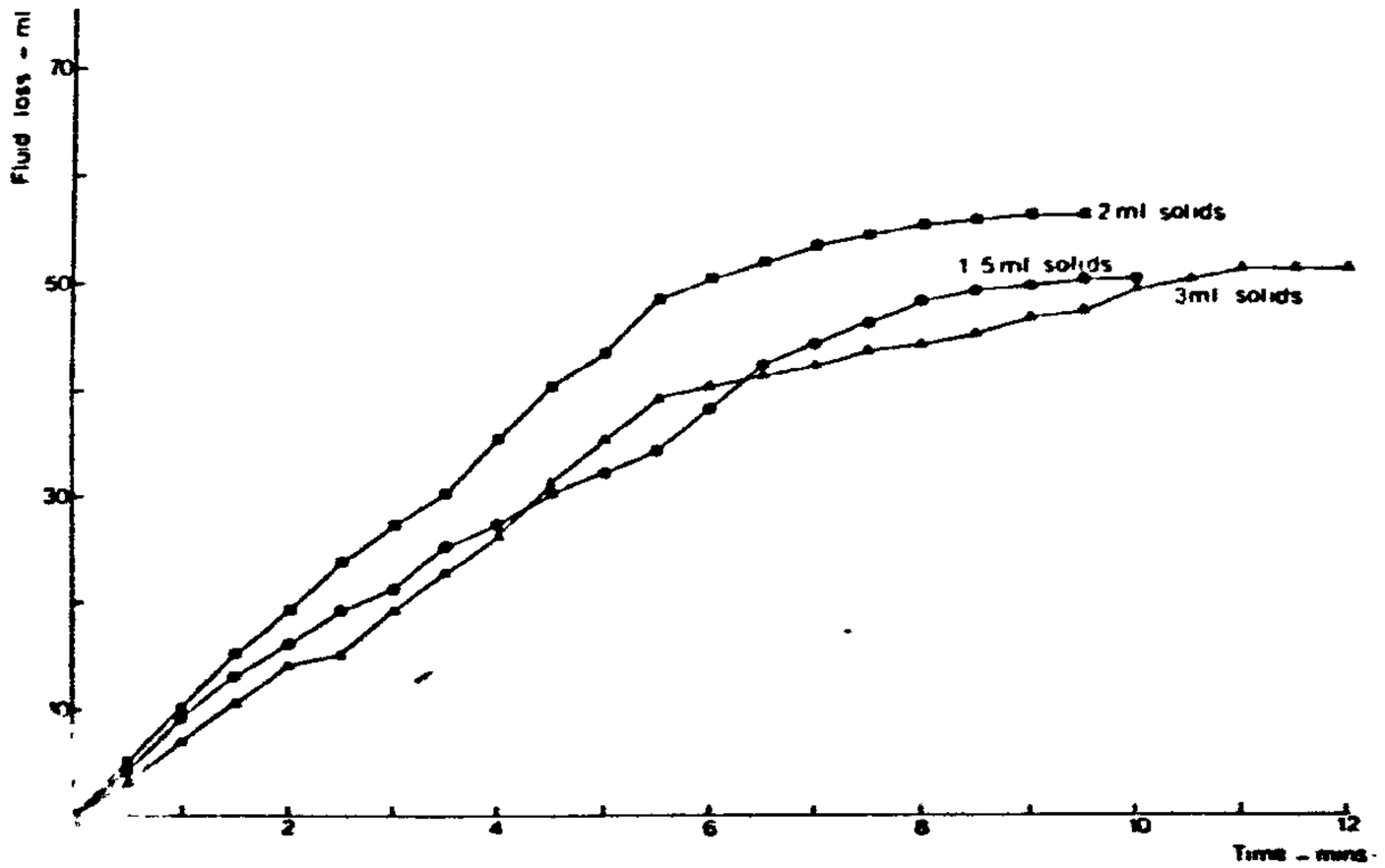

TABLE A.2

Fluid loss 6 minutes after the start of the test for the medium workability concrete.

Applied pressure kN/m^2	Fluid Loss, ml					
	Batch 1			Batch 2		
	1st test	2nd test	3rd test	1st test	2nd test	3rd test
35	35	12	17	17	27	13
70	54	50	47	24	46	38
85	45	26	37	26	25	28
105	63	46*	72	35	36	17
140	61	60	72	38	27	31

* extrapolated result

These blow outs could be avoided by fitting the piston with a valve. With the valve open, the piston would be lowered onto the concrete surface and this would prevent air being trapped between the concrete and piston. After closing the valve, the test would proceed in the normal manner.

The results from these trials were not consistent between nor within batches. There was no correlation between the fluid loss and the order of testing (Table A.2), but there is a correlation between high fluid loss and a large loss of solids. The fluid being expelled from the concrete was not uniform in appearance and was often clear or opaque until there was a blow out at which most of the solids would be discharged. When there is a blow out there is a high loss of solids and a high fluid loss, but it is not proven that all high fluid losses are the results of blow outs.

The occurrence of blow outs is not the only cause of the varibility of the results. At an applied pressure of 35 kN/m^2, it would be easy to dismiss the variability of the results as being solely due to the experimental technique and equipment, but these variations occurred at all the applied pressures. This suggests that the variability of the results might be due to the random way in which the particle structure is formed and therefore a function of the concrete and not the test method.

Figure A.4 shows a test in which the pressures was maintained for one hour. It has the same shape as the consolidation curves for soils[15]. It was impractical to continue all the tests until there was no further fluid loss. The trends of the curves at any applied pressure gave no indication that the final fluid loss would always be the same.

The tests with high workability concretes gave relatively small losses of solids. Comparing Figures A.8 and A.10, at a pressure of 140 kN/m^2 the fluid loss with the high workability concrete was slightly higher than the medium workability concrete samples which gave an equivalent loss of solids, but lower than the medium workability concretes with large losses of solids. At 70 kN/m^2 applied pressure, Figures A.5 and A.9, the high workability concrete had both a lower fluid and solids

loss than all but one of the medium workability concrete samples. This one exception had an equivalent solids loss, but a lower fluid loss.

The results of these trials gave water losses of up to 26 percent of the total free water. In formwork this is equivalent to a consolidation of 46 mm per metre height of section which is a consolidation far in excess of that observed. Therefore it can be concluded that concrete in normal sections never reaches the fully consolidated state.

CONCLUSIONS

1. The standard equipment lacks sufficient sensitivity to give reliable results below an applied pressure of 70 kN/m^2.

2. The escape of trapped air has distorted many of the results by causing blow outs. This problem could be prevented by careful design.

3. At pressures equivalent to the static weight of concrete, water movements will occur in the concrete.

4. For a fixed applied pressure, the fluid losses were not consistent between nor within batches.

5. The rate of loss of solids was not uniform, but there was an association between high fluid loss and high loss of solids.

6. The variability of the results is not only due to experimental error and blow outs.

7. At equivalent losses of solids; the high workability concrete gave higher fluid losses at 140 kN/m^2 and lower fluid losses at 70 kN/m^2 than the equivalent tests with medium workability concretes.

8. The fluid losses represented losses of up to 26 percent of the total free water.

9. The fluid losses measured by these experiments are far in excess of that observed in normal sections.

10. In normal sections, full consolidation is never achieved.